THE EFFECT OF PHARMACOLOGICAL AND DIETARY MODULATORS OF

LIPID METABOLISM ON GENE EXPRESSION IN A PORCINE MODEL

Except where reference is made to the work of others, the work described in this dissertation is my own or was done in collaboration with my advisory committee. This dissertation does not include proprietary or classified information.

_____

Ling Tang

Certificate of Approval:

_____	_____
Kevin W. Huggins Assistant Professor Nutrition and Food Science	Werner G. Bergen, Chair Professor Animal Sciences
_____	_____
Douglas C. Goodwin Associate Professor Chemistry	Russell B. Muntifering Professor Animal Sciences

_____

Stephen L. McFarland
Dean
Graduate School

THE EFFECT OF PHARMACOLOGICAL AND DIETARY MODULATORS OF LIPID METABOLISM ON GENE EXPRESION IN A PORCINE MODEL

Ling Tang

A Dissertation

Submitted to

the Graduate Faculty of

Auburn University

in Partial Fulfillment of the

Requirements for the

Degree of

Doctor of Philosophy

Auburn, Alabama
December 15, 2006

THE EFFECT OF PHARMACOLOGICAL AND DIETARY MODULATORS OF

LIPID METABOLISM ON GENE EXPRESSION IN A PORCINE MODEL

Ling Tang

_____

Signature of Author

_____

Date of Graduation

DISSERTATION ABSTRACT

THE EFFECT OF PHARMACOLOGICAL AND DIETARY MODULATORS OF LIPID METABOLISM ON GENE EXPRESION IN A PORCINE MODEL

Ling Tang

Doctor of Philosophy, December 15, 2006
(M.S., China Agriculture University, 2000)
(B.S., Xinjiang Agriculture University, 1996)

322 Typed Pages

Directed by Werner G. Bergen

Modifying the size and/or carcass distribution of adipose tissue in meat producing animals by nutritional and pharmacological means has long been of interest to animal scientists. In pigs, as in other meat animals, a more complete understanding of lipid metabolism and its regulation at the molecular level will be necessary to develop more effective strategies to modify fat deposition in different tissues of animals to improve muscle food quality and production efficiency. Studies in this dissertation describe an experimental model system to determine gene expression responses to dietary catecholamine analog in porcine adipose tissue and to a sudden change of dietary fat content in adipose, skeletal muscle, liver and intestinal epithelium in finishing pigs.

Studies described herein were designed to test the hypothesis that: 1) Ractopamine (a catecholamine) modulates lipid metabolism in adipose tissue of pigs in vivo through

transcriptional control of genes involved in fatty acid synthesis, fatty acid oxidation transcription factors, and regulatory pathways. 2) Feeding a high fat diet modulates transcription of genes involved in nutrient metabolism pathways, especially those involved in lipid and carbohydrate metabolism in the liver, adipose and muscle tissues of the pig. 3) A sudden shift from a typical high carbohydrate, low fat diet to a fat-supplemented diet in finishing pigs results in metabolic adaptations and changes in transcription of genes associated with triacylglycerol and cholesterol trafficking in the pig.

Collectively, results of the first two studies established that microarray can be used as a tool with which to detect transcription changes in the porcine tissues. The first study clearly indicated that long-term (28 days) exposure to the cAMP-elevating agent ractopamine was negative for the expression of genes in fatty acid synthesis in porcine adipose tissue. The second study showed that the short-term (14 days) of a fat enriched diet affected the transcription of lipid metabolism genes in different tissues of the pig. The third study determined the distribution pattern of genes ACAT, LCAT, apoB and HL in the porcine liver, subcutaneous adipose, gut and skeletal muscle tissues, and found that high fat diet depressed the transcription of ACAT in porcine liver.

ACKNOWLEDGEMENTS

The author would like to thank Dr. Werner Bergen for his dedication, mentoring, support, unending patience, and encouragement of critical thinking. The author thanks members of her doctoral advisory committee for their teaching, assistance, guidance, and patience during the process; Dr. Douglas Goodwin, Dr. Kevin Huggins and Dr. Russell Muntifering, with special thanks to Dr. Russell Muntifering, for his dedication as an outstanding graduate program officer. The author also wishes to express her gratitude to Dr. Anthony Moss for his encouragement, patience and assistance during the dissertation writing and final oral exam.

The author would also like to especially acknowledge the members of Dr. Frank Bartol's lab, especially Anne Wiley for her unending technical advice in the microarry analysis. Special thanks go to all the members of the Bergen lab, especially Julia Bartosh, whose technical assistance was dedicated and helpful. She also wishes to thank all the faculty and graduate students in the Department of Animal Sciences for making my graduate study enjoyable. The author would further like to thank Dr. Meng-min Liu, her boyfriend for his encouragement and help with data analysis and dissertation writing.

Finally, the author wishes to thank her parents and her sisters and brother for their love and support during her entire academic career.

Style manual or journal used Journal of Nutrition

Computer software used Microsoft Word 2003

TABLE OF CONTENTS

LIST OF TABLES..... x

LIST OF FIGURES..... xi

I. INTRODUCTION..... 1

II. LITERATURE REVIEW..... 6

Lipid metabolism overview……..…..…...…. 6
Fatty acid biosynthesis and triacylglycerol synthesis……. ……..... 7
TAG mobilization and fatty acid oxidation ……. 9
Fat deposition in pig……. 11
Regulation of gene expression by dietary fat……...….. 14
PPAR……..... 16
SREBP……... 18
Lipoprotein metabolism ……..…….…..... 19
Lipoprotein formation and transportation……...…….…..... 19
Effects of dietary fat on lipoprotein metabolism……... 22
Cyclic AMP and lipolysis…….……... 25
Cyclic AMP system…….……..……... 25
β adrenergic agonists…….……..... 27
Ractopamine…….…..…… 29
Efect of Ractopamine on the adipose tissue metabolism…… 29
Microarray technology in pig genome research……... 31
Gene expression analysis…….…….…..... 31
Microarray technology…….…….……... 32

III. EFFECTS OF DIETARY RACTOPAMINE ON PORCINE ADIPOSE GENE EXPRESSION ……...…… 38
Introduction……...……... 38
Materials and methods……. 41
Results and discussion...……..... 67
Conclusion…….……... 94

IV. OLIGOMER ARRAY ANALYSIS OF TRANSCRIPTION RESPONSE OF PORCINE TISSUES TO A SUDDEN DIET SHIFT FROM LOW FAT DIET TO HIHG FAT DIET…… ……... 106

Introduction…….. 106
Materials and methods……. 109
Results and discusison…… 113
Conclusion……... 138

V. EXPRESSION OF PORCINE GENES RELATED TO FATTY ACID AND CHOLESTEROL METABOLISM IN DIFFERENT PORCINE TISSUES…….. 152
Introduction……. 152
Materials and methods…… 155
Results……. 164
Discussion……... 168
Conclusion……..... 172

VI. CONCLUSIONS AND PERSPECTIVES…..... 180

BIBILIOGRAPHY…….……. 186
APPENDICES..... 210
Appendix A. Images of total RNA resolved on the agarose gel…….. 210
Appendix B. Microarray Analysis Protocol…… 216
Appendix C. Images of fluorescent dye Cy5-labeled cDNA probe for slides hybridization in microarray analysis…….. 221
Appendix D. Pig Genome Oligo Set and Pig Genome Oligo Extension Set 1.0……. 229
Appendix E. Microarray images of Ractopamine experiment ……... 238
Appendix F. M-A plots of pro- and post- LOWESS normalization for Ractopamine experiment (Chapter III)……. 241
Appendix G . Microarray images of diet shifting experiment (Chapter IV) 245
Appendix H. M-A plots of pro- and post- LOWESS normalization for diet shifting experiment (Chapter IV)…… 256
Appendix I. List of transcripts highly up/down regulated (top 200 highest/lowest Log2ratio value) by dietary ractopamine supplement or dietary shifting (including Log2ratio value for each replication)……..... 268
Appendix J. An example of searching tentative biological information for one unknown transcript (gene)…….. 308

LIST OF TABLES

III.
1. An example of the information recorded for MIAME compliance…… 42
2. Pig identification number, length of treatment, amount of treatment, and the date of sample collection for the pigs in the Eli Lilly feeding trial….. 44
3. Part of GenePix Arrya List (GAL) file. It presents genes information corresponding to each spot…….. 58
4. Part of GenePix Result (GPR) file. The head of GPR file describes all the parameters used when scanning the array. The main body of GPR file list the determined and calculated values for each spot (gene)…… 60
5. Interesting gene list used to filter results…… 95
6. Filtered SAM result……. 103

IV.
1. Composition of feed given to the pigs in the dietary shifting from low fat diet (LFD) to high fat diet (HFD) experiment…….. 110
2. Pig identification number, diet treatment, and the date of sample collection for the pigs……. 110
3. Differential transcription responses in liver to feeding LFD and HFD to pigs.. 143
4. Differential transcription responses in adipose tissue to feeding LFD and HFD to pigs…….. 146
5. Differential transcription responses in skeletal muscle to feeding LFD and HFD to pigs…… 149
6. Number and percentage of detected (present) and undetected (absent) out of 13297 genes among tissues studied……. 115
7. Number and percentage of differently expressed transcripts by SAM…….. 115

V.
1. Composition of feed given to the pigs in the dietary shifting from low fat diet (LFD) to high fat diet (HFD) experiment……... 156
2. Identification numbers, assigned dietary treatment, and the date of sample collection for experimental pigs……. 156
3. DNA sequence of the primers, annealing temperature used, and number of PCR cycles performed for the semi-quantitative RT-PCR…… 159
4. Final body weights at slaughter and plasma cholesterol and triglycerate concentration…….. 164

LIST OF FIGURES

II.

1. Overview of lipoprotein metabolism……. 20
2. Overview of the steps involved in oligonucleotide microarray experiments… 35

III.

1. Cy5-labeled RNA on a 2% agarose gel at 130V for 45 minutes, the gel was imaged on Typhoon 9410 at PMT 600 using emission filter for Cy5 (laser 633 nm). …..……... 52
2. An example of M-A plot before and after LOWESS normalization…… 64
3. RNA integrity categories…… 72
4. Electropherograms of microcapillary electrophoresis from four RNA samples 73
5. An example of boxplot of different arrays before and after LOWESS normalization…… 81
6. Effect of feeding 0, 20, 60 ppm of ractopamine on mRNA abundance of FAS, SREBP, GLUT4, SCD-1 and housekeeping gene (actin,) in porcine adipose tissues from corssbred pig. …...……. 93

V.

1. Intact total RNA resolved on a 1.0% agarose gel at 120V for 30 minutes…… 158
2. Tissue distribution patterns of expression the four genes…….. 166
3. Gel image of relative RT-PCR in porcine liver, adipose and gut tissues…….. 166
4. Relative gene expression in pigs fed HF diet (n=4) vs. the HCHO diet (n=4).. 167
5. Comparison of LCAT sequences (cds) between pig (AY349156) and human (BC014781.1) by LASTn…… 174
6. Comparison of ACAT sequences (5'UTR) between pig (AY676347) and human (L21934.2) by BLASTn……. 175
7. Comparison of LCAT protein sequences between pig (AAQ24609.1) and human (AAA59500.0) by BLASTp…….. 176
8. Multiple sequence alignment of human apoB 100 protein (NP_000375.1), apoB48 (AAA51741.1) and translated fragment of pig apoB mRNA…….. 177

I. INTRODUCTION

Consumer acceptance of pork products is a major factor for the sustainability of the pork industry. Elevated intakes of saturated fatty acids are associated with an increased incidence of heart disease, diabetes and obesity. Increased saturated fatty acids (SFAT) consumption has been associated with an overall increase in diabetes, obesity, cardiovascular disease. Because animal products are higher in SFAT, animal production research has focused new strategies to lower carcass SFAT. Fat deposition in meat animals is affected by genetics (breed) and nutritional conditions (1). An animal has to process a large number of different nutrients and other diet components, but nutrients can reach high concentrations without becoming toxic. Each nutrient can also bind to numerous targets with different affinities and specificities.

Genetic selection, pharmacological agents and production strategies are major tools to reduce fat content in pork. These include changes in feed components during specific growth phases and administration of exogenous agents such as β adrenergic agonists (2).

Despite advances in providing acceptable pork products for today's market, overall regulatory mechanisms of porcine lipid metabolism are not well characterized. Deeper understanding of the effects of dietary and hormonal factors on regulation of lipid metabolism will aid in developing future production strategies to provide juicier and healthy pork products.

Essentially every metabolic process represents regulated interactions of a large number of proteins encoded by their respective mRNA molecules as they are expressed in given cells, organs and organisms (3). Alterations of mRNA abundances and consequently the corresponding protein amounts are critical in controlling the flux of metabolites or nutrients through a biochemical pathway (4). Protein, fat and carbohydrates in feed/food may affect every successive step in the flow of genetic information, thereby altering metabolic functions (5).

The cyclic AMP system regulates lipolysis in fat cells by activating protein kinase A and hormone sensitive lipase. cAMP-elevating agents regulate lipid metabolism via a beta-adrenergic receptor-G protein-adenylyl cyclase-protein kinase A cascade in porcine adipose tissue (2). Catecholamines and β-adrenergic agonists are compounds that bind to membrane β-adrenergic receptors. Porcine adipocytes contain 73% β1, 20% β2, and 7% β3 adrenergic receptors. Ractopamine ((1R*, 3R*), (1R*, 3S*)-4-hydroxy-alpha-[[[3-(4-hydroxyphenyl)-1-methylpropyl]-amino] methyl]benzenemethanol) is a β1, β2 -sensitive-adrenergic agonist used in livestock production to decrease fat accretion and increase lean growth (9). Ractopamine in porcine adipose tissue binds to β-adrenergic agonist receptors and activates adjacent G_s proteins which catalyze adenosine triphosphate (ATP) conversion to cyclic adenosine-monophosphate (cAMP). Ractopamine decreased relative mRNA abundance of acetyl Co-A carboxylase (ACC), fatty acid synthase (FAS), malic enzyme (ME) and glycerol phosphate dehydrogenase (GPDH) in adipogenic cell line TA1(2). In this dissertation, (Chapter III), the effect of ractopamine on the gene transcription response in adipose tissue in finishing pigs was determined using microarray technology.

Comprehensive understanding of porcine genome function is critical to understanding how dietary nutrients affect complex metabolic processes and fat deposition. However, presently little is known how genomic/molecular regulation of lipid metabolism in pigs is coordinated across liver, skeletal muscle and adipose tissue during the growing and finishing phases of production. Coordinated gene expression responses to a sudden change of lipid metabolism, brought about by changing dietary nutrient composition have not been evaluated. Thus, assessment of the molecular events underlying metabolic adaptation of pigs switched from a typical corn-based high carbohydrate, low-fat diet (LFD) to a tallow-based high-fat diet (HFD) should provide a model for exploring differential gene expression for lipid metabolism in pigs.

Fat concentration may vary from 2% to more than 40% of dry matter in diets of animals and humans. Besides providing energy for the animal, long-chain fatty acids are ligands for nuclear receptors, peroxisome proliferators activated receptors (α and γ) and liver X receptor (PPAR and LXR), which in turn control metabolic pathways (6). The sterol regulatory element binding protein (SREBP) family is another group of transcription factors regulated by fatty acids. SREBP-1c regulates expression of a number genes involved in *de novo* lipogenesis (7). In rodents, polyunsaturated fatty acids (PUFA) depress SREBP and lipogenesis, but saturated fatty acids have little ability in depressing SREBP (8). In the pig, saturated fat has similar effect in depressing fat deposition (9), but the molecular mechanism is still not clear. In modern swine industry, domestic pigs consume a large proportion of carbohydrate and relatively low- fat (4%) from the diet. Therefore, the rate of *de novo* synthesis of long-chain fatty acids is rapid in well-fed pigs (10). In this study a high-dietary-fat intake model was specifically applied to study lipid

metabolism in pigs (see Chapters IV and V). In one set of experiments in this dissertation, I used a shift from a control high-carbohydrate, low-fat diet to a high-saturated-fat diet to study effects of fat on gene expression pattern in different porcine tissues. The adaptation to a sudden diet shift requires rapid and sustained coordinated responses in gene expression and specific regulation signals to enzymes and other proteins across all tissues in pigs.

Research of triacyglycerol and cholesterol metabolism, and lipoprotein synthesis and export have been studied in rodent liver (11, 12), but differences exists among animals(13). It is thus necessary to collect gene transcription data and elucidate the control of fatty acid metabolism at the molecular level in pigs. Such knowledge of pig lipid biology will be the basis for further utilizing pigs as an animal model in biomedical research and for developing new techniques to improve pork quality in the future.

During industry-wide programs to significantly lower total fat in pork over the last 25 years, finishing programs had been modified and pigs with much lower propensity to deposit fat were utilized. Today the industry is attempting to promulgate a new production strategy that will result in relatively low subcutaneous and visceral fat accumulation coupled with some intramuscular fat deposition. Based on what is known about the biology of fat deposition in storage depots and muscle in pigs, such new strategies will not emerge without a more complete understanding of the temporal and tissue-specific regulation of fat deposition in pigs. Dietary nutritents and pharmacological agents are strategies used to modify fat deposition in meat animals. Therefore, experiments presented in this dissertation were designed to determine: 1) Long-term effects (28 days) of cAMP-elevating agent Paylean™ (ractopamine hydrochloride) on the

gene expression profile in porcine adipose tissue; 2) transcription response of the pig genome to a sudden diet shift from high-carbohydrate, low-fat diet (LFD) to high-fat diet (HFD).in porcine liver, adipose and muscle tissues; 3) expression of triacyglycerol and cholesterol trafficking associated genes after shifting from a high-carbohydrate, low-fat diet to a high-fat diet.

II. LITERATURE REVIEW

LIPID METABOLISM OVERVIEW

As a major fuel source in the animal, fat is stored as triacylglycerol (TAG) in the adipose tissue and mobilized in the form of plasma free/ nonesterified fatty acids (FFAs). Long chain fatty acids are also critical structural components as parts of phospholipid molecules of cellular membranes.

After dietary TAG enters the small intestine, TAGs are hydrolyzed to monoglycerides and free fatty acids (FFA) by the action of specific lipases. FFA or non-esterified fatty acids (NEFA) readily aggregate to form micelles until they are taken up individually by the enterocytes. The FFAs inside the enterocytes are reesterified into TAGs and packaged with lipoproteins and phospholipids to form chylomicrons. Chylomicrons enter the lymphatic system and eventually pass into the circulatory system via the thoracic duct. In the adipose and muscle, TAG of chylomicrons is hydrolyzed to release FFA by lipoprotein lipase, an enzyme attached to the endothelial cells primarily lining the capillaries. Released FFAs bind with serum albumin and are transported to peripheral tissues. In adipose tissue, the FFAs are primarily reesterified and stored as TAGs; in other organs, such as muscle and liver, small amounts of TAG are stored intracellularly. The stored TAG is mobilized in the form of plasma FFAs when energy is required by the animal. In human and rodents, the primary sites of FFA oxidation are cardiac skeletal muscle and liver. The liver and muscle oxidizes FFA to help fuel their

various metabolic activities, through sequential formation of acetyl-CoA through β oxidation, completely oxidation of acetyl-CoA in TCA cycle and transferring electrons into oxidative phosphorylation to produce ATP.

Regulation of fat metabolism has been extensively studied in rodents and humans because intake of a high level saturated fat from the diet is linked to the development of cardiovascular disease, insulin resistance, diabetes and obesity. For example, increased muscle accumulating TAG contributes to the development of insulin resistance. In meat animals, understanding lipid metabolism and the mechanism of its regulation underlies the development of strategies for modifying fat deposition in different tissues of animals and improving meat quality. In the review below, multiple lipid metabolism pathways will be discussed. Most of metabolic pathways will be described based on rodent and humans studies; specific research in the pig will be emphasized based on the limited literature.

Fatty Acids Biosynthesis and Triacylglycerols Synthesis

Fatty acids biosynthesis occurs in the cytosol with the growing fatty acid chains esterified to acyl-carrier protein (14). Long-chain fatty acid synthesis occurs in two stages: First, the conversion of acetyl-CoA to malonyl-CoA is catalyzed by acetyl-CoA carboxylase (ACC) and, secondl, acetyl-CoA and malonyl-CoA are converted to palmitate in the presence of NADPH, a process catalyzed by fatty acid synthetase (FAS) (15). Malonyl-CoA is the immediate precursor in fatty acid biosynthesis. Fatty acid precursor, acetyl-CoA is transferred from the mitochondrion to the cytosol as citrate via the tricarboxylate transport system and citrate cleavage. Palmitate is the primary product

of fatty acid biosynthesis in animals. Longer chain fatty acids and unsaturated fatty acids are synthesized from palmitate (16:0) by elongation and desaturation reactions (16).

After fatty acids are synthesized, they must be activated by acyl-CoA synthetase to produce acyl-CoA, and then combine with glycerol-3-phosphate to form triacylglycerols (17). Glycerol kinase catalyzes the activation of glycerol to glycerol-3-phosphate in the liver, and glycerol-3-phosphate dehydrogenase catalyzes the formation of glycerol-3-phosphate from dihydroxyacetone phosphate (17). Glycerol-3-phosphate acyltransferase (GPAT) catalyzes the synthesis of triacylglycerols from fatty acyl-CoA esters and glycerol-3-phosphate. Glycerol-3-phosphate acyltransferase prevents fatty acyl-CoA from undergoing lipid oxidation and leads fatty acyl-CoA to triacylglycerol synthesis (10). Triacylglycerols synthesized in the liver are transported via VLDL to adipose tissue and then hydrolyzed by lipoprotein lipase (LPL) before fatty acid storage in adipose-synthesized TAG.

Fatty acid synthesis is controlled by both short-term and long-term regulation (18). Acetyl-CoA carboxylase (ACC) catalyzes the first committed step of this pathway. ACC is inhibited by palmitoyl-CoA and by a glucagon-stimulated cAMP-dependent increase in phosphorylation, and it is activated by citrate and by insulin-stimulated dephosphorylation (19). Lipid synthesis is also controlled by long-term regulation, with insulin via SREBP-1c stimulating the synthesis of ACC and FAS. Dietary poly unsaturated long-chain fatty acids (PUFA) decrease the concentration of liver ACC and FAS (20).

De novo fatty acid synthesis or lipogenesis (DNL) is inhibited by free or non-esterified fatty acids by inhibiting cytosolic acetyl-CoA carboxylase activity (21). For

fatty acid synthesis in the rodent liver, PUFA are highly effective DNL inhibitors, but saturated NEFA have a lesser effect (22). PUFA reduce mRNA levels of lipogenic enzymes via gene expression or mRNA decay (23).

However, species differences exist in lipid metabolism. In humans and rodents, liver is the primary site of *de novo* lipogenesis (DNL), with adipose tissue is a secondary DNL site. However, in pigs, DNL takes place primarily in the adipose tissue while the liver synthesizes relatively low amounts of fatty acids for metabolic function (13). When animals ingest carbohydrates exceeding the amount required for energy expenditure, the excess carbohydrates are stored as TAG in the adipose tissue through fatty acid and TAG synthesis. In domestic pigs, daily intake of energy is usually provided from dietary carbohydrates. Fatty acids are synthesized from glucose in the adipose tissue of swine (13). Adipose tissue is the major glucose-utilizing tissue and metabolizes 40% of the daily glucose uptake in pigs (24). Glycolysis is the fate of glucose in the adipose tissue. The end product of glycolysis, pyruvate, is then converted to acetyl-CoA by pyruvate dehydrogenase. Acetyl-CoA from glycolysis is the precursor for the *de novo* fatty acid synthesis in the adipose tissue (17).

TAG Mobilization and Fatty Acid Oxidation

During states of negative energy balance, TAG in adipose tissue is mobilized to provide energy. The hydrolysis of TAG to FFA is catalyzed by hormone-sensitive lipase (HSL), which is the rate-limiting enzyme in lipolysis (25, 9). The free fatty acids arising from lipolysis bind with serum albumin and are transported to various tissues for further oxidation by fatty acid binding proteins (26).

Uptake of FFA by tissues for subsequent oxidation occurs via the plasma membrane, and FFAs are esterified to coenzyme (CoA) via fatty acyl–CoA synthetase on entering the cell. The resulting fatty acyl–CoA is then transported to the matrix through the inner membrane of the mitochondrion. This transport is mediated via carnitine and the enzyme carnitine palmitoyltransferase I (CPT-I) and carnitine palmitoyltransferase II (CPT-II). Once inside the mitochondrial matrix, the fatty acyl–CoA enters β-oxidative pathway and sequentially yields acetyl-CoA.

During β -oxidation of even chain fatty acyl-CoA, 2-carbon units are successively removed as the acyl-CoA is reduced to multiple acetyl CoA (17). This oxidative pathway includes FAD-dependent dehydrogenation of an alkyl group, hydration of the resulting trans 2,4 enoyl CoA , NAD^+-dependent oxidation of this hydroxy acid to a ketone, and C-C bond cleavage to form acetyl-CoA and a new fatty acyl-CoA with two fewer carbon atoms (27). Complete oxidation of the acyl-CoA, NADH and $FADH_2$ is achieved by the Krebs cycle and oxidative phosphorylation (28).

Fatty acid oxidation is regulated largely by the concentration of fatty acids in the blood, which is controlled by the hydrolysis rate of TAG in adipose tissue by hormone-sensitive lipase (29). HSL is regulated by phosphorylation and dephosphorylation in response to hormonally controlled cAMP levels. Glucagon, epinephrine and norepinephrine increase adipose tissue cAMP concentration (30). This second messenger activates cAMP-dependent protein kinase (cPKA), which in turn increases phosphorylation of perilipin and HSL. The phosphorylation of perilipin by PKA facilitates a large increase in the rate of lipolysis (31-33). HSL is both an abundant intracellular triacylglycerol lipase in adipocytes and a substrate for PKA; the

phosphorylation of PKA sites in HSL triggers the translocation of the lipase from the cytosol to the surfaces of lipid droplets (33-35) where lipolysis then occurs. A recent study has found that the presence of perilipin on the surfaces of lipid droplets is required to dock HSL onto lipid droplets (33), suggesting that perilipin may be HSL-binding proteins. After HSL is phosphorylated, it catalyses lipolysis in adipose tissue, elevating blood fatty acids levels, and finally activating the beta-oxidation pathway in other tissues such as liver and muscle (36). When cells experience an energy insufficiency, ATP becomes depleted and cellular AMP concentration rise (37). This results in activation of AMP-dependent protein kinase (AMPK), which lowers ACC activity and enhances fatty acid oxidation (37). Here, cAMP-dependent PKA, acting in concert with AMP-dependent protein kinase (AMPK), causes the inactivation of ACC; thus, cAMP-dependent phosphorylation simultaneously stimulates fatty acid oxidation and inhibits fatty acid synthesis (38).

According to Bergen and Mersmann (13): " The rodent adipocyte is responsive to a wide variety of endocrine entities including adrenergic hormones, insulin, somatotropin, adrenocorticotropin, thyrotrophin, thyroid hormones, and glucocorticoids. Adipocytes from other mammalian species exhibit less breadth of endocrine control with meager or no demonstrable response to many of these hormones (39)". In general, insulin stimulates fat deposition and inhibits lipid catabolism, whereas ß-adrenergic receptor (ßAR) agonists have the opposite effects (40).

Fat Deposition in Pigs

The literature on the effects of the type of dietary fat on lipogenesis is dominated by studies in rodent liver tissue. The degree of inhibition between saturated and

unsaturated fatty acids showed little difference in rodent adipose tissue, and the effects of degree of unsaturation are specific to liver (41). The difference indicates that the promoter regions of fatty acid synthase may differ between tissues (42). The overall DNL rates are low in the liver of pigs because of low lipogenic enzyme activity (43, 44).

The pig has a very high capacity for synthesis and storage of fatty acids. The amount of fattening depends on the age, sex and genetic lineage of the animal. Pigs from 5-7 months of age can deposit large amounts of fat with as much as 50% of daily energy intake being stored as fat (45). In fed pigs, fat is readily deposited in peripheral adipose tissue and body subcutaneous adipose tissue of the leg by converting carbohydrates to fatty acids (46-47).

Dietary fat alters triacylglycerol deposition in the pig based on dietary fat source (saturated or unsaturated), fat content, and duration of fat ingested (48). The intake of feed and feed quality may also affect the fat deposition in the pig (49). There are reports from three independent groups that inhibition of lipogenesis in adipose tissue of the pig is greater with saturated fat sources than with unsaturated sources (50-52). The nature of the dietary fats thus affects lipid homeostasis and body fat deposition. Ding et al. (53) found fatty acid composition in the plasma and adipose tissue was similar to the dietary fatty acid profile after young pigs were fed with either a tallow-based high fat or fish oil-based, high-fat diet for 2 weeks. They also found fatty acid profiles of liver and muscle reflected dietary specific fatty acids to a greater degree than plasma free fatty acids and adipose tissue. In pig, the major changes of fatty acid profiles in adipose tissue TAG fatty acids were observed only after a dietary fat source had been consumed for 4-5 weeks (54).

Porcine adipocytes are distinct from rodent adipocytes in a number of ways. Rodent adipocytes are highly insulin-sensitive, but porcine adipocytes are less sensitive (55). The hormonal and growth factor-driven differentiation of adipocytes may be different between rodent and porcine adipocytes (56). Extensive information about porcine adipocyte differentiation has been reviewed by Hausman (57) and is beyond the scope of this dissertation.

Models of mammalian hepatic lipid catabolism are based largely on data from adult rats, emphasizing formation of ketone bodies as primary adjuncts to mitochondrial matrix β-oxidation. Clearly, lipid metabolism in swine liver is not adequately described by rodent models of beta-oxidation that emphasize accelerated ketogenesis concomitant with enhanced mitochondrial flux of fatty acids (58). In neonatal rabbits (59) as well as mature rats (60-61), *in vitro* rates of liver β-oxidation were higher than in liver from new born pigs (60, 62-63). Adams (64) observed that *in vitro* hepatic O_2 consumption in piglets was only 50% of that noted in rats. The relatively low rate of β-oxidation in baby pigs can be explained in part by a lower overall metabolism and that the mitochondria contribute significantly to acetogenesis. The low rate of fatty acid oxidation in swine liver might be related to a lower tissue-specific metabolic rate (O_2 consumption per unit mass) resulting from lower energy need to meet cellular ATP requirements (65). Thus, low rates of β-oxidation and ketogenesis infer that alternative, nonketogenic routes of carbon flow may predominate in swine liver (62).

REGUALTION OF GENE EXPRESSION BY DIETARY FAT

Cells regulate gene expression in response to changes in the external environment. In unicellular organisms, specific mechanisms have evolved to allow the cells to metabolize fuels according to their availability in the external milieu (23). Most of the mechanisms involve conditional transcription of genes encoding enzymes specific to a metabolic pathway in response to an appropriate nutrient. The best-characterized examples are the nutritional regulation of the *lac* operon of *Escherichia coli* and the *gal* regulon of *Saccharomyces cerevisiae* (23). In multicellular organisms, the needs of the individual cell and of the whole organism must be managed. In mammals, most of the adaptations to environment are controlled by hormonal or neuronal signals. Major dietary components (protein and energy) or lesser (trace mineral, vitamin) dietary constituents may regulate gene expression in a hormonal-independent manner (66).

In preadipocyte**,** hormone-like effects have been attributed to fatty acids and their derivatives in the regulation of gene expression and consequent preadipocyte proliferation and differentiation (67). Regulation of expression of transcription factors, such as CCAAT/enhancer binding protein and peroxisome proliferator activated receptors, during early adipocyte development has been attributed to long-chain saturated and unsaturated fatty acids (68). Some fatty acids or their metabolites act like hormones to control the activity or abundance of specific transcription factors. These transcription factors interact with specific target genes through *cis*-regulatory elements and interface with common components of the transcriptional apparatus (69).

Activities of lipogenic genes are principally regulated at the transcription level (20-21, 70). Recent research results with rodents and humans showed that dietary fatty acids

had clearly enhanced gene expression, resulting in changes in metabolism, growth and cell differentiation (71). Storlien (72) found ingestion of diets high in saturated fat (>45% as calories) for several weeks increased serum TAG and promotes insulin resistance, and obesity in rodents. High-fat diets (>65% of energy as lipids) increased expression of fatty acid translocase and beta-hydroxyacyl-CoA dehydrogenase genes, but did not change the mRNA concentration of epithelial membrane fatty acid binding protein, mitochondrial carnitine palmitoyltransferase I, and uncoupling protein 3 in human skeletal muscle (73).

The domestic pig can easily consume dietary energy in excess of its needs and hence is prone to deposit excess fat as indicated above. Domestic pigs typically are given a small amount of fat from the diet (2%-4%), except in a production setting where fat replaces some dietary corn to lower feed cost. Dietary fat has profound effects on gene expression, leading to changes in metabolism and growth. The effects of dietary fat on gene expression reflect an adaptive response to changes in the quantity and type of fat ingested. Regulation of gene transcription by fatty acids seems to be due to changes in the activity or abundance of at least 4 transcription factor families: PPAR (peroxisome proliferator-activated receptor), LXR (liver x receptor), HNF-4α (hepatic nuclear factor 4) and SREBP (sterol regulatory element binding protein) (74). Except for SREBP, all these transcription factors are members of the steroid and thyroid hormone nuclear receptors superfamily (75).

Several mechanisms have been proposed to clarify the molecular basis for fatty acid regulation of gene transcription. Below, more detail is presented as to how fatty acids regulate gene expression through two families of transcription factors, the PPARs and SREBPs**.**

PPAR (Peroxisome Proliferator-Activated Receptors)

Peroxisome proliferator-activated receptors (PPARs) are members of the superfamily of ligand-activated nuclear transcription factors (76). The active transcriptional form of PPARs are heterodimeric complexes with retinoid X receptor (RXR). This heterodimer binds to specific DNA recognition sequences, PPAR response elements (PPRE), in the promoter region of target genes (77). In rodents, three PPAR subtypes have been identified, which are encoded by three separate genes and demonstrate tissue specificity in expression. The transcription factor PPARα is expressed in hepatocytes, cardiomyocytes, renal proximal tubule cells, and enterocytes (69). PPARδ is expressed in more tissues than PPARα, but most importantly in skeletal muscle (78); PPARγ is expressed in adipose tissue, spleen, retina, hematopoietic cells, and epithelial cells of the colon, prostate, and mammary gland (79). In pigs, PPARα is abundant in the porcine liver and muscle. PPARα and PPARγ are both expressed in adipose tissue; while PPARγ is the predominant form in adipose tissue (56). PPARγ isoforms, PPARγ1 and γ2, result from different splicing of same gene (80).

PPARs are activated by numerous fatty acids including: palmitic (16:0), oleic (18:1, n-9), linoleic (18:2 n-6), arachidonic (20:4 n-6) acids and eicosanoids. These nuclear receptors appear to act as sensors for fatty acids (81).

Many genes involved in fatty acid metabolism are regulated by one of the three members of the PPAR family (82). It has been shown that PPARα regulates pathways of fatty acid oxidation, while PPARγ modifies fatty acid synthesis and storage in adipose tissues (83). PPARγ2 is involved in the induction of genes encoding enzymes involved in lipid storage in adipocytes. Fatty acids and some prostanoids induce adipocyte

differentiation. In the process of adipocyte differentiation, the mRNA abundance of enzymes in the lipogenic and triglyceride synthesis pathways, fatty acid transport, fatty acid binding, as well as various lipogenic and lipolytic hormone receptors are up regulated (84).

PPARs are among several nuclear receptors that requireRXR as a heterodimer partner for DNA binding (78). The effect of fatty acid on RXR abundance or activity may impact other signaling systems utilizing RXR as a heterodimer partner (85).

PPARα is proposed to regulate peroxisomal and mitochondrial fatty acid oxidation by modulating the expression of peroxisomal acyl coA oxidase (AOX) and mitochondrial carnitine palmitoyltransferase (CPT-1) (86). PPARα, AOX and CPT-1 are expressed at high levels in rodent liver; while PPARα is not expressed in rodent adipose with a modest extent expression of AOX and CPT-1 in rodent adipose. This observation has led to the conclusion that fatty acid oxidation is unlikely in adipose tissue; an idea that underscores the primary function of adipose tissue as a TAG storage depot. In pigs however, expression of PPARα appears higher in adipose tissue than in liver (87), suggesting that swine adipose tissue may oxidize fatty acids. However, Sundvold et al. (88) demonstrated PPARα was mainly expressed in kidney and liver but not in adipose in mature swine. PPARα is also expressed in skeletal muscle, and promotes fatty acid oxidation, ketone body synthesis, and glucose sparing when activated by a fatty acid ligand in the rodent and human (86).

SREBP (Sterol Regulatory Element-Binding Proteins)

SREBP transcription factor family has emerged as regulating factors in lipid and cholesterol metabolism (70, 89). SREBPs belong to the basic helix-loop-helix-leucine zipper family of transcription factors and are synthesized as inactive precursors bound to the endoplasmic reticulum (ER) (90). Three ancillary proteins, SREBP cleavage-activating protein (SCAP), site-1 protease (S1P) and site-2 protease (S2P) are required for SREBP maturation (91). SREBPs directly targets expression of more than 30 genes involved in the synthesis and uptake of cholesterol, fatty acids, triglycerides, and phospholipids, as well as the NADPH coenzyme (92). When SREBPs are overexpressed under special experimental circumstances, each SREBP isoform can activate genes involved in synthesis of fatty acids, triglycerides and cholesterol (93). SREBP-1a is a ubiquitous activator of all SREBP-responsive genes. These include enzymes that mediate the synthesis of cholesterol, fatty acids, and triglycerides (94). Transcription of genes needed for DNL are preferentially regulated by SREBP-1c but not for cholesterol synthesis under physiological conditions. The target genes of SREBP-1c include in order: ATP citrate lyase, acetyl-CoA carboxylase (ACC), fatty acid synthase (FAS), stearoyl-CoA desaturase (SCD), glycerol-3-phosphate acyltransferase(GPAT) (95-96). Characterized by a longer transcriptional activation domain, SREBP-2 preferentially stimulates cholesterol biosynthesis (97). SREBP-1c and SREBP-2 activate three genes required to generate NADPH, malic enzyme, glucose-6-phosphate dehydrogenase (G6PD), and 6-phosphogluconate dehydrogenase (PGDH). NADPH is required for reduction steps in lipid biosynthetic pathways (96).

Regulation of SREBPs occurs at transcriptional and posttranscriptional levels. The transcription of SREBP-1c is selectively regulated by insulin, glucagon , and liver X-activated receptors (LXRs),.In the presence of LXR agonists, SREBP-1c expression is activated via a LXR binding site in the SREBP-1c promoter (98, 99). One of the properties of insulin is to stimulate DNL during carbohydrate excess. This action of insulin is counteracted by glucagon, which increases cellular cAMP . Many researhers suggest that insulin's stimulation of DNL is modulated by SREBP-1c (100-101). In isolated rat hepatocytes *in vitro*, insulin treatment simultaneously increases the abundance of mRNA for SREBP-1c and its target genes (102).

Although cholesterol biosynthesis depends almost entirely on SREBPs, fatty acid synthesis is only partially dependent on the expression of SREBPs. In liver, the gene encoding fatty acid synthase (FAS) can be transcriptionally activated by upstream stimulatory proteins (USP) that act in concert with SREBPs (103). The FAS promoter also contains an LXR element that permits a low-level response to LXR ligands even when SREBPs are suppressed (104). Regulation of liver SREBP-1c emerges to be quite complex, and SREBP-1c is highly sensitive to dietary polyunsaturated fatty acids (PUFA) in rodents and pigs (105-106). The SREBP-1 processing includes tethered nascent SREBP-1c processing by SCAP and SP1 and SP2, degradation of SREBP-1c mRNA (107) and ubiquitination of nSREBP and subsequent proteasomal degradation (106).

LIPOPROTEIN METABOLISM

In animals and humans, three major pathways of lipoprotein metabolism are tightly interrelated and interdependent: (1) the transport pathway of dietary or exogenous fat; (2) the transport pathway of hepatic or endogenous fat; and (3) the reverse cholesterol

transport pathway. Similar to the work on the effects of dietary fatty acid on lipid metabolism, research on the lipoprotein metabolism and its control by dietary factors has been almost exclusively conducted in rodents and humans.

Lipoprotein Formation and Transportation

An overview of lipoprotein physiology is depicted in Figure 1 and then described below. In the figure, A-1, B, C-II, and E represent the various apolipoproteins. Lipid is insoluble in aqueous media, and its transportation in the animal is performed by lipoproteins. Lipoprotein particles are the aggregates of proteins and lipids (23). Dietary fat is secreted from intestinal cells as chylomicrons, a process that requires apolipoprotein B (apoB).

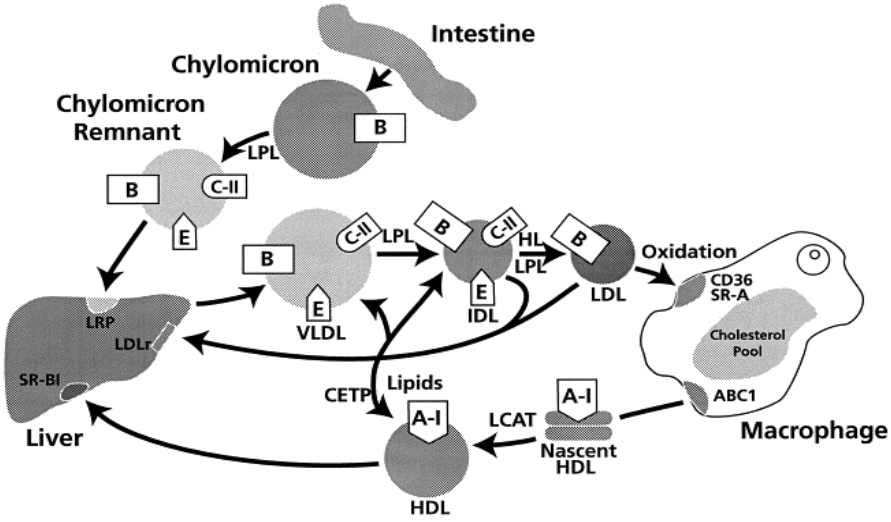

Fig 1. Overview of lipoprotein metabolism (108)

Chylomicrons are synthesized in the intestine and found in lymph and plasma after a fat-containing meal (109). The TAG within the chylomicrons is hydrolyzed by lipoprotein lipase (LPL) with apolipoprotein C-II (apo C-II) as cofactor, producing a

chylomicron remnant that is taken up by the low-density lipoprotein-like receptor protein (LRP) in the liver. Very low-density lipoprotein (VLDL) is secreted from the liver, and the TAG in the core of the VLDL is hydrolyzed in various tissues by LPL and apo C-II to produce intermediate-density lipoprotein (IDL). The liver takes up some IDL particles through the interaction of apo E with the LDL receptor; other IDL particles produce low-density lipoprotein (LDL) after hydrolysis by hepatic lipase (HL). If LDL is oxidized, it can enter macrophages via the scavenger receptors, CD36 and SR-A. Nascent HDL particles are made in the liver and intestine. They are secreted as particles containing mainly phospholipid and apo A-I. The nascent HDL interacts with peripheral cells such as macrophages and removes unesterified cholesterol through the ATP-binding cassette 1 (ABC1) transporter protein. The cholesterol in the nascent HDL is then esterified to a fatty acid derived from lecithin by lecithin cholesterol acyl transferase (LCAT) and its co-factor, apo A-I, producing a spherical, mature HDL particle. The cholesteryl ester in the core of HDL is then returned to the liver, either by the interaction of HDL with the SR-B1 receptor, or transferred to the apo B-containing lipoproteins by cholesteryl ester transfer protein (CETP) (Fig 1). In the liver, Acyl-CoA:cholesterol acyltransferase (ACAT) catalyzes the transfer of fatty acid from coenzyme A to the hydroxyl group of cholesterol, converting the cholesterol into a more hydrophobic from. Cholesteryl esters are transported in secreted lipoprotein particles to other tissues that use cholesterol, or are stored in the liver. A severe reduction in the cholesteryl ester content of hepatoma cells reduces apoB secretion (110). Description of above lipoprotein pathways are based on research in rodents and guinea pigs. The lipoprotein pathways in domestic pigs are not

completely similar. For example, it is still not clarified if gene CETP exists in domestic pig (111).

Effects of Dietary Fat on Lipoprotein Metabolism

Effects of fatty acids on lipoprotein metabolism are dependent on the chain length and degree of saturation. A saturated fatty acid diet (31% coconut oil) alone caused elevations of total, IDL, and LDL cholesterol when normolipidemic adult males were supplied with a high-fat diet for 9 days (112). Goldberg et al. (113) showed that diets supplemented with C-12 and C-14 saturated fatty acids increased serum cholesterol levels compared with polyunsaturated fatty acid containing diets in humans. In guinea pigs dietary fat saturation influences secretion rate of VLDL from the liver and the composition of nascent VLDL (114). Saturated fat-enriched diets increased secretion rate of smaller VLDL particles rich in cholesterol compared with a polyunsaturated fatty acid-enriched diet in guinea pigs (114). Using guinea pigs the effects of chain length and saturation of fatty acids on hepatic VLDL synthesis have been studied (115). Guinea pigs fed a palm kernel oil (PK) diet exhibited the greatest plasma LDL-cholesterol (LDL-C) levels, followed by those fed palmitate rich palm oil. The lowest plasma LDL-C concentrations were seen upon feeding coconut oil (114,116-117). In addition, significant differences in LDL composition have been noted in guinea pigs fed PK, lard or CO diets. Guinea pigs fed a saturated fatty acids (SAT) diet have cholesterol ester (CE) –enriched LDL that are associated with higher circulating concentrations of LDL-C. However, when guinea pigs are given PUFA diets, LDL particles are CE-poor, exibit 1.5 times faster turnover in plasma than the larger LDL particles from guinea pigs fed the SAT diet (117).

ApoB-100 is required for the assembly and secretion of VLDL by the liver. Dashti et al. (118) compared the effects of different fatty acids on the composition and concentration of apoA-I and apoB containing lipoproteins using $HepG_2$ cells. They observed that saturated fatty acids increased plasma concentration of apoA-I and apoB, while monounsaturated fatty acids decreased plasma apoA-I level. Hepatic microsomal TAG transfer protein (MTP) mRNA levels have been shown to be influenced by dietary fats, with levels being increased by saturated fatty acids compared with monounsaturated and n-6 PUFAs (119). For example, guinea pigs fed the PK diet exhibit the highest apoB secretion rate (120).

Feeding high-saturated-fat diets affected apoE levels and distribution among the lipoproteins in plasma. Cole et al. (121) found an increase in total apoE and apoE containing lipoprotein in rats fed a SAT diet for 2 weeks. Fisher et al. (112) found that apoE was redistributed on the saturated fat diet in adult males, such that apoE in VLDL, IDL and LDL were increased while apoE was decreased in heavier HDL fractions.

Acyl coenzyme A:cholesterol acyltransferase (ACAT) is the intracellular enzyme responsible for catalyzing cholesterol esterification in liver and other organs (37). In the human, there are two isoforms of ACAT. ACAT1 is expressed in all tissues while ACAT2 is present mainly in liver and intestine. ACAT2 is responsible for supplying cholesteryl ester for VLDL (122). Saturation of dietary fat and cholesterol content change liver ACAT activity in guinea pigs (123). Monounsaturated fatty acids increased ACAT activity in contrast to saturated fatty acids or PUFA. Increasing cholesterol concentration in the diet resulted in matching increases in liver ACAT activity.

Lecithin:cholesterol acyltransferase (LCAT) is responsible for cholesterol ester formation in the plasma compartment (37). VLDL cholesterol in guinea pig is mostly derived from LCAT activity, as is also the case in humans. LCAT activity may also contribute to the formation of CE (cholesterol ester) in VLDL (124). Fernandez et al. (125) found higher LCAT activity in guinea pigs fed high-fat diets (35 or 45% total dietary energy from fat) than those fed low-fat diets (10 or 19% total energy from fat), which correlated with the higher concentration of VLDL cholesterol.

Lipoprotein lipase (LPL) is present within intracellular pools in adipocytes and muscle cells and acts on TAG-rich lipoprotein and hydrolyzes the TAG. Apolipoprotein C-II (apoC-II), a protein constituent of human VLDL, is the activator for lipoprotein lipase (126). ApoC-III depress the action of of LPL. The regulation of LPL is tissue-specific. LPL has an important role in directing VLDL TAG to muscle tissues during fasting. Under condition of scarcity, adipocycte LPL expression is reduced, while expression in muscle cells is increase which is related to the need to supply fatty acids to muscle for oxidative metabolism (127).

Substituting dietary carbohydrates for fat affects the metabolism of all the lipoprotein fractions, especially for VLDL-TAG and apoB metabolism because of carbohydrate-induced hypertriglyceridemia, but this required excess dietary energy intakes (128-129). Observations on the effects of a high-carbohydrate diet (as compared with a higher-fat diet) on LDL apoB metabolism are conflicting and likely depend on total energy intake (130).

Various animal models have been employed to access the role of diet on lipoprotein metabolism and concentration. A big problem in interpreting these studies is that animal

species can vary greatly in their distribution of plasma cholesterol among lipoproteins that may not be comparable to men and women (131, 13). A recent review on the latest updates on mechanism by which fatty acids modulate plasma lipids has been published (132).

CYCLIC AMP AND LIPOLYSIS

Cyclic AMP System

The cyclic AMP system plays an important role in the regulation of lipolysis in fat cells. The receptor-controlled incremental production of intracellular cAMP promotes activation of cAMP-dependent protein kinase A (PKA) which phosphorylates a serine residue on hormone sensitive lipase (HSL) and promotes its activation and translocation towards the lipid droplet (37, 133). HSL catalyzes the rate-limiting step in TAG breakdown or lipolysis in adipose tissues (134). Insulin, functionally an antilipolytic hormone, causes dephosphorylation of HSL which results in its deactivation. The final breakdown of the monoacylglycerols that appear after the activation of HSL involves a monoacylglycerol lipase that is not directly under hormonal control (135). Adenylyl cyclase which catalyzes the formation of cAMP, is the key enzyme for activating the lipolytic cascade. The adenylyl cyclase system is composed of three major classes of membrane proteins; i.e., receptors (beta adrenergic receptors), coupling proteins (heterotrimeric G proteins) and effector units of the cyclase enzyme (136). Most of the physiological regulators of adenylyl cyclase interact with membrane-bound stimulatory or inhibitory receptors. These ligands through the receptor modulate the activity of effector units of adenylyl cyclase through signal transducing proteins; i.e. the guanine nucleotide-sensitive coupling proteins, (G-proteins) that bind and hydrolyze guanosine

triphosphate (GTP) (137). Several forms of G-proteins exit in fat cell membranes and are referred to as Gsά,β,γ or Giά,β,γ (17). Gs (stimulatory G protein), one form of G proteins, activates adenylyl cyclase when coupled with various beta-adrenoceptors (138). The membrane complex consisting of the adrenergic receptor and G proteins belong to a G protein, seven transmembrane protein domain superfamily referred to as G protein coupled receptors (GPCR) (139).

In addition to HSL, the best-identified substrates for PKA in fat cells are cGMP-inhibited, low Km cAMP-phosphodiesterase, glucose transporter, phosphorylase kinase, glycogen synthase, acyl-CoA carboxylase, and the β1 and β 2-adrenoceptors (140). These enzymes are controlled by allosteric and covalent regulation. The variety of potential phosphorylation sites in these enzyme proteins may actually control the sequential phosphorylation of sensitive sites in an order that depends on the intensity of the stimulatory signal that initiates from cAMP increments (141). Further research is needed to better understand how putative physiological substrates or ligands modulate/determine priority of PKA sensitive sites in some sort of hierarchical fashion to regulate lipid metabolism enzymes in the animal.

Lipid metabolism in adipose tissues is regulated by catecholamines that bind to membrane GPCR (β-adrenergic receptors) to activate through the cAMP –PKA cascade, adipose HSL (covalent modification; lipolytic response) and other genes by transcriptional regulation (32). Agents that enhance cAMP content (cAMP elevating agents) generally induce lipolysis in fat cells but cAMP-elevating agents may also decrease expression of lipogenic enzymes during differentiation of adipocytes (142). Cyclic AMP regulates the transcription of its target genes through cAMP response

elements (CRE) that are distinct DNA sequences present in the promoter regions of target genes. These elements are recognized by the cAMP response element binding protein, a transcription factor that is able to activate target gene transcription when it is phosphorylated by PKA (143). The complexity of cAMP-dependent regulation of gene expression was extended by the discovery of a family of CREB proteins and of a cAMP-responsive element modulator (CREM) which affects CREs in a negative fashion (144). CREB is a substrate for PKA, and it is the only transcription factor known that may bind cAMP response elements in the promoter region of various lipogenic and lipid oxidative genes (145). CREB may play an important role in the control of expression of fat cell-specific genes containing CREs (146).

B-Adrenergic Receptors (β-AR)

Beta adrenergic agonists /catecholamines (β-AA) stimulate porcine adipose lipolysis and attenuate fatty acid synthesis and activity of lipogenic enzymes (13). This is accomplished via binding of β-AA on transmembrane beta receptors (GPCR) present in membranes of porcine adipose tissues. By strategic use of beta adrenergic antagonists, it was confirmed in numerous studies that in pigs, β-AA act specifically by binding to porcine adipose GPCR or β-AR (13). The β-AR is cell surface receptors that belong to the large superfamily of 7-transmembrane domain proteins. A subset of these proteins is a large family of G-protein coupled receptors (GPCR) to which the β-AR belong (147).

Three subtypes of β-adrenergic receptors (β1 AR, β2 AR and β3 AR) have been identified in adipose tissue and other mammalian tissues. All three β-AR subtypes have been cloned in several species including swine (148-150). The β-AR subtypes share approximately 50% sequence homology with the highest homology in the trans

membrane domains associated with ligand binding pockets. The subtype distribution, however, in adipose and other tissues is species specific. In rodent adipose, the predominant subtype is β3-AR, but this subtype is basically absent in almost all other species (13). The distribution of β AR subtypes in pigs has been quantified by mRNA abundance determinations (151) and receptor binding studies (152). In pigs, while β3AR mRNA is detectable in several tissues including skeletal muscle, heart and adipose tissue, it represents a small number of all subtypes present in these major tissues. The β1AR subtype is the predominant subtype in most tissues, comprising nearly 80% in adipose, 72% in heart, 65% in lung, 60% in skeletal muscle, and 50% in liver (153). In rodents, β-AR subtypes exhibit ligand selectivity such that the rank order of affinity for norepinephrine is β1-AR> β2-AR> β3-AR. Subtypes β1-AR and β2-AR are co-expressed in most tissues of the body, but the ratio of each can vary. For example, the major isoform of the β-AR in the rat heart is β1AR, while in guinea pig lung it is β2AR. In contrast, β3AR is found mainly in rat adipose tissue as noted above. There are species variations in tissue subtype distributions (e.g., human heart has 65% β1-AR and porcine adipocytes have less than 10% β3-AR) (154). In addition, the amino acid sequence of all β-AR subtypes varied among species, Hence, it may be expected that some βAR agonists would have divergent effects in the same tissue among species because of different βAR subtype distributions and (or) amino acid sequences and consequently ligand binding affinity. Subtypes also differ in G-protein selectivity, and regulation by gene expression and phosphorylation (147).

Ractopamine

The chemical structure of ractopamine is similar to the natural catecholamines epinephrine and norepinephrine, and it binds to β AR in pig adipose and muscle tissue with high affinity. In cultured fat cells, ractopamine suppressed via a beta receptor/GPCR-cAMP-protein kinase A-dependent mechanism, fat accumulation and expression of lipogenic genes (2,154). Ractopamine contains two chiral centers and a possible four sterioisomers, RR, RS, SR, and SS (155). The RR isomer is the most lipolytic and accounts for enhanced growth in rats (154). Pig β AR selectivity for ractopamine stereoisomers has been studied using cloned β1AR and β2AR expressed in Chinese hamster ovary cells (157). The RR isomer has the highest affinity for each subtype. Experimental receptor activation and adenylate cyclase stimulation indicated that the β2AR was a more functional target than the β1AR (158).

Effect of Ractopamine on the Lipid Metabolism in the Pig

In the development of ractopamine, a family of phenethanolamine/ catecholamine ligands for βAR was first screened for their anti-obesity properties. Therefore, it was expected that administration of these types of pharmacological agents to pigs would result in lowered adipose tissue accretion. Direct ligand activation of βAR in adipose tissue enhanced PKA and causes activation and translocation of hormone-sensitive lipase and TAG hydrolysis (151) Activation of PKA is anti-lipogenic due to phosphorylation and inactivation of GLUT4 and acetyl-CoA carboxylase, and reduced expression of other lipogenic genes (2, 145, 151). Pigs fed ractopamine in the 1980s had a lower carcass fat than control pigs (159); however, a lowered rate of fat accretion has not been consistently observed in all animal trials by other workers using more contemporary, leaner pigs

(160). In addition, Purdue workers reported that expression and activity attenuation of lipogenic genes may only be present for up to a week (161), while Merkel et al. (9) showed that adipose fatty acid synthesis and lipogenic enzyme activities were attenuated up to 42 days by ractopamine in finishing pigs. In addition, Halsey (162) and Reiter (163) found that mRNA abundance of FAS was significantly lowered in pigs fed ractopamine for 42 to 54 days. Other results indicated that administration of ractopamine to pigs resulted in an acute (short time spike), but not chronic, increase in plasma non-esterified fatty acids *in vivo* (164). Such results have cast doubt on any long term effect of ractopamine on lipolysis and lipogenesis in finishing pigs. The response to ractopamine may be short-lived because adipose membrane βAR is desensitized by nearly 50% within the first 7 days of administration (165).

Ractopamine, however, consistently increased muscle protein accretion in pigs. Utilizing *in vivo* protein synthesis procedures with radiolabeled amino acids, Bergen et al. (166) reported that fractional protein synthesis rate in skeletal muscle of ractopamine fed pigs was significantly elevated after 14 and 28 days over controls. Others have reported that protein accretion responses were maximal within the first week and declined toward zero over 4 to 6 weeks (25). Clearly, there are divergent views from different laboratories on the long-term effectiveness of ractopamine to enhance lean deposition and lower fat accretion. Based on recent translational studies, the manufacturer of commercial ractopamine recommends a treatment period of up to 28 days to optimize effects both on lean and fat deposition (167). The mechanism whereby ractopamine isomers specifically down-regulating porcine βAR has not been delineated; however, there is consensus in the literature (160-161) that classic receptor down-regulation as described in rodents may

limit the effectiveness of ractopamine because of variable results in effects on fat deposition. Implementing feeding strategies to circumvent down-regulation of the receptors may enhance the ability of ractopamine to reduce fat accretion more consistently (168).

In this dissertation, the cAMP-elevating agent/ catecholamine Paylean™ (commercial name for ractopamine) was used to explore its effects on transcription of lipid metabolism genes in porcine adipose tissue. Paylean™ is the product of Elanco Animal Health, a division of Eli Lilly and Company, and was approved for finishing swine by the Food and Drug Administration (FDA) in 1999. The active ingredient in Paylean ^{TM}, ractopamine hydrochloride, is a member of beta-adrenergic agonist family. The commercial product contains four ractopamine stereoisomers.

APPLICATION OF MICROARRAY TECHNOLOGY IN PIG GENOME RESEARCH

Gene Expression Analysis

The ultimate goal of genomics is to understand how DNA encodes life; more specifically, to characterize the genetic programs which the genome employs to manifest a multitude of different cell functions and physiological characteristics (169). Genomic DNA becomes biologically/functionally "active" when transcribed into RNA, particularly mRNA. The collection of mRNA transcripts that are expressed or transcribed from genomic DNA, also named "transcriptome", is a major determinant of the cellular function and phenotype (169). The process of transcription affects the subsequent process of protein synthesis, thus alteration of gene expression reflects phenotypic differences and cellular responses to environmental stimuli (17).

The transcriptome is highly dynamic and changes rapidly and dramatically in response to exogenous and endogenous stimuli ranging, for example, from types of nutrients consumed to endocrine secretions (170). To understand gene function, knowing when, where and to what extent a gene is expressed is essential to understand the activity and biological roles of its encoded protein. Furthermore, changes in the multi-gene expression patterns can provide clues about regulatory mechanisms and broader cellular functions and biochemical pathways (171).

It is well known that cells respond with altered gene expression to the change of environments and that nutrition can influence the proliferation and differentiation of cells (172). Diet is possibly the most important environmental factor that organisms encounter that has a long-lasting effect on the genome. The relationship between specific nutrients or diet composition and gene expression could help to identify effects of nutrients or dietary ingredients components at the molecular level.

Genomes can respond in a rapid and specific manner by selectively increasing or decreasing the expression of specific genes, and these responses can be utilized to investigate the molecular events by which the genomes perceive nutritional signals and mobilize the organism to respond (173). Dietary nutrients can affect gene expression at the molecular level through the interactions with receptors, metabolic pathways and signals (174).

Microarray Technology

Microarrays are a technology for simultaneously measuring the number of copies of many distinct DNA or RNA fragments in a complex mixture. Microarrays work by exploiting the ability of complementary DNA strands to selectively bind (hybridize) to

each other, even in the presence of a large background of non-complementary competing fragments. Microarrays primarily use short oligonucleotides (15-25nt), longer oligonucleotides (50-120nt) or PCR-amplified cDNAs (100-3,000 base pairs) as array elements (175) but such short oligos are not sufficiently discriminatory in binding complementary target gene fragments with high fidelity. Oligonucleotides (40-80 bases in length) may be treated as "short cDNAs" and there is much less chance of spurious cross-hybridization with unrelated sequences compared with short oligonucleotides (176).

In microarrays, typically specific target (single strand) cDNA fragments or oligonucleotides are deposited on a surface in a way that keeps distinct fragments spatially separated, and a labeled (fluorescent or radioactive) probe mixture of (single strand) fragments is applied and allowed to hybridize to the target strands. The amount of each distinct probe fragment is measured by detection of the signals from the probe labels bound at each target site on the surface. This accomplishes a large number of measurements in a small area, so that a single hybridization reaction can provide simultaneous quantity measurements for tens of thousands of target DNA fragments.

The simplest realization of this technology is the spotted cDNA or oligonucleotides microarray, combined with two-color fluorescent detection, and this is the approach used in this study. With the progress of oligonucleotide synthesis methodology, synthesized oligos are now used much more frequently than cDNA fragments in microarray platform design and construction. The oligonucleotides (typically 70 mer) can be printed onto the same slides as cDNAs, with the same printing device, the hybridization and washing conditions are similar, and no new analytical programs for expression analysis is required

(177). In this approach, distinct long oligonucleotide (70 mer) fragments are printed as an array of distinct spots on a suitably treated glass microscope slide. The oligomers are spotted with a mechanical robotic system. Two distinct probe DNA (or RNA) mixtures - the control and the experimental sample - are given fluorescent red and green labels and are combined in solution and applied to the array. After hybridization, slides are scanned to generate fluorescent images from the two channels as depicted in Fig 2 (178). The fluorescent intensities of red and green detected from each spot reflect the relative numbers of red and green labeled fragments conjugated at the spot, and hence the relative numbers of fragments in the control and experimental samples.

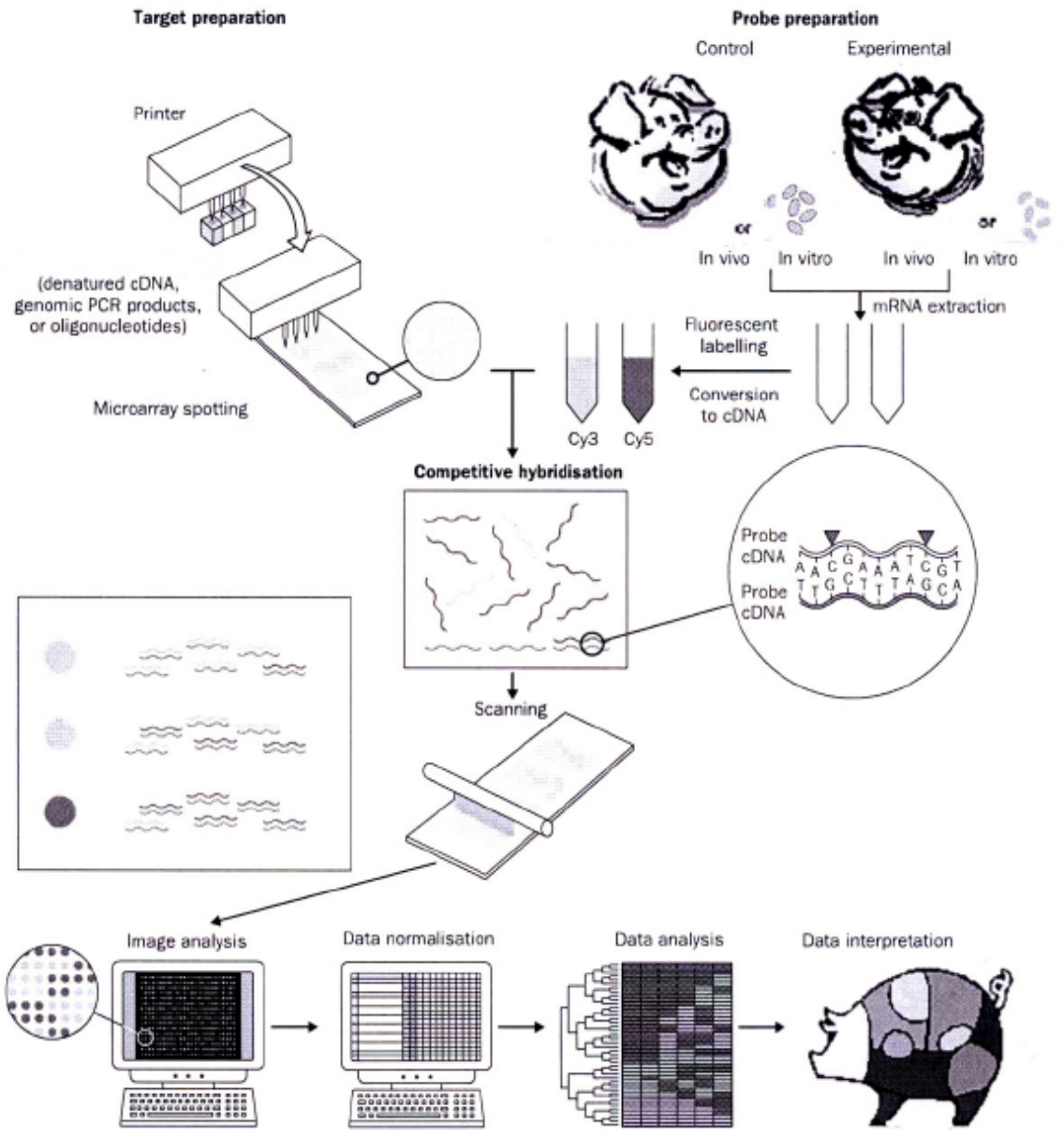

Fig 2. Overview of the steps involved in oligonucleotide microarray experiments (178)

The design of the oligonucleotides to be spotted on the microarray slides is the most important for success in utilizing this functional genomics technology. Basically, the oligonucleotides should have very similar melting temperature or G-C content, have very little homology with other oligonucleotides, be entirely contained within an exon, and have no repetitive- or hairpin sequences (179). When every oligo in a spotted microarray is of the same length and has almost the same melting temperature and G-C content, hybridization conditions are consistent for every gene on the array (180). Since 70 mer oligos are single stranded, they do not require a denaturation step as with the cDNA format during the procedure; this also eliminates the problem of renaturation, which can decrease hybridization efficiency (181).

A highly useful application of microarray technology is to assess global gene expression (mRNA abundance). Microarray technology enables large numbers of genes to be screened simultaneously, giving a comprehensive, detailed picture of changes in gene expression, thereby shedding light on complex regulatory interactions (182). The integration of microarray analysis into basic and applied nutrition research may provide new insights into the effects of nutrition and food ingredients like fats, carbohydrates, proteins, vitamins, minerals at the molecular level (183).

Because only a small portion of genes in the porcine genome have been cloned, cDNA probes for standard mRNA abundance studies with Northern blotting for many genes are not available in the pig. Furthermore, there is limiting coding fragment sequence data in the porcine genome to design primers and develop a qRT-PCR approach on a gene-by-gene basis to exploit differential gene expression to diet or pharmacological agents in pigs. Thus, development of the 70mer oligonucleotide spotted slide platform

designed by the Iowa State Porcine Genomics Center provides researchers interested in pigs a front-end analytical resource for across-tissues-integrated gene expression analysis for various physiological and nutritional states. The Iowa State porcine oligonucleotide array was used in this research to establish gene expression patterns in porcine lipid metabolisms experimental models (such as feeding catecholamines and high-fat diets) in a much more favorable time frame and comprehensiveness than a long tedious gene by gene approach. Not only will we be able to determine expression patterns of known genes involved in lipid metabolism in liver, adipose tissue and skeletal muscle, we will also likely encounter expression responses to our experimental porcine models for genes hitherto not recognized as participants in lipid metabolism. Once global expression patterns have been established, more specific analytical platforms and confirmatory procedures can be developed or applied with a clearer focus of what genes to study in order to better understand whole-animal lipid metabolism in pigs. This knowledge is critical if we want to minimize fat accumulation in pigs during production (fattening, per se, is inefficient use of feed and other economic resources) while enhancing intramuscular fat deposition to provide tasty and juicy porcine muscle foods.

III. EFFECTS OF DIETARY RACTOPAMINE (PAYLEAN^{TM}) ON PORCINE ADIPOSE GENE EXPRESSION

INTRODUCTION

The long-term goal of pork industry is to maximize the production efficiency and minimize the pollution to surrounding environment, to ensure that pig production is sustainable. Genetics, nutrition and facility management strategies have been implemented to increase pork quality and decrease the effects of animal production on the environment.

In food animals, BAA depresses fat deposition by increasing lipolysis and depressing lipogenesis and triacylglycerol synthesis. Increased lipolysis is dependent on increased activity of triacylglycerol lipase (9, 191). Decreased lipogenesis in adipose tissue is due to lowered activity of lipogenic enzymes, partly attributable to allosteric regulation through phosphorylation by cAMP-dependent kinase (191). In rat liver, cAMP also directly lowers expression of fatty acid synthase (37). In addition, BAA diverts dietary energy from fat deposition toward enhancement of muscle fiber hypertrophy characterized by increased deposition of skeletal muscle protein in the ham, belly, and shoulder in meat animals (184).

Duration of BAA treatment also affects the magnitude of growth response because of the putative down regulation phenomenon of GPCR, particularly in pig adipose tissues (192-193). Dunshea et al (24) found that strongest response to RAC occurred during the

first week of treatment and then declined. Others investigated the temporal response to RAC over a seven-week period and found that the greatest growth response to RAC occurred from day 6 to 22, after which time there was a linear decline in the magnitude of the response (194).

Ractopamine (RAC), a beta-adrenergic agonist (BAA), marketed as Paylean^{TM}, is an epinephrine analogue that binds to beta adrenergic receptors in the meat animals. Researches demonstrated that RAC improves average daily gain, stimulates muscle growth, decreases fat content in pigs and several other species (185-187), and reduces days to market. (184). Merkel et al (188) found that RAC lowered subcutaneous adipose depot size in finishing pigs nearly 20% and lowered carcass total fat percentage by 20 to 24%. Besides modifying carcass of meat animals, the use of RAC in animal production can potentially reduce the environment pollution caused by excretion. In a study by Sutton et al (189), barrows were used to determine effects of RAC and crude protein (CP) level on nitrogen (N) and phosphorus (P) retention, and excretion in urine and feces of finishing pigs. Average excreta output was reduced by 3.9% in pigs fed RAC, and N excretion was reduced by 10.7 to 34.2%. During anaerobic storage of manure arising from RAC-fed pigs, reduced levels of N, NH_3 emissions, and volatile fatty acids were observed (190).

There is still incomplete understanding of putative molecular mechanisms whereby RAC or other BAA affect fat deposition and muscle growth in pigs. The Bergen laboratory has shown that RAC lowered mRNA-abundance of lipogenic genes in the adipogenic cell line TA1 (2). Furthermore, results indicate that cAMP is directly involved because exogenously administrated, non-metabolizable cAMP analogs attenuated

lipogenic gene expression in cultured TA1 cells (2). Several studies (162-163) by the Bergen lab observed lower mRNA abundance of FAS, SREBP-1 and GLUT4 in adipose tissue when pigs were fed a 60-ppm RAC-supplemented diet for 28 days (162-163). In addition Thacker (Reiter) (163) found that RAC attenuated adipose SCD expression in RAC fed pigs, while in a separate study RAC increased expression of lipoprotein lipase (LPL) in porcine muscle (195).

While only limited studies on the effect of RAC on regulation of lipogenesis have been conducted, the role of BAA in adipose lipolysis has been more clearly delineated. Bergen and Merkel (9) proposed that BAA modulates lipid metabolism via the beta receptor-G protein-coupled adenylyl cyclase-PKA cascade in porcine adipose tissues. BAAs stimulate cAMP production and induce protein kinase A (PKA) activity, which stimulates hormone-sensitive triacylglycerol lipase in adipose tissue and subsequent mobilization of storage triacylglycerol. As noted previously, limited work with cultured fat cells have shown that BAA also inhibits lipogenesis (2). Thus, combining anti-lipogenic and pro-lipolytic effects of BAA, the overall net effect of BAA feeding is a depression of fat accretion, increase in lipolysis and possibly increased fatty acid oxidation. This effect would redirect energy from fat deposits toward tissue (skeletal muscle) to promote increased protein deposition.

Based on these previous findings and interpretations about the effect of RAC on the expression of a few key genes in the fatty acid metabolism, I proposed that RAC modulates fat deposition in pigs at the transcription level through regulating expression of genes in the lipid metabolism and regulation pathways. The work in this study thus emphasized the expression of genes associated with lipid metabolism in adipose tissue

and was designed to explore the global mRNA esponse to ractopamine treatment in porcine adipose tissue. We utilized an oligonucleotide microarry analysis platform to quantify the expression of 13,297 porcine transcripts simultaneously. this study was designed to explore the effect of RAC over a 28-day period on the relative abundance of mRNA of 13,297 transcripts in the middle layer of subcutaneous adipose tissue of pigs.

MATERIALS AND METHODS

In the area of global gene expression analysis, certain guidelines have been established for conducting and reporting such extensive data sets. In this study, *Minimum information about a microarray experiment* (MIAME), was used to guide the development of describing the experimental methods and the analysis and subsequent reporting of data sets. MIAME is a standard designed to contain the minimum information required to ensure that microarray data can be interpreted and that the resulting derived data can be independently ratified (196). MIAME can be broken down into four different areas: experimental design, sample description, software and techniques for the analysis and interpretation of data, and the array design (197). Table 1 shows an example of the information recorded for MIAMI compliance (198).The microarray data in this study will be deposited at the NCBI Gene Expression Omnibus (GEO) that is data repository of high-throughput gene expressions and hybridization arrays. In this study, the pig array was obtained through U.S. Pig Genome Coordination Program (http://www.animalgenome.org/ pigs/resources/ array_request.html). Information about oligo probe design, location of each spot in the array and gene information of each spot are described below.

Table 1. An example of needed information to be recorded for MIAME compliance (198)

Title and type of experiment	**Time course, control vs treatment, mutant vs wildtype?**
Authors	Names and addresses of researchers
Background	Important publications justifying the experimental use of arrays
Experimental design	
Species used	Worm, fly, plant, animal?
Strain/genotype of species	What, if any genetic manipulations have the species being used undergone?
Tissue/sample type	Whole organism or specific tissue type? muscle, nervous tissue?
Sex of species used	Male, female or hermaphrodite?
Maintenance of organism	Conditions on which that organism is routinely maintained
Method of sample collection	Dissection method used
Dates of collection	References to lab book
Sample storage	Temperature (−80°C), location
Sample manipulations	
RNA extraction method	How was the RNA extracted, what chemicals/kits were used?
RNA storage	Temperature (−80°C), location?
Gel/bioanalyser	Gel images or Agilent bioanalyser output demonstrating quality of RNA
Amplification protocol	Was an amplification step required?
Labeling protocol	How was the RNA labeled?
Hybridization protocol	How was the hybridization performed?
Chip identification number	Has the ID of the array used been included?
Data analysis	
Raw data	Are the raw data readings included and how were they produced?
Normalized data	Is the normalized data included and how were they produced?
Analysis methods	What analysis methods or programs were used?
Results	Final list of genes with changed expression values

Animal Feeding Trial in Eli Lilly & Co (Greenfield, IN)

This study used porcine adipose tissues collected from an animal feeding trial in Eli Lilly & Co conducted in 1996. The feeding trial was originally designed to study the effect of ractopamine on gene expression with gene-by-gene methods such as Northern blots. Previous graduate students in our lab conducted Northern blot analyses on the same tissue samples. Microarray analysis was applied in this study to the same samples.

Six finishing pigs (white large composite castrated males) were provided *ad libitum* access to a 16% crude protein corn-soybean meal diet, supplemented with 0 or 60 ppm Paylean™ for 28 days. The diet met all nutrient requirements for finishing pigs (199). Pigs did not fast prior to slaughter and were slaughtered at 28 days of the trial. The middle layer subcutaneous adipose tissue was collected. The pig feeding, slaughter, and sampling protocols were approved by the Lilly Research Laboratory Institutional Animal Care and Use Committee. Tissue samples from 0 and 60 ppm Paylean™ treated pigs for 28 days were used in the following oligonucleotide microarray analysis. Pig identification number, length of treatment, amount of Paylean™ treatment, and the date of sample collection are presented in Table 2.

Table 2. Pig identification number, length of treatment, amount of treatment, and the date of sample collection for the pigs in the Eli Lilly feeding trial. Finishing diets were supplemented with 0 or 60 ppm Paylean™ for 28 days.

Pig ID#	Length of Treatment (days)	Amount of Paylean™ (ppm)	Date of Samples Collection
787	28	0	9/24/1996
807	28	0	9/24/1996
826	28	0	9/24/1996
779	28	60	9/24/1996
784	28	60	9/24/1996
796	28	60	9/24/1996

Animal Slaughter and Tissue Collection

Pigs were slaughtered by electrical stunning followed by exsanguination. Middle-layer subcutaneous adipose tissues were removed immediately, snap-frozen in liquid nitrogen, and stored at minus 80ºC after samples were collected.

Experimental Design of Oligomer Microarray Analysis of Gene Expression

In this experiment, microarray analyses were performed with a pool of control RNA isolated from the adipose tissues of three pigs fed 0 ppm Paylean™ (control) and individual adipose RNA preparations from each pig fed 60 ppm Paylean™ diet (n=3; experimental). The labeling dyes Cyanine 3 (Cy3) and Cyanine 5 (Cy5) were randomly assigned between pooled control RNA and experimental RNA from each 60 ppm Paylean™ treated pig (200).

RNA isolation

Total RNA was isolated by using the one-step guanidinium-phenol-chloroform extraction method (201). One-half gram of frozen adipose tissue from each pig was

powdered using a hammer-driven, stainless steel mortar and pestle that was constantly cooled with liquid nitrogen. The tissue was then placed in a 50 ml conical tube containing 10 ml of TriZol reagent (Invitrogen Corp, Carlsbad, CA), and RNA was isolated according to the instructions provided. The RNA concentration was determined using an Ultrospec 3000 UV/ visible spectrophotometer (Amersham Pharmacia Biotech; Piscataway, NJ) by reading optical density (OD) at 260 nm (by using an OD_{260} unit equivalent to 40 µg/ml). Quality of the RNA was evaluated by gel electrophoresis of ~1 µg RNA on an 1% agarose 0.5X tris(hydroxymethyl)aminomethane (Tris)-borate-EDTA buffer (TBE) gel containing ethidium bromide at 120V for 30 minutes using 0.5X TBE as the running buffer. Images of the gels were taken under ultraviolet (UV) light using Polaroid instant film number 55 (Polaroid Corporation, Waltham, MA) to generate printed image of the gel. The RNA quality was evaluated by observing smearing at 18s and 28s bands, band intensity of 18s and 28s, and DNA contamination. No analysis was performed on any sample with degraded RNA appearance. RNA samples were stored at −80°C in 1µl of RNA Secure/ µg of RNA (Ambion; Austin, TX) until subsequent analyses. Gel images of RNA used in the microarray analysis were present in Appendix A.

RNA purification

DNA contamination can seriously affect the validity of reverse transcription (RT) reaction. To remove genomic DNA in the RNA sample, RNA samples were purified using DNA-free™ kit (Ambion, Austin, TX) according to the manufacturer's protocol. 0.1 volume 10X DNase I buffer and 1µl rDNase I (2U/ µl) were added to each RNA sample followed by the addition of RNase free water to bring the total volume to 50 µl.

The solution was mixed and incubated at 37^{o}C for 20-30 min. After incubation, 5 µl DNase inactivation reagent was added and incubated at room temperature for 2 min. Then, the resultant solutions were centrifuged at 10,000 x g for 1.5 min in a 16M Microcentrifuge (Labnet International Inc, Edison, NJ), and the RNA was transferred to a new tube.

The purified RNA was analyzed by measuring UV absorption at 260nm and 280nm. To assess the RNA quality, 1 µg purified RNA sample was processed, stained with ethidium bromide and resolved on a 1.0% agarose gel. After DNaseI treatment, control RNA samples from three pigs were pooled, and another UV absorbance reading was taken at 260nm and 280 nm to determine the pooled RNA concentration and assess the pooled RNA quality.

Besides checking RNA quality by agarose gel electrophoresis, DNA contamination was also assessed by attempting PCR amplification of the RNA with primers targeting at a fragment of intron of stearoyl CoA desaturase (SCD) using a PTC100 programmable thermal controller (MJ Research, Waltham, MA). The primer was designed based on pig SCD complete mRNA sequence (GenBank accession number: AY487830) using on-line software Primer3 (http://frodo.wi.mit.edu/cgi-bin/primer3/primer3_www.cgi). The sense primer sequence was: CAGCCACCTTTTTCGAGTTGT, and the antisense primer sequence was: AAATTGGGGAGGAGGGTGAAA .The expected PCR amplicon is 219 basepair (bp). 20 µl of resulting PCR amplicon was loaded on a 1.0% agarose gel to check if there was amplified molecule from DNA. Since the SCD primers targeted at a fragment of intron sequences, the primers could not anneal on the RNA and no amplicon

was produced by PCR. Therefore, the PCR amplicon was observed only when RNA was contaminated by genomic DNA.

Synthesis of Experimental Probes for Porcine Purified RNA Using Reverse Transcription

First strand cDNA synthesis with aminoallyl dNTP

The first strand of cDNA for each sample was synthesized using the Superscript II cDNA synthesis kit (Invitrogen Corp., Carlsbad, CA) according to the manufacturer's protocol. 18 μg of total RNA which had been purified with DNase I treatment was mixed with 2 μl oligo dT18-20 primer (0.5 μg/μl) (Invitrogen Corp., Carlsbad, CA) and the final volume was brought up to 18.5 μl with RNase-free water. Then the solution was incubated at 70^{o}C in a dry bath incubator (Fisher Scientific, Pittsburgh, PA) for 10 min. After this incubation, this solution was mixed with 6 μl 5X first strand buffer, 3 μl 0.1M DTT, 0.6 μl 50X aminoallyl-dNTP mix (Appendix B), 2 μl SuperScript IIRT, and 0.5 μl RNAse inhibitor (Ambion Incorporation; Austin, TX). The final reaction cocktail was gently mixed and incubated overnight at 42^{o}C in a micro-hybridization incubator (Robbins Scientific, Sunnyvale, CA).

RNA hydrolysis and neutralization after reverse transcription

After incubation overnight at 42^{o}C, 10 μl NaOH (1M) and 10 μl EDTA (0.5 M) were added to the RT reaction tubes (cDNA solution) and incubated at 65^{o}C for 15 minutes. After incubation, 10μl HCl (1 M) was added to neutralize the solution. This is an important step since DNA binds to Qiagen column at pH below 7.5 in the next purification step. Immediately after neutralization, the cDNA mixture was purified by the steps described below.

Purification of aminoallyl labeled cDNA

The purification protocol was modified from the Qiagen QIAquick PCR purification kit (Qiagen Inc, Valenica, CA) protocol. The phosphate wash and phosphate elution buffers (Appendix A) were substituted for the Qiagen-supplied buffers because the Qiagen buffers contain free amines that compete with the Cyanine (Cy) dye coupling reaction in the down stream steps. First, 300 µl (5X reaction volume) buffer PB was added to the cDNA and transferred to a QIA-quick column. Then the column was placed in a 2-ml collection tube and centrifuged at 10,000g for 1 min. The collection tube was emptied after centrifugation. Continuing the process, 750 µl phosphate wash buffer was then added to the column, and the column was centrifuged at 10,000g for 1 minute. After emptying the collection tube, the wash and centrifugation steps were repeated once. Then the flow-through in the collection tube was discarded and the column was centrifuged at 10,000g for another 1 min at maximum speed. Thereafter, the column was transferred to a new 1.5-ml microfuge tube, and 30 µl phosphate elution buffers were carefully added to the center of the column membrane. Then the collection tube was incubated for 1 minute at room temperature, and the cDNA was eluted by centrifugation at 10,000g for 1 min. The elution step was repeated in the same tube with another 30ul phosphate elution buffer. Finally the eluted cDNA sample was dried to completion about 45 min in a Savant SC100 Speed Vac concentrator (Savant, San Joes, CA).

Coupling aminoallyl-cDNA to Cyanine (Cy) dye ester

The coupling procedure was conducted under light-safe conditions. The completely dried aminoallyl-labled cDNA was resuspended in 4.5 µl 0.1M sodium carbonate buffer (Na_2CO_3). Then 4.5 µl of the appropriate Cy dye (Amersham Pharmacia Biotech,

Piscataway, NJ) was added to each tube and mixed. To prevent photobleaching of the Cy dyes, all reaction tubes were wrapped in foil and kept away from light. After dye addition, the reaction mixture was incubated for 1 hr at room temperature. Thereafter, the reaction mixture was purified in the following steps to remove uncoupled Cy-dye.

Purification of Cy-dye coupled cDNA

The purification steps were performed under light-safe conditions. The Qiagen QIAquick PCR purification kit was used. First, 35 µl 3M sodium acetate was added to the Cy-dye coupled cDNA solution. Then, 250 µl buffer PB (DNA binding buffer, supplied by Qiagen) was added and the mixture was applied to a QIA quick spin column that was placed in a 2 ml collection tube. The column then was centrifuged at 10,000g for 1 min, and the flow-through was discarded. Then, 0.75 mL buffer PE (washing buffer, supplied by Qiagen) was added to the column and centrifuged at 10,000g for 1 minute. After discarding the flow-through, the column was centrifuged for an additional 1 minute at maximum speed. Then, the column was placed in a clean 1.5-mL microfuge tube and 40 µL Buffer EB (elution buffer,supplied by Qiagen) was carefully added to the center of the column membrane. After incubation for 1 min at room temperature, the column was centrifuged at 10,000g for 1 min. The elution step was repeated another time in the same tube. The final elution volume should be around 80ul. Then, the tube was wrapped with aluminum foil, and the Cy dye-coupled cDNA containing solution from porcine adipose RNA was analyzed employing the following steps.

Analysis of labeling reaction

This step was conducted in the dark. An Ultraspec 300 UV/Visible spectrophotomer and a 50µl Beckman quartz MicroCuvette (Beckman Coulter Inc, Fullerton,CA) was used

to analyze the entire undiluted Cy-dye coupled cDNA solution. The cuvette was washed with MilliQ water and blow dried with a compressed air duster. For each sample the absorbance at 260 nm and either 550 nm for Cy3 or 650 nm for Cy5 were measured for each sample. Finally, the dye-coupled cDNA solution was pipetted back into the original sample tube.

To determine concentration and purity of dye labeled aminoallyl-cDNA, the following formulas were used to calculate total picomoles of cDNA synthesized as described by Hedge et al. (202).

$$\text{pmol nucleotides} = \frac{[OD_{260} * \text{volume } (\mu L) * 37 \text{ ng}/\mu L * 1000 \text{ pg/ng}]}{324.5 \text{ pg/pmol}}$$

$$= OD_{260} * \text{volume } (\mu L) * 114.02$$

1 OD_{260} = 37 ng/μL for cDNA; 324.5 pg/pmol is the average molecular weight of dNTP

For each sample the total picomoles of dye incorporated (Cy3 or Cy5 as appropriate) and the nucleotides/dye ratio were calculated using formula (195):

$$\text{pmol Cy3} = OD_{550} * \text{volume } (\mu L) / 0.15$$

$$\text{pmol Cy5} = OD_{650} * \text{volume } (\mu L) / 0.25$$

$$\text{nucleotides/dye ratio} = \text{pmol cDNA/pmol Cy dye}$$

For the formula, 0.15and 0.25 are correction factors for Cy3 and Cy5 respectively, which are corrected by extinction factors of Cy3 ($\varepsilon = 150000\ M^{-1}cm^{-1}$) and Cy5 (ε = 250000 M-1cm-1) molecules (202).

Fragmentation of Cy-labeled cDNA will cause low hybridization of cDNA with the oligo probes on the array. It is important to check the quality of Cy-labeled cDNA at this step. Cy5-labeled cDNA 2 μg was resolved by electrophoresis on 2% agarose gel at

130V for 45 minutes in the dark. Then the gel was wrapped with aluminum foil and imaged on Typhoon 9410 (Amersham Pharmacia Biotech, Piscataway, NJ) at photomutiplier tube (PMT) 600 using emission filter for Cy5 (excitation at 633nm). An example of Cy5-labeled cDNA is presented in Fig 1. Gel images of Cy5-labeled cDNA used in each slide bybridization are presented in Appendix C.

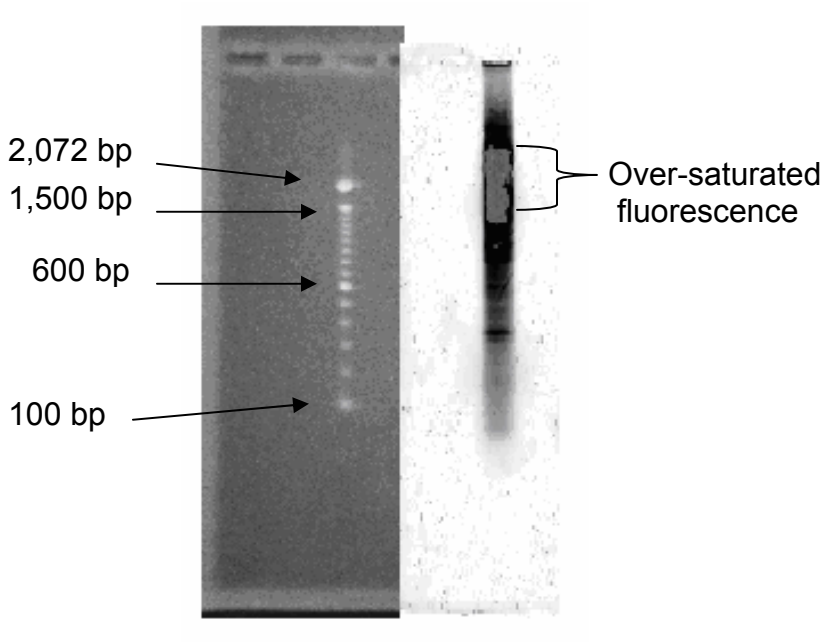

Fig 1. Cy5-labeled cDNA on a 2% agarose gel (right) at 130V for 45 minutes, the gel was imaged on Typhoon 9410 (Amersham Pharmacia Biotech, Piscataway, NJ) at PMT 600 using emission filter for Cy5 (laser 633nm). DNA ladder was resolved on another 2% agarose gel (left) under identical electrophoresis condition to identify the size of the Cy5-labeled cDNA. The fluorescently labeled cDNA population was mainly distributed from 600 bp to 2,000 bp with weak distribution in the range smaller than 400 bp. These data exhibited no fragmentation of cDNA and reflected the intactness of RNA.

Only purified unfragmented Cy labeled aminoallyl-cDNA probes were used for hybridization on the spotted slides. Then, equal pmol of Cy3 and Cy5 labeled cDNA solutions were mixed together, and the mixed cDNA solution was completely dried in a aluminum foil covered Savant SC100 Speed Vac concentrator for 2 hr.

Gene Expression Analyses Utilizing the Pig Genome Center pig Microarray Platform

The pig microarray

In this study, a pig-based 70mer oligomicroarray was used. The pig microarray was distributed by U.S. Pig Genome Coordination Program (Iowa State University, Ames, Iowa), produced with the QIAGEN Array-Ready Oligo Set for the Pig Genome (version 1.0) and the Pig Genome Oligo Extension Set (version 1.0) (Qiagen, Valencia, CA). The Pig Genome Oligo set contains 10,665 70-mer probes representing S*us scrofa* gene sequences with a hit to human, mouse, or pig gene transcript. Some sequences contain a 3' expressed sequence tag (EST). The Pig Genome Oligo Extension Set contains 2,632 S*us scrofa* gene sequences with at least one 3' EST. In total, 13,297 transcripts probes are included in this pig microarray. The gene-lists, data sheets, and product profiles of the Pig Genome Oligo Set Version 1.0 and Pig extension Genome Oligo Set Version 1.0 are available from Qiagen (http://omad.operon.com/download/index.php).

All spotted probes were designed from TIGR Gene Index SsGI (*Sus scrofa* Gene Index) Release 5.0 (http://www.tigr.org/tigr-scripts/tgi/T_index.cgi?species=pig). Details and criteria for selecting these particular 70-mer probes are given in Appendix D. Each 13,297 element oligo set was printed onto one single slide at the Microarray Printing

Facility at the University of Minnesota, Minneapolis. The pig microarrays (slides) were stored under dry and dark conditions before their use.

Pre-hybridization of slides

Briefly, the oligo array slides were plunged into a Coplin jar (Fisher Scientific) filled with boiling MilliQ water and immediately shaken vigorously for 2 minutes. Then slides were transferred to 95% ethanol for 15 seconds and dried by spinning at 500g for 1 minute in RT6000B refrigerated centrifuge (Sorvall, Thermo Electron Corporation, Asheville, NC). Thereafter, slides were put in a Coplin jar filled with pre-hybridization buffer [5X SSC (0.75M NaCl and 0.075M NaCitrate), 0.1% SDS, 1% BSA] and incubated in a Precision Model 181water bath (Precision Scientific. Inc, Chicago, IL) for 45 min at 42^{o}C. After pre-incubation, slides were washed with MiliQ water 5 times and then washed in isopropanol. Finally, slides were dried by centrifugation at 500g for 1 minute and put into a Corning Hybridization chamber (Corning, Corning, NY) with the spotted side upward.

Preparation of the hybridization chamber

Dry LifterSlips (Fisher Scientific) were cleaned with clean dry air, and put on the slide gently with the white-edged side downward to the slide. To prevent arrays from drying during the following hybridization process, two thin strips 6.25cm of Whatman filter paper (Whatman Inc, Florham Park, NJ), were placed into the wells located on either end of the hybridization chamber, and the filter paper was saturated with 20 µl MilliQ H_2O.

Hybridization

The hybridization steps were conducted under light-safe conditions. Twenty µl of human Cot 1 (Invitrogen Corp), 2 µl poly A (Invitrogen Corp) and 13.6 µl H_2O were

added to the completely dried cDNA mixture. The solution (hybridization mixture) was mixed by pipetting up and down and heated at 95 ^{o}C for 5 min in a dry bath incubator (Fisher Scientific). The hybridization mixture was centrifuged at 10,000 g for 1 minute to pellet any particle material. The upper clear solution was carefully transferred to a new tube avoiding any sediment material. The hybridization mixture was carefully pipetted onto the oligo array while it rested within the hybridization chamber. The hybridization mixture was slowly pipetted to spread the hybridization solution evenly across the array surface. When the hybridization mixture had diffused out completely under the cover slip, the hybridization chamber was quickly sealed to keep the moisture within the chamber. Thereafter, the hybridization chamber was wrapped with aluminum foil without touching the top of hybridization chamber. Finally, the wrapped hybridization chamber was placed overnight in the 42^{o}C serological water bath (Boekel Scientific, Feasterville, PA).

Post hybridization array washing procedure

The following washing steps were conducted in the dark. After hybridization overnight in the water bath at 42^{0}C, the wrapped slide was removed from the water bath with the spotted side facing upwards. The foil was carefully removed without touching the slide. Then, the exterior of the hybridization chamber was dried with a Kimwipe (Kimtech Science, Erie, PA), and was unsealed carefully to avoid water entering the chamber. The slide was removed from the chamber and quickly put into a Coplin jar filled with 1X SSC, 0.2% SDS buffer (Appendix D). To make the LifterSlip fall away from the slide, the Coplin jar was incubated for 4 min at room temperature with gentle mixing on a BellyDancer with speed 4 (Strovall, Greensboro, NC). The slide without

cover slips was transferred to another Coplin jar filled with 0.1X SSC, 0.2 % SDS buffer and incubated for 4 min at room temperature with gentle mixing on the BellyDancer with speed 4. For the third washing, the slide was quickly transferred to a Coplin jar filled with 0.1X SSC, and incubated for another 4 min at room temperature with gentle mixing on an orbital shaker with speed 4. Thereafter, the slide was dried by spinning at 1000 g in RT6000B refrigerated centrifuge for 1 minute. Then, the slide was put into a foil-wrapped 50-ml conical tube, and scanned with a Gene Pix 4000B simultaneous dual wavelength scanner as soon as possible (Axon Instruments, Inc., Union City, CA).

Scanning of arrays

The scanner was turned on 15 minutes before the slide scanning. Then, the slide was loaded onto the scanner with the spot side downward in the dark. After launching the GenePix Pro 4.0 software, the slide was quickly read by clicking "Prescan" button in order to locate the scan zone of the slide. Several scans at various level of photomultiplier tube (PMT) were conducted to establish the PMT offset. After optimizing PMT level, separate images were acquired for each fluorophore at a resolution of 10 μm per pixel. For scaling of the two channels with respect to signal intensity, PMT and laser power settings were adjusted to achieve a signal ratio of channel 635 nm/channel 532 nm as close to 1.0 as possible. According to the GenePix Pro manual, the acceptable signal ratio ranges from 0.8~1.2. All along the scan, the "histogram" panel was observed to verify that the image was correctly equilibrated; the two curves corresponding to the two channels should be superimposed for intensities greater than the background. After finishing scanning, two single-channel (channel 635 and channel 532) images and one ratio image were automatically created by GenePix Pro and were saved with tagged

image file format (TIFF). All array images of this experiment are presented in the Appendix E.

Image analysis

The combined ratio image of the two single-channel images (Cy3 and Cy5) was used for image analysis with GenePix Pro 4.0 software. First GenPix Array List (GAL) file, provided by Qiagen, was loaded to the image. The GAL file was used to link the information from the slides printing process to the image analysis. Gene names and identifiers are located to corresponding spots on the image. A partial GAL file is presented in Table 3. In the next step, a grid mask was used to aid align the blocks on the array. Each block was placed exactly over the corresponding spots by adjusting the position of the grid mask. After aligning the blocks, all the spots were flagged to evaluate the spot quality using the standard set by GenePix Pro software and the flagged values were stored in the final results table. Finally, the image analysis process extracted fluorescence intensity data from the validated spots. Results and related calculated values were automatically saved in the GenePix Result(GPR) file. The GPR file was applied in the following data processing and analysis steps. An example of partial GPR file was presented in the Table 4.

Table 3. Part of GenePix Array List (GAL) file. It presents genes information corresponding to each spot. Each spot is located by the block, row and column number, and has a unique identification number.

Block48=16500, 61160, 160, 18, 240, 17, 240				
Supplier=BioRobotics				
ArrayerSoftwareName=TAS Application Suite (MicroGrid II)				
ArrayerSoftwareVersion=2.2.2.8				
Block	Column	Row	ID	Name
1	1	1	SS00013045	unknown
1	1	2	SS00011959	unknown
1	1	3	SS00011151	unknown
1	1	4	SS00000701	heat shock protein 70.2 [Sus scrofa]
1	1	5	SS00010360	unknown
1	1	6	SS00009274	unknown
1	1	7	SS00008466	unknown
1	1	8	SS00007748	unknown
1	1	9	SS00006940	unknown
1	1	10	SS00005854	PIR|A40915|OKHUR2 protein kinase (EC 2.7.1.37) cAMP-dependent type II-beta regulatory chain - human, partial (14%)
1	1	11	SS00005046	homologue to SP|O97704|NPT2_SHEEP Renal sodium-dependent phosphate transport protein 2 (Sodium/phosphate cotransporter 2) (Na(+)/Pi, partial (47%)
1	1	12	SS00004328	similar to SP|P49916|DNL3_HUMAN DNA ligase III (EC 6.5.1.1) (Polydeoxyribonucleotide synthase [ATP]). [Human] {Homo sapiens}, partial (27%)
1	1	13	SS00003520	homologue to GP|14388542|dbj|BAB60792. hypothetical protein {Macaca fascicularis}, partial (44%)
1	1	14	SS00002434	PIR|JE0272|JE0272 low density lipoprotein receptor-related protein 6 - human, partial (12%)
1	1	15	SS00001626	homologue to GP|12654407|gb|AAH01029.1 N-Acetylglucosamine kinase {Homo sapiens}, complete
1	1	16	SS00000908	delayed rectifier potassium channel Kv2.1 [Sus scrofa]
1	1	17	SS00000100	SP|Q99832|TCPH_HUMAN T-complex protein 1 eta subunit (TCP-1-eta) (CCT-eta) (HIV-1 Nef interacting protein). [Human], partial (36%)

1	2	1	SS00013069	unknown
1	2	2	SS00011983	unknown
1	2	3	SS00011175	unknown
1	2	4	SS00000701	heat shock protein 70.2 [Sus scrofa]
1	2	5	SS00010384	unknown
1	2	6	SS00009298	unknown
1	2	7	SS00008490	unknown
1	2	8	SS00007772	unknown
1	2	9	SS00006964	unknown
1	2	10	SS00005878	homologue to GP|14035806|emb|CAC38499. unnamed protein product {Homo sapiens}, partial (59%)
1	2	11	SS00005070	homologue to GP|2078323|gb|AAB54006.1| Ch-1PTPase delta form {Homo sapiens}, partial (19%)
1	2	12	SS00004352	similar to GP|12803737|gb|AAH02705.1 chromosome 22 open reading frame 3 {Homo sapiens}, partial (43%)
1	2	13	SS00003544	similar to GP|12804035|gb|AAH02870.1 Unknown (protein for MGC:11266) {Homo sapiens}, partial (30%)
1	2	14	SS00002458	homologue to GP|11322247|emb|CAC16786. nucleolar protein No55 {Homo sapiens}, partial (36%)
1	2	15	SS00001650	homologue to GP|12804063|gb|AAH02884.1 hypothetical protein similar to beta-transducin family {Homo sapiens}, partial (27%)
1	2	16	SS00000932	protein carboxyl-o-methyltransferase [Sus scrofa domestica]
1	2	17	SS00000124	homologue to GP|1815762|gb|AAB42020.1| gamma-glutamylcysteine synthetase {Mus musculus}, partial (42%)
1	3	1	SS00013093	aromatase type II [Sus scrofa]aromatase cytochrome P450 [Sus scrofa]aromatase cytochrome P450 [Sus scrofa]type I cytochrome p450 aromatase [Sus scrofa]type II cytochrome p450 aromatase [Sus scrofa]
1	3	2	SS00012285	unknown
1	3	3	SS00011199	unknown
1	3	4	SS00001180	glyceraldehyde-3-phosphate dehydrogenase [Sus scrofa]glyceraldehyde-3-phosphate dehydrogenase [Sus scrofa] glyceraldehyde-3-phosphate dehydrogenase [Sus scrofa]glyceraldehyde 3-phosphate d
1	3	5	SS00010408	unknown

Table 4. Part of GenePix Result (GPR) file. The head of GPR file describes all the parameters used when scanning the array including PixelSize, FocusPosition, Temparature, PMTGain, and ScanPower. The main body of GPR file list the determined and calculated values for each spot (gene), such as median/mean spot foreground and background pixel intensity at each channel (532 nm and 635 nm), calculated median/mean of ratios, sum of medians/means, the signal-to-noise-ratio etc.

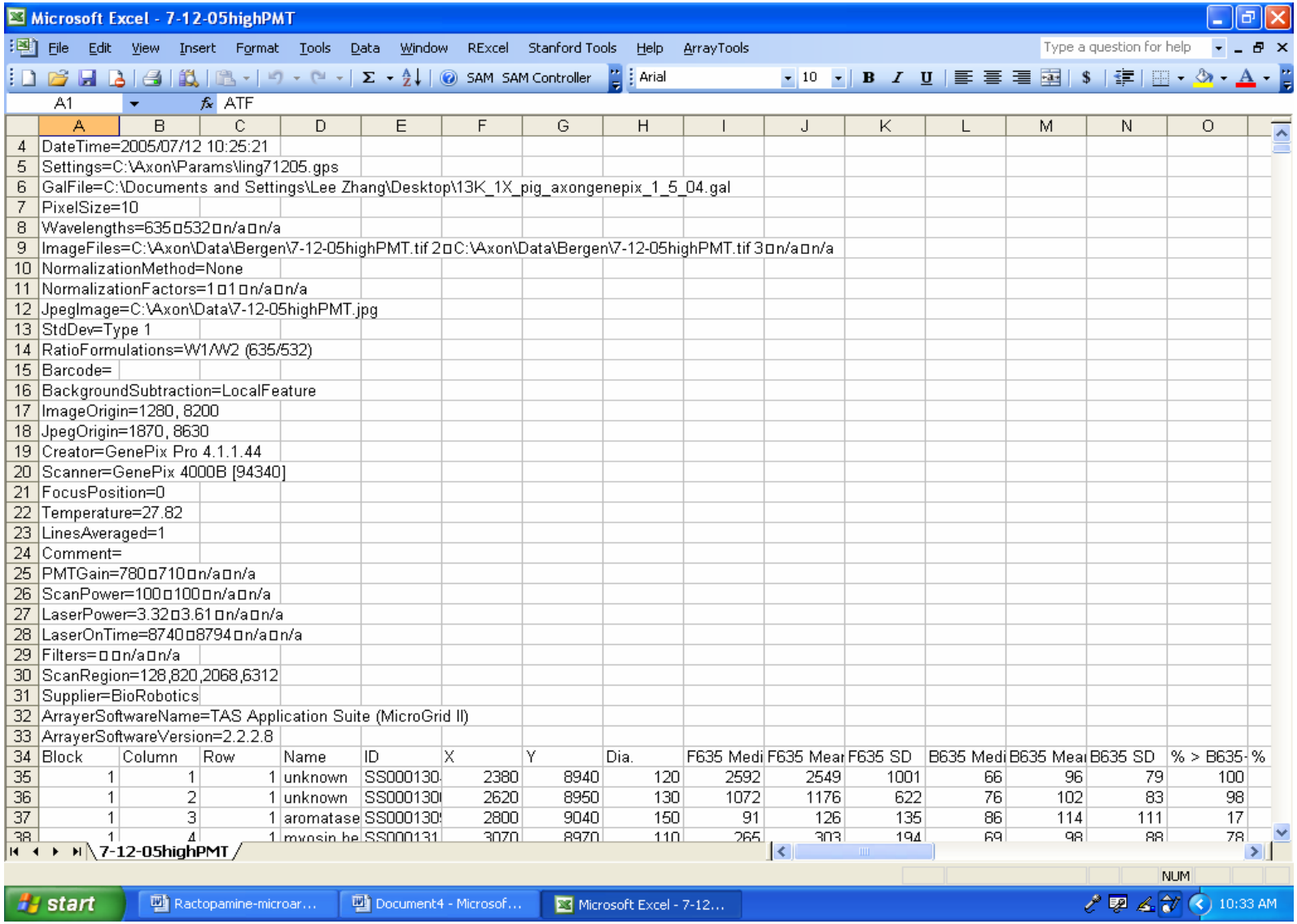

Microsoft Excel - 7-12-05highPMT

File Edit View Insert Format Tools Data Window REXcel Stanford Tools Help ArrayTools

Type a question for help

SAM SAM Controller

Arial 10

A1 ATF

	A	B	C	D	E	F	G	H	I	J	K	L	M	N	O
4	DateTime=2005/07/12 10:25:21														
5	Settings=C:\Axon\Params\ling71205.gps														
6	GalFile=C:\Documents and Settings\Lee Zhang\Desktop\13K_1X_pig_axongenepix_1_5_04.gal														
7	PixelSize=10														
8	Wavelengths=635□532□n/a□n/a														
9	ImageFiles=C:\Axon\Data\Bergen\7-12-05highPMT.tif 2□C:\Axon\Data\Bergen\7-12-05highPMT.tif 3□n/a□n/a														
10	NormalizationMethod=None														
11	NormalizationFactors=1□1□n/a□n/a														
12	JpegImage=C:\Axon\Data\7-12-05highPMT.jpg														
13	StdDev=Type 1														
14	RatioFormulations=W1/W2 (635/532)														
15	Barcode=														
16	BackgroundSubtraction=LocalFeature														
17	ImageOrigin=1280, 8200														
18	JpegOrigin=1870, 8630														
19	Creator=GenePix Pro 4.1.1.44														
20	Scanner=GenePix 4000B [94340]														
21	FocusPosition=0														
22	Temperature=27.82														
23	LinesAveraged=1														
24	Comment=														
25	PMTGain=780□710□n/a□n/a														
26	ScanPower=100□100□n/a□n/a														
27	LaserPower=3.32□3.61□n/a□n/a														
28	LaserOnTime=8740□8794□n/a□n/a														
29	Filters=□□n/a□n/a														
30	ScanRegion=128,820,2068,6312														
31	Supplier=BioRobotics														
32	ArrayerSoftwareName=TAS Application Suite (MicroGrid II)														
33	ArrayerSoftwareVersion=2.2.2.8														
34	Block	Column	Row	Name	ID	X	Y	Dia.	F635 Medi	F635 Mear	F635 SD	B635 Medi	B635 Mea	B635 SD	% > B635	%
35	1	1	1	unknown	SS000130	2380	8940	120	2592	2549	1001	66	96	79	100	
36	1	2	1	unknown	SS000130	2620	8950	130	1072	1176	622	76	102	83	98	
37	1	3	1	aromatase	SS000130	2800	9040	150	91	126	135	86	114	111	17	
38	1	4	1	myosin he	SS000131	3070	8970	110	265	303	194	69	98	88	78	

7-12-05highPMT

NUM

start Ractopamine-microar... Document4 - Microsof... Microsoft Excel - 7-12... 10:33 AM

Normalization

Microarray data normalization is an important step for obtaining data that are reliable and usable for subsequent analysis. In this study, a robust local regression technique, locally weighted scatterplot smoothing (LOWESS) algorithm was used to normalize all the data by GenePixpro package. In experiments where two fluorescent dyes (Cy3 and Cy5) have been used, intensity-dependent variation in dye bias may introduce spurious variations in the collected data. LOWESS normalization assumes that the dye bias is dependent on spot intensity and applies a spot intensity dependent smoothing adjustment to remove dye bias. All samples in the dataset are corrected independently in LOWESS. The adjusted ratio is computed by:

$\log(R/G) = \log(R_0/G_0) - c(A)$

In the above formula, R and G are normalized fluorescent intensity of Cy3 (red) and Cy5 (green) respectively for a spot; R_0 and G_0 are non-normalized fluorescent intensity of Cy3 (red) and Cy5 (green) respectively for the identical spot; c(A) is the Lowess fit to the log(R/G) vs log(sqrt(R*G)) plot. If green has been chosen as the treatment dye and red as the control dye, then R and G are reversed in the above formula (203).

Potential dye intensity biases in the microarray data sets were visualized using M vs. A scatter plots constructed for each array, where log intensity ratios $M = \log_2(Cy3/Cy5) = \log_2 Cy3 - \log_2 Cy5$ were plotted against mean log intensities $A = (\log_2 Cy3 + \log_2 Cy5)/2$ for each array spot (204). The efficiency of LOWESS normalization was assessed by monitoring *M-A* plots for data from each array before and after LOWESS normalization. An example of *M-A* plots before and after LOWESS normalization is presented in Fig 2. All M-A plots of this experiment are presented in Appendix F. The log transformed ratios

by LOWESS normalization were used in the following analysis. The log transformation of data reduced skew and produced desirable variance properties. Thus, the distribution of transformed data was closer to the normal distribution. More discussion about choosing normalization methods is in the discussion part of this chapter.

Fig 2. M-A plot before and after LOWESS normalization

For the X axis, A = ($\log_2 Cy3 + \log_2 Cy5$)/2, reflecting the spot intensity; for the Y axis, $M = \log_2(Cy3/Cy5) = \log_2 Cy3 - \log_2 Cy5$, reflecting the expression difference between the two channels. In this example, in the M-A plot after normalization, the fluorescence intensity (A value) of spots ranged from 0-16 with a few spot in the lowest and highest part, which means the scanner laser intensity was set properly to detect spots with low fluorescence intensity. Only a few spots were saturated. Before the normalization, The M-A plots exhibited systematic trends which depended on the value of A; therefore, local intensity-dependent regression lines through the data were fitted using the lOWESS fit function to remove the spot intensity dependent dye bias. After LOWESS normalizatrion, The difference between Cy5 and Cy3 labeling spots (M value) were symmetrically spread with the center of M=0, which means dye bias was minimized.

Fig 2. A) M-A plot before LOWESS normalization

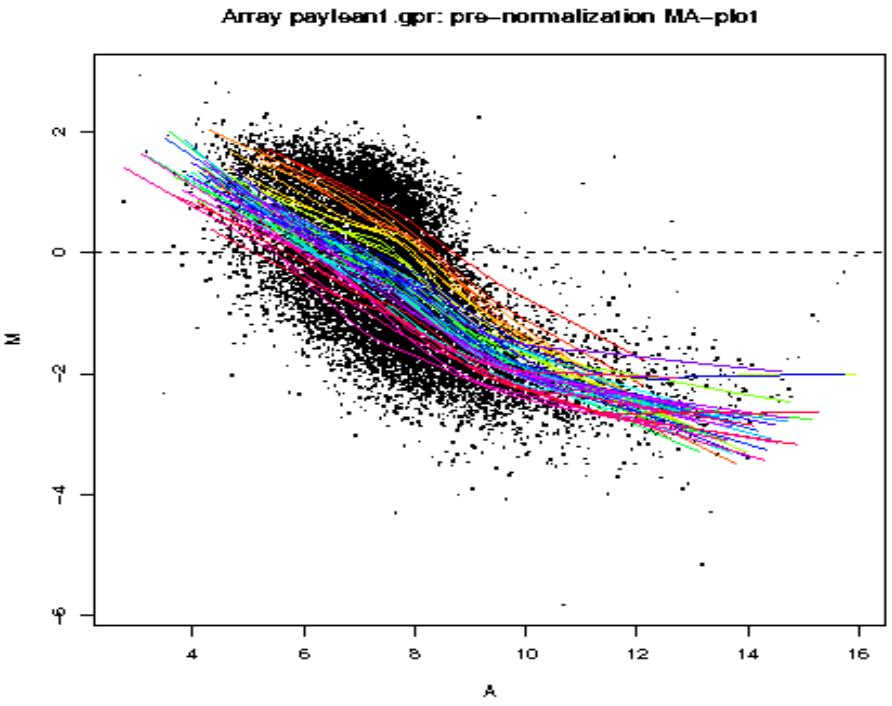

B) M-A plot after LOWESS normalization

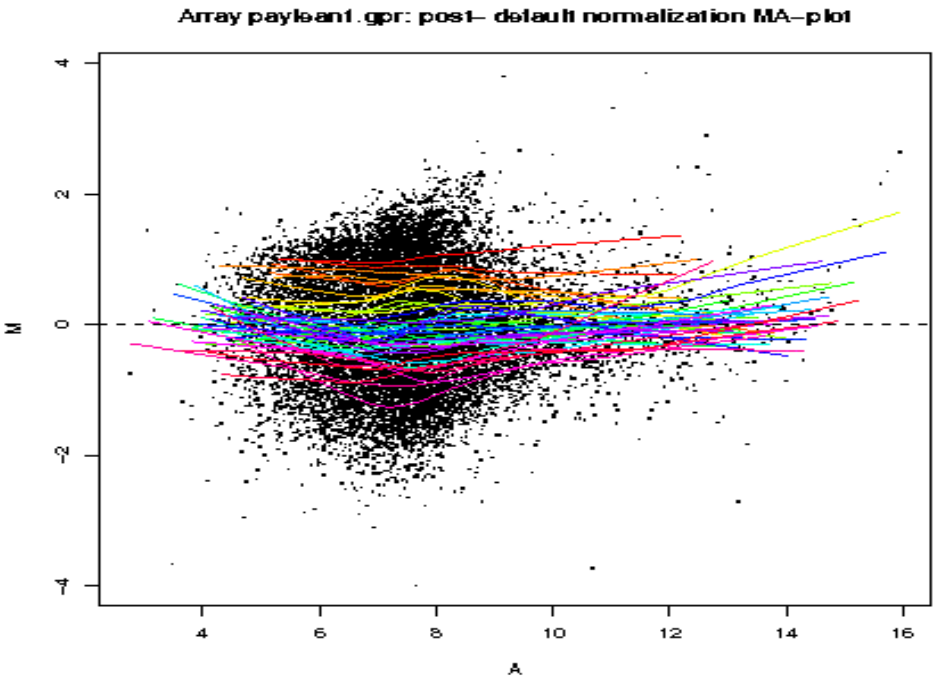

Statistical Analysis

To search differently expressed genes between control (0 ppm Paylean) and treatment (60 ppm Paylean) groups, Significant Analysis of Microarray (SAM) software (http://www-stat.stanford.edu/~tibs/SAM/) was used to conduct statistical analysis in this study (205).

The SAM (version 1.12) add-in to Microsoft Excel was used for comparisons of replicate array experiments. SAM assesses the difference between two mean values when taking into account the standard errors of those means. The significance of that difference is estimated by comparing it against the probability of it's occurrence once. The model of chance occurrence is generated by permutation of the input data, rather than a predetermined model (e.g., a normal distribution) in the standard t-test. The SAM algorithm was used instead of the standard *t* test because SAM was proved to have a better ability to scale down to small numbers of replicates (n=3 in this study) (205).

SAM computes a statistic d_i for each gene i, measuring the strength of the relationship between gene expression and the response variable. It uses repeated permutations of the data to determine if the expression of any gene is significantly related to the response. The cutoff value for significance is determined by a tuning parameter delta (Δ), which is chosen by a user to obtain different false positive rate. More discussion about application of statistical methods is in the discussion part of this chapter.

In this study SAM was employed using the one-class response with 1,000 permutations to determine genes whose expression was significantly different from zero. Significant genes were determined by setting the number of falsely called genes to less than one and choosing similar false discovery percentage medians for each biological

replicates. At these values, the false discovery rate (FDR) for the positive genes was 0.05 (5%) and the q value (a measure of significance in terms of the false discovery rate) for all biological replicates were less than 0.003.

After obtaining a list of significantly differentially expressed genes from SAM, in order to focus our attention on genes related to the hypothesis of the researches in this dissertation, a list including genes of interest (named genes of interest list) was constructed which includes genes for transcription factors, carbohydrate, lipid and cholesterol metabolism, electron transport, oxidative phosphorylation, and the cAMP pathway. The above genes of interest were randomly spotted on the pig array. This gene list was used to filter the SAM results and these filtered results are reported in Table 5.

RESULTS AND DISCUSSION

Issues in Evaluating RNA Quality from Porcine Adipose Tissue

The assessment of RNA integrity can be accomplished by various methods: traditional agarose gel-electrophoresis, innovative lab-on-chip technologies like Bioanalyzer 2100 (Agilent Technologies) and Experion (Bio-Rad Laboratories), and modern OD measurement via NanoDrop.

Absorption at 260 nm and 280 nm indicates the presence of nucleic acids and proteins respectively. The ratio of the absorbance at 260nm and 280nm has been used to measure the purity of isolated RNA for a long time. For instance, when using a spectrophotometer, a ratio of absorbances at 260 and 280 nm (A_{260}:A_{280}) greater than 1.8 is traditionally considered to be an acceptable indicator of RNA purity (206). However, the accuracy of A_{260}:A_{280} ratio method has been questioned. The pH and ionic strength of the solution significantly affect the A_{260}:A_{280} ratio of nucleic acids (207). Warburg and

Christian (208) showed that the ratio was a good indicator of contamination of protein preparation by nucleic acid, but the ratio did not reflect the contamination of nucleic acid by protein. Because the extinction coefficient of nucleic acid at 260nm and 280nm are much greater than that of proteins, significant contamination with protein will not greatly change the A_{260}:A_{280} ratio of a nucleic acid solution (209).

In the traditional method of assessing RNA quality, RNA integrity is evaluated using agarose gel electrophoresis (denaturing gel is preferred) stained with ethidium bromide, which produces a well-established banding pattern. Typically, gel images show two bands comprising the 28S and 18S ribosomal RNA (rRNA) species and other bands where smaller RNA species are located (210). Mammalian 28S and 18S rRNAs are approximately 5 kb and 2 kb in size. The theoretical 28S:18S rRNAs is approximately 2.7:1(212). The proportion of the ribosomal bands (28S:18S) has conventionally been viewed as the primary indicator of RNA integrity, with a ratio of 2.0 considered to be typical of 'high quality' intact RNA (211). Total RNAs from mammalian tissues rarely have a 28S:18S rRNA ratio of 2.0 or greater because 28S rRNA structure is unstable relative to the 18S rRNA. The instability of 28S rRNA results from its size and its high degree of secondary and tertiary structures (212).

Certainly total RNA with a 28S:18S rRNA ratio of 2.0 denotes high quality. However, the total RNA with lower rRNA ratios (<1.8) is not necessarily of poor quality especially for downstream applications if no degradation products can be observed in the electrophoretic trace (211). Visual assessment of the 28S:18S rRNA ratio on agarose gels is subjective because interpretation of gel images is dependent on individual and the resulting data cannot be processed digitally. Appearance of rRNA bands is affected by

electrophoresis conditions, amount of RNA loaded, and saturation of ethidium bromide fluorescence (213). Because of lack of reliability, the 28S:18S rRNA ratios may not be used as a gold standard for assessing RNA integrity. Imbeaud et al. (211) did not find clear correlation between 28S:18S rRNA ratio and RNA integrity in some samples although RNAs with 28S:18S >2.0 were usually of high quality. Moreover, most of the RNAs (83%) displaying a 28S:18S > 1.0, could be considered of good quality. This was determined after those RNAs were applied to determine the expression of four house-keeping genes using real-time quantitative reverse transcription PCR methods.

The Agilent 2100 Bioanalyzer provide a framework for the standardization of RNA quality control. RNA samples are electrophoretical separated on a micro-fabricated chip and subsequently detected via laser induced fluorescence detection. A RNA ladder is used as a mass and size standard during electrophoresis, which allows the estimation of the RNA band sizes (214). The integrity of the RNA may be assessed by visualization of the 18S and 28S ribosomal RNA bands. An elevated threshold baseline and a decreased 28S:18S ratio are both indicative of degradation. Degradation of the RNA sample produces a shift in the RNA size distribution toward smaller fragments and a decrease in fluorescence signal as dye intercalation sites are destroyed (215).

RNA Integrity Number (RIN) was developed to assess RNA quality for the lab-on-chip capillary gel-electrophoresis used in the Bioanalyzer 2100 (215). The RIN algorithm allows calculation of RNA integrity using a trained artificial neural network based on the determination of the most informative features that can be extracted from the electrophoretic traces out of 100 features identified through signal analysis (215). The selected features which collectively catch the most information about the integrity levels

include the total RNA ratio (ratio of area of ribosomal bands to total area of the electropherogram), the height of the 18S peak, the fast area ratio (ratio of the area in the fast region to the total area of the electropherogram) and the height of the lower marker (214).

The RIN algorithm allows the classification of total RNA on a numbering system from 1 to 10, with 1 being the most degraded profile and 10 being the most intact (Fig 3). A smearing of either 28S and 18S peaks, or a decrease in their intensity ratio indicates degradation of the RNA sample. In this way, interpretation of an electropherogram is facilitated, comparison of samples is enabled and repeatability of experiments can be assessed (211, 215).

While intact RNA obviously constitutes the best representation of the natural state of the transcriptome, there are situations in which gene expression analysis may be satisfactory even on partially degraded RNA. Schoor *et al.* (216) found gene expression profiles obtained from partially degraded RNA samples with still visible ribosomal bands exhibit a high degree of similarity compared to intact samples. They concluded that RNA samples of suboptimal quality might therefore still lead to meaningful results if used carefully. Moreover, Auer *et al*. (217) recently concluded that degradation does not preclude microarray analysis if comparison is done using samples of comparable RNA integrity. Imbeaud et al. (211) reported collection of reasonable microarray data and meaningful results from RNA samples of impaired quality. Schroder *et al.* (218) observed RIN shows a strong correlation to the expression value of house keep genes, while the ribosomal ratio (28S:18S) exhibited weak correlation to the expression value of the housekeeping genes.

In this study, RNA concentration and purity were evaluated by UV measurement after resolving on the agarose gel. RNA quality was assessed by visualizing smearing on 28S and 18S bands, DNA contamination, and the relative intensity of bands for 28S and 18S. The gel pictures for RNA samples used in this study are present in Appendix A.

Because interpreting an RNA gel image is subjective, remaining four adipose RNA samples from the microarray analysis (totally six RNA samples in the RAC study) were analyzed using Agilent Bioanalyzer 2100 after receiving comments and suggestion. These remaining original RNAs had been stored at -80^{o}C for 6-8 months when they were analyzed with an Agilent Bioanalyzer 2100. These four adipose RNA samples from different pigs were run in accordance with the manufacturer's instructions (http://www.cbse.ucsc.edu/pdf_library/Bioanalyzer%20protocol071304.pdf). The electropherograms are presented in Fig 4.

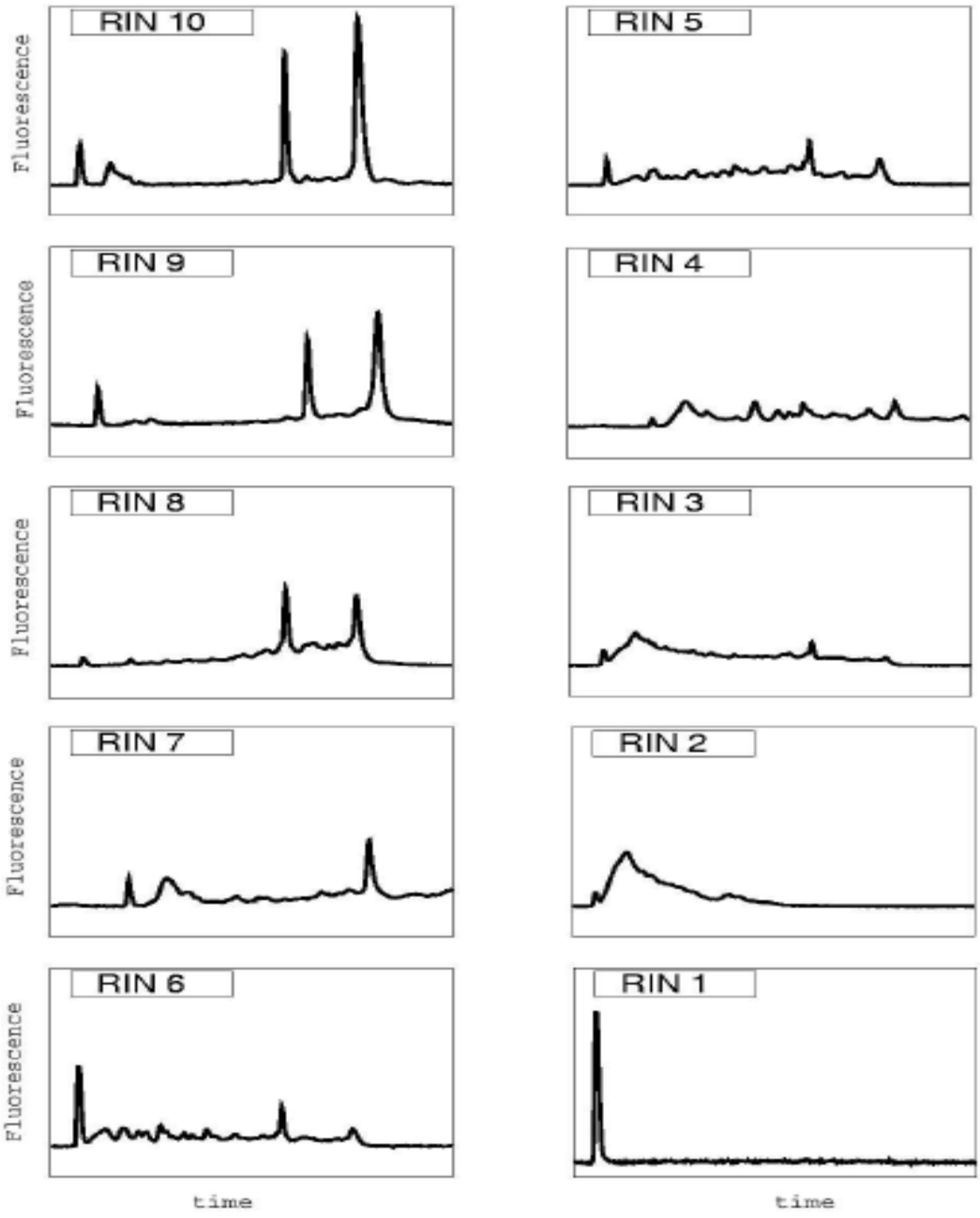

Fig 3. RNA integrity categories. The figure shows typical representatives of the ten integrity categories. RIN values range from 10 (intact) to 1 (totally degraded). The gradual degradation of rRNA is reflected by a continuous shift towards shorter fragment sizes (218).

Fig 4. Electropherograms of microcapillary electrophoresis from four RNA samples. Electropherogram of RNA includes a clearly visible 28S:18S rRNA peak, showing slight degradation with a little elevating of baseline. RNA degradation is progressive: as the area of the 28S rRNA peak decreases, reflecting breakdown, there is first a rise in the baseline between the 18S and 28S rRNA and then a progressive increase in the baseline area below the 18S rRNA that spreads as the 28S rRNA fragments become smaller.

Sample 1 (#826)

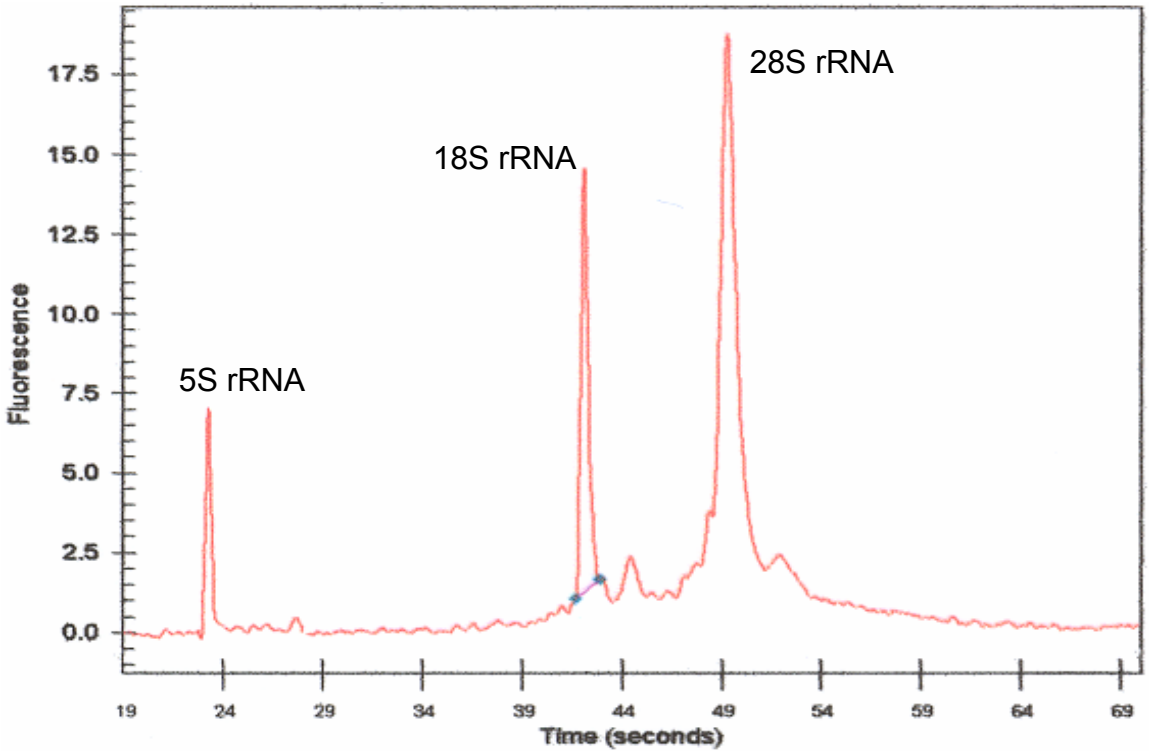

Sample 2 (#779)

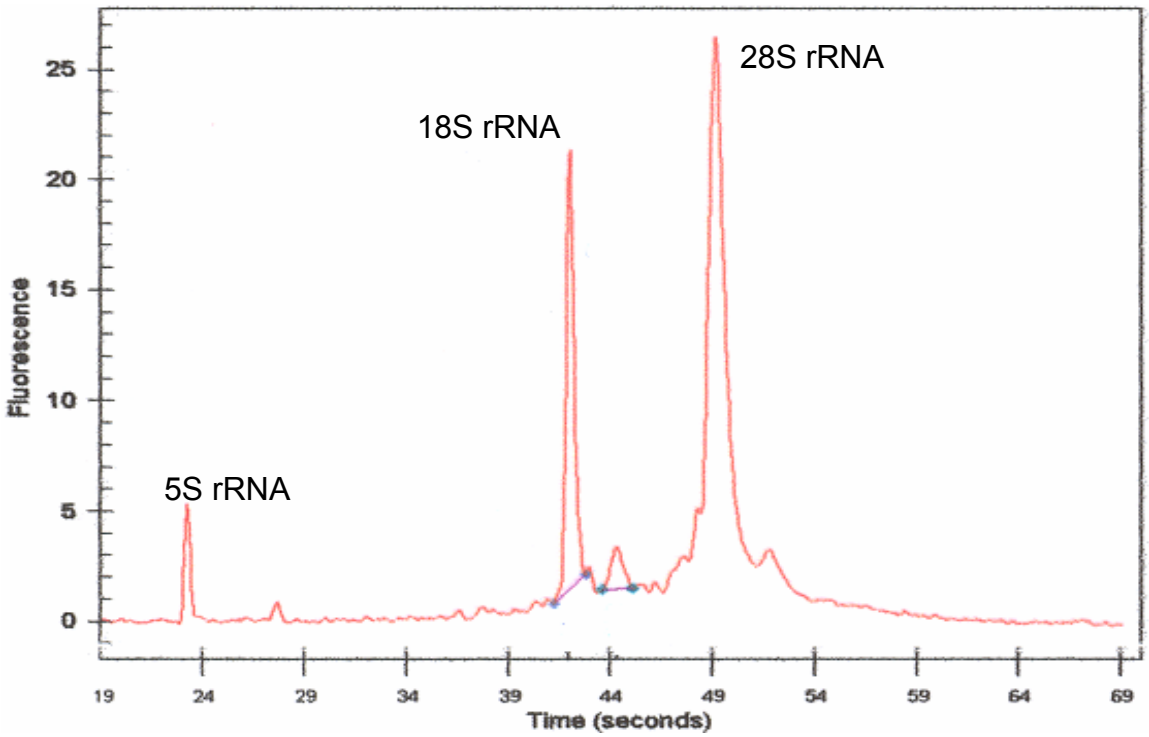

Sample 3 (#796)

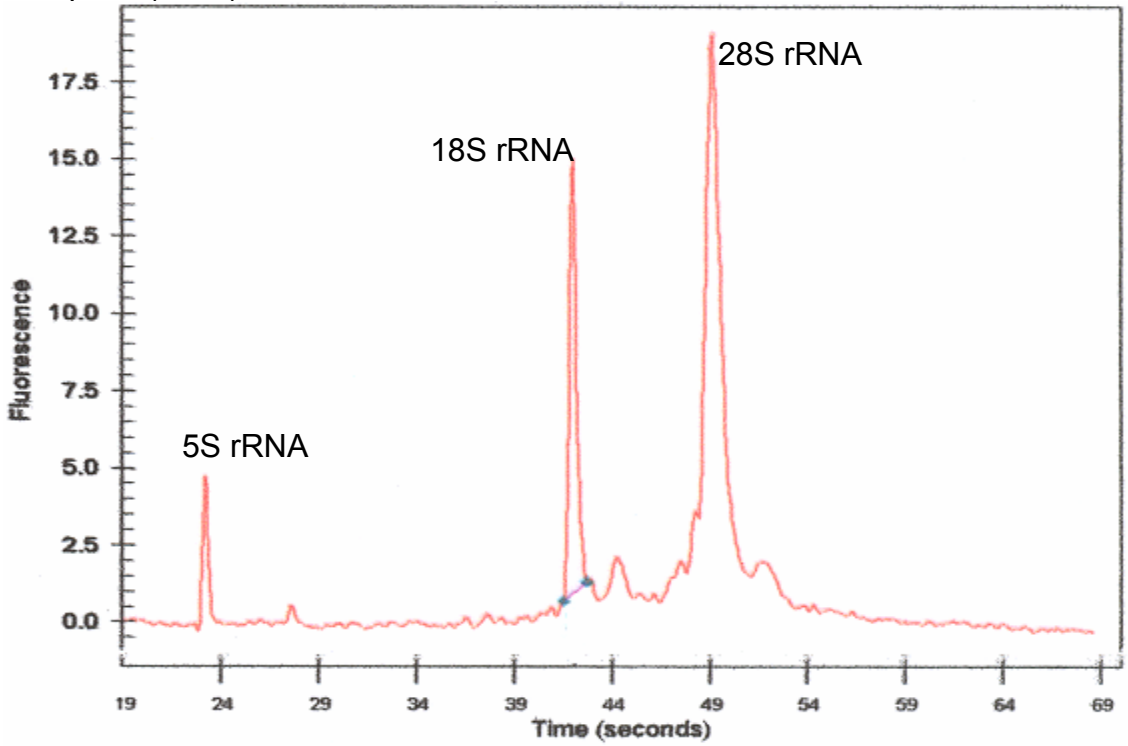

Sample 4 (#784)

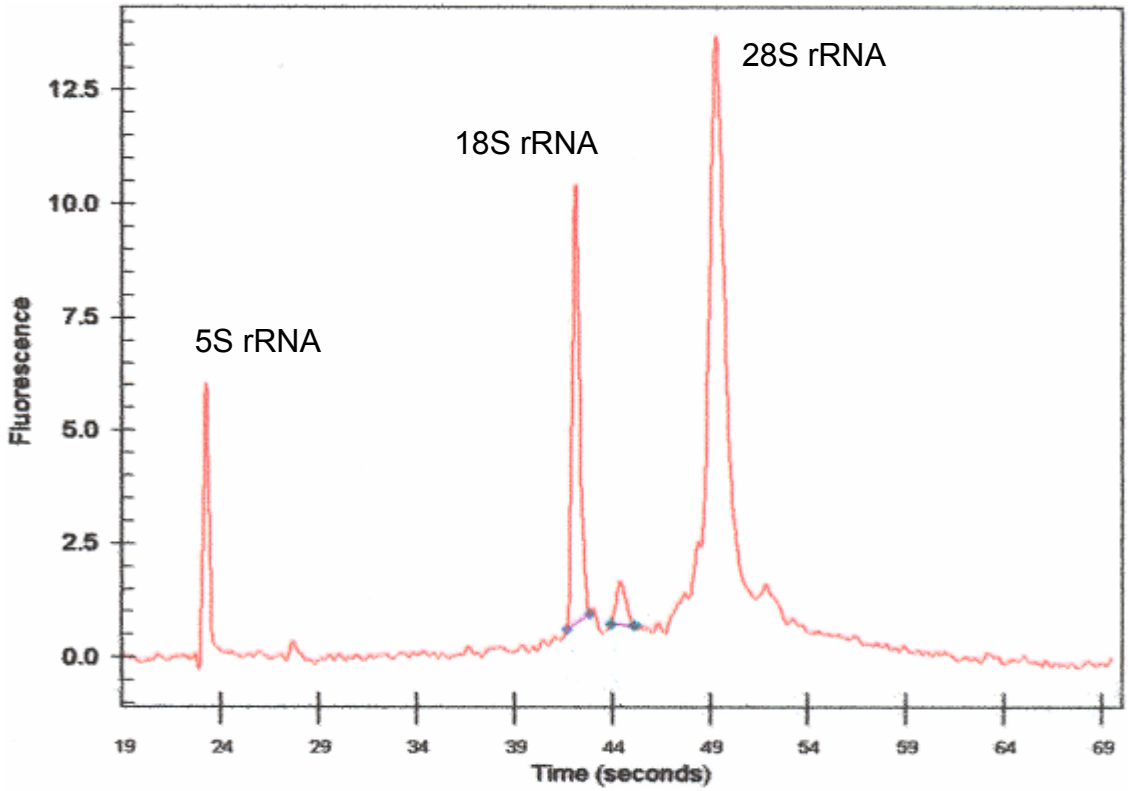

Issues in Choosing Microarry Experimental Design

An experiment utilizing a spotted 70mer-oligo microarray is in fact a competitive hybridization between one RNA sample that is labeled with the red-fluorescent dye Cyanine 5 (Cy5) and the other RNA sample that is labeled with the green-fluorescent dye Cyanine 3 (Cy3) to a single spotted oligo probe or vice verse. Hybridization of two dye labeled aminoallyl-cDNA (which represent the mRNA from the preparation on the oligo probes (spotted slides) are inherently comparative. Therefore the pairing of RNA samples (as the labeled cDNAs) for hybridization leads to relative/differential expression data. Each microarray run provides investigators with the relative abundance of two sets of mRNA to each other. When designing a microarray experiment, besides constraints such as the number of slides available, the amount of RNA available and other cost considerations, the most important design issues are to determine which RNAs are to be hybridized together on the same slide, which RNAs are to be labeled with which fluorescent dye, and how many biological replicates are necessary to estimate variation among the biological samples by statistical methods (219).

An experimental design should ensure that efficient use is made of the available resources, that obvious inherent experimental biases will be avoided and that the data obtained will provide useful information on treatment-driven differential gene expression. In this study, the primary objective was to identify differentially expressed genes in the adipose tissue upon RAC feeding to pigs for 28 days. Comparison of gene expression of two groups (0ppm Paylean vs. 60ppm Paylean) directly on the same array is the most efficient method. While there is heterogeneity among pigs used here, they were highly selected and represented an identical genotype. In order to be able to conduct this

differential gene expression experiment in a cost effective manner, the RNAs from control group (0ppm Paylean group) were mixed to provide the pooled control RNA. The RNA from each pig in the 60ppm Paylean group was hybridized with the pooled control RNA in order to get biological replicates (n=3).

In essence, replication allows averaging, and averages are less variable than their component terms. Lack of replication greatly restricts the ability to use statistical tests to determine whether a given intensity log ratio value is significantly different from zero (200). In particular, biological replication is essential to estimate the variance of the log ratios across slides. Replication is intimately connected with the statistical extrapolation from sample to population. Although almost all experiments that use statistical inference require biological replication, technical replicates are almost never required when the aim is to make inferences about populations that are based on sample data, as is the case in most microarray studies (200). There is no consensus about the necessary number of biological replicates in microarray analysis. Lee et al. (221) indicates that three replicates are sufficient for robust statistical analysis. However, other evidence indicates that a minimum of 5 biological cases per group should be analyzed for designs in which two groups of cases are evaluated for differential expression (222-224).

Another important design issue is to determine which RNAs are to be labeled with which fluorophore. Most microarray experiments show systematic differences between the red and green intensities because different incorporation efficiencies and quantum efficiencies between dye Cy3 and Cy5 (225). Because labeling dye Cy5 is less efficiently incorporated into nucleotides than Cy3, low expression genes in the Cy5-labeled comparative sample are likely to be incorrectly identified as being down-regulated.

Therefore, in the biological replications of miroarray analysis, labeling RNA samples from same treatment group with identical fluorescent dye should be avoided because color bias might persistent and accumulative (226). The dye-labeling bias can be effectively alleviated by two methods. One method is reverse labeling design (dye-swap design). Reverse labeling offers useful protection against the non-linearity of label normalization without the need to explicitly model the non-linearity. Reverse labeling increases the experimental cost but does not improve the number of biological replicates. Another useful alternative for dye error is performing non-linear normalization which corrects the systematic differences of Cy3 and Cy5, based on the fact that systematic trends by dye labeling are due to the inadequacy of linear normalization (227). In this study, besides performing non-linear normalization on all the data, random dye assignments was used for RNA arising from either 0 (pooled) and 60 ppm RAC-fed pigs.

Gene-label interaction is another factor that may influence the accuracy of microarray analysis. Use of two labels may also introduce gene-label interactions. For example, Cy3-dCTP may be preferentially incorporated into a specific sequence, relative to Cy5-dCTP. Theoretically, some degree of gene-label interaction may exist. However, this interaction appears to be insignificant in magnitude compared with other sources of variation (228).

Issues in Choosing Methods for Microarray Data Normalization

After extracting data from image analysis, systematic errors need to be removed before the data are applied to downstream statistical analysis. Any spot with intensity lower than the background plus two standard deviations should be excluded. On the other hand, the intensity ratios should be log-transformed so that upregulated and

downregulated values are on the same scale and comparable (229). Normalization is a data processing tool applied to remove systematic errors by balancing the fluorescence intensities of the two labeling dyes. The dye bias comes from various sources including differences in dye labeling efficiencies, heat and light sensitivities, as well as scanner settings for scanning two channels (230). When microarray analysis initially emerged as a tool for measuring differences of gene expression on a large scale, three methods are commonly used to calculate normalization factor including: (i) global normalization that uses all genes on the array (ii) housekeeping genes normalization that uses constantly expressed housekeeping/invariant genes; and (iii) internal controls normalization that uses known amount of exogenous control genes added during hybridization (229). With the development of mciroarray techniques, new normalization methods were developed to replace above three normalization methods. The shortcoming of the three methods arises from the fact that dye bias may be dependent on spot intensity and spatial location on the array. Furthermore, housekeeping genes are not as consistently expressed has been previously assumed, thus, using housekeeping genes normalization might introduce another potential source of error (231). Dye-swapping experiments are viewed as a plausible solution to reduce the dye bias problem, but may be impractical because of the limited supply of certain precious samples.

Global locally weighted scatterplot smoothing (LOWESS) has become a widely used normalization method after it was first utilized in microarray data analysis (232). LOWESS is a non-linear normalization method on the basis of gene intensity and spatial information which experts agree is superior to other methods (229). LOWESS applies a smoothing adjustment to obtain the calibration factor and remove dye bias based on the

spot intensity and location (232). Compared with other techniques like housekeeping-based normalization or dye-swap experiments, scatter plot-based normalization is more robust in many types of scenarios where the assumption of constantly expressed genes may break down (226). In this study, all image analysis data were normalized by LOWESS due to the robustness of fit in the presence of a few extreme outliers. An M-A plot was produced to investigate the log-intensity after microarray image was normalized by LOWESS. The plots show $\log_2$ of the expression ratio versus average spot intensity. After removing the dye labeling effect, in an ideal M-A plot, the center of the distribution of log-ratios should be zero. The log-ratios should be independent of spot intensity, and the fitted line should be parallel to the intensity axis (233). After LOWESS normalization within each microarray slide, normalization between slides may be applied dependent on the dispersion of M-values of all slides study. Boxplots are used for between-slides normalization. Boxplots involve comparing the ranges of the regression-corrected *M*-values across the slides, and scaling them so that M-values on each slide span symmetrically around zero (234). For example, between-slides normalization of 3 slides in RAC study is presented in the Fig 5. Notice that there is some variation in the average intensity between hybridizations. There are several factors that can cause this. Perhaps one array got slightly more DNA (the right one), or maybe there are slight variations during the production of the arrays. Maybe there were variations in the laboratory environment (temperature or humidity) during the preparation of these samples that influenced the readings (234).

A) Boxplots of the pre-normalization of M-value for three microarray slides

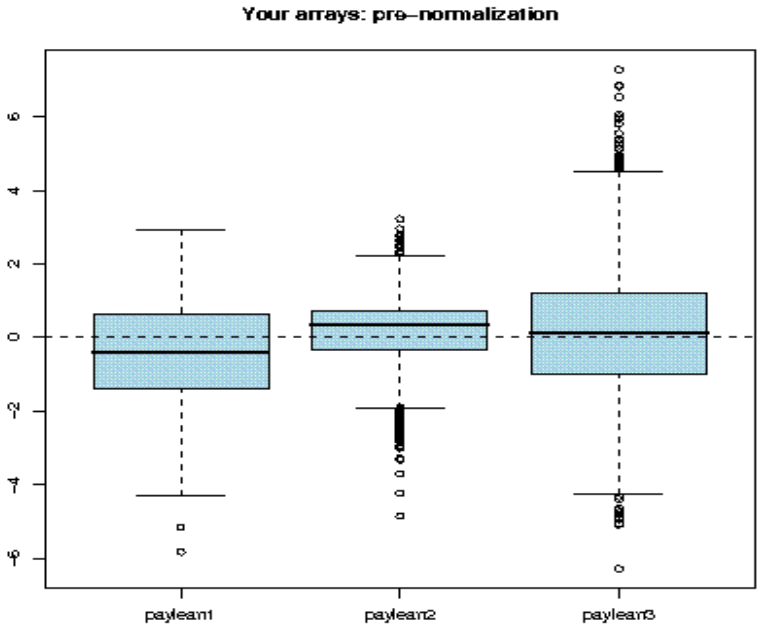

B) Boxplots of the post-normalization of M-value for three microarray slides

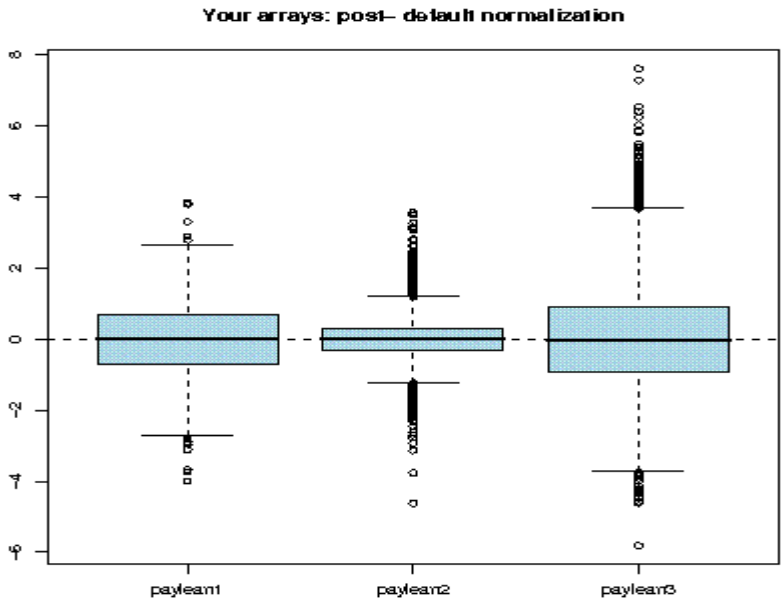

Fig 5. Boxplots of three microarray slides before and after normalization in RAC study

Issues in Choosing Method for Statistical Analysis to Identify Significantly Differentially Expressed Genes

Since microarry analysis is still developing, scientists working in bioinformatics are trying different statistical methods to analyze microarray data to identify genes whose expression changes across experimental paradigms, such as variants of F-statistics, modified t-test, non-parametric approaches and empirical Bayesian methods (235).

A fixed threshold cut off method (i.e. a two-fold increase or decrease) was used to identify differentially expressed genes during early stage of microarry work. However, this method is not efficient statistically, the main reason being that there are numerous systemic and biological variations that occur during a microarray experiment (236). Although some of the systemic variations such as dye bias can be effectively removed by normalization, random biological variations such as sample-to-sample and physiological variations are more difficult to handle (237-238). Because of these underlying variations, merely using a fixed threshold to infer significance might increase the proportion of false positives or false negatives. A better framework of inference of significance includes calculation of a statistic ranking genes according to their possibilities of differential expression (based on replicate array data), and selection of a cut-off value for rejecting the null-hypothesis that the gene is not differentially expressed (239).

Setting a cut-off for differential expression is tricky, because one has to balance the false positives (Type I error) and the false negatives (Type II error). Furthermore, performing statistical tests for tens of thousands of genes creates a multiple hypothesis-testing problem. For example, in an experiment with a 10,000-gene array in which the significance level α is set at 0.05, $10{,}000 \times 0.05 = 500$ genes would be inferred as

significant even though none is differentially expressed (236). Therefore, using a *p*-value of 0.05 is likely to exaggerate Type I errors. The multiple hypothesis testing problems is conventionally tackled by conservative approaches that control the family-wise error rate (FWER). Controlling the FWER limits the probability of making one or more type I errors to less than the α-value across the entire experiment, which limits the power to identify significantly differentially expressed genes (240). It is often acceptable for biologists to have few false positives if the majority of true positives are chosen, For example, an investigator might specify that it is acceptable for a small proportion of findings (for example, a maximum of 10%) to be wrong. Therefore, it is more practical to control the false discovery rate (FDR), the expected proportion of false positives among the number of rejected hypotheses (241).

SAM as was used here, a highly preferable new method for microarray data analysis, has been developed to utilize this FDR concept as a tool to assist in determining a cut-off after performing adjusted *t*-tests (http://www-stat.stanford.edu/tibs/SAM) (242).

Overview of Microarray Studies in the Porcine Adipose upon RAC Feeding

To the best of my knowledge, this study provides, for the first time with pigs, new insights into gene expression occurring in adipose tissue after 4 week RAC exposure. This was performed with the aid of microarray technology. A gene-by-gene approach would be very time consuming and technically challenging in this case because it would be difficult to obtain a global picture of differential gene expression patterns because there are insufficient individual porcine gene sequence data available to design primers for the many qRT-PCR runs required to test so many genes. In addition, at the present time there are a limited number of appropriate porcine specific cDNA are available for

Northern analysis of mRNA abundance. Thus, the decision was made to embark on a path using microarray technology which at least theoretically allows for expression analysis of thousands of mRNAs from a given tissue at once, and should provide a comprehensive assessment of multiple gene expression responses to given experimental variables.

In order to further explore mechanisms associated with RAC supplementation, we conducted a genomic analysis on adipose tissue collected on day 28 of the feeding trial. The microarray system returned 8,157 spots suitable for data analysis. Among 8,157 spots, 3,607 spots represented unknown genes. In this dissertation, unknown genes refer to spots whose oligo probe sequences were designed based on EST and whose spotted targets (their transcripts) were never annotated. After SAM analysis, 1,128 transcripts were detected as significantly different in the transcription level. Five hundred sixty-nine transcripts were down regulated, of which 284 out of the 569 transcripts were un-annotated genes. Five hundred fifty-nine transcripts were up regulated, and of those, 254 were non-annotated genes. In this microarray platform, nearly half of spotted targets (transcripts) were not annotated, and a large proportion of known transcripts are either involved in pathways unrelated to the purpose of this research or their functions are unknown. Based on the objectives of this study, we focused our attention on genes involved in the cAMP pathway, lipid metabolism, glycolysis pathway, TCA cycle and oxidative phosphorylation. The $\log_2$ratio values of genes of interest were presented in Table 6. In addition, for most up/down regulated top 200 genes, I presented the $\log_2$ratio value from each microarray analysis (representing each biological replication) in the Appendix I.

The expression concentration of PPARα, a transcription factor associated with regulation of fatty acid oxidation, was higher in the RAC-treated pigs. Expression of the gene CPTII was up regulated but expression of gene peroxisomal acyl-CoA oxidase was down regulated with RAC treatment (Table 6). The gene for leptin, an adipocyte –derived hormone, had a low expression level in the adipose tissue of RAC-treated pigs (Table 6). In RAC-treated pigs, we observed decreased expression of genes encoding key enzymes in lipogenesis such as acetyl-CoA carboxylase (ACC), fatty acid synthase (FAS), stearoyl-CoA desaturase (SCD), glucose transpoter 4 (GLUT4), fatty acid biding protein (FABP), long-chain fatty acid-CoA synthetase, and diacylglycerokinase in the adipose. For genes encoding for β-oxidation, expression of enoylCoA hydratase and hydroxyacyl-CoA dehydrogenase were down-regulated in RAC feeding pigs, but no difference was observed in ketoacyl-CoA thiolase (Table 6).

This study also found significant decreases in expression of genes participating in electron transport and oxidative phosphorylation in the adipose tissue after RAC treatment. Some of the most notable genes include those that encode pyruvate kinase, isocitrate dehydrogenase, succinate dehydrogenase, NADH dehydrogenease, cytochrome b, and ATPase (Table 6). The expression results for FAS, SCD, ACC, GLUT4 and leptin have been confirmed by independent experiments using Northern-blot in our laboratory (see discussion).

Pig has not been a model animal in genetics or genomics analysis, thus, the availability of pig microarray slides is quite restricted. The pig array used in this study is limited by the current state of research in pig genetics. Many genes which are potentially very important for this study such as lipoprotein lipase, aP2 (adipose fatty acid binding

protein), uncoupling protein, PPARγ, protein kinase A, and hormone sensitive lipase are unfortunately not included in this pig array.

Expression of Genes Involved with Fatty Acid Oxidation

In rodents and humans, the primary sites of fatty acid β oxidation are mitochondria within skeletal muscle, heart and liver (37), with adipose tissue representing a tissue that does not exhibit extensive fatty acid oxidation or need for ATP synthesis. Hence, the significance of changes in expression of genes involved in β oxidation, TCA cycle and electron transport pathways needs be further studied from a physiological perspective. These changes may or may not be of great physiological importance. PPARs belong to a family of nuclear transcription factors that function in a ligand-dependent manner. The tissue-specific expression pattern of PPAR isoforms is indication of their functions. In rodents and humans, PPARα is most abundant in liver although found in kidney, brown adipose tissue and heart (243), and it targets genes involved in fatty acid catabolism (β and ω oxidation pathways). In pigs, the expression of PPARα appears higher in adipose tissue than in liver (87), and the mechanism of PPARα activating fatty acid β oxidation pathways has not been well documented. In this study, the expression level of PPARα (log_2ratio=1.05) and CPT-II (log_2ratio=1.17) was significantly increased in RAC-treated pigs, but expression of genes in β-oxidation were not up-regulated by RAC. PPARα may act simply as a general sensor of overall tissue bulk fatty acid supply, providing coordinated changes in the capacity for fatty acid oxidation to prevent excessive triacylglycerol accumulation and subsequent development of obesity (72). In a circumstance of chronic stimulation of lipolysis by a catecholamine within a tissue with

limited oxidative capacity for fatty acids, the implication of increased PPARα expression is not clear.

Expression of CPTII (log_2ratio=1.17) was increased RAC-treated pigs. CPT-II, an enzyme that is associated with inner mitochondrial membrane, catalyzes the transfer of acyl residues from carnitine to CoA to form acyl-CoA thioesters that then enter β oxidation spiral. Here we have a coordinated expression between PPARα and CPTII; however, other genes encoding enzymes in the β oxidation pathway were down regulated in RAC-treated pigs, including short-chain acylCoA dehydrogenase and hydroxyacylCoA dehydrogenase. Ractopamine binds porcine ßAR and stimulates lipolysis (161, 165). Peterla et al. (244) found lipolysis (release of glycerol and free fatty acids) was stimulated by RAC in porcine adipose tissue explants *in vitro*. In well-fed pigs, adipose is a major energy storage tissue not a major energy mobilizing tissue. From the findings of enhanced lipolysis by BAA *in vivo*, it is safe to say that arising fatty acids in response to BAA are not reincorporated into adipose storage TAG or oxidized to produce energy in the adipose under chronic RAC influence, but would become available for oxidation in skeletal muscle and liver. The microarray analysis was only conducted on adipose tissue, thus there are no data about overall gene expression pattern in other tissues upon RAC feeding. However, in other studies on RAC-fed pigs, Halsey (162) and Gottschalk (195) presented some preliminary data that RAC increased mRNA abundance of acyl-CoA dehydrogenase (ACDH), CPT1 and lipoprotein lipase (LPL) in porcine longissimus muscle tissue.

HSL is the primary enzyme that hydrolyzes triacylglycerol stored in adipose tissue. Agonist stimulation of β-adrenergic receptors ultimately activates HSL via PKA-

dependent phosphorylation (29) and immunoassays have suggested that the activity of HSL is primarily regulated by covalent modification via reversible phosphorylation (245). Thus, HSL activity is principally controlled at the post-translational level (246). Because an oligo probe of HSL was not included in the present pig array platform, no information about any putative effect of RAC on gene expression of HSL could be obtained from this study.

Peffer et al. (247) found that supplementation of clofibrate, a strong PPARα expression enhancer, did not result in measurable changes in expression of PPARα and CPT-1 in the liver of young pig. However, Odle et al. (248) found a 5 fold induction of CPT-1 activity coincident with elevated mRNA abundance for PPARα upon clofibrate supplementation in young pigs. Thus, work form the same laboratory led to opposite finding in young piglets and the relationship between PPARα (transcription factor promoting fatty acid oxidation) and CPT-1 (rate limiting enzyme for fatty acid flux into mitochondria) at gene expression level needs be further studied. Peffer et al. (247) also found no changes in rates of hepatic β oxidation of [1-^{14}C]-palmitate and CPT-1 activities when suckling piglet were treated by isoproterenol (another BAA) for 12 days. Thus, BAA did not activate CPT-1 and β oxidation in the liver of young pigs. More research is needed to clarify if the mechanism of PPARα regulating β oxidation exists in porcine adipose tissue and if BAA attenuates fat deposition through regulatory mechanism involving PPARα. To what degree these dissimilarities in gene expression behavior are related to differences in the age of the pigs and liver versus adipose tissue can not be discerned based on limited literature in the pig study.

Expression of Genes Involved in Fatty Acid Synthesis

This study showed significant decreases in the expression of genes encoding key enzymes in *de novo* fatty acid synthesis and triacyglycerol synthesis, such as FAS (log_2ratio= –1.16), ACC (log_2ratio= –1.28), malate dehydrogenase (log_2ratio= –1.04) and fatty acid binding protein (FABP) (log_2ratio= –1.45). FAS and ACC are the principal enzymes for *de novo* fatty acid synthesis, and malate dehydrogenase is involved in NADPH generation for lipogenesis. FABP binds long-chain fatty acids and plays important roles in fatty acid uptake, transport and metabolism.

Expression of Stearoyl CoA desaturase SCD (log_2ratio= –2.76) was depressed in response to RAC. SCD is the rate-limiting enzyme in the *cis*-desaturation process of FA. The oxidative reaction converts saturated FA myristic, palmitic and stearic acid into their corresponding delta-9 monounsaturated FA (249). SCD gene expression is activated through cAMP during early preadipocyte differentiation (250). However, this cAMP induction of SCD transcripts has only been shown in pre-adipocytes and not in mature adipocytes (250). The induction of SCD expression directly corresponds to accumulation of fat droplets. Cyclic AMP response element binding protein (CREB) is the transcription factor often responsible for mediating cAMP induction, but no CREB response elements have been identified in the SCD promoter (250). In this study, decreased SCD expression by RAC might relate to effect of RAC in attenuating fat deposition in the porcine adipose tissue, but the mechanism is unknown.

Expression of Glucose Transporter 4 (GLUT4) (log_2ratio= –0.77) was shown a decreased tendency in response to RAC**.** The first step of glucose metabolism is the transport of glucose across the plasma membrane of glucose-sensitive tissues by glucose

transporters (37). The major isoform of this protein in muscle and adipose tissues is GLUT4. Glucose uptake is an insulin-stimulated process in the adipocyte. Glycolysis is the fate of glucose in the adipose tissue. Porcine adipose tissue specifically is the major glucose utilizing tissue and metabolizes 40% of the daily glucose uptake (37). The expression of GLUT4, therefore, can be a direct reflection of lipogenic activity in the pig. Exposure of 3T3-L1 adipocyte to cAMP for 24 h causes a down-regulation of GLUT4, both at mRNA and protein levels, and a decrease in insulin-mediated glucose transport (251). Vinals et al. (252) demonstrated that presence of cAMP analogues repressed GLUT4 protein and mRNA expression in cultured cells, but the mechanism is not clear because of limit information about promoter structure of GLUT4 gene.

The down-regulated expression of genes involved in lipogenesis indicated that effect of RAC in modifying pork quality involved controlling expression of genes in lipid metabolism, and this was consistent with my hypothesis for this study. Other studies from the Bergen lab using Northern blots, conducted before the present study with the same pig adipose tissue, have showed that expression of genes for FAS, SREBP, GLUT4 and SCD was decreased in response to RAC, indicating that the data for these genes obtained from the present oligo array analysis are confirmed (162-163).

Decreased expressions of genes encoding enzymes in energy metabolism (glycolysis, citric acid cycle and electron transport chain) were observed in the present study in adipose tissue of RAC-treated pigs, including pyruvate kinase (log_2ratio= –1.58), isocitrate dehydrogenase (log_2ratio= –1.22), succinate dehydrogenase (log_2ratio= –1.75), NADH dehydrogenase (log_2ratio= –1.36), cytochrome b (log_2ratio= –1.31), and ATPase (log_2ratio= –1.56). Because most of above enzymes are also controlled by allosteric and

covalent regulation, it is not appropriate to make inference about the activities of related metabolic pathways based on the transcription response alone. In a tissue not predominantly involved in oxidative metabolism, the physiological implications of these results are unclear.

In RAC-treated pigs, I found decreased expression of leptin (log_2ratio= –1.5) in the adipose tissue. Thacker (163) also found that RAC lowered leptin expression in the adipose tissue using Northern blotting. Leptin is the product of the ob gene, a protein predominately secreted by adipocytes (253). Leptin action is exerted through specific receptors that are highly expressed in many tissues (254). Leptin acts on the brain to control food intake, energy expenditure and endocrine functions (255-256). The primary role of leptin is still unclear; however, it is thought that the protein may serve in the feedback regulation of adipose mass on feed intake. Furthermore, studies in rats have shown that leptin simultaneously induces lipolysis and lipid oxidation (222,257). It has been demonstrated that body fat content correlates with circulating plasma leptin concentration in human (258-259) but Wauters (260) suggested that the vast majority of human obesity can not be attributed to defects in leptin or its receptors, since they observed elevated concentration of leptin in obese people (260). The connection between leptin, lipogenesis and energy metabolism is still unclear. Further research is needed to find correlations between RAC, leptin and fat deposition in pigs.

Limited Independent Verification of Microarry Analysis Data

It is necessary to confirm microarray data using an alternate technology, such as quantitative real-time PCR, Northern blot or *in situ* hybridization (261). Validation does not necessarily need to be performed for every gene of interest, but should be related to

the biological conclusion generated from the data. There is no absolute requirement for the amount of validation that needs to be included, but the more verification has been included, the more reliable the data will be deemed and the more useful any such study will become (262).

The microarray data from this study can be confirmed by the previous work in our lab. Previous members of our lab determined the expression of some key genes related to lipid metabolism by Northern blot using same adipose tissue from same pigs. Expression of SREBP-1, FAS, SCD, and GLUT4 was lower ($P<0.05$) in the adipose tissue when pigs were treated by 60ppm ractopamine for 28 days (Fig6). mRNA abundance of leptin in the porcine tissues was also decreased by RAC using Northern blotting (237). In this oligo array study, the $\log_2$ (60ppm/0ppm) values for SREBP-1, FAS, SCD, GLUT4 and leptin were -0.76, -1.16, -2.76, -0.77 and -1.5 respectively.

Fig 6. Effect of feeding 0, 20, 60 ppm of ractopamine on mRNA abundance of FAS, SREBP-1, GLUT4, SCD and housekeeping gene (β-actin) in porcine adipose tissues from crossbreed pig (162-163). mRNA abundances were measured by Northern blotting as described in the thesis of Halsey (162) and Thacker (163). A, SREBP-1; B, FAS; C, GLUT4; D. SCD (day 28). For each gene, blots displayed above the tabulated data in graph from show the gene of interest on the upper and housekeeping gene on the lower portion on day 28 of the study. Lanes of blots are from left to right: 1 and 2, 0ppm; 3 and 4, 20 ppm and 5 and 6, 60ppm ractopamine respectively. For each lane data are from an individual pig. Expression data (normalized using β actin) for each gene are presented in

a graphical format for all sampling times (n=3). Columns not sharing common letter (within gene/day category) were significantly different ($P<0.05$).

CONCLUSION

Feeding RAC to pigs induces changes in the gene expression of adipose tissue. These changes mainly involve increases in the transcription of PPARα and CPTII genes, decreases in fatty acid oxidizing enzymes and decreases in genes encoding enzymes in fatty acid synthesis and electron transport. These data provide an overview of RAC action on the RNA abundance of genes in the adipose tissue. This research revealed some candidate genes, such as cytosolic phospholipase A2 (log_2ratio= -1.555), porcine interleukin2 (log_2ratio=1.899) apolipoprotein precursor (log_2ratio= - 2.158), that might be useful to elucidate mechanisms underlying the anti-adipogenic effect of RAC in pigs in the future research. Other mRNA quantification assays are necessary to confirm results of microarray analysis, and further assays to measure enzyme activities or protein concentration of key enzymes are important to determine the physiological changes of pigs in response to RAC supplemention in the diet.

Table 5. List of metabolic pathways and genes of interest for this dissertation present on the pig array

Genbank/ embl Accession No.	Gene Name
fatty acid oxidation and Lipolysis	
P23786	Carnitine O-palmitoyltransferaseII[Human], partial (34%)
NM_213897	long-chain acyl-CoA dehydrogenase [Sus scrofa]
NM_213898	short-chain acyl-CoA dehydrogenase [Sus scrofa]
NM_001359	mitochondrial 2,4-dienoyl-CoA reductas[human]
AY344366	peroxisome proliferator activated receptor alpha [Sus scrofa]
NM_213901	Propionyl-CoA carboxylase beta chain precursor [Sus scrofa]
AAH08906.1	enoyl Coenzyme A hydratase short chain 1 mitochondrial {Homo sapiens}, partial (50%
O02691	3-hydroxyacyl-CoA dehydrogenase type II [Bovine] complete
AAB30019.2	peroxisomal acyl-coenzyme A oxidase {Homo sapiens}, partial (52%)
AAF12736.1	acyl-Coenzyme A dehydrogenase-8 precursor {Homo sapiens}, partial (54%)
EGAD45512	3-hydroxyisobutyryl-coenzyme A hydrolase {Homo sapiens}, partial (49%)
AAH12172.1	acetyl-CoA synthetase {Homo sapiens}, partial (33%)
Q99424	Acyl-coenzyme A oxidase 2 peroxisomalpartial (15%)
AAH11968.1	2 4-dienoyl CoA reductase 2 peroxisomal {Homo sapiens}, partial (58%
AAH00286.1	malonyl-CoA decarboxylase {Homo sapiens}, partial (46%)
AAF60277.1	carnitine palmitoyltransferase I {Ovis aries}, partial (32%)
BAA29057.1	very-long-chain acyl-CoA dehydrogenase {Homo sapiens}, partial (27%)
AAH01964.1	acyl-Coenzyme A dehydrogenase family member 8 {Homo sapiens}, partial (42%)
AF185048	acyl-CoA oxidase [Sus scrofa]
NM_213966	long-chain 3-ketoacyl-CoA thiolase [Sus scrofa]
NM_214315	hormone-sensitivelipaseHSL[Susscrofa]
CAB76256.1	enoyl coA/acyl coA hydratase/dehydrogenase complete
Fatty acid synthesis and triacylglycerate synthesis	
Z97186	stearoyl-CoA desaturase [Sus scrofa]
NM_214051	diacylglycerol acyltransferase [Sus scrofa]
NM_001004046	liver fatty acid binding protein [Sus scrofa]
AY700218	CCAAT/enhancer binding protein alpha [Sus scrofa]
U97256	cytosolic glycerol-3-phosphate dehydrogenase [Sus scrofa]
NM_214060	esterase D [Sus scrofa]
X98558	heart fatty acid-binding protein [Sus scrofa]
AJ416020	partial mRNA for adipocyte fatty acid-binding protein [Sus scrofa]
X94251	glyceraldehyde-3-phosphate dehydrogenase [Sus scrofa]
Q06055	ATP synthase lipid-binding protein mitochondrial precursor, complete{Homo sapiens}

AAH01918.1	acetyl-Coenzyme A acyltransferase 2 {Homo sapiens}, partial (20%)
P33121	HUMAN Long-chain-fatty-acid--CoA ligase 2 partial (24%)
P55052	BOVIN Fatty acid-binding protein epidermal (E-FABP), complete
BAA00401.1	mitochondrial acetoacetyl-CoA thiolase precursor {Rattus sp.}, partial (40%)
P36956	HUMAN Sterol regulatory element binding protein-1 (SREBP-1), partial (21%)
G01880	fatty-acid synthase (EC 2.3.1.85) (version 2) - human, partial (7%
BAA95446.1	acetyl-CoA transporter {Rattus norvegicus}, partial (41%)
AAC50478.1	diacylglycerol kinase zeta {Homo sapiens}, partial (28%)
P48201	HUMAN ATP synthase lipid-binding protein mitochondrial precursor, complete
EGAD 125291	ATP lipid-binding protein P1 precursor {Sus scrofa}, complete
AAH00618.1	elongation of very long chain fatty acids {Homo sapiens}, complete
O95573	HUMAN Long-chain-fatty-acid--CoA ligase 3
BAA86054.1	fatty acid coenzyme A ligase 5 {Homo sapiens}, partial (14%)
AAK84175.1	diacylglycerol acyltransferase 2 {Mus musculus}, partial (49%)
AAA41145.1	fatty acid synthase {Rattus norvegicus}, partial (6%)
BAB47242	CREB/ATF family transcription factor {Homo sapiens}, partial (32%)
Q9TTS3	BOVIN Acetyl-CoA carboxylase 1partial (7%)
AAK01477.1	C/EBP-induced protein {Homo sapiens}, partial (25%)
AY496867	adipocyte determination and differentiation-dependent factor 1 [Sus scrofa]
AF175308	acetyl-CoA carboxylase [Sus scrofa]
AF103945	CCAAT/enhancer binding protein beta [Sus scrofa]
AF252267	acetyl-CoA carboxylase alpha [Sus scrofa]
BAA20097.1	CCAAT/enhancer-binding delta protein {Bos taurus}, partial (54%)
Glycolytic/glucogenesis pathway	
L06944	succinyl-CoA synthetase beta-subunit
J03489	pyruvate dehydrogenase (lipoamide) [Sus scrofa domestica]
A29170	phosphopyruvate hydratase alpha - human, complete
AJ251197	pyruvate kinase [Sus scrofa]
AF217652	glucose-6-phosphatase catalytic subunit [Sus scrofa]
Q16654	HUMAN [Pyruvate dehydrogenase [lipoamide]] kinase isozyme 4 mitochondrial precursor, partial (18%)
AF008589	succinyl-CoA synthetase alpha subunit [Sus scrofa]
X17058	glucose transport protein [Sus scrofa]
M21197	citrate synthase precursor
M86719	NADPH-specific isocitrate dehydrogenase
NM_213980	UDP glucose pyrophosphorylase [Sus scrofa]
M16427	malate dehydrogenase precursor
AF061966	ATP-specific succinyl-CoA synthetase beta subunit [Sus scrofa]
A29170	phosphopyruvate hydratase alpha - human, complete
AJ300475	succinate dehydrogenase {Sus scrofa}, complete
P00883	RABIT Fructose-bisphosphate aldolase A [Rabbit], partial (24%)
P70404	MOUSE Isocitrate dehydrogenase [NAD] subunit gamma mitochondrial

	precursor, complete
P12382	MOUSE 6-phosphofructokinase liver type, partial (33%)
AAH01454.1	phosphoenolpyruvate carboxykinase 2 (mitochondrial) {Homo sapiens}, partial (23%)
AF054835	glucose transporter type 2; GLUT-2 [Sus scrofa]
AF141956	GLUT4 [Sus scrofa]
P00883	Fructose-bisphosphatealdolase A(EC4.1.2.13)(Muscle-typealdolase).[Rabbit].partial(24%)
S52485	glucokinase regulator - human, partial (26%)
AAB59563.1	glucokinase {Homo sapiens}, partial (40%)
AJ557236	pyruvate kinase M2 {Sus scrofa}, complete
AAH05811.1	pyruvate dehydrogenase kinase isoenzyme 2 {Homo sapiens}, partial (53%)
A54113	pyruvate kinase - rabbit, partial (13%)
Cholesterol/sterol metabolism	
CV876047	3-beta-hydroxysteroid dehydrogenase/delta-5-delta-4 isomerase [Sus scrofa]
U84399	steroidogenic factor-1 SF-1 [Sus scrofa]
NM_213911	steroid membrane binding protein [Sus scrofa]
AF414124	11-beta hydroxysteroid dehydrogenase isoform 1 [Sus scrofa]
CAB41234.1	(sterol regulatory element binding transcription factor 2) {Homo sapiens}, partial (18%)
AAC39922.1	sterol/retinol dehydrogenase {Homo sapiens}, complete
AAH10570.1	3-hydroxymethyl-3-methylglutaryl-Coenzyme A lyase (hydroxymethylglutaricaciduria) {Homo sapiens}, complete
Q15738	HUMAN NAD(P)-dependent steroid dehydrogenase, partial (53%)
CAC88111	17beta hydroxysteroid dehydrogenase {Homo sapiens}, partial (23%)
DQ020476	sterol regulatory element binding protein-2 [Sus scrofa]
S79678	3-hydroxy-3-methylglutaryl coenzyme A reductase/HMG-CoA reductase [Sus scrofa]
NM_213988	steroid 5-alpha-reductase 2 [Sus scrofa]
Q15800	C-4 methyl sterol oxidase. [Human] {Homo sapiens}, partial (43%)
NM_214306	17beta-estradiol dehydrogenase [Sus scrofa]
AAH00054.1	7-dehydrocholesterol reductase {Homo sapiens}, complete
A42912	3alpha(or 20beta)-hydroxysteroid dehydrogenase - pig, complete
Lipid transport, Lipoprotein/apolipoprotein	
M22646	apolipoprotein B
NM_001002801	apolipoprotein C-III
AJ222966	apolipoprotein A-IV [Sus scrofa]
AF467889	high density lipoprotein receptor SR-BI [Sus scrofa]
NM_214308	apolipoprotein-E [Sus scrofa]
X59414	apolipoprotein A-I [Sus scrofa]
AF118147	low density lipoprotein receptor [Sus scrofa]
AAB36587.1	ABC-transporter {Gorilla gorilla}, partial (54%)
S71363	probable ATP-binding cassette transporter ABC-3 - human, partial (10%)

AAH14305.1	Similar to high density lipoprotein binding protein (vigilin) {Homo sapiens}, partial (23%)
P18656	Apolipoprotein A-II precursor (Apo-AII). [Crab eating macaque Cynomolgus monkey], complete
AAD15748.1	ATP-binding cassette protein M-ABC1 {Homo sapiens}, partial (31%)
AF074421	putative ABC-transporter [Sus scrofa]
Q07954	HUMANLow-densitylipoproteinreceptor-relatedprotein1precursor(LRP).partial(5%)
AAH14305.1	Similartohighdensitylipoproteinbindingprotein(vigilin){Homosapiens}.partial(23%)
JE0272	lowdensitylipoproteinreceptor-relatedprotein6-human.partial(15%)
Amino acid/protein metabolism	
O15371	Eukaryotic translation initiation factor 3 subunit 7 (eIF-3 zeta){Homo sapiens}, partial (72%)
Q07205	IF5_RAT Eukaryotic translation initiation factor 5 (eIF-5). {Rattus norvegicus}, partial (32%)
P29562	Eukaryotic initiation factor 4A-I (eIF4A-I) (Fragment). [Rabbit] {Oryctolagus cuniculus}, partial (63%)
AAG34759.1	amino acid transporter SLC3A1 {Canis familiaris}, partial (20%)
P23588	HUMAN Eukaryotic translation initiation factor 4B (eIF-4B). {Homo sapiens}, partial (27%)
P17425	RAT Hydroxymethylglutaryl-CoA synthase cytoplasmic (HMG-CoA synthase), partial (28%)
P50441	PIG Glycine amidinotransferase
NM_001005208	albumin [Sus scrofa]
NM_214048	arginase I [Sus scrofa]
X86791	beta-globin [Sus scrofa]
AY013261	glycoprotein [Sus scrofa]
AJ429141	ribosomal protein S4 [Sus scrofa]
NM_214066	D-amino acid oxidase (EC 1.4.3.3)
NM_213927	cytosolic aspartate aminotransferase
NM_001001638	60S ribosomal protein L35 [Sus scrofa]
NM_214363	40S ribosomal protein S12 [Sus scrofa]
D13308	glycine N-methyltransferase [Sus scrofa]
AF044259	non-muscle myosin light chain [Sus scrofa]
AF239165	serine hydroxymethyltransferase [Sus scrofa]
D00524	acylamino acid-releasing enzyme [Sus scrofa]
D89497	smooth muscle myosin light chain kinase [Sus scrofa]
Z84093	L-aromatic amino acid decarboxylase, pkDDC [swine, kidney]
NM_213896	aminoacylase-I [Sus scrofa]
T08757	probable translation initiation factor eIF-2B delta chain - human (fragment), partial (61%
P04720	HUMAN Elongation factor 1-alpha 1 (EF-1-alpha-1)

P23396	HUMAN 40S ribosomal protein S3
A39760	ribosomal protein S16 cytosolic [validated] - human, partial (65%)
JC2369	ribosomal protein L15 cytosolic [validated] - rat, complete
AAG15419.1	eukaryotic translation initiation factor 3 subunit p42/p44 {Homo sapiens}, complete
AAC84044.1	translation initiation factor eIF3 p40 subunit; eIF3p40 {Homo sapiens}, partial (44%)
Q16576	HUMAN Histone acetyltransferase type B subunit 2, partial (19%)
P25112	40S ribosomal protein S28. {Rattus norvegicus}, complete
AAL31549.1	glutathione transferase T1-1 {Homo sapiens}, complete
AAK20884.1	arginine N-methyltransferase p82 isoform {Cricetulus longicaudatus}, partial (26%)
O15372	Eukaryotic translation initiation factor 3 subunit 3 (EIF-3 gamma). [Human], partial (41%)
S49172	translation initiation factor eIF-4 gamma - human (fragment), partial (14%)
Q28690	Translation initiation factor eIF-2B beta subunit (eIF-2B GDP-GTP exchange factor). [Rabbit], partial (50%)
P34897	Serine hydroxymethyltransferase mitochondrial precursor (Serine methylase), partial (31%)
AAB71410.1	eukaryotic translation initiation factor XeIF-4AIII {Xenopus laevis}, partial (33%)
GP 5107727	Human Translation Initiation Factor Eif1 Nmr 29 Structures, partial (89%)
S18294	translation elongation factor eEF-2 - human, partial (19%)
P56537	Eukaryotic translation initiation factor 6 (eIF-6) (B4 integrin interactor), complete
S25432	translation elongation factor eEF-1 beta chain - human, complete
AAC28633.1	putative nuclear protein {Homo sapiens}, partial (60%)
AAH05392.1	eukaryotic translation initiation factor 4E-like 3 {Homo sapiens}, partial (89%)
AAH16670.1	Similar to argininosuccinate lyase {Mus musculus}, partial (56%)
P49410	Elongation factor Tu mitochondrial precursor.{Bos taurus}, partial (66%)
AAF21465.1	kidney and liver proline oxidase 1 {Homo sapiens}, partial (47%)
A53048	translation initiation factor eIF-2 gamma chain [validated] - human, partial (29%)
P23588	Eukaryotic translation initiation factor 4B (eIF-4B). {Homo sapiens}, partial (33%)
AAK11184.1	histone deacetylase 3 {Rattus norvegicus}, partial (50%)
AAA52524.1	glutamate dehydrogenase {Homo sapiens}, partial (53%)
Q27991	BOVIN Myosin heavy chain nonmuscle type B (Cellular myosin heavy chain type B), partial (19%)
Q9QZ81	Eukaryotic translation initiation factor 2C 2 (eIF2C 2) (Golgi ER protein 95 kDa), partial (38%)
AAB48437.1	arginine N-methyltransferase 2 {Homo sapiens}, partial (29%)
B31486	translation initiation factor eIF-5A [validated] - human, complete
AAA62667.1	myosin-IC {Homo sapiens}, partial (28%)
S18294	translation elongation factor eEF-2 - human, partial (25%)
Q9TSZ7	Aminomethyltransferase mitochondrial precursor (Glycine cleavage system

	T protein), partial (29%)
P20132	L-serine dehydratase{Homo sapiens}, partial (37%)
P26443	Glutamate dehydrogenase mitochondrial precursor{Mus musculus}, partial (32%)
Q9XSJ7	Collagen alpha 1(I) chain precursor.{Canis familiaris}, partial (5%)
S31212	collagen alpha 1(XIV) chain precursor short form - chicken, partial (12%)
O46392	Collagen alpha 2(I) chain precursor.{Canis familiaris}, partial (12%)
BAA01185.1	alanine aminotransferase {Rattus norvegicus}, partial (24%)
A26711	translation initiation factor eIF-2 alpha chain - rat, partial (62%)
EGAD 136325	neutral and basic amino acid transporter protein {Sus scrofa}, complete
AF044969	collagen VIII alpha 1 [Sus scrofa]
AF041024	alpha-1 type VII collagen [Sus scrofa]
AF222917	myosin light chain kinase[Sus scrofa]
NM_214136	myosin heavy chain [Sus scrofa]
AF437511	carbamoyl-phosphate synthetase 1 [Sus scrofa domestica]
EGAD 4603	collagen type VI alpha 1 {Homo sapiens}, partial (7%)
Q04857	Collagen alpha 1(VI) chain precursor. [Mouse]partial (13%)
AAC31665.1	Myosin heavy chain (MHY11) (5'partial) {Homo sapiens}, partial (10%)
M21683	non-histone protein HMG1
CAA57702.1	glutamine--phenylpyruvate aminotransferase {Homo sapiens}, complete
AY372187	beta-lactoglobulin [Sus scrofa]
S32425	glutathione transferase - human, complete
AAD02563.1	mitochondrial branched chain aminotransferase precursor; BCATm {Ovis aries}, partial (21%)
Q28640	(Histidine-proline rich glycoprotein) (HPRG) (Fragment)., partial (34%)
CAC22253	alanine:glyoxylate aminotransferase 2 homolog 1 splice form 1 {Homo sapiens}, partial (28%)
AJ309014	myosin heavy chain [Sus scrofa]
U11771	fast myosin heavy chainmyosin heavy chain [Sus scrofa]
AAB65435.1	elongation factor 1 alpha {Bos taurus}, partial (24%)
A53019	collagen alpha 1(XVIII) chain - human (fragment), partial (17%)
P12234	Phosphate carrier protein mitochondrial precursor (PTP). {Bos taurus}, partial (54%)
P52943	Cysteine-rich protein 2 (CRP2) {Homo sapiens}, partial (35%)
Electron transport and oxidative phosphorylation	
S27226	NADH dehydrogenase (ubiquinone) (EC 1.6.5.3) 14.5K chain - bovine, complete
P34943	BOVIN NADH-ubiquinone oxidoreductase 39 kDa subunit mitochondrial precursor, partial (37%)
AY786556	cytochrome c oxidase subunit I [Sus scrofa]
AW574405	NADH2 [Sus scrofa]
AW574375	NADH3 [Sus scrofa]
DQ020119	cytochrome b [Sus scrofa]
AW584050	NADH4 [Sus scrofa
P24311	Cytochrome c oxidase polypeptide VIIb mitochondrial precursor. [Human]

	{Homo sapiens}, complete
AAG28221.1	ATPase6{Susscrofa}.partial(71%)
O14521	HUMAN Succinate dehydrogenase [ubiquinone] cytochrome B small subunit mitochondrial precursor (CybS), complete
NM_214291	(H++K+)-ATPase
	ATPasealpha-subunit(aa1-1021)[Susscrofa]
X16951	Ca(2+)-transportATPase(class2)[Susscrofa]
AAH06949.1	SimilartoATPaseclassIItype9A{Musmusculus}.partial(19%)
P11019	BOVINVacuolarATPsynthasesubunitE.partial(76%)
O75185	robablecalcium-transportingATPase{Homosapiens}.partial(40%)
CAB96823.1	(novelATPase){Homosapiens}.partial(41%)
P12953	HUMANVacuolarATPsynthasesubunitd.partial(81%)
P79251	BOVINVacuolarATPsynthasesubunitG1.complete
cAMP pathway	
AF319662	G protein-coupled receptor[Sus scrofa]
AJ005981	cAMP-regulated phosphoprotein [Sus scrofa]
U12148	5'-AMP-activated protein kinase catalytic alpha-2 subunit
U95009	cyclic AMP-responsive element binding protein, delta variant [Sus scrofa]
Q01518	Adenylyl cyclase-associated protein 1 (CAP 1). [Human] {Homo sapiens}, complete
P18848	HUMAN Cyclic-AMP-dependent transcription factor ATF-4 (Activating transcription factor 4), complete
Q9Y2B9	cAMP-dependent protein kinase inhibitor gamma form (PKI-gamma). [Human] {Homo sapiens}, complete
P43250	G protein-coupled receptor kinase GRK6 {Homo sapiens}, partial (30%)
AAC51339.1	CREB-binding protein {Homo sapiens}, partial (41%)
BAB47242	CREB/ATF family transcription factor {Homo sapiens}, partial (32%)
P54619	5'-AMP-activated protein kinase gamma-1 subunit (AMPK gamma-1 chain) (AMPKg). [Human], partial (53%)
AJ251728	alpha-1A adrenergic receptor [Sus scrofa]
NM_214138	protein kinase A anchoring protein
B31927	GTP-binding regulatory protein Gs alpha chain (adenylate cyclase-stimulating) splice form 2 -, partial (54%)
BAB47242	CREB/ATFfamilytranscriptionfactor{Homosapiens}.partial(32%)
Q9Y2D1	HUMANCyclic-AMP-dependenttranscriptionfactorATF-5(Activatingtranscriptionfactor5).partial(24%)
P18848	HUMANCyclic-AMP-dependenttranscriptionfactorATF-4.complete
Miscellanous (transcription factor, hormones, phosphatase)	
AAH01221.1	nuclear receptor binding protein {Homo sapiens}, partial (53%)
AF053922	retinoid X receptor beta [Sus scrofa domestica]
AF102858	insulin receptor [Sus scrofa]
AF128438	insulin receptor precursor [Sus scrofa]
NM_213840	leptin[Susscrofa]
AF184172S2	Sus scrofa leptin receptor (LEPR) gene, exon 4 and partial cds
O08950	RATTranscriptioninitiationfactorIIAgammachain(TFIIAP12subunit).comple

	te
S12741	transcriptionfactorATF-a-human.partial(35%)
Q63801	TranscriptioninitiationfactorTFIID70kDasubunit(TAFII-70)[Rat].partial(59%)
Q16594	TranscriptioninitiationfactorTFIID31kDasubunit(TAFII-32).[Human].partial(41%)
Q15544	HUMANTranscriptioninitiationfactorTFIID28kDasubunit(TAFII28).partial(54%)
T03829	transcriptionfactorTFII-I-human.partial(9%)
Q16514	HUMANTranscriptioninitiationfactorTFIID20/15kDasubunits.partial(68%)
P29053	TranscriptioninitiationfactorIIB(TFIIB).[Rat].partial(80%)
AAD46767.1	TFIIDsubunitTAFII55{Musmusculus}.partial(20%)
Q92759	HUMANTFIIHbasaltranscriptionfactorcomplexp52subunit(Basictranscriptionfactor52kDasubunit).partial(44%)
AAK28025.1	proteintyrosinephosphataseTD14{Homosapiens}.partial(11%)
S44454	transcriptionfactorBTF2chainp44-human.partial(41%)
S10099	transcriptionfactorITF-1-human(fragment).partial(37%)
AAH01454.1	phosphoenolpyruvatecarboxykinase2(mitochondrial){Homosapiens}.partial(23%)
AAC24498.1	phospholipaseD2{Homosapiens}.partial(47%)
AAD15617.1	similartoGilamonsterphospholipaseA2{Homosapiens}.partial(81%)
CAC69306	phospholipaseA2{Homosapiens}.partial(38%)
AAD32135.1	cytosolicphospholipaseA2beta;cPLA2beta{Homosapiens}.partial(18%)
AAK14906.1	phospholipaseCbeta-3{Rattusnorvegicus}.partial(28%)
Q15172	HUMANSerine/threonineproteinphosphatase2A56kDaregulatorysubunitalphaisoform.partial(59%)
AAL09472.1	groupXIIIsecretedphospholipaseA2{Homosapiens}.partial(93%)
AAD30424.1	calcium-independentphospholipaseA2{Homosapiens}.partial(13%)
Q28653	RABITSerine/threonineproteinphosphatase2A56kDaregulatorysubunitdeltaisoform.partial(25%)
S28173	phosphoproteinphosphatase(EC3.1.3.16)Xcatalyticchain-human.partial(48%)
AB016735	proteinphosphatase-1delta[Susscrofa]
AAF64456.1	ELKLmotifkinase2shortform{Musmusculus}.partial(65%)
P67776	proteinphosphatase2Aalphasubunit
M80709	20-beta-hydroxysteroiddehydrogenase

Table 6. Statistic analysis was performed by SAM. One-class response with 1,000 permutations was used to determine genes whose expression was significantly different from zero (log_2ratio=log_2treatment/control). At these analysis parameters, the false discovery rate (FDR) for the positive genes was 0.05 (5%); the q value (a measure of significance in terms of the false discovery rate) for all biological replicates were less than 0.003. Different from normal t-test, FDR instead of q value was used to control limits of significant analysis as described in the Material and Methods. In this table, the genes with bold log_2ratio values are differently expresses genes. Positive value means higher expression in treatment group (60ppm Paylean); negative value means lower expression in treatment group.

Gene	log_2ratio
fatty acid oxidation	
CarnitineO-palmitoyltransferaseIImitochondrialprecursor (CPTII). {Homosapiens}.partial(34%)	**1.17323**
mitochondrial2.4-dienoyl-CoAreductase{Homosapiens}.	**-1.27451**
Peroxisomeproliferatoractivatedreceptoralpha(PPARα)[Susscrofa]	**1.04572**
enoylCoenzymeA hydrataseshortchain1, mitochondria {Homosapiens}.partial(50%)	**-2.47947**
hydroxyacyl-CoAdehydrogenasetypeII(TypeIIHADH).[Bovine] complete	**-1.73103**
peroxisomalacyl-coenzymeAoxidase{Homosapiens}.partial(52%)	**-1.81188**
very-long-chainacyl-CoAdehydrogenase{Homosapiens}.partial(27%)	0.73684
long-chain3-ketoacyl-CoAthiolase[Susscrofa]	-0.66613
fatty acid synthesis	
stearoyl-CoAdesaturase[Susscrofa]	**-2.76398**
esteraseD[Susscrofa]	**-1.56863**
Fattyacid-bindingproteinepidermal(E-FABP).	**-1.45161**
fatty-acidsynthase (version2)-human.partial(7%)	**-1.15948**
diacylglycerolkinasezeta{Homosapiens}.partial(28%)	**-1.09199**
ATPsynthaselipid-bindingproteinmitochondrialprecursor	**-1.99459**
HumanLong-chainacyl-CoAsynthetase3(LACS3)	**-1.77748**
fattyacidcoenzymeAligase5 {Homosapiens}.partial(14%)	**-1.30171**
Acetyl-CoAcarboxylase1(ACC-alpha) [Susscrofa]	**-1.13074**
acetyl-CoAcarboxylase[Susscrofa]	**-1.28647**

cAMP pathway	
Gprotein-coupledreceptor3[Susscrofa]	0.47979
cAMP-regulatedphosphoprotein[Susscrofa]	-0.46759
5'-AMP-activatedproteinkinasecatalyticalpha-2subunit3	-0.54501
HuamnCyclic-AMP-dependenttranscriptionfactorATF-4(Activatingtranscriptionfactor4) complete	**-1.63231**
HUMANcAMP-dependentproteinkinase inhibitorgammaform(PKI-gamma).{Homosapiens}complete	0.46832
proteinkinaseAanchoringprotein3	**0.81146**
proteinphosphatase-1delta[Susscrofa]	**-1.46678**
Serine/threonineproteinphosphatase2A56kDaregulatorysubunitdeltaisoform.{Homosapiens}.partial(25%)	**-1.6**
lipoprotein	
apolipoproteinC-III3	**1.48956**
highdensitylipoproteinreceptorSR-BI[Susscrofa]3	**-1.1438**
weaklysimilartoPIRS71363S71363probableATP-bindingcassettetransporterABC-3-human.partial(10%)3	**1.25436**
homologuetoGP15679991gbAAH14305.1Similartohighdensitylipoprotein bindingprotein(vigilin){Homosapiens}.partial(23%)3	**-1.13628**
Carbohydrate metabolism	
succinyl-CoAsynthetasebeta-subunit3	**-0.9844**
pyruvatekinase[Susscrofa]	**-1.58221**
UDPglucosepyrophosphorylase[Susscrofa]	**-1.00408**
malatedehydrogenaseprecursor	**-1.04048**
HUMANSuccinatedehydrogenase[ubiquinone]	**-1.95208**
succinatedehydrogenase{Susscrofa}.	**-1.75676**
MOUSEIsocitratedehydrogenase[NAD]	**-1.22769**
Phosphopyruvatehydratase alpha-human.complete	**-2.16842**
GLUT4 [Sus scrofa]	**-0.77164**
Electron trnsport	
NADHdehydrogenase(ubiquinone)	**-1.36497**
NADHdehydrogenasesubunit2[Susscrofa]	**-2.07052**
NADH3[Susscrofa]	**-1.88885**
cytochromeb[Susscrofa]	**-1.3111**
NADH4[Susscrofa]NADH5[Susscrofa]NADH6[Susscrofa]	**-1.58104**
54kDavacuolarH(+)-ATPasesubunit[Susscrofa]	**-1.56453**
Ca(2+)-transportATPase(class2)[Susscrofa]	**-1.58707**
Others	
leptin[Susscrofa]]	**-1.50565**
transmembraneleptinreceptor[Susscrofa]	**1.52401**
homologuetotranscriptionfactorBTF2chainp44-human.partial(41%)	**1.02749**
insulinreceptor[Susscrofa]	**1.43410**
insulinreceptorprecursor[Susscrofa]	0.70099
CREB/ATFfamilytranscriptionfacto	**-1.10598**

r{Homosapiens}.partial(32%)	
similartoGilamonsterphospholipaseA2{Homosapiens}.partial(81%)	**1.0616**
cytosolicphospholipaseA2beta;cPLA2beta{Homosapiens}.partial(18%)	**-1.55553**
groupXIIIsecretedphospholipaseA2{Homosapiens}.partial(93%)	**1.18925**
hydroxymethylglutaryl-CoAsynthasecytoplasmic (HMG-CoAsynthase). {Homosapiens}.partial(28%)	-0.23794

IV. OLIGOMER ARRAY ANALYSIS OF TRANSCRIPTION RESPONSES OF PORCINE TISSUES TO A SUDDEN SHIFT FROM LOW FAT DIET TO HIGH FAT DIET

INTRODUCTION

Contemporary societies across the globe are facing an ever increasing incidence in diabetes and obesity. Changes in nutrition that often accompany the emergence of populations from subsistence nutrition to plentiful available food commodities as well as unintended life-style changes, such as increased reliance on restaurant/fast foods in the developed world, appear to be among the underlying causative factors of massive weight gains observed in many people. Epidemiological observations indicate that in particular excessive consumption of diets rich in energy, with the nutrition being provided primarily by lipids, are a major contributor to the development of obesity (263). Pigs frequently overeats, therefore our lab has sought to utilize late finishing pigs as a model for the molecular adaptation of liver, adipose tissue and skeletal muscle to a diet containing at least 40% fat energy.

In the modern US swine industry, finishing diets are principally composed of corn and soybean meal. Hence, excess energy intake is accompanied by *de novo* lipogenesis (DNL) from the glucose released from dietary starch coupled with active deposition of triacylglycerol in adipose tissues. In the US, humans do not exhibit high DNL since most consume diets in which energy arising from lipids is greater than 40% and long chain

acyl CoAs inhibit DNL by allosteric mechanisms. Allee et al. (46) demonstrated in pigs that 10% dietary corn oil and 10% dietary beef tallow were equally effective in depressing lipogenesis in porcine adipose tissue, suggesting that unsaturated and saturated fatty acids were similar in their effects on DNL. Often a much more pronounced effect by PUFA rather than a saturated FA on DNL is noted in laboratory animals (66). Smith (52) found that both fatty acid chain length and extent of de-saturation are determinants for the effects of dietary fat on the DNL in pigs. Recently it was reported that, when rats were fed a high fat diet for one week, unexpectedly fatty acid oxidation was not enhanced but intramyocellular lipid content was elevated (264). Feeding extra fat to pigs in the finishing phase to enhance intramuscular fat deposition has been tried and was only partially successful. This strategy has been seldom used at the commercial level because of potential lowering of feed intake and diet mixing problems during incorporation of fat (265).

Recent studies in vertebrates have identified a number of molecules that regulate nutrient signaling and metabolic activity with respect to lipid metabolism. Such molecules include transcription factors that control a battery of genes involved in lipid metabolism, such as ADD1/SREBP1, PPARs, C/EBPs (266, 267) and adipokines such as leptin, which controls fat homeostasis and feeding behavior (268). Pigs differ in lipid biology from rodents and humans in one key aspect in that the primary site of *de novo* lipogenesis in pigs is adipose tissue while in humans liver is the primary DNL site with adipose as secondary site. Lipid biology in pigs has been studied to limit excessive fat deposition, while enhancing pork quality. In addition, researchers have attempted to adapt pigs as a model for human lipid metabolism (13).

Comprehensive understanding of porcine genome function is critical to understanding how dietary nutrients affect complex metabolic processes and fat deposition. However, presently little is known how genomic/molecular regulation of lipid metabolism in pigs is coordinated across liver, skeletal muscle and adipose tissue during the growing and finishing phases of production. Coordinated gene expression responses to a sudden change of lipid metabolism, brought about by changing dietary nutrient composition have not been evaluated. Thus, assessment of the molecular events underlying metabolic adaptation of pigs switched from a typical corn-based high carbohydrate, low-fat diet (LFD) to a tallow-based high-fat diet (HFD) should provide a model for exploring differential gene expression for lipid metabolism in pigs. The USDA group at Baylor University reported differential expression results of a few genes key to fatty acid metabolism in liver, adipose tissue and muscle in young pigs fed a 40% fat energy diet (48). These results showed an increase in mRNA abundance for acyl-CoA oxidase and CPT-1 in muscle and a decline in SREBP-1 in liver. Expression of four other genes studied was not affected. In the present work, a 13,297 gene array was utilized to obtain a much broader/global expression pattern in pigs fed a high fat diet in liver, adipose and skeletal muscle.

In this study I propose that feeding a diet of high fat content will modulate transcription of genes involved in nutrient metabolism pathways, especially those involved in lipid and carbohydrate metabolism. Therefore this study was designed to determine the impact of high dietary fat on the transcription response of genes involved in nutrient metabolism in liver, adipose and muscle tissues of finishing pigs using microarray techniques.

MATERIALS AND METHODS

Animal Feeding Trial

Eight adult castrated crossbred male pigs were provided *ad libitum* access toeither a corn and soybean-based, low-fat diet [LFD] (n=4) or a tallow/corn oil-supplemented high fat diet [HFD] (n=4) for 14 days. For the LFD, 4.3% diet energy was from fat contributed mainly by the corn, while, in the HFD, 40% diet energy was from a supplemental fat source of 4:1 saturated fat (beef tallow) and a PUFA source (corn oil; added to maintain a constant PUFA to SFA ratio for both diets). The composition of the feed offered for the 14 days before slaughter is presented in Table 1. The calculated crude protein concentration in the experimental diet were 20% and 19%, respectively, and both diets met or exceeded all NRC (199) requirements for finishing pigs. The average body weights on slaughter were 105.1± 5.4 kg and 106.1±2.93 kg for LFD and HFD treated pigs respectively, and they were not significantly different in statistics (P-value=0.34).

This experiment was approved by the Auburn University Institutional Animal Care and Use Committee (IACUC #0207-R-2448). The pigs were slaughtered at 14 days and liver, subcutaneous adipose and skeletal muscle tissues were collected. Pig identification number, diet treatment for each pig, and the day the samples were collected are presented in the Table 2.

Table1. Composition of feed given to the pigs

Ingredient	Control (%)	High Fat (%)
Corn	68.05	51.65
Starch	51.04	38.74
Fat source (Tallow/Sat Fat /corn oil/equiv)	0	13.25 3.25
Soybean Meal	29.00	29.00
Premix		
Di-Calcium Phosphate	1.00	1.00
Limestone, grd	0.80	0.80
Salt	0.35	0.35
Vit & TM	0.2	0.2
Additive/fiber	0.5	0.5
Calculated analysis		
Kcal/gm	4.1	5.2
Total Protein	20%	19%
Polyunsat to saturated fatty acid	0.2	0.2

*Meets all NRC (1998) requirements for finishing pigs
*The formulations are presented as feed ingredients (not dry matter corrected). These diets were not formulated to be iso-energetic.

Table2. Pig identification number, diet treatment, and the date of sample collection for the pigs.

Pig	Length of Treatment (days)	Fat Supplemented to diet (%)	Date of Samples Collection
4901	14	0 (LFD)	11/19/2003
5504	14	0 (LFD)	11/19/2003
5205	14	0 (LFD)	11/19/2003
6002	14	0 (LFD)	11/19/2003
4905	14	16.5 (HFD)	11/19/2003
5207	14	16.5 (HFD)	11/19/2003
5502	14	16.5 (HFD)	11/19/2003
6001	14	16.5 (HFD)	11/19/2003

Tissue Collection

All the pigs were killed at the Auburn University Meat Laboratory by electrical stunning followed by exsanguinations under USDA/APHIS inspection. Liver, subcutaneous adipose and skeletal muscle tissues were removed immediately, snap-frozen in liquid nitrogen prior to scalding and dehairing of the carcass. Liver samples were removed from the right lobe, adipose tissue samples were removed from the middle layer of subcutaneous adipose depot near 12^{th} rib, and skeletal muscle samples were removed from the longissimus muscle between the 10^{th} and the last ribs. This procedure minimized contamination and eliminated product rejection for the further processing of the carcass for human consumption.

Experimental Design

Microarray analyses were conducted on the liver, adipose and muscle tissues. For each tissue, I used a pooled control RNA preparation isolated from the four LFD pigs and individual RNA preparations from each HFD pig (n=4). Images of gel for all RNA preparations are presented in Appendix A. The labeling dye Cyanine 3 (Cy3) and Cyanine 5 (Cy5) were assigned randomly between control pool RNA and RNA from each HFD-treated pigs such that there were 2 controls pools with Cy3 and 2 HFD pigs with Cy5, and 2 control pools with Cy5 and 2 HFD pigs with Cy3. Our laboratory did not have the resources to conduct a dye swap for each control RNA (LFD) and each of the 4 individual RNAs from the four HFD pig combinations.

Microarray Analysis

The experimental procedures for isolating RNA**,** synthesizing cDNA, aminoallyl labeling cDNA, hybridizing labeled cDNA with oligos on the pig array are described in

the Chapter III. Images of fluorescent dye Cy5 labeled cDNA are presented in Appendix C. Similar procedures were also performed to scan the slides and conduct image analysis, normalization and statistics. All array images of this experiment are presented in Appendix G.

Normalization

To remove systematic error in the experimental analysis, as described in the Chapter 2, LOWESS was used to normalize all the slides. M-A plots for all experimental runs before and after LOWESS normalization are presented in Appendix H.

Statistical Analysis

SAM was employed using the one-class response with 1,000 permutations to determine genes whose expression was significantly different from zero. Differently expressed genes were determined by setting the number of falsely called genes to less than one and choosing similar false discovery percentage medians for each of the biological replicates. In the SAM analysis, a similar false discovery rate (FDR=5%) was chosen for each tissue analysis. Then, as described in the chapter III, all significantly differently expressed genes from the SAM list for each tissue were filtered by the genes of interest list. The differential expression results for the predetermined genes of interest list (filtered results) for liver, adipose and muscle are reported in Tables 3-5 respectively. In addition, for the top 200 genes in each tissue, I presented the $\log_2$ratio value from each microarray analysis (representing each biological replication) in the Appendix I.

RESULTS AND DISCUSSION

General Pattern of Gene Expression and Its Changes in Expression of Porcine Tissues

Utilizing the Iowa State Porcine Genomic Center oligo pig array, differential expression of 13,297 70 mer spot targets was measured. The oligo probe (sequence) of each spot was designed based on known gene sequences or expressed sequence tags (ESTs). Six thousand, six hundred and fifty (50.01%) of the oligo probes were designed based on ESTs. Of the total 13,297 specific 70mer spots or genes, 52.47%, 48.59% and 47.73% did not achieve any visible hybridization for liver, adipose and muscle tissues respectively. These are called "absent genes", and the variation of total absent genes among tissues was only 4.74%. This result shows that essentially the same spotted gene targets hybridized to the prepared dye-aminoallyl cDNA probes across all three tissues. Genes or spots on slides to which the dyed cDNA did hybridized were 47.5% for liver, 51.4% for adipose and 52.3% for muscle. These genes are called "present genes". Out of the "present genes" 71.3% (liver), 44.5% (adipose tissue) and 41.9% (muscle) were not annotated or based on EST in the Qiagen-provided list of gene spots, and these spots are called "unknown genes". A summary of the overall performance results of the spotted arrays is presented in Table 6.

The percentage of differentially expressed genes (from a total of 13,297 genes) identified by SAM were 7.9% (liver), 6.4% (adipose tissue) and 8.5% (muscle) in liver, adipose and muscle tissue respectively. Such a finding is consistent with the overall theory (182) about absolute expression data using microarray analysis, in that from any given sample or source most of genes on an array are not differently expressed. As can be

seen in Table 7, “unknown genes” accounted for a large proportion in the differentially expressed genes. Approximately 1000 genes were either up or down regulated by the dietary regime. Numeric details on the up/down regulated genes resulting from the diet shift across three tissues are presented in Table 7.

Table 6 Number and percentage of detected (present) and undetected (absent) out of 13,297 genes among tissues studied.

	Liver	Adipsoe	Muscle
Absent genes out of total	6977 (52.5%)	6461 (48.6%)	6347 (47.7%)
Present genes out of total	6320 (47.5%)	6836 (51.4%)	6950 (52.3%)
Unknown genes out of present	4504 (71.3%)	3039 (44.5%)	2912 (41.9%)

Table 7 Number and percentage of differently expressed transcripts by SAM

	Liver	Adipose	Muscle
Significantly differentially expressed genes (number) and (% out of total)	1055 (7.9%)	847 (6.4%)	1138 (8.6%)
Up-regulated (number)	440 (41.7%)	552 (65.2%)	416 (36.6%)
Unknown genes out of up-regulated total	339 (77.1%)	293 (53.1%)	84 (20.2%)
Down-regulated (number)	615 (58.3%)	295 (34.8%)	722 (63.4%)
Unknown genes out of down-regulated total	407 (66.3%)	102 (34.6%)	207 (28.7%)

Microarray Study in the Liver

Table 3 shows the effect of comparing LFD and HFD on differential transcription of genes in liver. In spite of a less than primary role of liver in porcine fat anabolism, gene expression in liver was affected by HFD. All results are expressed as $\log_2$ratio. For each transcript, ratio = $\frac{\text{normalized pixel intensity labeling HFD RNA}}{\text{normalized pixel intensity labeling LFD RNA}}$

The HFD when fed to finishing pigs decreased the mRNA abundance of SREBP-1($\log_2$ratio=–1.15) and other genes in involved in triacylglycerol (TAG) synthesis including diacylglycerol acyltransferase ($\log_2$ratio= –1.77), and glycerol-3-phosphate dehydrogenase ($\log_2$ratio= –2.4). Gene expressions of enzymes in the fatty acid β-oxidation pathway were depressed by the fat supplement, including long-chain-fatty acid-CoA synthetase ($\log_2$ratio= –1.519), long-chain acyl CoA dehydrogenase ($\log_2$ratio= –1.14), and enoylCoA hydratase ($\log_2$ratio= –1.57). HFD did not alter mRNA abundance of PPARα, a transcription factor regulating fatty acid oxidation. However, expression of acyl CoA oxidase ($\log_2$ratio= –2.9), an enzyme in peroxisome fatty acid oxidation pathway and target gene of PPARα, was down-regulated in response to HFD. In the liver of rodents and humans, mechanism of PPARα activating expression of genes in fatty acid β oxidation has been well documented (269-271). As described in chapter 2, PPARα is highly expressed in the liver and not expressed in the adipose tissue of rodents and human, but PPARα is expressed more abundant in the adipose tissue than the liver in the pig (44). Peffer et al. (247) did not observe a positive relationship of expression of PPARα and genes in fatty acid β oxidation in the porcine liver. Similarly, the data in this study did not show a positive relationship between expression of PPARα and genes in

fatty acid β oxidation in the liver upon HFD. Effects of PPARα on fatty acid β oxidation in the pig need more research to be confirmed.

Expression of SREBP-1 (log_2ratio= –1.2) in the liver was significantly suppressed by high saturated fat in finishing pigs. When young pigs were fed tallow-supplemented high-fat diet or low-fat corn-soybean meal diets for 2 weeks, Ding et al. (48) found, that liver transcript concentration of SREBP-1 mRNA tended to be decreased in high-fat (tallow) fed pigs compared with the low-fat-fed pigs (P=0.06) in the liver.

SREBPs belong to the helix-loop-helix family of transcription factors. SREBP-1 regulates the expression of genes in lipid synthesis while SREBP-2 has been shown to control genes important to cholesterol homeostasis (97, 272-273). However, SREBPs themselves are not very potent activators of transcription and require the actions of ancillary proteins to affect transcription of target genes (274). Therefore, reduced expression of lipogenic enzyme genes (see below) by high fat in our study may be related to the low expression of SREBP-1.

Results of this study showed lower mRNA abundance of fatty acid synthase (FAS) (log_2ratio= –0.91) and ACC (log_2ratio= –1.51 and log_2ratio= –1.93 for sus scrofa and bovine ACC respectively) in the liver after diets were shifted to HFD in the pigs. FAS and ACC are rate-limiting enzymes for long-term fatty acid biosynthesis. FAS is a multienzyme complex that synthesizes long-chain, saturated fatty acids (primarily palmitic acid) from acetyl-CoA, malonyl-CoA, and NADPH (275). FAS is not always limited to the production of palmitate; it can also construct longer fatty acids like stearate (but independent elongases appear to be more important in mammalian cells) and shorter

fatty acids like myristate, or other shorter fatty acids (276). It should be noted that independent elongases appear to be more important in mammals.

Yin et al. (277) found that the abundance of FAS mRNA in porcine liver was responsive to hormonal manipulation as shown with recombinant porcine somatotropin. Irrespective of that fact, less than 20% of total body fatty acid synthesis may be attributed to the liver (13). As indicated previously, most of the fat deposited in pigs under production conditions is derived from *de novo* fatty acid synthesis in the adipose tissue when typical farm diets, which contain a large proportion of the corn; i.e., dietary starch, are used. In contrast, in rodents, adipose tissue *de novo* fatty acid synthesis accounts for less than 50% of the total carcass fatty acid synthetic capacity (13). The relative contribution of each tissue to total carcass lipogenesis may also vary somewhat with age of the animal and dietary composition.

The expression of lipogenic enzymes is dependent on the nutritional status of the animal and the composition of dietary energy (46, 277-278). Diets high in fat have been reported to suppress the expression of genes coding for lipogenic enzymes in the rodents (279, 280). Similarly, expression of lipogenic genes was down-regulated in response to HFD in porcine liver.

While Ding et al. (48) observed a lowered SREBP-1 expression, they found no expression differences in the transcript concentration of FAS in the liver and adipose tissues between young pigs fed corn-based, low-fat diet or tallow-based, high-fat diet for 2 weeks. As noted above, in the present study, decreased transcription of FAS and ACC was observed when diet was shifted from LFD to HFD in pigs. These different findings between Ding et al. and my study may be related with the different developmental phase

of the pigs. In this study finishing pigs were used and the final average bodyweights were 104.06±5.37 kg and 105.08± 2.90 kg for LFD and HFD groups, respectively, while the pigs used in the experiment by Ding et al. (48) were young pigs with average initial bodyweights of 6.16± 1.01kg.

Like FAS, ACC is also a multi-protein subunit enzyme complex. Acetyl-CoA carboxylase catalyzes the first committed reaction in fatty acid synthesis from acetyl-CoA. This enzyme catalyzes the ATP- and biotin-dependent carboxylation of acetyl CoA to malonyl CoA (17). This response is mediated when the intake of dietary carbohydrates exceeds the amount of energy required by the animal. The activity of ACC is controlled by allosteric regulation (long chain fatty acids) and cAMP –PKA-directed covalent modification by phosphorylation. In either case, ACC activity may be lowered rapidly via allosteric and covalent regulation, and under such circumstances ACC is the rapid-response, rate-limiting enzyme in lipogenesis. In addition, other dietary and pharmacological factors may also regulate ACC via gene expression (17, 37)

In this study, expression of liver fatty acid binding protein (L-FABP) was depressed (log_2ratio= –1.18) in the HFD animals, while the mRNA abundance of FABP was increased in the adipose and muscle tissue (see Table 4 & 5). Liver fatty acid binding protein is a member of the genetically related cytosolic FABP family (281). The FABPs are a class of soluble proteins that function by facilitating the intracellular diffusion of fatty acids between cellular compartments and/or enzymes. FABPs reversibly bind hydrophobic ligands, including long-chain fatty acids (LCFA), LCFA-CoA, phospholipids, peroxisome proliferators, and other hydrophobic molecules (282, 283). The transcription rate of the L-FABP gene is tightly regulated and induced by LCFA

through a peroxisome proliferator-activated receptor (PPAR)-responsive element located in the proximal part of the promoter in the rodent model (283).

Wolfrum (284) proposed that L-FABP is the gateway by which hydrophobic compounds influence gene transcription. L-FABP and PPAR-α exhibit a similar ligand-binding spectrum (285). Wolfrum et al. (282) and Tan et al. (286) convincingly demonstrated that L-FABP was able to activate PPAR-α in hepatoma and COS cells, respectively. Furthermore, numerous reports imply that L-FABP has a critical role in LCFA metabolism by modulating availability of substrate and increasing enzymatic capacity through activation of PPAR-α and possibly other transcription factors (284-286). Hung et al. (287) determined the FABP protein abundance and correlated its levels with the extent of LCFA metabolism in the rats and found that L-FABP was important in hepatic LCFA metabolism. Erol et al. (288) confirmed that L-FABP is a cell-intrinsic stimulator of LCFA oxidation *in vivo*, but they found that L-FABP effects on fatty acid oxidation might vary with physiological condition. These workers showed that both *in vivo* and in hepatocyte incubations (*in vitro*), L-FABP is a limiting factor in the production of ß-hydroxybutyrate, the final product of (mainly) hepatic fatty acid oxidation. They concluded that FABPs might be important for the action of cognate PPARs only under conditions of low lipid metabolism.

In this dissertation, the mRNA abundances of FABP ($\log_2$ratio= –1.18) and genes in fatty acid β-oxidation were decreased but PPARα was not changed in the liver in response to HFD in pigs. Because this study only determined transcription responses, the regulatory mechanism of L-FABP on PPARα and fatty acid β-oxidation could not be fully described nor could any definite conclusion be reached about the role of

triacylglycerol under the experimental conditions at this time. More research is needed to clarify if the L-FABP has a regulatory role on fatty acid oxidation at the transcription level in pig and if similar response exists for protein concentration and enzyme activity upon high influx of NEFA/LCFA in the porcine liver.

Fatty acid supply and cellular uptake of fatty acids has been shown to parallel the level of liver fatty acid binding protein (L-FABP) in rats (289). mRNA abundance of FABP in the liver was decreased (ratio= –1.18) in response to the high fat diet. L-FABP is not only way for fatty acid to get in liver. Fatty acids can cross plasma membrane with the help of the protein fatty acid translocase (37). As a non-adipose tissue, liver has limited ability to handle extra fatty acids. When lipids overaccumulate in the liver, they may enter deleterious nonoxidative pathways leading to cell injury and death (290). A single *in vitro* study in endothelial cells and cardiac myocytes has suggested that accumulation of FFAs may result in lysosomal permeabilization (291) Furthermore, lysosomal breakdown with cathepsin B (ctsb) release into the cytosol is a feature of TNF-α signaling cascades (292). The reason for decreased expression of FABP in porcine liver upon a large influx of LCFA/NEFA from the diet are not clear. The general down regulation of genes in lipid metabolism may relate to the protective reaction of liver in the condition of excess influx of fatty acids, or may relate to a lesser role of porcine livers in lipid metabolism than has been observed in rodents. Clearly, the LFD-to-HFD induced down-regulated expression of FABP and genes in the fatty acid β-oxidation was unexpected in the liver. It is not correct to make further inference without assays in histology and proteins on liver tissue, and I will not speculate on the underlying mechanism without more data.

The first step of glucose metabolism is the transport of glucose across the plasma membrane of glucose-sensitive tissues aided by glucose transporter (293). Glucose transporter (GLUT) facilitates transporting glucose down the concentration gradient; the major isoform of this protein in the liver is GLUT2. Transcription of GLUT2 (log_2ratio= –1.9) was lower in the pigs fed HFD. It has been demonstrated that glucose induces GLUT2 expression due to transcription activation of gene GLUT2 (294). Gremlich et al. (295) demonstrated that palmitic acid induced a decrease in GLUT2 mRNA abundances, but it did not induce consistent changes in GLUT2 protein expression. Therefore, the decreased mRNA abundance of GLUT2 in the liver may be related to the high saturated fat content in HFD. Once inside the cell, the glucose is activated by phosphorylation to form glucose-6-phosphate. This metabolite may be further metabolized via glycolysis and/or the pentose phosphate pathway or utilized for glycogen synthesis in the liver and other tissues (17).

Transcription of pyruvate kinase (log_2ratio=0.9934), a regulatory and irreversible enzyme in glycolysis catalyzing formation of pyruvic acid from phosphenolpyruvic acid, was up regulated in the HFD pigs. The activity of pyruve kinase is also controlled by allosteric and covalent regulation. For example, in the liver, activity of pyruvate kinase is inhibited by cAMP-dependent phosphorylation (17). Correspondingly, expression of key enzymes in gluconeogenesis and glycogen synthesis, glucose-6-phosphatase (log_2ratio= –2.94), phosphoenolpyruvatecarboxykinase 2 (log_2ratio= –3.7527), and UDP glucose pyrophosphorylase (log_2ratio= –1.612), were down-regulated in HFD pigs. Because pyruvate kinase, phosphoenolpyruvatecarboxykinase 2 and glucose 6 phosphatase are

also controlled by allosteric and covalent regulation, the real change of glycolysis and glucogenesis in the liver may be better observed by assaying activities of those enzymes.

The mRNA abundance of pyruvate dehydrogenase (PDH) (log_2ratio= –1.8422) in the liver was decreased in HFD treated pigs (Table 3). Pyruvate dehydrogenase (PDH) catalyzes the production of acetyl-CoA from pyruvate. Pyruvated dehydrogenase is inhibited by high-energy potential and when fatty acids are being oxidized (37). The pyruvate dehydrogenase is primarily regulated by phosphorylation/dephosphorylation (297). Pryuvate dehydrogenase kinase phosphorylates and inactivates pyruvate dehydrogenase. Expression of pryuvate dehydrogenase kinase (log_2ratio= –4.2257) was greatly down-regulated upon HFD. PDH kinase is activated by increases in the [ATP]/[ADP], [acetyl-CoA]/[CoA], and [NADH]/[NAD^+] ratios (297). The great decrease of mRNA concentration of pryuvate dehydrogenase kinase might lead to lower expression of the protein. The decreased expression of Pryuvate dehydrogenase kinase might relate with the decreased energy potential connecting with down-regulated expression of genes in fatty acid oxidation, glycolysis and TCA-cycle in the porcine liver in response to the HFD. The regulation mechanism between pyruvate dehydrogenase and pyruvate dehydrogenase kinase happens by phosphorylation at the protein level. Herein, I can not completely explain the extremely low mRNA abundance of pryuvate dehydrogenase kinase and middle low mRNA abundance of pyruvate dehydrogenase in porcine livers upon HFD.

Expression of gene succinyl-CoA synthetase (log_2ratio= –1.5813) in the liver was decreased in response to HFD diet, but gene expression of two regulatory enzymes in the TCA cycle, NADPH-specific isocitrate dehydrogenase (log_2ratio= –0.3766) and succinate

dehydrogense (log_2ratio=0.3003), was not altered upon the HFD in the liver. No differences were observed in the mRNA abundance of genes involved in electron transport and the oxidative phosphorylation process by HFD, such as cytochrome b, cytochrome c oxidase subunit, NADH dehydrogenase, and $H^{(+)}$-ATPase.

Transcriptions of genes in fatty acid oxidation, fat synthesis and glucogenesis were all lowered in the liver after dietary shifting from LFD to HFD. This may infer some type of negative feedback of the liver in response to high levels of LCFA, particular on lipid and energy metabolism enzymes. It must be stressed that actual activities of glucose and lipid metabolism are not clear based on transcription response alone, because mRNA stability and translation, enzyme phosphorylation and enzyme degradation also have important roles in controlling the overall activity of metabolic pathways.

In response to HFD treatment pigs, expression of gene HMG-CoA synthase (log_2ratio=0.0974) was not changed. However, the mRNA abundance of HMG-CoA reductase (log_2ratio= –2.1), rate-limiting enzyme in the overall cholesterol biosynthesis pathway was decreased in HFD pigs. A number of genes involved in regulating cellular cholesterol homeostasis are controlled at the level of transcription by nutrients. For example, addition of cholesterol to the diets of mice led to a rapid 5-10 fold decline in the mRNA abundances for HMG-CoA synthase, HMG-CoA reductase, farnesyl diphosphate and the LDL-receptor (124). HMG-CoA reductase expression is also controlled by changes in mRNA translation and stability and protein stability. In addition, enzyme activity is modulated by phosphorylation, making it one of the most highly regulated enzymes. The decreased mRNA abundance of HMG-CoA reductase may relate to the down regulated genes in fatty acid β oxidation which provide acetyl-CoA, the precursor

of cholesterol biosynthesis. However, nearly no literature is available about the effect of dietary fat on the expression of genes involved in cholesterol biosynthesis in the pig. Harris et al. (256) found the cholesterol content of liver was lower in pigs fed a high-fat, high-cholesterol diet than a low-fat, low-cholesterol diet fed pigs (starting at 12 week of age) for 92 days, but no difference was observed in cholesterol content and percentage of fat in the cerebrum, fat, heart, ileum, kidney, and muscle tissues. Harris et al. (256) concluded that the serum cholesterol or dietary fat and cholesterol content did not influence the cholesterol accretion in most tissues of pigs, and liver is a modulator of cholesterol homeostasis in the pig.

In this experiment about 440 genes not involved in lipid, carbohydrate and energy metabolism were up-regulated (significant $\log_2$ ratio; see Appendix G). This included endothelin receptor ($\log_2$ratio=3.59), ligatin ($\log_2$ratio=2.73), neuritin ($\log_2$ratio=2.477), calcineurin catalytic subunit ($\log_2$ratio=2.42), and Rho-related GTP-binding protein ($\log_2$ratio=2.139) (Appendix G). This would indicate that the dietary shifting from LFD to HFD broadly affected expression of genes in the liver, not restricted in energy metabolism pathways. In this study, I made no further attempt to identify or work with any genes that were filtered out by our pre-experimentally genes of interest list.

Finally, it is worth reiterating that I observed changes in gene expression. However, I have tried to focus these results on metabolism and its regulation with the clear reservation that metabolic pathways are not solely regulated at the gene expression level. Obviously, verifying the above gene expression response through determining protein concentration and enzyme activity is crucial to know the metabolic adaptation of liver

upon the HFD, specifically those rate-limiting enzymes and regulatory enzymes in the lipid and carbohydrate metabolism pathways.

Microarray Studies in the Adipose Tissue

Expression results for adipose tissue are presented in Table 4.

In this study, after the diet shift from LFD to HFD there were no changes in the mRNA abundances of genes involved in the long-chain fatty acid mobilization including CPTII (log_2ratio=0.3925), long-chain acyl-CoA dehydrogenase (log_2ratio=0.5026), acyl-CoA oxidase ((log_2ratio=0.6129), enoyl-CoA hydratase (log_2ratio=0.678) and 2,4-dienoyl-CoA reductase (log_2ratio=0.5058).

No change was observed in genes involved in *de novo* fatty acid synthesis SREBP-1 (log_2ratio=0.0242), ACC (log_2ratio=0.0847) and FAS (log_2ratio= –0.4467), although mRNA abundances of pyruvate kinase (log_2ratio=0.6373) and pyruvate dehydrogenase (log_2ratio=0.6096) tended to be higher in HFD pigs. My data are in agreement with previous findings reported by Ding et al. (48). In their study, no changes were observed in the transcription level of FAS and aP2 after young pigs were fed a tallow-based high fat diet for 2 weeks. Allee (46) found that, in porcine adipose tissue, fatty acid synthesis and the total activity of lipogenic enzymes were reduced by dietary fat, and that this reduction was dependent on the amount of fat in the diet.

Previously published research indicates that feeding high-fat diets to rodents will modulate adipose lipogenesis. Weaning mice onto a high-fat, low-carbohydrate diet prevented the rise in adipose tissue FAS and ACC mRNA associated with weaning onto a typical high-carbohydrate laboratory chow type diet (278). Pape et al. (279) found that resuming feeding of previously unfed rats with a high-fat diet blocked the induction of

ACC mRNA in adipose tissue. Clarke et al. (298) found that when carbohydrate intakes were maintained constant among animals fed diets containing fat, the expression of lipogenic enzymes was not suppressed by dietary fats. Jump et al. (101) in a recent review concluded that the inhibition of *de novo* fatty acid synthesis by dietary fat likely reflects an acute allosteric feedback inhibition mechanism (suppression of acetyl-CoA carboxylase catalytic efficiency) rather than a primary adaptive change in expression of genes coding for lipogenic enzymes (101).

In adipose of our pigs, mRNA abundance of genes involved in TAG synthesis were increased including glycerol-3-phosphate dehydrogenase (G-3PDH; $\log_2$ratio=0.9255), diacylglycerol acyltransferase (DGAT; $\log_2$ratio=0.8850), and fatty acid-CoA ligase ($\log_2$ratio=0.7823). The up-regulation of genes in TAG synthesis may be related to the increased expression of FABP. Transcription of FABP ($\log_2$ratio=1.1244) was up-regulated in the adipose tissue and this may enhance fatty acid uptake by adipose tissues. Working with a diet-induced obesity rodent model using excessive dietary fat intake, Li et al. (299) noted that after a 1-week exposure to a high-fat diet, several adipogenic genes, in particular those involved with TAG synthesis, such as G-3 PDH, DGAT, were upregulated in adipose tissue as noted in my study. Because genetic regulation of adipogenesis is complex, any putative increase in overall adiposity upon HFD would result in a mixture of new adipocytes at various stages of development. Micorarray results in this study reflected an overall multiple-step process and gene expression profile. This scenario may result in complex and sometimes inconsistent gene expression patterns in the process of expanding adipose tissue.

In adipose, expression of fructose-bisphosphate aldolase A (log_2ratio=0.9142) in finishing pigs was increased by HFD while transcription of other genes in glycolytic and TCA pathways tended to be slightly up-regulated by dietary high fat including pyruvate kinase (log_2ratio=0.6373), pyruvate dehydrogenase (log_2ratio=0.6096), succinate dehydrogenase (log_2ratio=0.6685). Such up regulation of genes in glycolysis may be related to increased expression of TAG synthesis genes in the adipose tissue since adipose is a major storage site for TAG (300). If large amounts of LCFA were taken up by adipose tissue upon action of LPL in HFD fed pigs, then significant amounts of glycerol 3- phosphate would be required for esterification. Porcine adipose tissues lack glycerol kinase, an enzyme which phosphorylates endogenous glycerol arising from hydrolysis of stored TAG to produce glycerol 3-phosphate (301). Since the HFD diet was not really lacking glucose precursors (starch), adequate glucose was likely available to support sufficient adipose glycolysis and ultimately generate glycerol 3-phosphate to enable TAG deposition.

The results in this study further showed that the diet shift to HFD did not change the transcription of SREBP-2 (log_2ratio=0.3377) and genes involved or associated with cholesterol biosynthesis. These results are consistent with the finding by Harris et al. (229) as described above and the known function of SREBP-2 in regulation of cholesterol synthesis (65). In addition, porcine adipose may not be an important site for cholesterol synthesis.

This study did not observe changes in the transcription of genes of β-oxidation pathway in the adipose tissue after the diet shift to HFD. No change was observed in the transcription of CPT-II (log_2ratio=0.3925) and in the genes encoding different types of

acyl-CoA dehydrogenase, such as very-long-chain acyl-CoA dehydrogenase (log_2ratio=0.4309), long-chain acyl-CoA dehydrogenase (log_2ratio=0.5026) and short-chain acyl-CoA dehydrogenase (log_2ratio=0.2494). My CPT-II results are consistent with the report by Ding et al. (48) who found no differences in CPT-1 transcript concentration between control and high fat fed pigs. Acyl-CoA dehydrogenase catalyzes the initial step of the mitochondria fatty acid β-oxidation pathway. Consistent with the expression results for acyl-CoA dehydrogenase, expression of down-stream genes in β-oxidation was not changed in porcine adipose tissue by HFD, including 2,4-dienoyl-CoA reductase (log_2ratio=0.5058), enoyl CoA hydratase (log_2ratio=0.648) and long-chain-3-ketoacyl-CoA thiolase (log_2ratio=0.2841). CPT-II catalyzes the release of acyl-CoA from acyl-carnitine for β-oxidation in the mitochondria matrix, and CPT-II is thought to play an important role in the rapid transfer of activated long-chain fatty acids into mitochondrial matrix for β-oxidation (302).

Acyl-CoA oxidase expression was not enhanced (log_2ratio=0.6129) by feeding HFD. Acyl-CoA oxidase catalyzes the commitment step in peroxisomal lipid oxidation by converting fatty acyl-CoA to 2-*trans*-enoyl-CoA and H_2O_2 (303). Fatty acid substrates for the enzyme include very-long-chain, long-chain, and some medium-chain fatty acids. Various AOX isoforms located in the peroxisome metabolize either straight or branched-chain fatty acids (304). Expression of AOX is regulated by PPAR which binds to PPRE in the AOX promoter region. The peroxisomal proliferator-induction of AOX varies between tissues and among species. In our study, mRNA abundance of AOX was not altered by high fat. This is consistent with the report by Ding et al. (48) who also noted

no difference in AOX transcript abundance between young pigs fed a corn-based, low-fat diet and tallow-based, high fat diet for 2 weeks.

Detection of altered transcription in tissues in response to feeding HFD to pigs may depend on the timing of the transcripts measurements. Modifications of adipose tissue transcripts concentrations by dietary lipids have been demonstrated after feeding high fat experimental diets for various lengths of time. For example, PPARγ and aP2 mRNA concentrations were decreased when rat were fed a high fat vs. low-fat diet for 8 days, but the two transcripts were increased when the same treatment lasted for 30 Days (305). Pigs fed high fat diets for 12 wk have increased adipose tissue PPARγ mRNA concentrations (306). Unfortunately, only a PPARα but not a PPARγ probe was spotted on the pig array platform used here. In addition all my results are from a single 14 day experimental HFD feeding period. Future work should include longer experimental periods and should include expression of PPARγ and its target gene aP2, which may help understand how supplemental fat modifies porcine adipose lipid metabolism.

Triacylglycerols in adipose tissues are continually being hydrolyzed and resynthesized. The glucose concentration within adipose cells is a major factor determining whether fatty acids are released into the blood after TAG hydrolysis. Fatty acids from TAG hydrolysis are released to the plasma as NEFA if glycerol-3-phosphate is scarce because of low availability of glucose (17). As noted above, glucose was unlikely to be limiting factor of TAG synthesis. An increased TAG accumulation also depends on the concentration of exogenous fatty acids (i.e., the higher the concentration of fatty acids, the more the lipid accumulation will likely occur (307). In this study, it is

very possible that increased expression of genes involved in TAG synthesis was the result of the high-fat diet coupled with adequate glucose supplies.

In porcine adipose, expression of gene GLUT4 (log_2ratio = 0.5715) was not altered by HFD. This study did not observe significant alterations in the transcription of genes in the TCA cycle in response to HFD, i.e. succinyl-CoA synthetase (log_2ratio = 0.494), succinate dehydrogenase (log_2ratio = 0.6685). The main role of TCA cycle is to completely oxidize acetyl-CoA to provide energy. Considering pigs were well fed in the experimental condition and adipose was not the energy-producing tissue in the feeding and rest states, the lack of change in expressions of genes in TCA cycle upon HFD might relate to the lack of change of expression of genes in β oxidation and peroxisomal oxidations pathways.

No differences were observed for the transcription of genes in the electron transport and oxidative phosphorylation in porcine adipose tissue after HFD treatment including NADH dehydrogenase 4 (log_2ratio=0.5037), NADH dehydrogenase (log_2ratio=0.5219) and ATPsynthase subunit (log_2ratio=0.8818 for bovine subunit E and log_2ratio=0.2563 for human subunit D). This observation was consistent with no observed changes in the transcription of genes in β-oxidation and TCA cycle in the adipose tissue after abruptly dietary change from LFD to HFD in pigs.

In this study mRNA abundance of leptin tended to be increased (log_2ratio=0.622) when high fat was fed to pigs. Increased expression of leptin in the HFD fed pigs was likely a response to increased deposition of TAG in adipose depots. The adipocytokine leptin is secreted by adipose tissues and released in proportion to the size of body fat stores. Leptin is detected in the blood at concentrations that directly reflect the adiposity

of the animal, but more work in pigs will be necessary to delineate all functions and effects of this adipocytokine (245). Concentrations of leptin in serum from obese swine were 306% higher than concentrations in control, leaner pigs (302). During periods of energy excess, high levels of leptin interact with the hypothalamus to suppress appetite as well as increasing energy expenditure by enhancing fatty acid oxidation in liver and other tissues (308). Studies in rats have shown that leptin simultaneously induces lipolysis and lipid oxidation (309).

Finally transcription of a few genes that were included in the filtering process including various types of transcription initiation factors, transcription factors and components of signal pathways were found to be up regulated in adipose after pigs were fed a high fat diet for 14 days (Table 4).

Microarray Studies in the Longissimus Muscle Tissue

Results for the transcriptional profiling of genes involved in lipid and energy metabolism in skeletal muscle (longissimus muscle) are presented in Table 5.

In skeletal muscle, no change was observed in mRNA abundance of some β oxidation enzymes including long-chain acyl-CoA dehydrogenase (log_2ratio=0.6594), very-long-chain acyl-CoA dehydrogenase (log_2ratio=0.4263), short chain acyl-CoA dehydrogenase (log_2ratio= –0.1393) in response to HFD in pigs. For other genes associated with fatty acid oxidation, expression of 3-hydroxyacyl-CoA dehydrogenase (log_2ratio= –0.8938) was decreased and CPTI (log_2ratio= –0.7693) tended to be decreased by feeding HFD. For the genes involved in *de novo* fatty acid synthesis, no change was observed for FAS (log_2ratio= –0.3833), SCD (log_2ratio=0.282), pyruvate dehydrogenase (log_2ratio=0.1319) and pyruvate kinase (log_2ratio= –0.2641) expression in

the muscle after the 14 day shift to HFD. Expression of FABP (log_2ratio=1.2) was increased after high fat treatment. For the genes of TAG synthesis in muscle from HFD pigs, no changes were observed in the mRNA abundance of acetyl-CoA acyltransferase (log_2ratio=0.4629), diacylglycerol acyltransferase (log_2ratio= –0.09) although glycerol-3-phosphate-dehydrogenase expression was lowered (log_2ratio= –1.2937). No differences were observed in the mRNA abundance of genes involved in cholesterol and sterol biosynthesis in HFD pigs including SREBP-2, HMG-CoA reductase, 17 beta-estradiol dehydrogenase, and 20 beta-hydroxysteroid dehydrogenase. Similar to results in adipose tissue, expression of leptin (log_2ratio=0.711) tended to be elevated after pigs were fed HFD in muscle tissue (not a major site of leptin production).

For genes in the glycolytic pathway, based on this micro-array analysis, transcription of fructose-bisphosphate aldolase A (log_2ratio= –0.8919) was decreased by HFD. The transcription of glucose transport protein (log_2ratio=0.0623) was not changed in response to the high fat diet. No differences were observed in mRNA abundance of some genes involved in the TCA cycle such as succinyl-CoA synthetase α (log_2ratio=0.0739), β (log_2ratio=0.2177), and citrate synthase precursor (log_2ratio=0.2159).

In mature human, skeletal muscle is the predominant tissue for whole body energy substrate oxidation (either as glucose or fatty acids), and oxygen consumption accounts up to 90% of whole body oxygen consumption in total exercising muscle (310). During the resting state the energy requirements of muscle may be met with fatty acid oxidation (311). Typically skeletal muscle accounts for the majority of glucose utilization (312) but when people are obese or people or animals consume diets containing significant

amounts of fat, adjustments in the pattern of substrate oxidation are necessary that are not always accompanied by desirable outcomes. Thus, glucose oxidation may be compromised in muscle upon excessive fat intake/or fat deposition that results in hyperglycemia and potentially insulin resistance (312). Multiple sites of metabolic control exist within muscle that govern oxidative flux, although recent evidence indicates that substrate availability regulates the transcription of metabolic genes (313). Ellis et al. (314) found that the expression of genes important for fat oxidation tended to increase in both type I (slow twitch, oxidative) and type II (fast twitch, glycolytic) muscles after an HF dietary intervention for 8 weeks in the rats, but the expression of muscle-type carnitine palmitoyltransferase I was not increased in type II muscle.

Excess dietary fat has been implicated in the development of obesity and diabetes. In the skeletal muscle, fatty acid and glucose metabolism pathways are cross linked, and the regulatory mechanism of fatty acid and glucose oxidation by dietary nutrients is still unclear (315).

Randle et al. (316) introduced the glucose-fatty acid cycle in muscle suggesting that the availability of FFA determines the rates of fat oxidation, and an increased availability of FFA would then lead to an increased fat oxidation over glucose utilization. This glucose–fatty acid cycle was based on results from *in vitro* experiments on rat heart and diaphragm muscle metabolism. It may not be surprising that *in vivo* studies have yielded conflicting results regarding the effect of FFA on glucose oxidation. Some studies showed an inhibitory effect of fatty acids on glucose oxidation in rat skeletal muscle (317), while others found no such effect (318-319).

In humans there is no direct support for the glucose-fatty acid cycle as proposed by Randle et al. (316) to account for control of glucose metabolism by fatty acids. Changes were not observed in concentrations of either muscle citrate or glucose-6-phosphate when fatty acid concentrations were altered in various experiments (320-322). When glucose uptake is maintained at a constant high rate, a 10-fold increase in FFA concentration had no affect on glucose oxidation (323-324). In my study, the transcription of genes in the TCA cycle and most genes in glycolysis (except decreased mRNA abundance of fructose-bisphosphate aldolase A) were not changed in the muscle when diet was shifted from LFD to HFD. In this study, corn (starch) content was different between LFD and HFD besides the difference of fat content. The starch content in HFD was 38.74% compared with 51.04% in LFD. Glucose metabolites arising from glycolysis, TCA cycle and pentose phosphate pathways in themselves can act as intracellular signals that regulate metabolism by allosteric means or promote/ inhibit transcription of various other genes in liver, adipose, or muscle tissue (297). One of these is the recently described carbohydrate response element binding protein (ChREBP) gene whose expression is regulated by an intermediate in the pentose phosphate pathway (297). I am unable to arrive at any inference about the effect of lower dietary glucose from HFD on expression of genes in glucose and fat metabolism without exact feed intake data between LFD and HFD pigs.

The starch contents in LFD and HFD were 51.04% and 38.74% respectively. The feed intake for each pig was not available in this study because pigs were group-fed in an open pen ad libitum. Thus, the difference of carbohydrate intake between LFD and HFD pigs is not exactly known. The animal technician did not notice any changes in behavior

or an initial rejection of the HFD, and the body weights of pigs on slaughter were not different between LFD and HFD groups. It was possible that LFD pigs still got enough carbohydrate from the diet. Otherwise, the fat in the muscle would be mobilized to produce energy. However, in this study, expression of glucose transport protein (log_2ratio=0.0623) and genes in fatty acid β-oxidation was not changed in response to the diet shifting to HFD. In this study, dietary shifting from LFD to HFD did not increase expression of genes in fat oxidation, but I can not conclude that the unchanged expression of genes in fatty acid oxidation was caused by the constant high rate of glucose uptake from HFD without strict feed intake data for each experimental pig.

Some more recent newer observations also do not support the glucose-fatty acid cycle theory on the molecular level in explaining the effect of fatty acids on fat oxidation. Saha et al. (319) and Sidossia et al. (325-326) found that the availability of carbohydrate rather than that of fat determines the rate of fat oxidation. Sidossia et al. (325) observed that muscle long-chain acylcarnitine concentration was decreased after infusion of insulin and glucose into human experimental subjects who were constantly infused with long-chain fatty acids. Cameron-Smith (327) found that messenger RNA abundance of FABP, CPT I, and UCP-3 did not differ significantly when rats were fed either a high fat diet or a high carbohydrate diet. Schrauwen-Hinderling et al. (264) found that intramyocellular lipid content in rat skeletal muscle was increased after switching a normal fat diet to a HF diet for 1 week and accompanied by molecular adaptations that favored fat storage in muscle rather than oxidation. They found acetyl-CoA carboxylase 2 (regulator of malonyl-CoA which down regulates CPT-1 activity and thereby controls muscle β-oxidation) mRNA concentration tended to be increased while hexokinase II, glucose

transporter 4, and hormone-sensitive lipase mRNA were unchanged after the HF diet. In my study a tendency of down-regulation of CPT-1 was observed in the muscle after a diet shift from LFD and HFD. In the future studies, assaying the CPT-1 protein concentration and long-chain acylcarnitine concentration may help to determine whether the slightly lower CPT-1 mRNA abundance is related to the dietary starch concentration between LFD and HFD. Ding et al. (48) found that mRNA abundance of CPT-1 tended to be elevated in the muscle of high fat-fed young pigs (P=0.07). This finding would favor the Randle hypothesis. The differences between data from young pigs versus mature rats may be caused by a different developmental phase of animals in the two studies. My study used adult finishing pigs (initial weight was 104~105kg), while young pigs (initial weight was 6.16± 1.01kg) were used in the experiment by Ding et al. (48).

Muscle genes involved in the electron transport and oxidative phosphorylation were down regulated, including NADH-ubiquinone oxidoreductase (log_2ratio= –0.8985) and NADH dehydrogenase 4 (log_2ratio= –1.8858) when the diet was shifted from LFD to HFD in pigs. Sparks (328) et al. observed high fat diet decreased the transcription of six genes involved in oxidative phosphorylation when mice were given high fat diet for 3 weeks including: NADH dehydrogenase 1β subcomplex 3, NADH dehydrogenase 1β subcomplex 5, NADH dehydrogenase flavoprotein1, NADH dehydrogenase Fe-S protein, succinate dehydroganase complex, and solute carrier family 25.

In this study, the decreased transcription of oxidative phosphorylation associated genes may be related to the low mRNA abundance of CPT1 and 3-hydroxyacyl-CoA dehydrogenase in the muscle tissue of HFD pigs. In the high-fat-treated animals, expressions of some translation initiation factors and elongation factors in this array

profile were also depressed (Table 5); expression of ribosomal protein S4, β-globin, and non-histone protein, were slightly increased after high fat treatment. Conversely, for different types of collagen genes (collagen alpha 1, 2, VII alpha 1) expression was decreased. Feeding HFD also resulted in a significantly lowered mRNA abundance of myosin light chain kinase and myosin heavy chain in *Sus scrofa*. While beyond the limits set for this dissertation work, the results on muscle myofibrillar proteins warrant further investigation to explore any putative mechanism whereby dietary fat may modulate muscle protein synthesis, degradation and net accretion in pigs and other animals.

CONCLUSION

In the present study, the expressions of a set of metabolic genes were compared between LFD and HFD pigs among liver, adipose and muscle tissues. In the liver tissue, HFD down regulated most genes involved in lipid metabolism; in the adipose tissue, expression of genes in TAG synthesis was increased in response to HFD; in the muscle tissue, HFD did not alter expression of most genes involved in carbohydrate and lipid metabolism. Therefore, gene expression changes by HFD are different among tissues, which may be related to physiological functions of different tissues in the pig body.

Besides the genes mentioned above, I also found a group of unknown/unidentified genes and other genes in non energy and lipid associated metabolic pathways that were down/up regulated by feeding HFD to pigs. For example, the expression of a group of kinases or phosphatases was changed in liver, adipose and muscle tissue by the shifting from LFD to HFD. The phosphorylation/dephosphorylation cycle is involved in covalent regulation of activity of enzymes in lipid metabolism (i.e., ACC, HSL, 6-PFK) and other

data identified a kinase cascade that may be involved in signaling by glucose to transcriptional machinery (294).

Results need to be interpreted with prudence because this study determined transcription responses of genes using oligonucleotide microarray without confirming any results by an alternative method, and microarray analysis is a high throughout but low quality technique by nature. Changes in the abundance of mRNA of a given gene may reflect altered rates of gene transcription, mRNA processing, and (or) mRNA stability (329). The principal determinant of the abundance of mRNA may be dependent on developmental stage or may be tissue-dependent (330). Generally, the immediate biological response of cells to changes in the external milieu is regulated (within seconds or minutes) by modification of enzyme activity. In contrast, the adaptation to more prolonged changes depends on the regulation of gene transcription. How expression differences triggered by HFD will affect any final metabolic adaptations in finishing pigs is unclear. Considering that some enzymes in the lipid and carbohydrate metabolism pathways are also controlled by allosteric and covalent regulation, it would be incorrect to make conclusions about the metabolic changes only based on transcriptional responses of genes in biological organisms. Thus, this work was clearly discovery and exploratory in nature.

The consequences of consuming a diet of high saturated fat content on cellular activity may involve regulatory effects on gene expression, protein translation, processing, modification, and secretion. Certainly high PUFA containing diets regulate expression of lipogenic genes and affect SREBP processing in rodent liver (101). In this study, a genes of interest list was used to focus my attention on the genes related to

hypothesis of researches in this dissertation. To obtain further biological information from the microarray data, one strategy could be to focus on most changed (down-/up-regulated) 10-20 genes. Alternative gene expression techniques can be used to confirm the expression changes of those genes determined by microarray, and then extend the verification of those changes using protein expression and enzyme activity analysis. However it is clear that target genes must be chosen carefully because of the present absence of extensive information on specific sequences for many genes in the porcine genome. For example developing qRT-PCR assays will require designing of sense and antisense primer sequences and specific assay conditions on a gene by gene basis.

In summary, this experiment is unique in that, to our knowledge, it is the first to utilize functional genomic techniques to compare gene expression in three tissues in finishing pigs fed either a typical LFD or a tallow-based HFD. A long-range goal of this research is to better understand mechanisms whereby saturated fatty acids regulate expression of genes in lipid metabolism and fat deposition among the porcine tissues. This type of information will enable researchers to develop strategies to modify pork quality in the animal (swine) production in future translational research efforts.

Future Research on the Unknown Genes in the Array Platform

In this pig micro-array, there are a total of 13,297 spotted 70 mer probes (genes). 7739 probes were designed based on tentative consensus sequences (TCs), each of them containing at least one 3'expresses sequence tag (EST). Since about 58% of spotted probes of the pig array represent unknown or unidentified genes, not surprisingly, expressions of numerous unknown genes were determined to be significantly increased or decreased in finishing pigs when the diet was shifted from LFD to HFD. Therefore,

further research is necessary to explore/mine the biological information of the differently expressed unknown genes. Additional data mining of all the unidentified spotted genes that showed significant changes in mRNA abundance may well result in new and unique insights of the effect of high fat consumption on gene expression in pigs, but such a task is beyond the scope of this study. Here a simple process in searching for biological information of unknown genes is proposed; this process was tested for few differently expressed unknown genes. Researchers will likely choose the most differently expressed genes (i.e. a high $\log_2$ ratio) as candidate genes in the following activity after micro-array analysis. The following process is proposed to obtain relevant information about "unknown" genes. First, the location/identification number on the array from the Qaigen proprietary index for the 70 mer probes (Qaigen file) can be submitted to the TIGR Gene Index Database (SsGI 5.0) (http://www.tigr.org/tigr-scripts/tgi/T_index.cgi?species=pig). From here the consensus sequence (TCs) representing the unknown gene of interest can be obtained. These TCs may include multiple open reading frames (ORF) and/or correspond to multiple SsGI EST. Because limited annotation is provided by the SsGI EST, the TCs may then be aligned against GenBank by running BLASTn. BLASTn may then result in many hits to many genes in different species for the 70 mer probe sequence spotted on the array. Genes with highest BLAST percent identity score with a given 70 mer will then receive further attention. Although this procedure is not completely reliable to reach a final conclusion about the identity of an unknown gene of interest, the information obtained through the above process may be a starting point for future research. An example of searching tentative biological information of one unknown gene is presented in the Appendix J. Also, this process of identifying "unknown" differentially

expressed porcine genes will likely increase our understanding of genome sequence and function of the domestic pig.

Table 3. Differential transcription responses in liver to feeding LFD and HFD to pigs. Statistic analysis results presented for liver tissue obtained by SAM. One-class response with 1,000 permutations was used to determine genes whose expression was significantly different from zero (log_2ratio =log_2HFD/LFD). At these analysis parameters, the false discovery rate (FDR) for the positive genes was 0.05 (5%); the q value (a measure of significance in terms of the false discovery rate) for all biological replicates were less than 0.01. Different from normal t-test, FDR instead of q value was used to control limits of significant analysis as described in the Chapter 2. In this table, the genes with bold log_2ratio values are differently expresses genes. Positive value means higher expression in HFD pigs; negative value means lower expression in HFD group.

Gene name	Log_2(ratio)
Fatty acid oxidation	
long-chain acyl-CoA dehydrogenase [Sus scrofa]	**-1.1419**
propionyl-CoA carboxylase B [Sus scrofa]	-0.6905
enoyl Coenzyme A hydratase short chain 1 mitochondrial {Homo sapiens}, partial (50%)	**-1.5755**
peroxisomal acyl-coenzyme A oxidase {Homo sapiens}, partial (52%)	**-1.9594**
acyl-Coenzyme A dehydrogenase-8 precursor {Homo sapiens}, partial (54%)	**-1.5876**
Similar to 2 4-dienoyl CoA reductase 2 peroxisomal {Homo sapiens}, partial (58%)	**-1.7430**
very-long-chain acyl-CoA dehydrogenase {Homo sapiens}, partial (27%)	**-3.5427**
acyl-Coenzyme A dehydrogenase family member 8 {Homo sapiens}, partial (42%)	**-2.1410**
acyl-CoA oxidase [Sus scrofa]	**-2.882**
long-chain 3-ketoacyl-CoA thiolase [Sus scrofa]	**-1.7970**
novel enoyl coA/acyl coA hydratase/dehydrogenase type protein (isoform 1), complete	**-0.8277**
Fatty synthesis	
diacylglycerol acyltransferase [Sus scrofa]	**-1.7742**
liver fatty acid binding protein [Sus scrofa]	**-1.1816**
CCAAT/enhancer binding protein alpha [Sus scrofa]	**-1.7694**
cytosolic glycerol-3-phosphate dehydrogenase [Sus scrofa]	**-2.3805**
esterase D [Sus scrofa]	-0.6817
HUMAN ATP synthase lipid-binding protein mitochondrial precursor complete	**-1.2022**
acetyl-Coenzyme A acyltransferase {Homo sapiens}, partial (20%)	**-1.2472**
HUMAN Long-chain-fatty-acid--CoA ligase 2 (LACS 2)., partial (24%)	**-1.5190**
HUMAN Sterol regulatory element binding protein-1 (SREBP-1), partial (21%)	**-1.1527**

fatty-acid synthase - human, partial (7%)	**-0.9071**
diacylglycerol kinase zeta {Homo sapiens}, partial (28%)	**-1.5601**
HUMAN ATP synthase lipid-binding protein mitochondrial precursor complete	**-1.6980**
ATP lipid-binding protein P1 precursor {Sus scrofa}, complete	**-1.3098**
elongation of very long chain fatty acids-like 1 {Homo sapiens}, complete	**-2.0498**
glucokinase {Homo sapiens}, partial (40%)	**-1.4927**
HUMAN Long-chain-fatty-acid--CoA ligase 3 (Long-chain acyl-CoA synthetase 3) (LACS 3)., partial (11%)	-0.2393
fatty acid coenzyme A ligase 5 {Homo sapiens}, partial (14%)	**-1.4042**
fatty acid synthase {Rattus norvegicus}, partial (6%)	-0.1057
BOVIN Acetyl-CoA carboxylase 1 (ACC-alpha) partial (7%)	**-1.9277**
C/EBP-induced protein {Homo sapiens}, partial (25%)	0.43178
adipocyte determination and differentiation-dependent factor 1 [Sus scrofa]	-0.3364
acetyl-CoA carboxylase [Sus scrofa]	**-1.5148**
CCAAT/enhancer binding protein beta [Sus scrofa]	**-0.9312**
CCAAT/enhancer-binding delta protein {Bos taurus}, partial (54%)	**-1.9884**
Carbohydrate metabolism	
Fructose-bisphosphate aldolase A [Rabbit], partial (24%)	**-1.3850**
phosphoenolpyruvate carboxykinase 2 {Homo sapiens}, partial (23%)	**-3.7527**
succinyl-CoA synthetase beta-subunit	**-1.5813**
citrate synthase precursor	**-1.1381**
NADPH-specific isocitrate dehydrogenase	-0.3766
phosphopyruvate hydratase alpha - human, complete	-0.427
pyruvate kinase - rabbit, partial (13%)	**0.99343**
pyruvate dehydrogenase (lipoamide) [Sus scrofa domestica]	**-1.8422**
glucose-6-phosphatase catalytic subunit [Sus scrofa]	**-2.9442**
UDP glucose pyrophosphorylase [Sus scrofa]	**-1.6120**
ATP-specific succinyl-CoA synthetase beta subunit [Sus scrofa]	**-1.4984**
succinate dehydrogenase {Sus scrofa}, complete	0.3003
Pyruvate ddehydrogenase kinase	**-4.2257**
HMG-CoA lyase	**-1.557**
MOUSE 6-phosphofructokinase liver type (Phosphofructokinase 1) partial (33%)	**-2.0062**
fructokinase {Homo sapiens}, partial (38%)	**-2.0355**
glucose transporter type 2; GLUT-2 [Sus scrofa]	**-1.8929**
Cholesterol metabolism	
HUMAN C-4 methyl sterol oxidase [Human] partial (43%)	**-1.3338**
steroid membrane binding protein [Sus scrofa]	**-1.5844**
11-beta hydroxysteroid dehydrogenase isoform 1 [Sus scrofa]	**-2.4192**
3-beta-hydroxysteroid dehydrogenase/delta-5-delta-4 isomerase [Sus scrofa]	**-1.4822**
sterol/retinol dehydrogenase {Homo sapiens}, complete	**-1.0429**
3-hydroxymethyl-3-methylglutaryl-Coenzyme A lyase {Homo sapiens}, complete	**-1.2573**
17beta hydroxysteroid dehydrogenase {Homo sapiens}, partial (23%)	**-1.7631**
3-hydroxy-3-methylglutaryl coenzyme A reductase/HMG-CoA reductase [Sus scrofa]	**-2.1300**
steroid 5-alpha-reductase 2 [Sus scrofa]	**-0.8079**
17beta-estradiol dehydrogenase [Sus scrofa]	**-2.0963**

7-dehydrocholesterol reductase {Homo sapiens}, complete	**-3.7507**
(or 20beta)-hydroxysteroid dehydrogenase - pig, complete	**-2.1625**
high density lipoprotein receptor SR-BI [Sus scrofa]	0.4785
Similar to high density lipoprotein binding protein {Homo sapiens}, partial (23%)	**-2.4586**
apolipoprotein C-III	**-2.1489**
apolipoprotein E	**-1.3042**
apolipoprotein A-I	**-1.8754**
probable ATP-binding cassette transporter ABC-3 - human, partial (6%)	0.5269
Apolipoprotein A-II precursor (Apo-AII). [Cynomolgus monkey], complete	-0.4210
ATP-binding cassette protein M-ABC1 {Homo sapiens}, partial (31%)	**0.8241**
putative ABC-transporter [Sus scrofa]	-0.0700
Electron transport and ATP production	
NADH dehydrogenase (ubiquinone) 14.5K chain - bovine, complete	-0.5583
cytochrome c oxidase subunit I [Sus scrofa]	0.4094
cytochrome b [Sus scrofa]	-0.1405
NADH4 [Sus scrofa]NADH5 [Sus scrofa]NADH6 [Sus scrofa]	**1.21217**
54kDavacuolarH(+)-ATPasesubunit[Susscrofa]	-0.1581
sarcoendoplasmicreticulumcalciumATPase[Susscrofa]	**2.14926**
HUMAN Cytochrome c oxidase polypeptide VIIb mitochondrial precursor [Human] complete	**1.19173**
Others	
HUMAN Adenylyl cyclase-associated protein 1 (CAP 1){Homo sapiens}, complete	**-1.4561**
cAMP-dependent protein kinase inhibitor gamma form (PKI-gamma). {Homo sapiens}, complete	**1.4151**
HUMAN G protein-coupled receptor kinase GRK6 {Homo sapiens}, partial (30%)	**-1.7287**
CREB-binding protein {Homo sapiens}, partial (41%)	0.1304
insulin receptor [Sus scrofa]	-0.2312
alpha-1A adrenergic receptor [Sus scrofa]	**-1.7306**
retinoid X receptor beta [Sus scrofa domestica]	0.6841
proteinphosphatase2Aalphasubunit	**-2.0742**
|highdensitylipoproteinreceptorSR-BI[Susscrofa]	0.4785
RABITSerine/threonineproteinphosphatase2A.partial(25%)	**-1.4554**
proteinphosphatase-1delta[Susscrofa]	**-1.7588**

Table 4. Differential transcription responses in adipose tissue to feeding LFD and HFD to pigs. Statistic analysis results for adipose tissue were obtained by SAM. One-class response with 1,000 permutations was used to determine genes whose expression was significantly different from zero (log_2ratio =log_2HFD/LFD). At these analysis parameters, the false discovery rate (FDR) for the positive genes was 0.05 (5%); the q value (a measure of significance in terms of the false discovery rate) for all biological replicates were less than 0.01. Different from normal t-test, FDR instead of q value was used to control limits of significant analysis as described in the Chapter 2. In this table, the genes with bold log_2ratio values are differently expresses genes. Positive value means higher expression in HFD pigs; negative value means lower expression in HFD group.

Gene Name	Log_2(ratio)
Fatty acid oxiaiton	
Carnitine O-palmitoyltransferase II mitochondrial precursor (CPT II). [Human], partial (34%)	0.3925
long-chain acyl-CoA dehydrogenase [Sus scrofa]	0.5026
short-chain acyl-CoA dehydrogenase [Sus scrofa]	0.2494
mitochondrial 2,4-dienoyl-CoA reductase [Sus scrofa]	0.5058
propionyl-CoA carboxylase B [Sus scrofa]	0.4181
enoyl Coenzyme A hydratase short chain 1 mitochondrial {Homo sapiens}, partial (50%)	**0.6780**
3-hydroxyacyl-CoA dehydrogenase type II {Bos taurus}, complete	0.0518
peroxisomal acyl-coenzyme A oxidase {Homo sapiens}, partial (52%)	0.5765
acyl-Coenzyme A dehydrogenase-8 precursor {Homo sapiens}, partial (54%)	**0.6945**
Similar to 2 4-dienoyl CoA reductase 2 peroxisomal {Homo sapiens}, partial (58%)	0.2744
malonyl-CoA decarboxylase {Homo sapiens}, partial (46%)	-0.4141
very-long-chain acyl-CoA dehydrogenase {Homo sapiens}, partial (27%)	0.4309
acyl-Coenzyme A dehydrogenase family member 8 {Homo sapiens}, partial (42%)	0.3091
acyl-CoA oxidase [Sus scrofa]	**0.6129**
long-chain 3-ketoacyl-CoA thiolase [Sus scrofa]	0.2841
novel enoyl coA/acyl coA hydratase/dehydrogenase type protein (isoform 1), complete	0.3607
Fatty acid and TAG synthesis	
stearyl-CoA desaturase [Sus scrofa]	0.4286
diacylglycerol acyltransferase [Sus scrofa]	0.0450

cytosolic glycerol-3-phosphate dehydrogenase [Sus scrofa]	**0.9255**
esterase D [Sus scrofa]	0.0565
fatty acid-binding protein [Sus scrofa]	**1.1244**
HUMAN ATP synthase lipid-binding protein mitochondrial precursor complete	0.2422
acetyl-Coenzyme A acyltransferase 2 {Homo sapiens}, partial (20%)	0.1775
HUMAN Long-chain-fatty-acid--CoA ligase 2 partial (24%)	**0.7823**
pyruvate kinase M2 {Sus scrofa}, complete	**0.6373**
mitochondrial acetoacetyl-CoA thiolase precursor {Rattus sp.}, partial (40%)	0.5635
HUMAN Sterol regulatory element binding protein-1 (SREBP-1), partial (21%)	0.0242
fatty-acid synthase - human, partial (7%)	-0.4467
HUMAN ATP synthase lipid-binding protein mitochondrial precursor complete	**0.9169**
ATP lipid-binding protein P1 precursor {Sus scrofa}, complete	**0.8710**
elongation of very long chain fatty acids -like 1 {Homo sapiens}, complete	0.5452
HUMAN Long-chain-fatty-acid--CoA ligase partial (11%)	0.3355
diacylglycerol acyltransferase 2 {Mus musculus}, partial (49%)	**0.8850**
_BOVIN Acetyl-CoA carboxylase (ACC-alpha partial (7%)	0.0847
C/EBP-induced protein {Homo sapiens}, partial (25%)	-0.3895
CCAAT/enhancer binding protein beta [Sus scrofa]	**1.3706**
succinyl-CoA synthetase alpha subunit [Sus scrofa]	0.1135
CCAAT/enhancer-binding delta protein {Bos taurus}, partial (54%)	0.1274
Arabidopsis thaliana lipid transfer protein 6	0.4245
Carbohydrate metabolism	
succinyl-CoA synthetase beta-subunit	0.0985
glucose transport protein [Sus scrofa]	0.2785
citrate synthase precursor	**0.8103**
UDP glucose pyrophosphorylase [Sus scrofa]	**0.6706**
ATP-specific succinyl-CoA synthetase beta subunit [Sus scrofa]	0.4940
phosphopyruvate hydratase alpha - human, complete	**0.6518**
Pyruvate kinase M2 isozyme [Rabbit] {Oryctolagus cuniculus}, partial (26%)	0.4117
pyruvate dehydrogenase (lipoamide) [Sus scrofa domestica]	**0.6096**
HUMAN Succinate dehydrogenase [ubiquinone] complete	**0.6024**
succinate dehydrogenase {Sus scrofa}, complete	**0.6685**
Fructose-bisphosphate aldolase A (Muscle-type aldolase). [Rabbit], partial (24%)	**0.9142**
MOUSE 6-phosphofructokinase liver type (Phosphofructokinase 1) partial (33%)	0.1100
GLUT4 [Sus scrofa]	0.5715
Cholesterol metabolism	
HUMAN C-4 methyl sterol oxidase [Human] partial (43%)	0.2321
steroidogenic factor-1 SF-1 [Sus scrofa]	-0.0602
11-beta hydroxysteroid dehydrogenase isoform 1 [Sus scrofa]	-0.0102
sterol regulatory element binding transcription factor 2){Homo sapiens}, partial (18%)	0.3377
sterol/retinol dehydrogenase {Homo sapiens}, complete	0.4294
3-hydroxymethyl-3-methylglutaryl-Coenzyme A lyase {Homo sapiens}, complete	0.2074
17beta hydroxysteroid dehydrogenase {Homo sapiens}, partial (23%)	0.1299
steroid 5-alpha-reductase 2 [Sus scrofa]	-0.3321
17beta-estradiol dehydrogenase [Sus scrofa]	0.4718
3alpha(or 20beta)-hydroxysteroiddehydrogenase - pig, complete	**0.7596**

apolipoprotein B	-0.4293
apolipoprotein E [Sus scrofa]	**0.8726**
apolipoprotein A-I [Sus scrofa]	-0.1557
ABC-transporter {Gorilla gorilla}, partial (54%)	-0.4181
Similar to high density lipoprotein binding protein {Homo sapiens}, partial (23%)	**0.6129**
putative ABC-transporter [Sus scrofa]	-0.2150
Electron transport and ATP production	
NADH dehydrogenase (ubiquinone) 14.5K chain - bovine, complete	0.5219
NADH4 [Sus scrofa]NADH5 [Sus scrofa]NADH6 [Sus scrofa]	0.5037
H(+)-ATPasesubunit[Susscrofa]	0.5077
Na+./K+ATPasealpha1subunit[Susscrofa]	0.1220
Ca(2+)-transportATPase(class2)[Susscrofa]	0.2191
BOVINVacuolarATPsynthasesubunitE partial(76%)	**0.8818**
HUMANVacuolarATPsynthasesubunitd)(partial(81%)	0.2563
Others	
G protein-coupled receptor	-0.4972
cAMP-regulated phosphoprotein [Sus scrofa]	0.1242
5'-AMP-activated protein kinase catalytic alpha-2 subunit	-0.2688
HUMANCyclic-AMP-dependenttranscriptionfactorATF-4.complete	**1.0057**
nuclear receptor binding protein {Homo sapiens}, partial (53%)	0.3840
proteinphosphatase2Aalphasubunit	**0.6447**
actin-relatedprotein3[Susscrofa]	0.3594
leptin[Susscrofa]	**0.6220**
phospholipaseD2{Homosapiens}.partial(47%)	0.1718
phospholipaseCbeta-3{Rattusnorvegicus}.partial(28%)	0.3438
HUMANSerine/threonineproteinphosphatase2A.partial(59%)	0.3105
HUMANTranscriptioninitiationfactorTFIID31kDasubunit(TAFII-31Human].partial(41%)	0.3854
transcriptionfactorTFII-I-human.partial(9%)	0.4046
phosphoproteinphosphataseXcatalyticchain-human.partial(48%)	0.2520
HUMANLow-densitylipoproteinreceptor-relatedprotein1precursor(LRP)-2partial(5%)	0.4505
RATTranscriptioninitiationfactorIIB(TFIIB).[Rat].partial(80%)	**0.9901**
HUMANTFIIHbasaltranscriptionfactorcomplexp52subunitpartial(44%)	0.1995
RABITSerine/threonineproteinphosphatase2A56kDa partial(25%)	**0.9150**
BOVINVacuolarATPsynthasesubunitG1.complete	**0.9573**
RATTranscriptioninitiationfactorIIAgammachaincomplete	0.1436

Table 5. Differential transcription responses in skeletal muscle to feeding LFD and HFD to pigs. Statistical analysis results for muscle tissue was obtained by SAM. One-class response with 1,000 permutations was used to determine genes whose expression was significantly different from zero (log_2ratio =log_2HFD/LFD). At these analysis parameters, the false discovery rate (FDR) for the positive genes was 0.05 (5%); the q value (a measure of significance in terms of the false discovery rate) for all biological replicates were less than 0.01. Different from normal t-test, FDR instead of q value was used to control limits of significant analysis as described in the Chapter 2. In this table, the genes with bold log_2ratio values are differently expresses genes. Positive value means higher expression in HFD pigs; negative value means lower expression in HFD group.

Gen name	Log_2(ratio)
Fatty acid oxidation	
long-chain acyl-CoA dehydrogenase [Sus scrofa]	**0.6594**
short-chain acyl-CoA dehydrogenase [Sus scrofa]	-0.1393
Propionyl-CoA carboxylase beta chain precursor [Sus scrofa]	-0.2702
BOVIN 3-hydroxyacyl-CoA dehydrogenase type II (Type II HADH). [complete]	**-0.8938**
malonyl-CoA decarboxylase {Homo sapiens}, partial (46%)	-0.3163
carnitine palmitoyltransferase I {Ovis aries}, partial (32%)	**-0.7693**
very-long-chain acyl-CoA dehydrogenase {Homo sapiens}, partial (27%)	0.4263
novel enoyl coA/acyl coA hydratase/dehydrogenase type protein (isoform 1)), complete	-0.1240
Fatty acid and TAG synthesis	
stearyl-CoA desaturase [Sus scrofa]	0.2820
diacylglycerol acyltransferase [Sus scrofa]	-0.0920
CCAAT/enhancer binding protein alpha [Sus scrofa]	0.0413
cytosolic glycerol-3-phosphate dehydrogenase [Sus scrofa]	**-1.2937**
esterase D [Sus scrofa]	-0.0981
fatty acid-binding protein [Sus scrofa]	**1.2009**
acetyl-Coenzyme A acyltransferase 2 {Homo sapiens}, partial (20%)	0.4629
LCFB_HUMAN Long-chain-fatty-acid--CoA ligase 2 partial (24%)	0.2262
mitochondrial acetoacetyl-CoA thiolase precursor {Rattus sp.}, partial (40%)	0.1597
fatty-acid synthase - human, partial (7%)	-0.3833
ATP lipid-binding protein P1 precursor {Sus scrofa}, complete	0.1553
fatty acid coenzyme A ligase 5 {Homo sapiens}, partial (14%)	0.2210
C/EBP-induced protein {Homo sapiens}, partial (25%)	0.1980

CCAAT/enhancer binding protein beta [Sus scrofa]	**-0.8919**
HUMAN [Pyruvate dehydrogenase [lipoamide]] kinase isozyme 4 mitochondrial precursor partial (18%)	**-0.6925**
CCAAT/enhancer-binding delta protein {Bos taurus}, partial (54%)	**-0.7810**
Carbohydrate metabolism	
succinyl-CoA synthetase alpha subunit [Sus scrofa]	0.0739
succinyl-CoA synthetase beta-subunit	0.2177
glucose transport protein [Sus scrofa]	0.0623
citrate synthase precursor	0.2159
pyruvate dehydrogenase (lipoamide) [Sus scrofa domestica]	0.1319
Pyruvate kinase M2 isozyme [Rabbit], partial (26%)	-0.2641
malate dehydrogenase precursor	0.0976
ATP-specific succinyl-CoA synthetase beta subunit [Sus scrofa]	0.1448
Fructose-bisphosphate aldolase A (Muscle-type aldolase). [Rabbit], partial (24%)	**-0.8919**
Cholesterol metabolism	
3-beta-hydroxysteroid dehydrogenase/delta-5-delta-4 isomerase [Sus scrofa]	0.1527
sterol/retinol dehydrogenase {Homo sapiens}, complete	0.0742
3-hydroxymethyl-3-methylglutaryl-Coenzyme A lyase {Homo sapiens}, complete	-0.4520
sterol regulatory element binding protein-2 [Sus scrofa]	-0.2470
3-hydroxy-3-methylglutaryl coenzyme A reductase/HMG-CoA reductase [Sus scrofa]	-0.3022
17beta-estradiol dehydrogenase [Sus scrofa]	0.2636
3alpha(or 20beta)-hydroxysteroid dehydrogenase - pig, complete	0.1451
apolipoprotein C-III	0.0247
apolipoprotein E [Sus scrofa]	**-0.7275**
apolipoprotein A-I [Sus scrofa]	0.0503
Similar to high density lipoprotein binding protein (vigilin) {Homo sapiens}, partial (23%)	-0.3212
Apolipoprotein A-II precursor [Cynomolgus monkey], complete	-0.1147
ATP-binding cassette protein M-ABC1 {Homo sapiens}, partial (31%)	**-0.6341**
Protein metabolism	
Eukaryotic translation initiation factor 3 subunit 7 {Homo sapiens}, partial (38%)	**-0.8171**
beta-globin [Sus scrofa]	**0.9614**
ribosomal protein S4 [Sus scrofa]	0.4505
40S ribosomal protein S12 [Sus scrofa]	**0.6203**
smooth muscle myosin light chain kinase [Sus scrofa]	0.1456
HUMAN 40S ribosomal protein S6 (Phosphoprotein NP33). [Rat], complete	0.2182
probable translation initiation factor eIF-2B delta chain – human partial (61%)	0.1482
ribosomal protein L15 cytosolic [validated] - rat, complete	0.4368
eukaryotic translation initiation factor 3 subunit p42/p44 {Homo sapiens}, complete	**-1.1871**
HUMAN Histone acetyltransferase type B subunit 2 partial (19%)	0.1943
40S ribosomal protein S28. [Rat] {Rattus norvegicus}, complete	0.3755
arginine N-methyltransferase p82 isoform {Cricetulus longicaudatus}, partial (26%)	0.1196
eukaryotic translation initiation factor 4E-like 3 {Homo sapiens}, partial (89%)	**-0.6320**
Similar to argininosuccinate lyase {Mus musculus}, partial (56%)	0.1043
BOVIN Elongation factor Tu mitochondrial precursor. [Bovine] partial (66%)	-0.3424

histone deacetylase 3 {Rattus norvegicus}, partial (50%)	-0.4110
translation initiation factor eIF-5A [validated] - human, complete	**-0.8752**
Glutamate dehydrogenase mitochondrial precursor {Mus musculus}, partial (32%)	-0.4566
Collagen alpha 1(I) chain precursor. [Dog] partial (5%)	**-1.0131**
Collagen alpha 2(I) chain precursor. [Dog] partial (12%)	**-1.2133**
alanine aminotransferase {Rattus norvegicus}, partial (24%)	-0.0594
translation initiation factor eIF-2 alpha chain - rat, partial (62%)	-0.3298
collagen VIII alpha 1 [Sus scrofa]	**-0.9139**
myosin light chain kinase	**-0.9061**
myosin heavy chain [Sus scrofa]	-0.2212
homologue to EGAD|4603|4479 collagen type VI alpha 1 {Homo sapiens}, (7%)	-0.3651
Collagen alpha 1(VI) chain precursor. [Mouse] {Mus musculus}, partial (13%)	**-0.8547**
non-histone protein HMG1	0.2482
glutathione transferase class mu GSTM4 (version 2) - human, complete	0.1365
| mitochondrial branched chain aminotransferase precursor; {Ovis aries}, partial (21%)	-0.4397
myosin heavy chain [Sus scrofa]	**-1.4053**
elongation factor 1 alpha {Bos taurus}, partial (24%)	-0.3662
Electron transport and ATP synthesis	
BOVIN NADH-ubiquinone oxidoreductase subunit mitochondrial precursor (37%)	**-0.8985**
cytochrome b [Sus scrofa]	-0.3498
NADH4 [Sus scrofa]NADH5 [Sus scrofa]NADH6 [Sus scrofa]	**-1.8858**
Cytochrome c oxidase polypeptide VIIb mitochondrial precursor] {Homo sapiens}, complete	-0.4757
Na+/K+ATPasealpha1subunit[Susscrofa]	0.1782
H++K+)-ATPase	-0.2512
Others	
insulin receptor precursor [Sus scrofa]	-0.3208
CREB-binding protein {Homo sapiens}, partial (41%)	0.0973
cAMP-regulated phosphoprotein [Sus scrofa]	0.5336
cyclic AMP-responsive element binding protein, delta variant [Sus scrofa]	-0.5974
GTP-binding regulatory protein Gs alpha chain partial (54%)	0.4626
leptin[Susscrofa]	**0.7110**
transmembraneleptinreceptor[Susscrofa]	-0.2237
ProbablecalciumtransportingATPaseKIAA0703{Homosapiens}.partial(40%)	**1.0323**
CREB-RP(G13){Homosapiens}.partial(32%)	**-0.7468**
GeneencodinghumansecretedgroupIIIphospholipaseA2{Homosapiens}.partial(38%)	**-0.6353**
cytosolicphospholipaseA2beta;cPLA2beta{Homosapiens}.partial(18%)	-0.2098
HUMANTranscriptioninitiationfactorTFIID20/15kDasubunits, partial(68%)	0.2598
TranscriptioninitiationfactorIIB(TFIIB) Rat].partial(80%)	0.0618
calcium-independentphospholipaseA2{Homosapiens}.partial(13%)	-0.2182
sarcoendoplasmicreticulumcalciumATPase[Susscrofa]	-0.5584
|proteinphosphatase-1delta[Susscrofa]	**-0.6889**
RATTranscriptioninitiationfactorIIAgammachain(TFIIAP12subunit) (TFIIA-12)(TFIIAS).complete	0.2600
proteinphosphatase2Aalphasubunit	**0.7904**

V. EXPRESSION OF PORCINE GENES RELATED TO FATTY ACID AND CHOLESTEROL METABOLISM IN DIFFERENT PORCINE TISSUES

INTRODUCTION

Consumption of muscle foods has been typically associated with excess energy and saturated fatty acid intakes. American consumers are cognizant that excessive consumption of high-energy, predominantly saturated fatty acids containing foods may contribute to the onset of obesity, type 2 diabetes, and related cardiovascular maladies. Thus, through genetic selection for more rapidly growing and leaner pigs, through formulation of diets that precisely meet swine nutrient requirements, and through enhanced health care and management practices, over the last 25 years the US pork industry has attempted to produce muscle foods with lower fat content that are more in line with recommendations of the American Heart Association to keep fat calories near 30% of total calorie in the human diet. Unfortunately, this positive change in porcine muscle foods has a down-side in that lean pork lack the traditional taste and juiciness associated with pork. Since the seminal studies of Hammond (331), it has been understood that, in order to achieve fat deposition and the desired juiciness in muscle, subcutaneous and visceral storage lipid depots have to be "filled" first. Hence during the production cycle, shortly before harvest, pigs have been placed before harvest, on

finishing diets to ensure adequate rates of fat gain to promote some intramuscular fat deposition.

During industry-wide programs to significantly lower total fat in pork over the last 25 years, finishing programs had been modified and pigs with much lower propensity to deposit fat were utilized. Today the industry is attempting to promulgate a new production strategy that will result in relatively low subcutaneous and visceral fat accumulation coupled with some intramuscular fat deposition. Based on what is known about the biology of fat deposition in storage depots and muscle in pigs, such new strategies will not emerge without a more complete understanding of the temporal and tissue-specific regulation of fat deposition in pigs. As in humans or rodents, fat deposition in the pig is the result of complex interaction between genetic and a range of environmental influences including nutrition (1). Nutritional manipulation such as changing energy sources (fats and carbohydrates) and /or amounts in diets may have a significant effect on both fat accretion and muscle growth (332). The liver is the primary site for *de novo* fatty acid synthesis in humans and rodents, but adipose tissue in pigs (41) is the principal site of *de novo* fatty acid synthesis. While the pig has been used as an animal model to study the progression of excess energy intake on fat deposition, obesity and cardiovascular maladies for application to human medicine, many key aspects of lipid metabolism in pig are not exactly identical to human or rodents (13). Thus, to specifically target the pattern of tissue fat deposition in pigs during the finishing phase of production, regulation of porcine lipid metabolism across major tissues (liver, skeletal muscle and adipose tissue) must first be better understood at the molecular level to develop future strategies for specific tissue-targeted fat deposition.

Enhancing intramuscular fat accumulation in pigs by increasing dietary fat late during the finishing phase has been previously attempted (333), but has not become a common strategy in the pork industry. In the previous chapter IV described the effect of a sudden shift from a corn-soy low-fat diet to a corn-soy, tallow, corn oil-supplemented high-fat diet on global gene expression in skeletal muscle, liver and adipose tissue in finishing pigs, as evaluated with an oligo/DNA array spotted slide platform. In this chapter, emphasis is placed on expression responses of four targeted genes associated with lipoprotein, triacyglycerol, and cholesterol transport including acyl-CoA cholesterol acyltransferase (ACAT); lethicin-cholesterol acyltransferase (LCAT), ApoB and hepatic lipase (HL).

The purpose of this study was to compare the transcription response of these targeted genes after a shift from corn-based high-carbohydrate, low-fat diet (LFD) to a tallow-supplemented high-fat diet (HFD) fed for 2 weeks. The HFD contained a high proportion of saturated fat contributed by the tallow. I propose that an abrupt sudden shift from a typical finishing diet to a diet supplemented with saturated fatty acids in 90-100 kg pigs will result in metabolic adaptations and changes in transcription of genes involved in triacylglycerol and cholesterol trafficking in the animal. While the animal experiment was being conducted, an initial step of this study in the laboratory was to first partially clone a porcine cDNA fragment of LCAT and ACAT. Information provided from these porcine specific sequences along with sequence data for porcine HL and ApoB was then utilized to design primers to determine the expression pattern of these targeted four genes in porcine skeletal muscle, liver, adipose and small intestinal epithelium (gut) and then utilize a semi-quantitative reverse transcriptase-polymerase chain reaction (smqRT-

PCR) method to quantify the relative mRNA abundance of ACAT, LCAT, HL and ApoB between pigs fed the low and high fat diets.

MATERIALS AND METHODS

Animal Feeding Trial

Eight adult, crossbred pigs (90 kg) were provided *ad libitum* access to either a corn and soybean-based, low-fat diet (LFD) (n=4) or a tallow/ corn oil-supplemented high-fat diet (HFD) (n=4) for 14 days. For LFD, 4.3% diet energy was from fat contributed by the corn; while for HFD, 40% dietary energy was contributed by saturated fatty acids from beef tallow plus some additional corn oil. The composition of the diets fed to pigs for the 14 days before slaughter is presented in Table 1. The calculated protein concentration in the experimental diet was 20% and 19.3 %, respectively, for LFD and HFD. Both diets met or exceeded all nutrient requirements for finishing pigs as prescribed by the NRC (199).

This experiment was approved by the Auburn University Institutional Animal Care and Use Committee (IACUC #0207-R-2448). The pigs were slaughtered at 14 days, and liver, subcutaneous adipose tissue and skeletal muscle tissues were collected. Pig identification number, diet treatment for each pig, and the day the samples were collected are presented in the Table 2.

Table 1. Composition of diets fed to finishing pigs*

Ingredient	Control (%)	High Fat (%)
Corn	68.05	51.65
Fat source (Tallow/Sat Fat /corn oil/equiv)	0	13.25 3.25
Soybean Meal	29.00	29.00
Premix		
Di-Calcium Phosphate	1.00	1.00
Limestone, ground	0.80	0.80
Salt	0.35	0.35
Vitamins & trace mineral mix	0.2	0.2
Additive/fiber	0.5	0.5
Calculated analysis		
Kcal/gm	4.1	5.2
Total Protein %	20	19.3
Polyunsaturated to sat. fatty acid	0.2	0.2

*Meets all NRC (1998) nutrient requirements for finishing pigs
*The formulations are presented on a present as is feed ingredients (not dry metarial corrected). These diets were not formulated to be iso-energetic.

Table 2. Identification numbers, assigned dietary treatment, and the date of sample collection for experimental pigs.

Pig	Length of Treatment (days)	Fat Supplemented to diet (%)	Date Sample Collected
4901	14	0 (LFD)	11/19/2003
5504	14	0 (LFD)	11/19/2003
5205	14	0 (LFD)	11/19/2003
6002	14	0 (LFD)	11/19/2003
4905	14	16.5 (HFD)	11/19/2003
5207	14	16.5 (HFD)	11/19/2003
5502	14	16.5 (HFD)	11/19/2003
6001	14	16.5 (HFD)	11/19/2003

Tissue Collection

All the pigs were killed at the Auburn University Meat Laboratory by electrical stunning, followed by exsanguination under USDA/APHIS inspection. Liver, subcutaneous adipose, skeletal muscle and gut tissues were removed immediately snap-frozen in liquid nitrogen as described in the preceding chapter prior to scalding and de-hairing of the swine carcass. Liver samples were removed from the right lobe; tissue samples from the middle layer subcutaneous adipose were removed from the subcutaneous depot near 12^{th} rib, and skeletal muscle samples were removed from the longissimus muscle between the 10^{th} and the last ribs. This procedure minimized contamination and product rejection by the federal inspection system and allowed for the further processing of the carcass for eventual human consumption.

Analysis of Plasma Triacylglycerol and Cholesterol Concentration

Plasma was prepared from blood obtained during slaughter and frozen at -20 ºC until analyzed for total cholesterol and triglyceride concentrations by the Clinical Diagnostic Laboratory at the Auburn University College of Veterinary Medicine.

RNA Isolation

Total RNA was isolated by using a one step guanidinium-phenol-chloroform extraction procedure (201). One-half gram of frozen adipose tissue from each pig was powdered using a hammer-driven, stainless steel mortar and pestle that was constantly cooled with liquid nitrogen. The tissue was then placed in a 50-ml conical tube containing 10 ml of TriZol reagent (Invitrogen Corporation; Carlsbad, CA), and RNA was isolated according to the instructions provided. 0.5 μg of total RNA was dissolved in

100 µl of distilled, deionized RNase-free water, and RNA integrity was analyzed on a 1.0 % agarose gel to check the integrity of RNA. Total RNA was quantified using an Ultrospec 3000 UV/ visible spectrophotometer (Amersham Pharmacia Biotech; Piscataway, NJ), and the RNA quality was estimated by observing the smearing of 18S and 28S bands, intensities of the bands and DNA contamination. . Extracted RNA was stored at -80ºC in 1µl of RNA Secure/ µg of RNA (Ambion; Austin, TX). An example of the banding pattern of total RNA is presented in Figure 1.

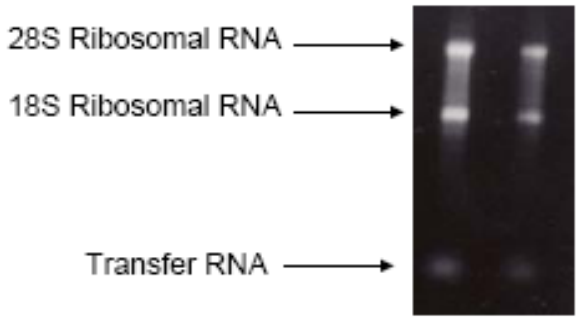

Fig 1. Intact total RNA resolved on a 1.0% agarose gel at 120V for 30 minutes. The bands represented from top to bottom are 28S ribosomal RNA, 18S ribosomal RNA, and transfers/small RNA.

Cloning of Porcine LCAT and ACAT Gene Fragments

Primer Design

Paired sense and anti-sense primers were designed based on known human sequences using the web-based computer software, Primer3 (http://frodo.wi.mit.edu/cgi-bin/primer3/primer3_www.cgi). LCAT and ACAT primers were designed referring to the human LCAT mRNA sequence (Accession No. BC014781.1) and human ACAT mRNA sequence (Accession No. L21934.2) found in GenBank. Primers were used in the following procedure to amplify porcine LCAT and ACAT fragments. The sequence of primers and the expected sizes of amplicons produced by the polymerase chain reaction (PCR) are listed in the Table 3.

Table 3. DNA sequence of the primers, annealing temperature used, and number of PCR cycles performed for the semi-quantitative RT-PCR

Gene identity	Primers	Source of primers	Annealing temperature	# of PCR cycles	Size, bp
LCAT(BC014781.1)	Forward: TTGATGGCTTCATCTCTCTTGG Reverse: TCATCACCATCCTCATAGAGCA	Human	59°C	35	453
ACAT(L21934.2)	Forward: CTTCCACCCCTTCTCCATCTTT Reverse: TGCCATAGTAGCCAATGGGATA	Human	59°C	35	815
ApoB(L11235.1)	Forward: TCTCCTTATGGGAAAAAGCAGG Reverse: GCCAACTCTGGAAGAGAAATCT	Pig	59°C	33	517
HL (J03540.1)	Forward: GAACGCACAAGATTGGGAGAAT Reverse: ATGATCAGCTCGCCGATATCC	Pig	59°C	33	697
β-actin(AY550069.1)	Forward: GGACTTCGAGCAGGAGATGG Reverse: GCACCGTGTTGGCGTAGAGG	Pig	59°C	24	233

Reverse Transcription-Polymerase Chain Reaction (RT-PCR)

One μg of total RNA from porcine adipose tissue was amplified in the presence of the LCAT or ACAT primer pairs by reverse transcription (RT) reaction and polymerase chain reactions (PCR). These reactions were conducted using the OneStep RT-PCR kit (Qiagen, Inc.) and a PTC-100 programmable thermal cycler (MJ Research, Inc.; Waltham, MA). Within each PCR cycle, the initial denaturation step was at 94^{o} C for one minute. This was followed by primer annealing step at 59^{o} C for one minute. Annealing was followed by a one minute extension step at 72^{o} C. The denaturation, annealing and extension steps were then sequentially repeated 29 more times followed by a final extension step at 72^{o} C for ten minutes. 20 μl of RT-PCR reaction product was run on a 1.0% agarose gel to determine if there was an amplicon of the expected length based on a standard 100 bp DNA ladder (Invitrogen Corporation). The expected product lengths derived from sequence data were 453 base pairs (bp), and 815 bp for LCAT and ACAT, respectively.

Cloning and Transformation of Porcine Partial Coding Sequences

Fresh reverse transcription-polymerase chain reaction products were directly ligated into a pCR-II TOPO vector (Invitrogen) and transfected into TOP10 or TOP10F' *E. coli* cells (Invitrogen) using the pCR-II TOPO Vector System. In the pCR-II TOPO Vector System there were two selection methods: ampicilin resistance and X-galactosidase (X-gal) activity. After ligation and transformation, 50 μl and 200 μl of the transformed bacteria in S.O.C. Media (0.5% Yeast extract, 2.0% tryptone, 10mM NaCl, 2.5mM KCl, 10mM $MgCl_2$, 20mM $MgSO_4$, 20mM glucose) were plated on LB (Luria-Betani) selective plates containing 200 μg/ml of ampicillin (Fisher Scientific; Hampton, NH), and

53.3 μg/ml X-gal (Fisher Scientific). For TOP10F' cells, plates also contained 0.13 mM Isopropyl-β-D-thiogalactoside (IPTG) (Fisher Scientific). Plates were incubated at 37°C for 12-16 hours. Positive colonies were selected from the smear plates, streaked on identically prepared LB plates, and incubated 12-15 hours at 37°C. Four colonies positive for the cloned vector containing the insert of interest were then selected from each plate. These colonies were used each to inoculate liquid cultures of 4 ml LB media with 200 μg/ml ampicillin. These small-scale cultures were incubated on a horizontal shaker at 37°C for 15 hours. Then, plasmid DNA was purified from 1.5 ml of each culture following the microcentrifuge protocol of the Qiaprep Spin Miniprep Kit (Qiagen, Inc.). The pCR II-TOPO cloning vector contains *EcoRI* restriction sites on either side of the inserted cDNA fragment. Once plasmid DNA was isolated, it was digested by cutting with EcoR1 (Invitrogen Corporation). Sizes of ligated inserts for LCAT and ACAT were verified by a restriction digestion of plasmid DNA with *EcoRI* restriction enzyme (Invitrogen Corporation) followed by electrophoresis through a 1.0% agarose gel.

To produce an ample quantity of cDNA fragments, large-scale cultures of plasmid DNA were obtained by inoculating 200 ml of LB Media containing 200μg/ml ampicillin with 2ml of culture from the colonies of choice in a one-liter culture flask. The cultures were incubated at 37°C for 15 hours with agitation. Plasmid DNA was purified following the Plasmid Purification Maxi Protocol using two Qiagen-tip 500 columns from a Qiafilter Maxi Kit (Qiagen, Inc.). As with the small-scale cultures, restriction digestions were performed and products were run on agarose gels to ensure that purified plasmids contained inserts of appropriate size. Plasmid DNA was prepared for long-term storage by freezing 400μl of culture in 200μl of sterol 100% glycerol at -80°C.

Sequencing

To confirm RT-PCR cloning and to determine the directionality of the insert, plasmids containing the LCAT and ACAT cDNA fragments were sequenced bi-directionally. Sense and antisense sequences were obtained for the inserts by sequencing with T7 and SP6 primers at the Auburn University Genomics and Sequencing Lab using a modification of the Sanger method (314) with fluorescent dideoxy termination in an automated capillary sequencer (Applied Biosystems; Foster City, CA).

The sequence of porcine LCAT and ACAT cDNA fragments were previously unknown. The partial fragment of the porcine LCAT and ACAT mRNA sequence was submitted to Genbank, accepted, and assigned Accession Number AY349156 for LCAT and AY676347 for ACAT. The fragment of pig LCAT is part of the coding region. The translated pig LCAT protein includes 150 amino acids and the protein accession number is AAQ24609 assigned by Genbank. The fragment of ACAT is part of 5' UTR (un-translated region). Sequences obtained from DNA sequencing were submitted to BLASTn (335) to determine the homology of the insert sequences with other sequences in GenBank. The LCAT and ACAT sequences generated here were found to have 92% and 99% homology with the human LCAT and ACAT mRNA sequence, respectively (Fig 5 and Fig 6). The translated partial LCAT protein sequence was submitted to BLASTp (336), and it was found to be 93% homologous with the human LCAT protein (Fig 7).

Determining Gene Expression Distribution by RT-PCT

Similar RT-PCR procedure as described above was performed to determine the expression pattern of ACAT, LCAT, HL and ApoB in porcine tissues, liver, adipose, muscle and gut (four tissues).

Determining Relative mRNA Abundance by Semi-quantitative PCR

A two-step semi-quantitative RT-PCR method was developed to measure gene expression in liver, adipose and gut tissues (337). During the preliminary stages of method development, linearity with respect to RNA and amplicon appearance and PCR cycle number were determined. In the final protocol, cDNA was first synthesized from total RNA using oligo-$(dT)_{18n}$ primers (Operon, Huntsville, AL) and the Omniscript Reverse Transcription Kit (Qiagen Inc.). In the next step, identical primers with those in the cloning of LCAT and ACAT porcine gene fragments were used for amplification of the cDNA. Primers for apolipoprotein B (ApoB), hepatic lipase (HL) and β -actin were designed based on the known pig ApoB mRNA sequence (Accession No.L11235.1), pig HL mRNA sequence (Accession No.J03540.1) and pig β-actin mRNA sequence (AY550069.1). Followig the reverse transcription step, cDNA from different tissues were amplified with ACAT, LCAT, apoB, and HL specific primers using the Taq PCR Core Kit (Qiagen Inc.). The optimal PCR annealing temperatures for each specific gene primer pair and number of PCR cycles to get linear amplification range are presented in Table 3. A housekeeping gene, β-actin was used as an internal control and normalization gene. During the PCR process for each specific gene, β-actin primers were added to the same tube when 24 cycles were remaining in each gene's specified linear amplification range. Finally, the PCR products were electrophoresed on 1.0% agarose gel and base pair sizes

of PCR product were determined relative to DNA ladder standards. The gel images were captured by digital still camera (Sony, Tokyo, Japan), and densitometry values were measured with the NIH image J program (http://rsb.info.nih.gov/ij/). RT-PCR values are presented as a ratio of the specified gene's signal in the selected linear amplification cycle divided by β-actin signal. Data were analyzed by t-test using SAS software.

RESULTS

The dietary shift was imposed on the selected pigs without any incremental adaptation. Overall, animal performance for the next 14 d was not affected by the abrupt sudden shift from the LFD to the HFD. Pigs were group-fed in an open pen ad libitum and the animal technician did not notice any changes in behavior or an initial rejection of the HFD. Based on observations only, the HFD was apparently more palatable to the finishing pigs than the control, corn-soy, low-fat diet, and there were no difference in dry matter intake between LFD and HFD pigs. Final bodyweights at slaughter and plasma cholesterol and triacylglycerol concentrations in the experimental animals are presented in Table 4.

Table 4. Final body weight of pigs, plasma cholesterol and triacylglycerol on day 14. Each of these physiological parameters is expressed as mean ±standard deviation (SD).

Group	LFD	HFD	P-value
Final body weight ±SD; kg	105.1 ± 5.4	106.1 ± 2.93	0.34
Plasma cholesterol (mg/100mL) ±SD	91.75± 8.92	101.33± 14.18	0.45
Plasma triacyglycerol (mg/100mL) ±SD	32.75± 6.65	52.33± 19.73	0.11

Both cholesterol and triacylglycerol concentrations were numerically higher in HFD fed pigs but the differences did not approach significance.

The tissue distribution pattern of the four genes was first determined by RT-PCR with RNA isolated from liver, adipose, skeletal muscle and gut epithelium. HL (as expected) was expressed only in the liver while apoB was detected in liver, adipose and gut epithelium. LCAT was found in all four tissues, while ACAT was only detected in liver and gut epithelium (Fig 2). ApoB expression was highest in liver, followed by gut and adipose (Fig 2, when normalized to β actin expression). This ApoB gene expression pattern is similar to that noted in humans and rodents; however, ApoB synthesis, while extremely critical for chylomicron formation (small intestine) and VLDL (liver) synthesis, is not principally regulated at the transcriptional level (338, 339). Based on the present results, the pattern of ApoB mRNA expression in finishing pigs is consistent with previous work (humans, rodents) showing that intestine and liver are primary tissues that export lipids to other tissues utilizing the ApoB protein as a lipoprotein carrier for chylomicrons and VLDL (340).

Comparing mRNA abundance/ expression of the four genes in different tissues between LFD and HFD fed pigs (Fig 3), dietary high fat significantly decreased ACAT transcription in porcine liver ($P<0.05$, Fig 3A). Although mRNA abundance of ACAT was lower in the gut of HFD pigs than LFD pigs from gel image analysis, these results were based on only two pigs (Fig 3C). No changes in mRNA abundance were observed for liver LCAT, ApoB and HL between LFD and HFD fed pigs (Fig 4 A). HFD also did not change the mRNA abundance of LCAT and apoB in the adipose tissue (Fig 4B).

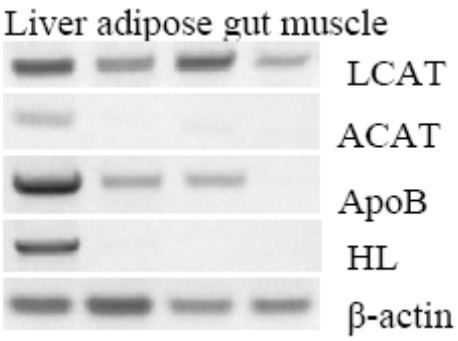

Fig 2. Gene distribution pattern in porcine tissues

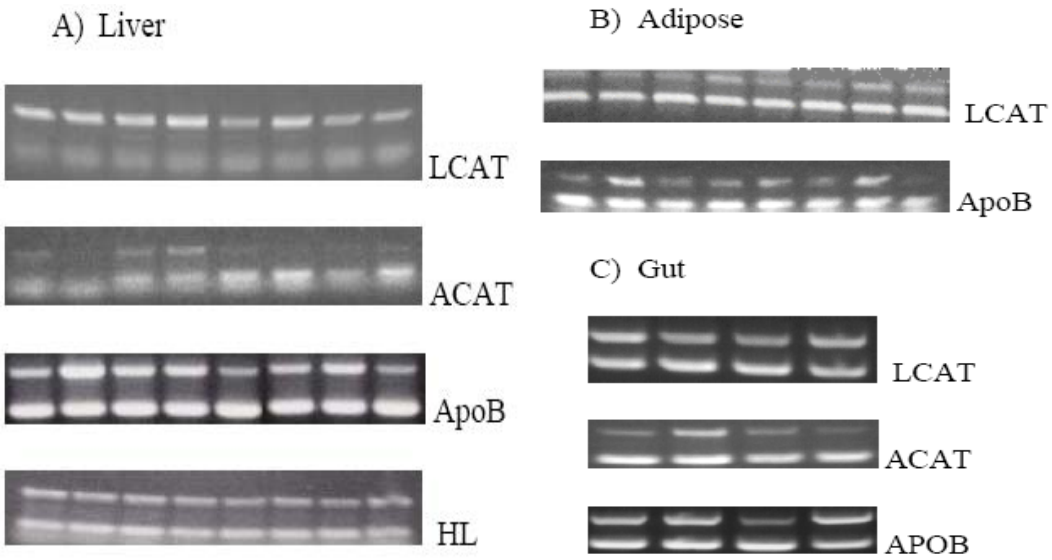

Fig 3. Gel image of relative RT-PCR in porcine tissues A) liver B) adipose C) gut. For A and B, lane 1-4: HCHO diet; lane 5-8: HF diet. For C, lane 1-2:HCHO diet; lane 3-4: HF diet.

Fig 4. Relative gene expression in pigs fed HF diet (n=4) relative to the HCHO diet (n=4), error bars represent standard deviation. Significant difference is represented as * (P<0.05). A) liver, B) adipose

A)

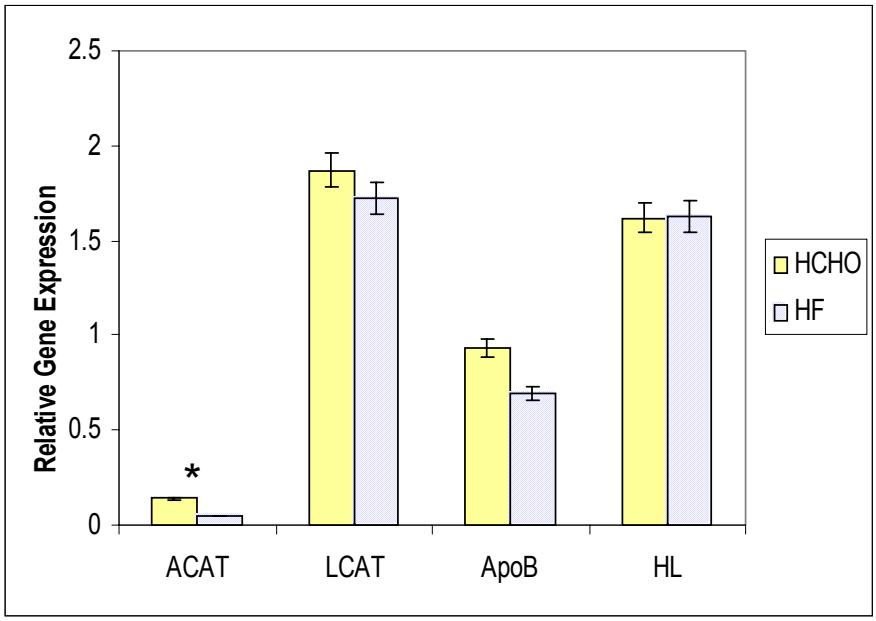

B)

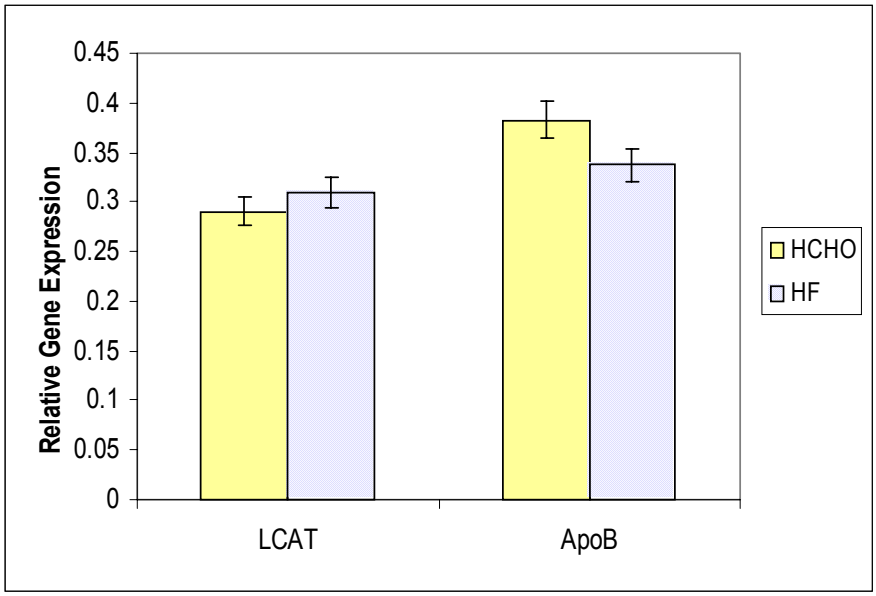

DISSUSION

Feeding diets containing 10% beef tallow to pigs depressed lipogenesis in porcine adipose tissue (46). These findings were based on lipogenic enzyme activity assays in adipose tissues. Since that work, very little new data have accrued on the regulation of lipogenesis, in particular at the gene expression level with respect to high fat/fatty acid intakes in pigs. Further, there are no data on transcription responses of lipid trafficking genes, such as LCAT, ACAT, ApoB and HL to dietary fat intake by pigs.

Liver plays an important role in cholesterol trafficking, uptake, excretion and endogenous synthesis in mammals, but such data are primarily from studies with rodents and primates (341). While liver is the primary site of fatty acid synthesis in human and rodents, only small quantities (342) of total *de novo* fatty acids synthesis occur in the porcine liver, and adipose is the primary tissue for synthesizing fatty acids in pig (343). The small intestinal (gut) epithelium plays an important role in dietary nutrients absorption and metabolism. This is particularly true for uptake of fatty acids arising from intestinal pancreatic lipase activity and consequent transport into the lymph of hydrophobic lipids as lipoproteins synthesized in the gut epithelium from the absorbed fatty acids and monoglycerides (37).

In the liver, ACAT catalyzes the esterification of cholesterol with long chain fatty acids, and the derived cholesterol esters are secreted as a component of very low density lipoprotein (VLDL) (344). Similar to the general down-regulated expression pattern of genes in lipid metabolism found in the liver tissue by microarray analysis in Chapter 3, results of semi-quantitative RT-PCR in this study also showed decreased mRNA abundance for ACAT after a diet shift from LFD to HFD in pigs after 14 days. In rodents,

high-fat diets are associated with increased synthesis of cholesterol and amounts of blood VLDL and LDL (345) usually necessitating increased ACAT activity. Seo et al. (346) found that dietary fat induced transcription of ACAT in human hepatoma cells. Likewise an increased mRNA abundance of liver ACAT was hypothesized/ anticipated for pigs in this experiment.

The lack of agreement between my results and work on primarily rodents may be related to the difference in the species, length of exposure to a high fat diet, and the effects of in *vitro* vs. *in vivo* experiments (i.e. cell cultures). Furthermore, because diets containing long-chain fatty acids depressed fatty acid synthesis in pigs (46, 347), it was very possible the HFD diet in this study depressed fatty acid synthesis in pigs. ACAT contributes to cellular cholesterol homeostasis by etherifying free cholesterol and the cholesteroyl ester is deposited in lipid droplets (348). Hence, after the diet shift to the HFD, this putative attenuated fatty acid synthesis, coupled with low dietary cholesterol, might lead to a decreased need for ACAT activity, which may be caused by decreased ACAT mRNA abundance in the liver. In the gut, ACAT plays a role in cholesterol absorption by maintaining a free cholesterol diffusion gradient across the enterocyte surface through the formation of intracellular cholesterol esters (349). The transcription of ACAT also appeared reduced in the gut, but these results are based on only two pigs (low number because of tissue harvesting difficulties beyond the control of the writer of this dissertation). Finally, the oligo array results (see Chapter 3) from liver revealed a basically across the board lowered mRNA abundance of almost all genes involved in lipid and energy metabolism of this set of finishing pigs fed the HFD for 14 days. It is conceivable that a sudden influx of large amount of fatty acids into liver upon the sudden

shifting to HFD may have produced a fatty acid overload condition in the liver, which resulted in a general down-regulation of genes in lipid metabolism in the liver to prevent over-accumulation of fat. Based on observation of increased expression of genes in TAG synthesis in the adipose tissue by microarray analysis in the chapter 3, adipose tissue had more potency to absorb and store fatty acids in response to the HFD. This conjecture can not be substantiated at present without fatty acid analysis in plasma and tissues.

LCAT catalyzes the initial step in reverse cholesterol transport, the esterification of cell-derived free cholesterol, concomitant with transfer of the esters into the core of high density lipoprotein (HDL) (350). In this study, LCAT was observed highly expressed in liver and adipose tissues, but there were no differences in LCAT mRNA abundance after between LFD and HFD treated pigs. Similar results were reported in mice. Deng et al. (345) found hepatic expression of LCAT was unchanged by high fat-enriched diets in the mice.

Hepatic lipase is synthesized and secreted by the hepatocyte. It catalyzes the hydrolysis of the intermediate density protein (IDL) triacylglycerol to produce low density protein (LDL) (351). More recent work has shown that cholesteryl ester transfer protein (CETP) during normal metabolism is responsible for IDL to LDL conversion and the role of HL is to hydrolyze triacylglycerol in HDL (37). CETP is expressed in pigs (AF333037); however, specific roles of HL and CETP in porcine reverse-cholesterol transport is unclear. We did not find any differences in mRNA abundance of HL in pigs fed either LFD to HDL.

ApoB is the apoprotein necessary in VLDL and LDL synthesis (37). Two isoforms of apoB, apoB100 and apoB48 have been identified in humans. ApoB100 exclusively is

synthesized in human liver, and intestine secretes mainly apoB48 with some apoB 100 (352). ApoB100 and ApoB48 are derived from a single gene, a major mRNA of ~14kb. In the human intestine, a stop codon at 6666 of the apoB messenger RNA terminates the translation and results in the production of a polypeptide known as apoB48 (48% of messenger RNA translated) (353). Therefore, apoB48 is the N-terminal, 48% of full-length apoB100 (354). The porcine apoB gene fragment used here to measure the transcription level in porcine tissues was analyzed to locate its relative position in the human apoB protein. In this process, the porcine mRNA fragment was first translated to obtain the corresponding protein sequence by the TranSeq online software (http://www.ebi.ac.uk/emboss/transeq/). Then the translated porcine apoB protein fragment was aligned with human apoB100 and apoB48 protein sequences (Fig 8). The alignment results showed that the present porcine protein fragment corresponds to a partial amino acid sequence in the C-terminal region of human apoB100. Thus, this particular porcine ApoB cDNA fragment and the resulting primers used here can identify ApoB , but cannot distinguish between ApoB 100 and ApoA 48. In this study, mRNA abundance of apoB was higher in liver than adipose and gut tissues, but mRNA abundance of ApoB in liver, adipose and muscle tissues were not different between LFD and HFD pigs. Previous work has indicated that dietary supply of triacylglycerol alone does not regulate ApoB secretion or plasma concentrations of ApoB (355). A lack of change in the transcription of ApoB in the high fat diet in the rat was previously reported (345). Deng et al. (345) did not detect significance alterations of VLDL apoproteins (apoB, apoE, apoCII, apoCIII) after rats were treated by menhaden oil diets (40% of calories from fat). Furthermore, it has been shown that, in humans, ApoB is mainly

regulated at the post-transcriptional level (356). Further research is needed to compare the ApoB protein concentration between LFD and HFD pigs, which may clarify the regulatory mechanisms for ApoB synthesis in the pig. Since this study focused on determination of transcription response of genes, it is impossible here to make any conclusion whether identical regulatory mechanism are applicable in pig as in human or rodents.

Lipoproteins transport the majority of cholesterol and triacylglyceride in the circulatory system (357). Further analysis and comparison the lipoprotein profiles of serum and fat content in liver, adipose and muscle tissues between LFD and HFD pigs will likely extend our understanding about the effects of dietary high fat on the expression of genes involved in inter-tissue transport of triacylglycrol and cholesterol. Such data may help explain the observed gene transcription response of these four lipoprotein associated genes upon a shift from LFD to HFD in pigs.

CONCLUSIONS

This study has established that four genes associated with inter tissue lipid trafficking appear more highly expressed in porcine liver than other tissues studied. These results also showed that a LFD to HFD shift did not change liver LCAT, HL and ApoB gene transcript abundance in pigs, indicating that this 14 day exposure to HFD did not affect the expression of these genes in the liver. Furthermore, no changes were observed in the mRNA abundance of LCAT and ApoB in the adipose tissue between LFD and HFD pigs.

This study demonstrated that the transcription response of ACAT differed in various tissues when pigs were shifted from an abundant carbohydrate, low-fat diet to a high-fat

diet. Substitution of dietary fat for carbohydrate down-regulated the transcription of ACAT in the porcine liver. To our knowledge, the current study represents the first report of LCAT and ACAT distribution in pigs and on the effect of dietary high fat on the expression of lipid-trafficking genes in pigs.

Fig 5. Comparison of LCAT sequences (cds) between pig (AY349156)

and human (BC014781.1) by BLAST

```
Score =  632 bits (319),  Expect = 2e-178
 Identities = 418/451 (92%), Gaps = 0/451 (0%)
 Strand=Plus/Plus
Pig   LCAT    1   AGGACCGCTTTATTGATGGCTTCATCTCTCTTGGAGCTCCCTGGGGTGGCTCCACCAAGC  60
                  |||||||||||||||||||||||||||||||| |||||||||||||||||| |||||
Human LCAT  669   AGGACCGCTTTATTGATGGCTTCATCTCTCTTGGGGCTCCCTGGGGTGGCTCCATCAAGC  728

Pig   LCAT    61  CCATGCTAGTCTTGGCCTCAGGTGACAACCAGGGCATCCCGATCATGTCCAGCATCAAAC  120
                  ||||||| |||||||||||||||||||||||||||||| |||||||||||||||| |
Human LCAT    729 CCATGCTGGTCTTGGCCTCAGGTGACAACCAGGGCATCCCCATCATGTCCAGCATCAAGC  788

Pig   LCAT    121 TGAAAGAGGAGCAGCGCATGACAACAACCTCCCCCTGGATGTTTCCCTCCAGCCACGTGT  180
                  |||||||||||||||||| || || ||||||||||||||||||||||  ||   | ||
Human LCAT    789 TGAAAGAGGAGCAGCGCATAACCACCACCTCCCCCTGGATGTTTCCCTCTCGCATGGCGT  848

Pig   LCAT    181  GGCCCGAGGACCATGTGTTCATTTCCACCCCCAGCTTCAACTACACAAGCCATGACTTCC  240
                  |||| |||||||| |||||||||||||| |||||||||||||||||| ||| ||||||||
Human LCAT    849  GGCCTGAGGACCACGTGTTCATTTCCACACCCAGCTTCAACTACACAGGCCGTGACTTCC  908

Pig   LCAT    241  AGCGCTTCTTTGCAGACCCGCACTTTGAGGAAGGCTGGTACATGTGGCTACAGTCACGTG  300
                  | ||||||||||||||| |||||||||||||||||||||||||||||| ||||||||||
Human LCAT    909  AACGCTTCTTTGCAGACCTGCACTTTGAGGAAGGCTGGTACATGTGGCTGCAGTCACGTG  968

Pig   LCAT    301  ACCTGCTGGCAGGCCTCCCAGCGCCTGGTGTGGAAGTATACTGTCTGTATGGTGTGGGCC  360
                  |||| |||||||| |||||||| ||||||||||||||||||||||| || || |||||||
Human LCAT    969  ACCTCCTGGCAGGACTCCCAGCACCTGGTGTGGAAGTATACTGTCTTTACGGCGTGGGCC  1028

Pig   LCAT    361  TGCCCACACCCCGCACCTACATCTTTGACCACGGCTTCCCCTACACGGACCCTGTGGATG  420
                  ||||||| |||||||||||||||  ||||||||||||||||||||||||||||||||| ||
Human LCAT    1029 TGCCCACGCCCCGCACCTACATCTACGACCACGGCTTCCCCTACACGGACCCTGTGGGTG  1088


Pig   LCAT    421  TGCTCTATGAGGATGGTGATGACACTGTGGC  451
                  |||||||||||||||||||||||| |||||
Human LCAT    1089 TGCTCTATGAGGATGGTGATGACACGGTGGC  1119
```

Fig 6. Comparison of ACAT sequences (5'UTR) between pig (AY676347) and human (L21934.2) by BLAST

```
Score =  950 bits (479),  Expect = 0.0
 Identities = 482/483 (99%), Gaps = 0/483 (0%)
 Strand=Plus/Plus

Pig   ACAT     333   CATGGAAAAGTTCTTTACTGGTGATTTCTGAGATTTTAGTTCACCCCTTATCCTGAGCAG  392
                     ||||||||||||||||||||||||||||||||||||||||||||||||||||||||||||
Human ACAT     636   CATGGAAAAGTTCTTTACTGGTGATTTCTGAGATTTTAGTTCACCCCTTATCCTGAGCAG  695

Pig   ACAT      393  TGTACACTGTTCCCAATATGTAGCCTTTTATCCCTCACCCCCTCTAAGTTCAAGAAGACT  452
                     ||||||||||||||||||||||||||||||||||||||||||||||||||||||||||||
Human ACAT      696  TGTACACTGTTCCCAATATGTAGCCTTTTATCCCTCACCCCCTCTAAGTTCAAGAAGACT  755

Pig   ACAT      453  ATGGTCCTGCAGAAAGCTTTATATGTAATTAACATATCTTTATCTTTATCTTTATAGGCA  512
                     ||||||||||||||||||||||||||||||||||||||||||||||||||||||||||||
Human ACAT      756  ATGGTCCTGCAGAAAGCTTTATATGTAATTAACATATCTTTATCTTTATCTTTATAGGCA  815

Pig   ACAT      513  GTAGACTCATCTTTTGAAACAGATTCCATTAAGAGTGAATGTGTACCCTCCCTCTAGCCT  572
                     ||||||||||||||||||||||||||||||||||||||||||||||||||||||||||||
Human ACAT      816  GTAGACTCATCTTTTGAAACAGATTCCATTAAGAGTGAATGTGTACCCTCCCTCTAGCCT  875

Pig   ACAT      573  TTATTATTACTGTTTTTGCTATTACATGTGTTAGTGTATGTGAATTTAATGCTTAAAAAT  632
                     ||||||||||||||||||||||||||||||||||||||||||||||||||||||||||||
Human ACAT      876  TTATTATTACTGTTTTTGCTATTACATGTGTTAGTGTATGTGAATTTAATGCTTAAAAAT  935

Pig   ACAT      633  GTATCCCATTGGCTACTATGGCAAAAGGTTGACTCATAAGAGTTTAGCACGGGTTAAGAT  692
                     ||||||||||||||||||||||||||||||||||||||||||||||||||||||||||||
Human ACAT      936  GTATCCCATTGGCTACTATGGCAAAAGGTTGACTCATAAGAGTTTAGCACGGGTTAAGAT  995

Pig   ACAT      693  CTGAAAGTTTTCCCCCAGCCTCTTATCACTGGCGCAGACTTCACAATTCATGGAAGCCAC  752
                     |||||||||||| ||||||||||||||||||||||||||||||||||||||||||||||
Human ACAT      996  CTGAAAGTTTTCTCCCAGCCTCTTATCACTGGCGCAGACTTCACAATTCATGGAAGCCAC  1055


Pig   ACAT      753  CAGTGAGATGACATTGCCTCAGGCAGTTACTATTTTTATATTCTATAACTCGAGGAGCTC  812
                     ||||||||||||||||||||||||||||||||||||||||||||||||||||||||||||
Human ACAT      1056 CAGTGAGATGACATTGCCTCAGGCAGTTACTATTTTTATATTCTATAACTCGAGGAGCTC  1115

Pig   ACAT      813  AGG  815
                     |||
Human ACAT      1116 AGG  1118
```

Fig 7. Comparison of LCAT protein sequences between pig (AAQ24609.1) and human (AAA59500.0) by BLAST

```
Score =  302 bits (774),  Expect = 2e-80
 Identities = 140/150 (93%), Positives = 142/150 (94%), Gaps = 0/150
(0%)

Query  212  DRFIDGFISLGAPWGGSIKPMLVLASGDNQGIPIMSSIKLKEEQRITTTSPWMFPSRMAW  271
            DRFIDGFISLGAPWGGS KPMLVLASGDNQGIPIMSSIKLKEEQR+TTTSPWMFPS   W
Sbjct  1    DRFIDGFISLGAPWGGSTKPMLVLASGDNQGIPIMSSIKLKEEQRMTTTSPWMFPSSHVW  60

Query  272  PEDHVFISTPSFNYTGRDFQRFFADLHFEEGWYMWLQSRDLLAGLPAPGVEVYCLYGVGL  331
            PEDHVFISTPSFNYT  DFQRFFAD HFEEGWYMWLQSRDLLAGLPAPGVEVYCLYGVGL
Sbjct  61   PEDHVFISTPSFNYTSHDFQRFFADPHFEEGWYMWLQSRDLLAGLPAPGVEVYCLYGVGL  120

Query  332  PTPRTYIYDHGFPYTDPVGVLYEDGDDTVA  361
            PTPRTYI+DHGFPYTDPV VLYEDGDDTVA
Sbjct  121  PTPRTYIFDHGFPYTDPVDVLYEDGDDTVA  150
```

Fig 8. Multiple sequence alignment of human apoB 100 protein (NP_000375.1), apoB48 (AAA51741.1) and translated fragment of pig apoB mRNA by CLUSTAL W (1.82)

Sequence 1 Human APoB100 precursor amino acids (aa) sequence: gi|4502153|ref|NP_000375.1
Note: In the apoB100 precursor, apoB 100 begins from 1670, the previous sequences contain regions for signal peptide, multiple disulfide bonds, glycosylation regions, variant regions and unknown function domains. (Knott,T.J, 1986)

Sequence 2 Human ApoB 48 amino acid sequence: gi|178732|gb|AAA51741.1 (Hardman,D.A.,1987)
Sequence 3 Translated pig amino acid sequence based on the sequenced PCR amplicons in this study: translated sequence

```
gi|4502153|ref|NP_000375.1|      MDPPRPALLALLALPALLLLLLAGARAEEEMLENVSLVCPKDATRFKHLR 50
gi|178732|gb|AAA51741.1|         --------------------------------------------------
translated                       --------------------------------------------------

                                 ..................

gi|4502153|ref|NP_000375.1|      GISTSATTNLKCSLLVLENELNAELGLSGASMKLTTNGRFREHNAKFSLD 1700
gi|178732|gb|AAA51741.1|         --------------------LNAELGLSGASMKLTTNGRFREHNAKFSLD 30
translated                       --------------------------------------------------

gi|4502153|ref|NP_000375.1|      GKAALTELSLGSAYQAMILGVDSKNIFNFKVSQEGLKLSNDMMGSYAEMK 1750
gi|178732|gb|AAA51741.1|         GKAALTELSLGSAYQAMILGVDSKNIFNFKVSQEGLKLSNDMMGSYAEMK 80
translated                       --------------------------------------------------

gi|4502153|ref|NP_000375.1|      FDHTNSLNIAGLSLDFSSKLDNIYSSDKFYKQTVNLQLQPYSLVTTLNSD 1800
gi|178732|gb|AAA51741.1|         FDHTNSLNIAGLSLDFSSKLDNIYSSDKFYKQTVNLQLQPYSLVTTLNSD 130
translated                       --------------------------------------------------

gi|4502153|ref|NP_000375.1|      LKYNALDLTNNGKLRLEPLKLHVAGNLKGAYQNNEIKHIYAISSAALSAS 1850
gi|178732|gb|AAA51741.1|         LKYNALDLTNNGKLRLEPLKLHVAGNLKGAYQNNEIKHIYAISSAALSAS 180
translated                       --------------------------------------------------

gi|4502153|ref|NP_000375.1|      YKADTVAKVQGVEFSHRLNTDIAGLASAIDMSTNYNSDSLHFSNVFRSVM 1900
gi|178732|gb|AAA51741.1|         YKADTVAKVQGVEFSHRLNTDIAGLASAIDMSTNYNSDSLHFSNVFRSVM 230
translated                       --------------------------------------------------

gi|4502153|ref|NP_000375.1|      APFTMTIDAHTNGNGKLALWGEHTGQLYSKFLLKAEPLAFTFSHDYKGST 1950
gi|178732|gb|AAA51741.1|         APFTMTIDAHTNGNGKLALWGEHTGQLYSKFLLKAEPLAFTFSHDYKGST 280
translated                       --------------------------------------------------

gi|4502153|ref|NP_000375.1|      SHHLVSRKSISAALEHKVSALLTPAEQTGTWKLKTQFNNNEYSQDLDAYN 2000
gi|178732|gb|AAA51741.1|         SHHLVSRKSISAALEHKVSALLTPAEQTGTWKLKTQFNNNEYSQDLDAYN 330
translated                       --------------------------------------------------

gi|4502153|ref|NP_000375.1|      TKDKIGVELTGRTLADLTLLDSPIKVPLLLSEPINIIDALEMRDAVEKPQ 2050
gi|178732|gb|AAA51741.1|         TKDKIGVELTGRTLADLTLLDSPIKVPLLLSEPINIIDALEMRDAVEKPQ 380
translated                       --------------------------------------------------

gi|4502153|ref|NP_000375.1|      EFTIVAFVKYDKNQDVHSINLPFFETLQEYFERNRQTIIVVVENVQRNLK 2100
gi|178732|gb|AAA51741.1|         EFTIVAFVKYDKNQDVHSINLPFFETLQEYFERNRQTIIVVLENVQRNLK 430
translated                       --------------------------------------------------

gi|4502153|ref|NP_000375.1|      HINIDQFVRKYRAALGKLPQQANDYLNSFNWERQVSHAKEKLTALTKKYR 2150
gi|178732|gb|AAA51741.1|         HINIDQFVRKYRAALGKLPQQANDYLNSFNWERQVSHAKEKLTALTKKYR 480
translated                       --------------------------------------------------

gi|4502153|ref|NP_000375.1|      ITENDIQIALDDAKINFNEKLSQLQTYMIQFDQYIKDSYDLHDLKIAIAN 2200
gi|178732|gb|AAA51741.1|         ITENDIQIALDDAKINFNEKLSQLQTYMIQFDQYIKDSYDLHDLKIAIAN 530
translated                       --------------------------------------------------

gi|4502153|ref|NP_000375.1|      IIDEIIEKLKSLDEHYHIRVNLVKTIHDLHLFIENIDFNKSGSSTASWIQ 2250
```

```
gi|178732|gb|AAA51741.1|        IIDEIIEKLKSLDEHYHIRVNLVKTIHDLHLFIENIDFNKSGSSTASWIQ 580
translated                      --------------------------------------------------

gi|4502153|ref|NP_000375.1|    NVDTKYQIRIQIQEKLQQLKRHIQNIDIQHLAGKLKQHIEAIDVRVLLDQ 2300
gi|178732|gb|AAA51741.1|        NVDTKYQIRIQIQEKLQQLKRHIQNIDIQHLAGKLKQHIEAIDVRVLLDQ 630
translated                      --------------------------------------------------

gi|4502153|ref|NP_000375.1|    LGTTISFERINDVLEHVKHFVINLIGDFEVAEKINAFRAKVHELIERYEV 2350
gi|178732|gb|AAA51741.1|        LGTTISFERINDVLEHVKHFVINPYWDFEVAEKINAFRAKVHELIERYEV 680
translated                      --------------------------------------------------

gi|4502153|ref|NP_000375.1|    DQQIQVLMDKLVELTHQYKLKETIQKLSNVLQQVKIKDYFEKLVGFIDDA 2400
gi|178732|gb|AAA51741.1|        DQHIQVLMDKLVELAHQYKLKETIQKLSNVLQQVKIKDYFEKLVGFID-- 728
translated                      --------------------------------------------------

gi|4502153|ref|NP_000375.1|    VKKLNELSFKTFIEDVNKFLDMLIKKLKSFDYHQFVDETNDKIREVTQRL 2450
gi|178732|gb|AAA51741.1|        --------------------------------------------------
translated                      --------------------------------------------------

gi|4502153|ref|NP_000375.1|    NGEIQALELPQKAEALKLFLEETKATVAVYLESLQDTKITLIINWLQEAL 2500
gi|178732|gb|AAA51741.1|        --------------------------------------------------
translated                      --------------------------------------------------

gi|4502153|ref|NP_000375.1|    SSASLAHMKAKFRETLEDTRDRMYQMDIQQELQRYLSLVGQVYSTLVTYI 2550
gi|178732|gb|AAA51741.1|        --------------------------------------------------
translated                      --------------------------------------------------

gi|4502153|ref|NP_000375.1|    SDWWTLAAKNLTDFAEQYSIQDWAKRMKALVEQGFTVPEIKTILGTMPAF 2600
gi|178732|gb|AAA51741.1|        --------------------------------------------------
translated                      --------------------------------------------------

gi|4502153|ref|NP_000375.1|    EVSLQALQKATFQTPDFIVPLTDLRIPSVQINFKDLKNIKIPSRFSTPEF 2650
gi|178732|gb|AAA51741.1|        --------------------------------------------------
translated                      --------------------------------------------------

gi|4502153|ref|NP_000375.1|    TILNTFHIPSFTIDFVEMKVKIIRTIDQMQNSELQWPVPDIYLRDLKVED 2700
gi|178732|gb|AAA51741.1|        --------------------------------------------------
translated                      --------------------------------------------------

gi|4502153|ref|NP_000375.1|    IPLARITLPDFRLPEIAIPEFIIPTLNLNDFQVPDLHIPEFQLPHISHTI 2750
gi|178732|gb|AAA51741.1|        --------------------------------------------------
translated                      --------------------------------------------------

gi|4502153|ref|NP_000375.1|    EVPTFGKLYSILKIQSPLFTLDANADIGNGTTSANEAGIAASITAKGESK 2800
gi|178732|gb|AAA51741.1|        --------------------------------------------------
translated                      --------------------------------------------------

gi|4502153|ref|NP_000375.1|    LEVLNFDFQANAQLSNPKINPLALKESVKFSSKYLRTEHGSEMLFFGNAI 2850
gi|178732|gb|AAA51741.1|        --------------------------------------------------
translated                      --------------------------------------------------

gi|4502153|ref|NP_000375.1|    EGKSNTVASLHTEKNTLELSNGVIVKINNQLTLDSNTKYFHKLNIPKLDF 2900
gi|178732|gb|AAA51741.1|        --------------------------------------------------
translated                      --------------------------------------------------

gi|4502153|ref|NP_000375.1|    SSQADLRNEIKTLLKAGHIAWTSSGKGSWKWACPRFSDEGTHESQISFTI 2950
gi|178732|gb|AAA51741.1|        --------------------------------------------------
translated                      --------------------------------------------------

gi|4502153|ref|NP_000375.1|    EGPLTSFGLSNKINSKHLRVNQNLVYESGSLNFSKLEIQSQVDSQHVGHS 3000
gi|178732|gb|AAA51741.1|        --------------------------------------------------
translated                      --------------------------------------------------

gi|4502153|ref|NP_000375.1|    VLTAKGMALFGEGKAEFTGRHDAHLNGKVIGTLKNSLFFSAQPFEITAST 3050
gi|178732|gb|AAA51741.1|        --------------------------------------------------
translated                      --------------------------------------------------

gi|4502153|ref|NP_000375.1|    NNEGNLKVRFPLRLTGKIDFLNNYALFLSPSAQQASWQVSARFNQYKYNQ 3100
gi|178732|gb|AAA51741.1|        --------------------------------------------------
translated                      --------------------------------------------------


gi|4502153|ref|NP_000375.1|    NFSAGNNENIMEAHVGINGEANLDFLNIPLTIPEMRLPYTIITTPPLKDF 3150
gi|178732|gb|AAA51741.1|        --------------------------------------------------
translated                      --------------------------------------------------

gi|4502153|ref|NP_000375.1|    SLWEKTGLKEFLKTTKQSFDLSVKAQYKKNKHRHSITNPLAVLCEFISQS 3200
gi|178732|gb|AAA51741.1|        --------------------------------------------------
translated                      --------------------------------------------------
```

```
gi|4502153|ref|NP_000375.1|      IKSFDRHFEKNRNNALDFVTKSYNETKIKFDKYKAEKSHDELPRTFQIPG 3250
gi|178732|gb|AAA51741.1|         ---------------------------------------------------
translated                       INSFNRHFETVRDKALDFFTESYNEIKITFDKYKVEKPLDQQPRTFQIPG

gi|4502153|ref|NP_000375.1|      YTVPVVNVEVSPFTIEMSAFGYVFPKAVSMPSFSILGSDVRVPSYTLILP 3300
gi|178732|gb|AAA51741.1|         ---------------------------------------------------
translated                       YTIPVINIDVSPFTVKMETFGYVIPKEISTPNITILGSGISVPSYTLGLQ


gi|4502153|ref|NP_000375.1|      SLELPVLHVPRNLKLSLPHFKELCTISHIFIPAMGNITYDFSFKSSVITL 3350
gi|178732|gb|AAA51741.1|         ---------------------------------------------------
translated                       FLELPALDVPRNLQISLPEL------------------------------

                        ..............................................................

gi|4502153|ref|NP_000375.1|      YMKLAPGELTIIL 4563
gi|178732|gb|AAA51741.1|         -------------
translated                       -------------
```

VI. CONCLUSION AND PERSPECTIVE

Genetic selection, and the development and application of repartitioning agents to shift nutrients from fat deposition to protein deposition in the production of leaner animals, are research areas of major economic importance to the livestock producer in providing food for improved nutrition and health of consumers. Nutritional manipulation of energy to protein ratio and feed energy intake during the production cycle is an additional option to reduce fatness without compromising efficiency of growth. The theory of nutrient partitioning, as originally proposed by Sir John Hammond, for the maintenance and growth of individual tissues occurs in a hierarchial manner to those tissues essential for survival of the species. In growing animals, muscle and adipose tissues (edible meat) develop relative to genetic potential, but are of low priority with respect to nutrient utilization for maintenance requirements (358). Nutrient partitioning to optimize efficiency of meat production can be gained 1) through improvement of genetic composition by selection or gene alteration, and 2) hormonal and neuroendocrine strategies to alter appetite, reduce stress and favor muscle accretion rather than adipose tissue deposition in a healthy environment for animal well-being (359).

From a genomics perspective, nutritients are dietary signals that are detected by the cellular sensor systems that influence gene expression, protein translation, and metabolite synthesis (360). Genomic tools can be used in two different but complementary strategies

in molecular nutrition research. One is the traditional hypothesis-driven approach: specific genes and proteins, the expression of which is influenced by nutrients, and identified using genomic tools (361). The other strategy is largely theoretical at this stage, is the "systems biology" approach where gene, protein and metabolite signatures that are associated with specific nutrients, or nutritional regimes, are catalogued, and might provide "early warning" molecular biomarkers for nutrient-induced changes to homeostasis (362).

In this dissertation, the first strategy was used but expanded to a discovery micorarray approach, to get detailed molecular data on whole genome responses in muscle, liver and adipose tissues in pigs administered RAC or fed high fat diets.

On the basis of my experiments, it seems prudent to conclude that

1) These studies showed that micro-arrays are able to detect transcriptional changes resulting from feeding 60 ppm ractopamine and an 16 % increase in dietary fat.

2) Ractopamine up regulated the expression of genes PPARa and CPTII, and decreased expression of genes encoding enzymes in fatty acid synthesis and electron transport in the adipose tissue in pigs fed the beta adrenergic agonist for 28 days.

3) After the diet was shifted from LFD to HFD, the mRNA level of genes in fatty acid synthesis, FABP and fatty acid oxidation were decreased in the liver; expression of FABP and genes in the TAG synthesis were increased in the adipose tissue; transcription of CPT1 and 3-hydroxyacyl-CoA dehydrogenase and some genes in the oxidative phosphorylation were up regulated in muscle tissue.

Comparing effects of RAC and high fat on the gene expression in pigs, RAC is a β-adrenergic agonist added to the diet as a pure compound in small doses, but RAC acts

with high affinity and selectivity for a limited number of biological targets. Most nutrients (carbohydrate, protein and fat) are softer dietary signals, and their net effect must be considered in the context of chronic exposure (363). An animal has to process a large number of different nutrients and other diet components, but nutrients can reach high concentrations without becoming toxic. Each nutrient can also bind to numerous targets with different affinities and specificities. In this study, the oligo-array analysis detected wider and stronger transcription response in RAC-treated pigs than those noted in pigs after the diet was shifted from LFD to HFD. In RAC study, transcription of 1,299 genes was altered while around 847 genes/ESTs in pig tissues switched to a HFD showed significant differences in expression.

One of the major challenges that remain from the work is how to interpret differently expressed genes/transcripts, such as a group of phosphatases in the muscle of high-fat treated pigs that were not part of the gene filter assignment corresponding to the hypothesis. Future data mining, even of results generated here, may be important to fully exploit my micro-array result. The type of follow-ups may range from bioinformatic analysis of presently non analyzed raw data in the arrays, application of real-time PCR analysis of specific genes, promoter function and structure analyses to designing new experiments to further explore gene expression changes from in pigs exposed to RAC or other dietary combinations.

Perhaps more importantly, my study showed that there are significant numbers of uncharacterized transcripts in this micro-array platform. Using bioinformaticsl tools and molecular methods, it is possible to discover new genes, which may provide opportunities

for characterization of encoded proteins of unknown function and their interaction in the process of metabolism pathways.

When I first joined the Bergen's laboratory, research activities focused on developing gene-specific cDNA probes by cloning new sequences/DNA fragments of genes rate limiting in porcine lipid metabolism and measuring or determining mRNA abundance of various transcripts in porcine adipose tissue using Northern blotting. Obviously, these methods were laborious, and the number of characterized genes available for such studies are limiting. My study was the first to comprehensively characterize expression responses in the porcine transcriptome to ractopamine and dietary high fat. If the high-fat study were to be repeated, I would first like to increase the dietary fat content; I would further increase the number of animals per group and measure the plasma metabolone and complete plasma lipoproteins profile for all treatments. In addition, I would confirm the many of differently expressed genes in high fat micro-array analysis with real-time PCR. This would require a lot of preliminary work to obtain appropriate primes for each of the genes, and would take extensive laboratory work to set up many qRT-PCR assays and would be quite costly. I would also like to expand the dietary lipid profile to include substantial amounts cholesterol and study its effect on the transcription of genes in lipoprotein and cholesterol metabolism pathways. Furthermore, I would add another experimental group with even higher fat content and thus lower dietary carbohydrate content to explore the expression of genes that may cross-talk in fatty acid and glucose oxidation. Additionally, I might recommend a study applying Western blot or enzyme activity analysis to determine if changes happened on the proteins encoded by genes with changed expression in transcription level. For those

genes expressing opposite changes of mRNA level in different tissues (e.g transcription of FABP was decreased in the liver but increased in adipose and muscle in response to high fat diet) if confirmed by qRT-PCR, there is a need to characterize the potential differences in the promoter regions of these gene isoforms in various tissues. Such a characterization may help to explain gene expression response differences observed in this study between tissues that use fatty acids, store fatty acids and in the adipose tissue lipogenic response to treatments.

Data presented in this dissertation provide the first description of the transcriptome response of lipid metabolism genes in the finishing pigs treated by ractopamine or high fat. In the absence of complete gene information in domestic pig, an oligo-array platform was used to determine the transcription profile of fatty acid metabolism in the pig. Data from Chapter 2 confirmed that short-term effects of ractopamine on decreasing fatty acid synthesis and increasing fatty acid β-oxidation at transcription level. Results in Chapter 3 presented evidence that transcription responses to dietary fat were specific in different tissues. This work provided a basis to understand the relationship between dietary fat and gene expression among tissues of pigs.

Micro-array from my experience is a useful tool to discover genes that may be important as targets in the further research. However, we should be aware that simply accumulating micro-array datasets alone can not lead to important insights. These data must be gathered in conjunction with appropriate functional studies using the knowledge of nutrient signals or systems biology driven analysis of signatures, to define molecular biomarkers responding to dietary variation.

Since microarray technology first was introduced to public (182), DNA microarray has been utilized in nearly every facet of biology. In this dissertation, a pig oligo array was used to investigate the global properties of genome transcription when pigs were administered ractopamine or fed a high fat. Both of these projects have provided new insights into the lipid metabolism and regulation mechanism and the data can be used to further explore pig biology at the molecular level.

BIBLIOGRAPHY

1. Berg, R. T. &Walters, L. E. (1983) The Meat Animal: Changes and Challenges. J Anim Sci 57: 133-146.

2. Bergen, W. G. (2001) The role of cyclic AMP elevating agents and somatotropin in transcriptional and posttranslational regulation of lipogenesis and lipolysis in Bos taurus and Sus scrofa. Recent Res. Devel. Lipids 4: 47-59

3. Seguin, C. & Hamer, D. H. (1987) Regulation in vitro of metallothionein gene binding factors. Science 235: 1383-1387.

4. Reusch, J. E. & Klemm, D. J. (1999) Nutrition and fat cell differentiation.[comment]. Endocrinology 140: 2935-2937.

5. Daniel, H. & tom Dieck, H. (2004) Nutrient-gene interactions: a single nutrient and hundreds of target genes. Biological Chemistry 385: 571-583.

6. Beigneux, A. P., Moser, A. H., Shigenaga, J. K., Grunfeld, C. & Feingold K. R. (2000) The acute phase response is associated with retinoid X receptor repression in rodent liver. J Biol Chem 275(21):16390-16399.

7. Maxwell, K. N., Soccio, R. E., Duncan, E. M., Sehayek, E. & Breslow, J. L. (2003) Novel putative SREBP and LXR target genes identified by microarray analysis in liver of cholesterol-fed mice. Journal of Lipid Research 44: 2109-2119.

8. Clarke, S. D. (1999) Nutrient regulation of gene and protein expression.. Current Opinion in Clinical Nutrition & Metabolic Care 2: 287-289.

9. Bergen, W. G. & Merkel, R. A. (1991) Body composition of animals treated with partitioning agents: implications for human health. FASEB Journal 5: 2951-2957.

10. Hood, R. L. &Allen, C. E. (1973) Lipogenic enzyme activity in adipose tissue during the growth of swine with different propensities to fatten. J Nutr 103: 353-362.

11. Wang, D. & Sul, H. S. (1998) Insulin stimulation of the fatty acid synthase promoter is mediated by the phosphatidylinositol 3-kinase pathway. Involvement of protein kinase B/Akt. Journal of Biological Chemistry 273: 25420-25426.

12. Azain, M. J. (2004) Role of fatty acids in adipocyte growth and development. Journal of Animal Science 82: 916-924.

13. Bergen, W. G. & Mersmann, H. J. (2005) Comparative aspects of lipid metabolism: impact on contemporary research and use of animal models. Journal of Nutrition 135: 2499-2502.

14. Moustaid, N., Sakamoto, K., Clarke, S., Beyer, R. S. & Sul, H. S. (1993) Regulation of fatty acid synthase gene transcription. Sequences that confer a positive insulin effect and differentiation-dependent expression in 3T3-L1 preadipocytes are present in the 332 bp promoter. Biochem J 292: 767-772.

15. Kolodziej, M. P. & Zammit, V. A. (1993) Mature carnitine palmitoyltransferase I retains the N-terminus of the nascent protein in rat liver. FEBS Letters 327: 294-296.

16. Hillgartner, F. B., Salati, L. M. & Goodridge, A. G. (1995) Physiological and molecular mechanisms involved in nutritional regulation of fatty acid synthesis. Physiological Reviews 75: 47-76.

17. Voet, D. V. (2003) Biochemistry, John Wiley and Sons, Etobicoke

18. Botion, L. M. & Green, A. (1691) Long-term regulation of lipolysis and hormone-sensitive lipase by insulin and glucose. Diabetes 48: 1691-1697.

19. Yin, D., Clarke, S. D. & Etherton, T. D. (2001) Transcriptional regulation of fatty acid synthase gene by somatotropin in 3T3-F442A adipocytes. Journal of Animal Science 79: 2336-2345.

20. Duplus, E., Glorian, M. & Forest, C. (2000) Fatty acid regulation of gene transcription. Journal of Biological Chemistry 275: 30749-30752.

21. Wahle, K. W., Rotondo, D. & Heys, S. D. (2003) Polyunsaturated fatty acids and gene expression in mammalian systems. Proceedings of the Nutrition Society 62: 349-360.

22. Duplus, E. & Forest, C. (2002) Is there a single mechanism for fatty acid regulation of gene transcription? Biochemical Pharmacology 64: 893-901.

23. Jump, D. B. (2004) Fatty acid regulation of gene transcription. Critical Reviews in Clinical Laboratory Sciences 41: 41-78.

24. Dunshea, F. R., Harris, D. M., Bauman, D. E., Boyd, R. D. & Bell, A. W. (1992) Effect of porcine somatotropin on in vivo glucose kinetics and lipogenesis in growing pigs. Journal of Animal Science 70: 141-151.

25. Antras, J., Lasnier, F. & Pairault, J. (1991) Beta-adrenergic-cyclic AMP signalling pathway modulates cell function at the transcriptional level in 3T3-F442A adipocytes. Molecular & Cellular Endocrinology 82: 183-190.

26. Tamaoki, H., Nishina, Y., Shiga, K. & Miura, R. (1999) Mechanism for the recognition and activation of substrate in medium-chain acyl-CoA dehydrogenase. Journal of Biochemistry 125: 285-296.

27. Engst, S., Vock, P., Wang, M., Kim, J. J. & Ghisla, S. (1999) Mechanism of activation of acyl-CoA substrates by medium chain acyl-CoA dehydrogenase: interaction of the thioester carbonyl with the flavin adenine dinucleotide ribityl side chain. Biochemistry 38: 257-267.

28. Boshart, M., Weih, F., Nichols, M. & Schutz, G. (1991) The tissue-specific extinguisher locus TSE1 encodes a regulatory subunit of cAMP-dependent protein kinase. Cell 66: 849-859.

29. Kraemer F. B. & Shen, W. J. (2002) Hormone-sensitive lipase: control of intracellular tri-(di-)acylglycerol and cholesteryl ester hydrolysis**.** J. Lipid Res. 43**:** 1585 - 1594.

30. Yeaman, S. J. (2004) Hormone-sensitive lipase--new roles for an old enzyme. Biochemical Journal 379: 11-22.

31. Anne Garcia, Vidya Subramanian, Anna Sekowski, Sucharita Bhattacharyya, Martha W. Love, and Dawn L. Brasaemle (2004) J Biol Chem. 279(9):8409-16

32. Souza, S. C., Muliro, K. V., Liscum, L., Lien, P., Yamamoto, M. T., Schaffer, J. E., Dallal, G. E., Wang, X., Kraemer, F. B., Obin, M., and Greenberg, A. S. (2002) Modulation of hormone-sensitive lipase and protein kinase A-mediated lipolysis by perilipin A in an adenoviral reconstituted system.J. Biol. Chem. 277, 8267-8272

33. Tansey, J. T., Huml, A. M., Vogt, R., Davis, K. E., Jones, J. M., Fraser, K. A., Brasaemle, D. L., Kimmel, A. R., and Londos, C. (2003) Functional studies on native and mutated forms of perilipins. A role in protein kinase A-mediated lipolysis of triacylglycerols.J. Biol. Chem. 278, 8401-8406

34. Sztalryd, C., Xu, G., Dorward, H., Tansey, J. T., Contreras, J. A., Kimmel, A. R., and Londos, C. (2003) Perilipin A is essential for the translocation of hormone-sensitive lipase during lipolytic activation J. Cell Biol. 161, 1093-1103

35. Brasaemle, D. L., Levin, D. M., Adler-Wailes, D. C., and Londos, C. (2000) The lipolytic stimulation of 3T3-L1 adipocytes promotes the translocation of hormone-sensitive lipase to the surfaces of lipid storage droplets.Biochim. Biophys. Acta 1483, 251-262

36. Greenberg, A. S., Shen, W. J., Muliro, K., Patel, S., Souza, S. C., Roth, R. A. & Kraemer, F. B. (2001) Stimulation of lipolysis and hormone-sensitive lipase via the extracellular signal-regulated kinase pathway. Journal of Biological Chemistry 276: 45456-45461.

37. Vance, D. E. & Vance, J. E. (2002) Biochemistry of Lipids, Lipoproteins and Membranes, 4th edition. Elsevier Science.

38. Londos, C., Brasaemle, D. L., Schultz, C. J., Adler-Wailes, D. C., Levin, D. M., Kimmel, A. R. & Rondinone, C. M. (1999) On the control of lipolysis in adipocytes. Annals of the New York Academy of Sciences 892: 155-168.

39. Ruderman, N. B., Kemmer, F. W., Goodman, M. N. & Berger, M. (1980) Oxygen consumption in perfused skeletal muscle. Effect of perfusion with aged, fresh and aged-rejuvenated erythrocytes on oxygen consumption, tissue metabolites and inhibition of glucose utilization by acetoacetate. Biochemical Journal 190: 57-64.

40. Akanbi, K. A. & Mersmann, H. J. (1996) Beta-adrenergic receptors in porcine adipocyte membranes: modification by animal age, depot site, and dietary protein deficiency. Journal of Animal Science 74: 551-561.

41. Shillabeer, G., Hornford, J., Forden, J. M., Wong, N. C. & Lau, D. C. (1990) Hepatic and adipose tissue lipogenic enzyme mRNA levels are suppressed by high fat diets in the rat. Journal of Lipid Research 31: 623-631.

42. Gondret, F., Ferre, P. & Dugail, I. (2001) ADD-1/SREBP-1 is a major determinant of tissue differential lipogenic capacity in mammalian and avian species. Journal of Lipid Research 42: 106-113.

43. Lee, K., Hausman, G. J. & Dean, R. G. (1998) Expression of C/EBP alpha, beta and delta in fetal and postnatal subcutaneous adipose tissue. Molecular & Cellular Biochemistry 178: 269-274.

44. Ding, S. T., Schinckel, A. P., Weber, T. E. & Mersmann, H. J. (2000) Expression of porcine transcription factors and genes related to fatty acid metabolism in different tissues and genetic populations. Journal of Animal Science 78: 2127-2134.

45. Mersmann, H. J., Houk, J. M., Phinney, G., Underwood, M. C. & Brown, L. J. (2001) Lipogenesis by in vitro liver and adipose tissue preparations from neonatal swine. American Journal of Physiology 224: 1123-1129.

46. Mersmann, H. J., Phinney, G., Sanguinetti, M. C. & Houk, J. M. (1973) Lipogenic capacity of liver from perinatal swine (Sus domesticus). Comparative Biochemistry & Physiology B: Comparative Biochemistry 46: 493-497.

47. O'Hea, E. K. & Leveille, G. A. (1968) Lipid metabolism in isolated adipose tissue of the domestic pig (Sus domesticus). Comp Biochem Physiol 26: 1081-1089.

48. O'Hea, E. K., and Leveille, G. A. (1969) Influence of feeding frequency on lipogenesis and enzymatic activity of adipose tissue and on the preformance of pigs. J Anim Sci 28, 336-341

49. Allee, G. L., Baker, D. H. & Leveille, G. A. (1972) Fat utilization and lipogenesis in the young pig. Journal of Nutrition 101: 1415-1421.

50. Allee, G. L., Baker, D. H. & Leveille, G. A. (1971) Influence of level of dietary fat on adipose tissue lipogenesis and enzymatic activity in the pig. Journal of Animal Science 33: 1248-1254.

51. Camara, M., Mourot, J. & Fevrier, C. (1996) Influence of two dairy fats on lipid synthesis in the pig: comparative study of liver, muscle and the two backfat layers. Annals of Nutrition & Metabolism 40: 287-295.

52. Smith, D. R., Knabe, D. A. & Smith, S. B. (1996) Depression of lipogenesis in swine adipose tissue by specific dietary fatty acids. J Anim Sci 74: 975-983.

53. Ding, S. T., Lapillonne, A., Heird, W. C. & Mersmann, H. J. (2003) Dietary fat has minimal effects on fatty acid metabolism transcript concentrations in pigs. Journal of Animal Science 81: 423-431.

54. Koch, D. E., Pearson, A. M., Magee, W. T., Hoefer, J. A. & Schweigert, B. S. (1968) Effect of Diet on the Fatty Acid Composition of Pork Fat. J Anim Sci 27: 360-365

55. Pope, T. S., Smart, D. A. & Rooney, S. A. (1988) Hormonal effects on fatty-acid synthase in cultured fetal rat lung; induction by dexamethasone and inhibition of activity by triiodothyronine. Biochim Biophys Acta 959: 169-177.

56. Ding, S. T., McNeel, R. L. & Mersmann, H. J. (1999) Expression of porcine adipocyte transcripts: tissue distribution and differentiation in vitro and in vivo. Comparative Biochemistry & Physiology. Part B, Biochemistry & Molecular Biology 123: 307-318.

57. Hausman, D. B., DiGirolamo, M., Bartness, T. J., Hausman, G. J. & Martin, R. J. (2001) The biology of white adipocyte proliferation. Obesity Reviews 2: 239-254.

58. Odle, J. (2005) New insights into the utilization of medium-chain triglycerides by the neonate: observations from a piglet model. Journal of Nutrition 127: 1061-1067.

59. Pegorier, J. P., Le May, C. & Girard, J. (2004) Control of gene expression by fatty acids. Journal of Nutrition 134.

60. Duee, P. H., Darcy-Vrillon, B., Blachier, F. & Morel, M. T. (1995) Fuel selection in intestinal cells. Proceedings of the Nutrition Society 54: 83-94.

61. Drackley, J. K. (2000) Lipid Metabolism, CAB International, New York.

62. Odle, J., Benevenga, N. J. & Crenshaw, T. D. (1991) Utilization of medium-chain triglycerides by neonatal piglets: chain length of even- and odd-carbon fatty acids and apparent digestion/absorption and hepatic metabolism. Journal of Nutrition 121: 605-614.

63. Pegorier, J. P., Duee, P. H., Girard, J. & Peret, J. (1983) Metabolic fate of non-esterified fatty acids in isolated hepatocytes from newborn and young pigs. Evidence for a limited capacity for oxidation and increased capacity for esterification. Biochemical Journal 212: 93-97.

64. Adams, S. H., Lin, X., Yu, X. X., Odle, J. & Drackley, J. K. (1641) Hepatic fatty acid metabolism in pigs and rats: major differences in endproducts, O2 uptake, and beta-oxidation. American Journal of Physiology 272.

65. Odle, J., Lin, X., van Kempen, T. A., Drackley, J. K. & Adams, S. H. (1995) Carnitine palmitoyltransferase modulation of hepatic fatty acid metabolism and radio-HPLC evidence for low ketogenesis in neonatal pigs. Journal of Nutrition 125: 2541-2549.

66. Soncini, M., Yet, S. F., Moon, Y., Chun, J. Y. & Sul, H. S. (1995) Hormonal and nutritional control of the fatty acid synthase promoter in transgenic mice. J Biol Chem 270: 30339-30343.

67. Yaqoob, P., Sherrington, E. J., Jeffery, N. M., Sanderson, P., Harvey, D. J., Newsholme, E. A. & Calder, P. C. (1995) Comparison of the effects of a range of dietary lipids upon serum and tissue lipid composition in the rat. International Journal of Biochemistry & Cell Biology 27: 297-310.

68. Worgall, T. S., Johnson, R. A., Seo, T., Gierens, H. & Deckelbaum, R. J. (2002) Unsaturated fatty acid-mediated decreases in sterol regulatory element-mediated gene transcription are linked to cellular sphingolipid metabolism. Journal of Biological Chemistry 277: 3878-3885.

69. Issemann, I. & Green, S. (1990) Activation of a member of the steroid hormone receptor superfamily by peroxisome proliferators.[see comment]. Nature 347: 645-650.

70. Horton, J. D., Goldstein, J. L. & Brown, M. S. (2002) SREBPs: transcriptional mediators of lipid homeostasis. Cold Spring Harbor Symposia on Quantitative Biology 67: 491-498.

71. Jump, D. B. & Clarke, S. D. (1999) Regulation of gene expression by dietary fat. Annual Review of Nutrition 19: 63-90.

72. Storlien, L. H., Tapsell, L. C. & Calvert, G. D. (2000) Role of dietary factors: macronutrients. Nutrition Reviews 58.

73. Cameron-Smith, D., Burke, L. M., Angus, D. J., Tunstall, R. J., Cox, G. R., Bonen, A., Hawley, J. A. & Hargreaves, M. (2003) A short-term, high-fat diet up-regulates lipid metabolism and gene expression in human skeletal muscle. American Journal of Clinical Nutrition 77: 313-318.

74. Olefsky, J. M. (2001) Nuclear receptor minireview series. Journal of Biological Chemistry 276: 36863-36864.

75. Lu, T. T., Repa, J. J. & Mangelsdorf, D. J. (2001) Orphan nuclear receptors as eLiXiRs and FiXeRs of sterol metabolism. Journal of Biological Chemistry 276: 37735-37738.

76. Barroso, I., Gurnell, M., Crowley, V. E., Agostini, M., Schwabe, J. W., Soos, M. A., Maslen, G. L., Williams, T. D., Lewis, H., Schafer, A. J., Chatterjee, V. K. & O'Rahilly, S. (1999) Dominant negative mutations in human PPARgamma associated with severe insulin resistance, diabetes mellitus and hypertension.[see comment]. Nature 402: 880-883.

77. Smith, S. A., May, F. J., Monteith, G. R. & Roberts-Thomson, S. J. (2001) Activation of the peroxisome proliferator-activated receptor-alpha enhances cell death in cultured cerebellar granule cells. Journal of Neuroscience Research 66: 236-241.

78. Kliewer, S. A., Xu, H. E., Lambert, M. H. & Willson, T. M. (2001) Peroxisome proliferator-activated receptors: from genes to physiology. Recent Progress in Hormone Research 56: 239-263.

79. Elbrecht, A., Chen, Y., Cullinan, C. A., Hayes, N., Leibowitz, M., Moller, D. E. & Berger, J. (1996) Molecular cloning, expression and characterization of human peroxisome proliferator activated receptors gamma 1 and gamma 2. Biochemical & Biophysical Research Communications 224: 431-437.

80. Vosper, H., Khoudoli, G. A., Graham, T. L. & Palmer, C. N. (2002) Peroxisome proliferator-activated receptor agonists, hyperlipidaemia, and atherosclerosis. Pharmacology & Therapeutics 95: 47-62.

81. Peters, J. M., Lee, S. S., Li, W., Ward, J. M., Gavrilova, O., Everett, C., Reitman, M. L., Hudson, L. D. & Gonzalez, F. J. (2000) Growth, adipose, brain, and skin alterations resulting from targeted disruption of the mouse peroxisome proliferator-activated receptor beta(delta). Molecular & Cellular Biology 20: 5119-5128.

82. Baumann, C. A., Chokshi, N., Saltiel, A. R. & Ribon, V. (2000) Cloning and characterization of a functional peroxisome proliferator activator receptor-gamma-responsive element in the promoter of the CAP gene. Journal of Biological Chemistry 275: 9131-9135.

83. Tontonoz, P., Hu, E. & Spiegelman, B. M. (1995) Regulation of adipocyte gene expression and differentiation by peroxisome proliferator activated receptor gamma. Current Opinion in Genetics & Development 5: 571-576.

84. Clinton, S. K.& Giovannucci, E. (1998) Diet, nutrition, and prostate cancer. Annu. Rev. Nutr. 18:413-40.

85. Hertz, R., Bishara-Shieban, J, & Bar-Tana, J. (1995) Mode of action of peroxisome proliferators as hypolipidemic drugs. J. Biol. Chem. 270:13470-75.

86. Ferre, P. (2004) The biology of peroxisome proliferator-activated receptors: relationship with lipid metabolism and insulin sensitivity. Diabetes 53.

87. Ajuwon, K. M., Kuske, J. L., Ragland, D., Adeola, O., Hancock, D. L., Anderson, D. B. & Spurlock, M. E. (2003) The regulation of IGF-1 by leptin in the pig is tissue specific and independent of changes in growth hormone. Journal of Nutritional Biochemistry 14: 522-530.

88. Sundvold, H., Grindflek, E. & Lien, S. (2001) Tissue distribution of porcine peroxisome proliferator-activated receptor alpha: detection of an alternatively spliced mRNA. Gene 273: 105-113.

89. Horton, J. D. & Shimomura, I. (1999) Sterol regulatory element-binding proteins: activators of cholesterol and fatty acid biosynthesis. Current Opinion in Lipidology 10: 143-150.

90. Horton, J. D., Shimomura, I., Ikemoto, S., Bashmakov, Y. & Hammer, R. E. (2003) Overexpression of sterol regulatory element-binding protein-1a in mouse adipose tissue produces adipocyte hypertrophy, increased fatty acid secretion, and fatty liver. Journal of Biological Chemistry 278: 36652-36660.

91. Goldstein, J. L., Rawson, R. B. & Brown, M. S. (2002) Mutant mammalian cells as tools to delineate the sterol regulatory element-binding protein pathway for feedback regulation of lipid synthesis. Arch. Biochem. Biophys. 397:139-148.

92. Horton, J. D. & Shimomura, I. (1999) Sterol regulatory element-binding proteins: activators of cholesterol and fatty acid biosynthesis. Current Opinion in Lipidology 10: 143-150.

93. Edwards, P. A., Tabor, D., Kast, H. R. & Venkateswaran, A. (2000) Regulation of gene expression by SREBP and SCAP. Biochim. Biophys. Acta. 1529:103-113.

94. Shimano, H., Yahagi, N., Amemiya-Kudo, M., Hasty, A. H., Osuga, J., Tamura, Y., Shionoiri, F., Iizuka, Y., Ohashi, K., Harada, K., Gotoda, T., Ishibashi, S. & Yamada, N. (1999) Sterol regulatory element-binding protein-1 as a key transcription factor for nutritional induction of lipogenic enzyme genes. Journal of Biological Chemistry 274: 35832-35839.

95. Horton, J. D., Shah, N. A., Warrington, J. A., Anderson, N. N., Park, S. W., Brown, M. S. & Goldstein, J. L. (2003) Combined analysis of oligonucleotide microarray data from transgenic and knockout mice identifies direct SREBP target genes. Proceedings of the National Academy of Sciences of the United States of America 100: 12027-12032.

96. Moon, Y.-A., Shah, N.A., Mohapatra, S., Warrington, J.A. & Horton, J.D. (2001) Identification of a mammalian long chain fatty acyl elongase regulated by sterol regulatory element-binding proteins. J. Biol. Chem. 276:45358-45366.

97. Brown, M. S. & Goldstein, J. L. (1997) The SREBP pathway: regulation of cholesterol metabolism by proteolysis of a membrane-bound transcription factor. Cell. 89:331-340.

98. Repa, J. J. et al. (2000). Regulation of mouse sterol regulatory element-binding protein-1c gene (SREBP-1c) by oxysterol receptors, LXR and LXRß. Genes Dev. 14:2819-2830.

99. Liang, G. *et al.* (2002). Diminished hepatic response to fasting/refeeding and liver X receptor agonists in mice with selective deficiency of sterol regulatory element-binding protein-1c. J. Biol. Chem. 277:9520-9528.

100. Foretz, M., Guichard, C., Ferre, P. & Foufelle, F. (1999) Sterol regulatory element binding protein-1c is a major mediator of insulin action on the hepatic expression of glucokinase and lipogenesis-related genes.[see comment]. Proceedings of the National Academy of Sciences of the United States of America 96: 12737-12742.

101. DeBose-Boyd, R. A., Ou, J., Goldstein, J. L. & Brown, M. S. (1477) Expression of sterol regulatory element-binding protein 1c (SREBP-1c) mRNA in rat hepatoma cells requires endogenous LXR ligands. Proceedings of the National Academy of Sciences of the United States of America 98: 1477-1482.

102. Shimomura, I., Bashmakov, Y., Ikemoto, S., Horton, J. D., Brown, M. S. & Goldstein, J. L. (1999) Insulin selectively increases SREBP-1c mRNA in the livers of rats with streptozotocin-induced diabetes.[see comment]. Proceedings of the National Academy of Sciences of the United States of America 96: 13656-13661.

103. Latasa, M. J., Moon, Y. S., Kim, K. H. & Sul, H. S. (2000) Nutritional regulation of the fatty acid synthase promoter in vivo: sterol regulatory element binding protein functions through an upstream region containing a sterol regulatory element. Proceedings of the National Academy of Sciences of the United States of America 97: 10619-10624.

104. Joseph, S. B., Laffitte, B. A., Patel, P. H., Watson, M. A., Matsukuma, K. E., Walczak, R., Collins, J. L., Osborne, T. F. & Tontonoz, P. (2002) Direct and indirect mechanisms for regulation of fatty acid synthase gene expression by liver X receptors. Journal of Biological Chemistry 277: 11019-11025.

105. Hannah, V. C., Ou, J., Luong, A., Goldstein, J. L. & Brown, M. S. (2001) Unsaturated fatty acids down-regulate srebp isoforms 1a and 1c by two mechanisms in HEK-293 cells. Journal of Biological Chemistry 276: 4365-4372.

106. Jump, D. B., Botolin, D., Wang, Y., Xu, J., Christian, B. & Demeure, O. (2005) Fatty acid regulation of hepatic gene transcription. Journal of Nutrition 135: 2503-2506.

107. Horton, J. D., Goldstein, J. L. & Brown, M. S. (2002) SREBPs: activators of the complete program of cholesterol and fatty acid synthesis in the liver. J. Clin. Invest. 109:1125-1131.

108. Kwiterovich, P. O., Jr. (2000) The metabolic pathways of high-density lipoprotein, low-density lipoprotein, and triglycerides: a current review. American Journal of Cardiology 86: 21.

109. Vitic, J. & Stevanovic, J. (1993) Comparative studies of the serum lipoproteins and lipids in some domestic, laboratory and wild animals. Comparative Biochemistry & Physiology B: Comparative Biochemistry 106: 223-229.

110. Contacos C, Barter PJ, Vrga L, Sullivan DR. (1998) Cholesteryl ester transfer in hypercholesterolaemia: fasting and postprandial studies with and without pravastatin. Atherosclerosis. 141(1):87-98.

111. Boekholdt SM, Kuivenhoven JA, Hovingh GK, Jukema JW, Kastelein JJ, van Tol A (2004).CETP gene variation: relation to lipid parameters and cardiovascular risk. Curr Opin Lipidol. 15(4):393-8.

112. Fisher, E. A., Blum, C. B., Zannis, V.I.& Breslow, J. L. (1983) Independent effects of dietary saturated fat and cholesterol on plasma lipids, lipoproteins, and apoprotein *E.* J. Lipid Res .24:1039-48.

113. Goldberg, A. C. & Schonfeld, G. (1985) Effects of diet on lipoprotein metabolism. Annual Review of Nutrition 5: 195-212.

114. Abdel-Fattah, G., Fernandez, M. L. & McNamara, D. J. (1998) Regulation of very low density lipoprotein apo B metabolism by dietary fat saturation and chain length in the guinea pig. Lipids 33: 23-31.

115. Fernandez, M. L. & McNamara, D. J. (1991) Regulation of cholesterol and lipoprotein metabolism in guinea pigs mediated by dietary fat quality and quantity. Journal of Nutrition 121: 934-943.

116. Fernandez, M. L., Lin, E. C. & McNamara, D. J. (1992) Regulation of guinea pig plasma low density lipoprotein kinetics by dietary fat saturation. Journal of Lipid Research 33: 97-109.

117. Fernandez, M. L., Lin, E. C. & McNamara, D. J. (1833) Differential effects of saturated fatty acids on low density lipoprotein metabolism in the guinea pig. Journal of Lipid Research 33: 1833-1842.

118. Dashti, N., Feng, Q. & Franklin, F. A. (1980) Long-term effects of cis and trans monounsaturated (18:1) and saturated (16:0) fatty acids on the synthesis and secretion of apolipoprotein A-I- and apolipoprotein B-containing lipoproteins in HepG2 cells. Journal of Lipid Research 41: 1980-1990.

119. Bennett, A. J., Billett, M. A., Salter, A. M. & White, D. A. (1995) Regulation of hamster hepatic microsomal triglyceride transfer protein mRNA levels by dietary fats. Biochemical & Biophysical Research Communications 212: 473-478.

120. Abdel-Fattah, G., Fernandez, M. L. & McNamara, D. J. (1188) Regulation of guinea pig very low density lipoprotein secretion rates by dietary fat saturation. Journal of Lipid Research 36: 1188-1198.

121. Cole, T. G., Patsch, W., Kuisk, I., Gonen, B. & Schonfeld, G. (1983) Increases in dietary cholesterol and fat raise levels of apoprotein E-containing lipoproteins in the plasma of man. Journal of Clinical Endocrinology & Metabolism 56: 1108-1115.

122. Temel, R. E., Gebre, A. K., Parks, J. S. & Rudel, L. L. (2003) Compared with Acyl-CoA:cholesterol O-acyltransferase (ACAT) 1 and lecithin:cholesterol acyltransferase, ACAT2 displays the greatest capacity to differentiate cholesterol from sitosterol. Journal of Biological Chemistry 278: 47594-47601.

123. Feldman, E. B., Russell, B. S., Chen, R., Johnson, J., Forte, T. & Clark, S. B. (1983) Dietary saturated fatty acid content affects lymph lipoproteins: studies in the rat. Journal of Lipid Research 24: 967-976.

124. Fernandez, M. L. & McNamara, D. J. (1994) Dietary fat saturation and chain length modulate guinea pig hepatic cholesterol metabolism. Journal of Nutrition 124: 331-339.

125. Fernandez, M. L., Sun, D. M., Montano, C. & McNamara, D. J. (1995) Carbohydrate-fat exchange and regulation of hepatic cholesterol and plasma lipoprotein metabolism in the guinea pig. Metabolism: Clinical & Experimental 44: 855-864.

126. Kinnunen, P. K., Jackson, R. L., Smith, L. C., Gotto, A. M., Jr. & Sparrow, J. T. (1977) Activation of lipoprotein lipase by native and synthetic fragments of human plasma apolipoprotein C-II. Proceedings of the National Academy of Sciences of the United States of America 74: 4848-4851.

127. Kris-Etherton, P. M. & Yu, S. (1997) Individual fatty acid effects on plasma lipids and lipoproteins: human studies. American Journal of Clinical Nutrition 65:1628S-1644S.

128. Fernandez, M. L., Vergara-Jimenez, M., Conde, K. & Abdel-Fattah, G. (1996) Dietary carbohydrate type and fat amount alter VLDL and LDL metabolism in guinea pigs. Journal of Nutrition 126: 2494-2504.

129. Kliewer, S. A., Sundseth, S. S., Jones, S. A., Brown, P. J. & Wisely, G. B. (1997) Fatty acids and eicosanoids regulate gene expression through direct interaction with peroxisome proliferator-activated receptors α and γ. Proc. Natl. Acad. Sci. 94:4318-23.

130. Fernandez, M. L. (2001) Guinea pigs as models for cholesterol and lipoprotein metabolism. Journal of Nutrition 131: 10-20.

131. Nicolosi, R.J., Wilson, T.A., Lawton, C., Rogers, E.J., Wiseman, S.A., Tijburg, L.B.M. & Kritchevsky, D. (1998) The greater athrrogenecity of nonpurified diets versus semipurified diets in hamsters is mediated via differences in plasma lipoprotein cholesterol distribution, LDL oxidative susceptibility, and plasma α-tocopherol concentration. J. Nutr. Biochem. 9: 591-597.

132. Fernandez, M. L. & West, K. L. (2005) Mechanisms by which dietary fatty acids modulate plasma lipids. Journal of Nutrition 135: 2075-2078.

133. Egan, J. J., Greenberg, A. S., Chang, M. K., Wek, S. A., Moos, M. C., Jr. & Londos, C. (1992) Mechanism of hormone-stimulated lipolysis in adipocytes: translocation of hormone-sensitive lipase to the lipid storage droplet. Proceedings of the National Academy of Sciences of the United States of America 89: 8537-8541.

134. Okazaki, H., Osuga, J., Tamura, Y., Yahagi, N., Tomita, S., Shionoiri, F., Iizuka, Y., Ohashi, K., Harada, K., Kimura, S., Gotoda, T., Shimano, H., Yamada, N. & Ishibashi, S. (2002) Lipolysis in the absence of hormone-sensitive lipase: evidence for a common mechanism regulating distinct lipases. Diabetes 51: 3368-3375.

135. Clifford, G. M., Londos, C., Kraemer, F. B., Vernon, R. G. & Yeaman, S. J. (2000) Translocation of hormone-sensitive lipase and perilipin upon lipolytic stimulation of rat adipocytes. Journal of Biological Chemistry 275: 5011-5015.

136. Champigny, O., Ricquier, D., Blondel, O., Mayers, R. M., Briscoe, M. G. & Holloway, B. R. (1991) Beta 3-adrenergic receptor stimulation restores message and expression of brown-fat mitochondrial uncoupling protein in adult dogs. Proceedings of the National Academy of Sciences of the United States of America 88: 10774-10777.

137. Inglese, J., Freedman, N.J., Koch, W.J. & Lefkowitz, R.J. (1993) Structure and mechanism of the G-protein-coupled receptor kinases. Journal of Biological Chemsitry 268: 23735-23738.

138. Spiegel, A. M., Shenker, A. & Weinstein, L. S. (1992) Receptor-effector coupling by G proteins: implications for normal and abnormal signal transduction. Endocrine Reviews 13: 536-565.

139. Bünemann, M., Lee, K. B., Pals-Rylaarsdam, R., Roseberry, A. G. & Hosey, M. M (1999) Desensitization of G-protein-coupled receptors in the cardiovascular system. Annual Review of Physiology 61: 169-192

140. Mermann, H. J. (1998) Overview of the effects of beta-adrenergic receptor agonists on animal growth including mechanisms of action. J Anim Sci 76, 160-172.

141. Reusch, J. E. & Klemm, D. J. (1426) Inhibition of cAMP-response element-binding protein activity decreases protein kinase B/Akt expression in 3T3-L1 adipocytes and induces apoptosis. Journal of Biological Chemistry 277: 1426-1432.

142. Spiegelman, B. M. & Green, H. (1981) Cyclic AMP-mediated control of lipogenic enzyme synthesis during adipose differentiation of 3T3 cells. Cell 24: 503-510.

143. Roesler, W. J., Vandenbark, G. R. & Hanson, R. W. (1988) Cyclic AMP and the induction of eukaryotic gene transcription. Journal of Biological Chemistry 263: 9063-9066.

144. Foulkes, N. S., Borrelli, E. & Sassone-Corsi, P. (1991) CREM gene: use of alternative DNA-binding domains generates multiple antagonists of cAMP-induced transcription. Cell 64: 739-749.

145. Mersmann, H. J. (1998) Overview of the effects of beta-adrenergic receptor agonists on animal growth including mechanisms of action. Journal of Animal Science 76: 160-172.

146. Bronnikov, G., Houstek, J. & Nedergaard, J. (2006) Beta-adrenergic, cAMP-mediated stimulation of proliferation of brown fat cells in primary culture. Mediation via beta 1 but not via beta 3 adrenoceptors. Journal of Biological Chemistry 267: 2006-2013.

147. Strosberg, A. D. (1993) Structure, function, and regulation of adrenergic receptors. Protein Science 2:1198-1209.

148. Liang, W. & Mills, S. E. (2002) Quantitative analysis of beta-adrenergic receptor subtypes in pig tissues. Journal of Animal Science 80: 963-970.

149. Cao, H., Bidwell, C. A., Williams, S. K., Liang, W. & Mills, S. E. (1998) Rapid communication: Nucleotide sequence of the coding region for the porcine beta1-adrenergic receptor gene. Journal of Animal Science 76: 1720-1721.

150. Smith, S. B., Garcia, D. K., Davis, S. K. & Anderson, D. B. (1989) Elevation of a specific mRNA in longissimus muscle of steers fed ractopamine. Journal of Animal Science 67: 3495-3502.

151. McNeel, R. L. & Mersmann, H. J. (1999) Distribution and quantification of beta1-, beta2-, and beta3-adrenergic receptor subtype transcripts in porcine tissues. Journal of Animal Science 77: 611-621.

152. Liang, W. & Mills, S. E. (2002) Quantitative analysis of beta-adrenergic receptor subtypes in pig tissues. Journal of Animal Science 80: 963-970.

153. Mills, S. E., Kissel, J., Bidwell, C. A. & Smith, D. J. (2003) Stereoselectivity of porcine beta-adrenergic receptors for ractopamine stereoisomers. Journal of Animal Science 81: 122-129.

154. Kissel, J. D., D. J. Smith, &S. E. Mills. (2001) Stereoselectivity of porcine β-adrenergic receptors for ractopamine isomers. J. Anim.Sci. 79:429(Abstr.).

155. Ricke, E. A., Smith, D. J., Feil, V. J., Larsen, G. L. & Caton, J. S. (1999) Effects of ractopamine HCl stereoisomers on growth, nitrogen retention, and carcass composition in rats. Journal of Animal Science 77: 701-707.

156. Yen, J. T., Mersmann, H. J., Hill, D. A. & Pond, W. G. (1990) Effects of ractopamine on genetically obese and lean pigs. Journal of Animal Science 68: 3705-3712.

157. Mills, S. E., Spurlock, M. E. & Smith, D. J. (2003) Beta-adrenergic receptor subtypes that mediate ractopamine stimulation of lipolysis. Journal of Animal Science 81: 662-668.

158. Mills, S. E., Kissel, J., Bidwell, C. A. & Smith, D. J. (2003) Stereoselectivity of porcine beta-adrenergic receptors for ractopamine stereoisomers. Journal of Animal Science 81: 122-129.

159. Maltin, C. A., Hay, S. M., Delday, M. I., Lobley, G. E., & Reeds, P. J. (1989) The action of the beta-agonist clenbuterol on protein metabolism in innervated and denervated phasic muscles. Biochem. J. 261:965–971.

160. Anderson, D. B., Kauffman, R. G. & Kastenschmidt, L. L. (1972) Lipogenic enzyme activities and cellularity of porcine adipose tissue from various anatomical locations. Journal of Lipid Research 13: 593-599.

161. Liu, C. Y., Grant, A. L., Kim, K. H., Ji, S. Q., Hancock, D. L., Anderson, D. B. & Mills, S. E. (1994) Limitations of ractopamine to affect adipose tissue metabolism in swine. Journal of Animal Science 72: 62-67.

162. Halsey C. H. C. (2003) The effect of the cAMP-elevating agent Paylean on the transcriptional control of lipogenesis and lipid oxidation in swine (MS thesis). Auburn University Auburn (AL).

163. Reiner, S. S. (2004) The effect of the cAMP-elevating agent Paylean on the transcriptional control of lipogenesis and lipid oxidation in swine (MS thesis). Auburn University Auburn (AL).

164. Watkins, L. E., Jones, D. J., Mowrey, D. H., Anderson, D. B. & Veenhuizen, E. L. (1990) The effect of various levels of ractopamine hydrochloride on the performance and carcass characteristics of finishing swine. Journal of Animal Science 68: 3588-3595.

165. Spurlock, M. E., Cusumano, J. C., Ji, S. Q., Anderson, D. B., Smith, C. K., 2nd, Hancock, D. L. & Mills, S. E. (1994) The effect of ractopamine on beta-adrenoceptor density and affinity in porcine adipose and skeletal muscle tissue. Journal of Animal Science 72: 75-80.

166. Bergen, W. G., Johnson, S. E., Skjaerlund, D. M., Babiker, A. S., Ames, N. K., Merkel, R. A. & Anderson, D. B. (1989) Muscle protein metabolism in finishing pigs fed ractopamine. Journal of Animal Science 67: 2255-2262.

167. Armstrong, T. A., Ivers, D. J., Wagner, J. R., Anderson, D. B., Weldon, W. C. & Berg, E. P. (2004) The effect of dietary ractopamine concentration and duration of feeding on growth performance, carcass characteristics, and meat quality of finishing pigs. J Anim Sci 82(11): 3245 - 3253.

168. McElligott, M. A., Chaung, L. Y. & Barreto, A., Jr. (1989) Effects of a beta-adrenergic agonist on protein turnover in muscle cells in culture. Biochemical Pharmacology 38: 2199-2205.

169. O'Brien, S. J., Menotti-Raymond, M., Murphy, W. J. & Yuhki, N. (2002) The Feline Genome Project. Annual Review of Genetics 36: 657-686.

170. Barlow, C. & Lockhart, D. J. (2002) DNA arrays and neurobiology--what's new and what's next? Current Opinion in Neurobiology 12: 554-561.

171. German, J. B., Roberts, M. A., Fay, L. & Watkins, S. M. (2002) Metabolomics and individual metabolic assessment: the next great challenge for nutrition.[see comment]. Journal of Nutrition 132: 2486-2487.

172. Swanson, K. S., Schook, L. B. & Fahey, G. C., Jr. (2003) Nutritional genomics: implications for companion animals. Journal of Nutrition 133: 3033-3040.

173. Daniel, H. (2002) Genomics and proteomics: importance for the future of nutrition research. British Journal of Nutrition 87.

174. Daniel, P. B., Walker, W. H. & Habener, J. F. (1998) Cyclic AMP, signaling and gene regulation. Annu. Rev. Nutr. 18:353-83.

175. Kane, M. D., Jatkoe, T. A., Stumpf, C. R., Lu, J., Thomas, J. D. & Madore, S. J. (2000) Assessment of the sensitivity and specificity of oligonucleotide (50mer) microarrays. Nucleic Acids Research 28: 4552-4557.

176. El Atifi, M., Dupre, I., Rostaing, B., Chambaz, E. M., Benabid, A. L. & Berger, F. (2002) Long oligonucleotide arrays on nylon for large-scale gene expression analysis. Biotechniques 33: 612-616.

177. Barrett, J. C. & Kawasaki, E. S. (2003) Microarrays: the use of oligonucleotides and cDNA for the analysis of gene expression.[see comment]. Drug Discovery Today 8: 134-141.

178. Bryant, P. A., Venter, D., Robins-Browne, R. & Curtis, N. (2004) Chips with everything: DNA microarrays in infectious diseases. The Lancet Infectious Diseases 4: 100-111.

179. Beaucage, S. L. (1213) Strategies in the preparation of DNA oligonucleotide arrays for diagnostic applications. Current Medicinal Chemistry 8: 1213-1244.

180. Li, F. & Stormo, G. D. (1067) Selection of optimal DNA oligos for gene expression arrays. Bioinformatics 17: 1067-1076.

181. Wagner, E. K., Ramirez, J. J., Stingley, S. W., Aguilar, S. A., Buehler, L., Devi-Rao, G. B. & Ghazal, P. (2002) Practical approaches to long oligonucleotide-based DNA microarray: lessons from herpesviruses. Progress in Nucleic Acid Research & Molecular Biology 71: 445-491.

182. Schena, M., Shalon, D., Davis, R. W. & Brown, P. O. (1995) Quantitative monitoring of gene expression patterns with a complementary DNA microarray.[see comment]. Science 270: 467-470.

183. Spielbauer, B. & Stahl, F. (2005) Impact of microarray technology in nutrition and food research. Molecular Nutrition & Food Research 49: 908-917.

184. See, M. T., Armstrong, T. A. & Weldon, W. C. (2004) Effect of a ractopamine feeding program on growth performance and carcass composition in finishing pigs. J Anim Sci 82(8): 2474 - 2480.

185. Lands, A. M., Luduena, F. P. & Buzzo, H. J. (1967) Differentiation of receptors responsive to isoproterenol. Life Sciences 6: 2241-2249.

186. Dalrymple, R. H., Baker, P. K., Gingher, P. E., Ingle, D. L., Pensack, J. M. & Ricks, C. A. (1984) A repartitioning agent to improve performance and carcass composition of broilers. Poultry Science 63: 2376-2383.

187. Schinckel, A. P., Herr, C. T., Richert, B. T., Forrest, J. C. & Einstein, M. E. (2003) Ractopamine treatment biases in the prediction of pork carcass composition. Journal of Animal Science 81: 16-28.

188. Bergen, W. G. & Merkel, R. A. (1991) Body composition of animals treated with partitioning agents: implications for human health. FASEB Journal 5: 2951-2957.

189. Sutton, A. L. & Richert, B. T. (2004) Nutrition and feed management strategies to reduce nutrient excretions and odors from swine manure. Water Science & Technology 49: 397-404.

190. Sutton, A. L., Kephart, K. B., Verstegen, M. W., Canh, T. T. & Hobbs, P. J. (1999) Potential for reduction of odorous compounds in swine manure through diet modification. Journal of Animal Science 77: 430-439.

191. Yang, Y. T. & McElligott, M. A. (1989) Multiple actions of beta-adrenergic agonists on skeletal muscle and adipose tissue. Biochemical Journal 261: 1-10.

192. Spurlock, M. E., Cusumano, J. C. & Mills, S. E. (1993) The affinity of ractopamine, clenbuterol, and L-644,969 for the beta-adrenergic receptor population in porcine adipose tissue and skeletal muscle membrane.[erratum appears in J Ani Sci 1993 Oct;71(10):2834]. Journal of Animal Science 71: 2061-2065.

193. Moody, D. E., Hancock, D. L. & Anderson, D. B. (2000) Phenethano-lamine repartitioning agents. In: J. P. F. D'Mello (ed.) Farm Animal Metabolism and Nutrition. pp. 65–96. CAB International, Wallingford, Oxon, U.K.

194. Williams, N. H., Cline, T. R., Schinckel, A. P. & Jones, D. J. (1994) The impact of ractopamine, energy intake, and dietary fat on finisher pig growth performance and carcass merit. Journal of Animal Science 72: 3152-3162.

195. Gottschalk, P. N. (2004) Effect of Paylean® administration on expression of selected transcription factors and their target genes in porcine skeletal muscle (MS thesis) Auburn University Auburn (AL).

196. Brazma, A., Hingamp, P., Quackenbush, J., Sherlock, G., Spellman, P., Stoeckert, C., Aach, J., Ansorge, W., Ball, C. A., Causton, H. C., Gaasterland, T., Glenisson, P., Holstege, F. C., Kim, I. F., Markowitz, V., Matese, J. C., Parkinson, H., Robinson, A., Sarkans, U., Schulze-Kremer, S., Stewart, J., Taylor, R., Vilo, J. & Vingron, M. (2001) Minimum information about a microarray experiment (MIAME)-toward standards for microarray data.[see comment]. Nature Genetics 29: 365-371.

197. Ball, C., Brazma, A., Causton, H., Chervitz, S., Edgar, R., Hingamp, P., Matese, J. C., Parkinson, H., Quackenbush, J., Ringwald, M., Sansone, S. A., Sherlock, G., Spellman, P., Stoeckert, C., Tateno, Y., Taylor, R., White, J., Winegarden, N. & Society, M. (2004) Standards for microarray data: an open letter. Environmental Health Perspectives 112.

198. Mee, C. J. (2005) Microarray methods in Drosophila neurobiology. Invertebrate Neuroscience 5: 189-195.

199. (1998) Nutrient Requirements of Swine. In, National Research Council, National Academy of Sciences, Wahington D.C.

200. Allison DB, Cui X, Page GP, Sabripour M. (2006) Microarray data analysis: from disarray to consolidation and consensus. Nat Rev Genet. 7(1):55-65.

201. Chomczynski, P. & Sacchi, N. (1987) Single-step method of RNA isolation by acid guanidinium thiocyanate-phenol-chloroform extraction. Analytical Biochemistry 162: 156-159.

202. Hegde, P., Qi, R., Abernathy, K., Gay, C., Dharap, S., Gaspard, R., Hughes, J. E., Snesrud, E., Lee, N. & Quackenbush, J. (2000) A concise guide to cDNA microarray analysis. Biotechniques 29: 548-550.

203. Berger, J. A., Hautaniemi, S., Jarvinen, A. K., Edgren, H., Mitra, S. K. & Astola, J. (2004) Optimized LOWESS normalization parameter selection for DNA microarray data. BMC Bioinformatics 5: 9.

204. Yang, Y. H., Dudoit, S., Luu, P., Lin, D. M., Peng, V., Ngai, J. & Speed, T. P. (2002) Normalization for cDNA microarray data: a robust composite method addressing single and multiple slide systematic variation. Nucleic Acids Research 30: 15.

205. Tusher, V. G., Tibshirani, R. & Chu, G. (2001) Significance analysis of microarrays applied to the ionizing radiation response.[erratum appears in Proc Natl Acad Sci U S A 2001 Aug 28;98(18):10515]. Proceedings of the National Academy of Sciences of the United States of America 98: 5116-5121.

206. Manchester, K L. (1995). Value of A260/A280 ratios for measurement of purity of nucleic acids. Biotechniques 19, 208-209.

207. Glasel, J A. (1995). Validity of nucleic acid monitored by 260nm/280nm absorbance ratios. Biotechniques 18, 62-63.

208. Warburg, O. and W. Christian. (1942). Isolation and Crystallisation of Enolase. Biochem. Z. 310:384-421.

209. Wilfinger, W W, Mackey, K and Chomczyski, P. (1997). Effect of pH and ionic strength on the spectrophotometric assessment of nucleic acid purity. Biotechniques 22, 474-481.

210. Sandrine Imbeaud*, Esther Graudens, Virginie Boulanger, Xavier Barlet, Patrick Zaborski, Eric Eveno, Odilo Mueller1, Andreas Schroeder1 and Charles Auffray (2005). Towards standardization of RNA quality assessment using user-independent classifiers of microcapillary electrophoresis traces. Nucleic Acids Research 33(6):e56

211. Sambrook J, Fritsch E, Maniatis T(1989). Molecular Cloning, a laboratory manual. 2nd edition. Cold Spring Harbor Laboratory Press, New York.

212. Agilent, . 2100 expert software. Tech Rep 5989-0112EN, Agilent Technologies, Software Data Sheet. (2004). http://www.agilent.com/chem/labonachip

213. The RIN-project(2001). http://www.agilent.com/chem/RIN, http://www.quantiom.com/RIN.

214. Manchester, K L. (1996). Use of UV methods for the measurement of protein and nucleic acid concentrations. Biotechniques 20, 968-970.

215. Simone Fleigea and Michael W. Pfaffl. (2006). RNA integrity and the effect on the real-time qRT-PCR performance. Mol Aspects Med. 27(2-3):126-39.

216. Schoor O, Weinschenk T, Hennenlotter J, Corvin S, Stenzl A, Rammensee HG, Stevanovic S . (2003). Moderate degradation does not preclude microarray analysis of small amounts of RNA. Biotechniques. 35(6):1192-6.

217. Auer, H., Lyianarachchi, S., Newsom, D., Klisovic, M.I., Marcucci, G., Kornacker, K., Marcucci, U. (2003) Chipping away at the chip bias: RNA degradation in microarray analysis *Nature Genet.*, 35: 292–293

218. Andreas Schroeder, Odilo Mueller, Susanne Stocker, Ruediger Salowsky, Michael Leiber, Marcus Gassmann, Samar Lightfoot, Wolfram Menzel, Martin Granzow and Thomas Ragg (2006). The RIN: an RNA integrity number for assigning integrity values to RNA measurements. BMC Molecular Biology 7:3

219. Yang, Y. H. & Speed, T. (2002) Design issues for cDNA microarray experiments. Nature Reviews Genetics 3: 579-588.

220. Wolfinger, R. D., Gibson, G., Wolfinger, E. D., Bennett, L., Hamadeh, H., Bushel, P., Afshari, C. & Paules, R. S. (2001) Assessing gene significance from cDNA microarray expression data via mixed models. Journal of Computational Biology 8: 625-637.

221. Lee, M. L., Kuo, F. C., Whitmore, G. A. & Sklar, J. (2000) Importance of replication in microarray gene expression studies: statistical methods and evidence from repetitive cDNA hybridizations. Proceedings of the National Academy of Sciences of the United States of America 97: 9834-9839.

222. Allison, D. B. et al. (2002). A mixture model approach for the analysis of microarray gene expression data. Comput. Stat. Data Analysis 39, 1–20.

223. Pavlidis, P., Li, Q. & Noble, W. S. (2003).The effect of replication on gene expression microarray experiments. Bioinformatics 19, 1620–1627

224. Tsai, C. A. , Hsueh, H. M. & Chen, J. J. (2003).Estimation of false discovery rates in multiple testing: application to gene microarray data. Biometrics 59, 1071–1081

225. Chen, Y., Kamat, V., Dougherty, E. R., Bittner, M. L., Meltzer, P. S. & Trent, J. M. (1207) Ratio statistics of gene expression levels and applications to microarray data analysis. Bioinformatics 18: 1207-1215.

226. Dobbin, K., Shih, J. H. & Simon, R. (2003) Questions and answers on design of dual-label microarrays for identifying differentially expressed genes. Journal of the National Cancer Institute 95: 1362-1369.

227. Wilson, D. L., Buckley, M. J., Helliwell, C. A. & Wilson, I. W. (2003) New normalization methods for cDNA microarray data. Bioinformatics 19: 1325-1332.

228. Tseng, G. C., Oh, M. K., Rohlin, L., Liao, J. C. & Wong, W. H. (2001) Issues in cDNA microarray analysis: quality filtering, channel normalization, models of variations and assessment of gene effects. Nucleic Acids Research 29: 2549-2557.

229. Quackenbush, J. (2002) Microarray data normalization and transformation. Nature Genetics 32: 496-501.

230. Bolstad, B. M., Irizarry, R. A., Astrand, M. & Speed, T. P. (2003) A comparison of normalization methods for high density oligonucleotide array data based on variance and bias. Bioinformatics 19: 185-193.

231. Lee, P. D., Sladek, R., Greenwood, C. M. & Hudson, T. J. (2002) Control genes and variability: absence of ubiquitous reference transcripts in diverse mammalian expression studies. Genome Research 12: 292-297.

232. Yang, Y. H., Buckley, M. J. & Speed, T. P. (2001) Analysis of cDNA microarray images. Briefings in Bioinformatics 2: 341-349.

233. Yang, Y. H., Dudoit, S., Luu, P., Lin, D. M., Peng, V., Ngai, J. & Speed, T. P. (2002) Normalization for cDNA microarray data: a robust composite method addressing single and multiple slide systematic variation. Nucleic Acids Research 30: 15.

234. Cleveland, W. S. & Guarino, R. (1978) The use of numerical and graphical statistical methods in the analysis of data on learning to see complex random-dot stereograms. Perception 7: 113-118.

235. Kaminski, N. & Friedman, N. (2002) Practical approaches to analyzing results of microarray experiments. Am J Respir Cell Mol Biol 27(2):125-32.

236. Leung, Y. F. & Cavalieri, D. (2003) Fundamentals of cDNA microarray data analysis. Trends in Genetics 19: 649-659.

237. Novak, J. P., Sladek, R. & Hudson, T. J. (2002) Characterization of variability in large-scale gene expression data: implications for study design. Genomics 79: 104-113.

238. Pritchard, C. C., Hsu, L., Delrow, J. & Nelson, P. S. (2001) Project normal: defining normal variance in mouse gene expression. Proceedings of the National Academy of Sciences of the United States of America 98: 13266-13271.

239. Nadon, R. & Shoemaker, J. (2002) Statistical issues with microarrays: processing and analysis. Trends in Genetics 18: 265-271.

240. Dudoit, S., Gentleman, R. C. & Quackenbush, J. (2003) Open source software for the analysis of microarray data. Biotechniques. Suppl.

241. Reiner, A., Yekutieli, D. & Benjamini, Y. (2003) Identifying differentially expressed genes using false discovery rate controlling procedures. Bioinformatics 19: 368-375.

242. Storey, J. D. & Tibshirani, R. (2003) Statistical methods for identifying differentially expressed genes in DNA microarrays. Methods in Molecular Biology 224: 149-157.

243. Chinetti, G., Fruchart, J. C. & Staels, B. (2000) Peroxisome proliferator-activated receptors (PPARs): nuclear receptors at the crossroads between lipid metabolism and inflammation. Inflammation Research 49: 497-505.

244. Peterla, T. A. & Scanes, C. G. (1024) Effect of beta-adrenergic agonists on lipolysis and lipogenesis by porcine adipose tissue in vitro. Journal of Animal Science 68: 1024-1029.

245. Holm, C., Osterlund, T., Laurell, H. & Contreras, J. A. (2000) Molecular mechanisms regulating hormone-sensitive lipase and lipolysis. Annual Review of Nutrition 20: 365-393.

246. Large, V., Arner, P., Reynisdottier, S., Grober, J., Van Harmelen, V., Holm, C. & Langin, D. (1998) Hormone-sensitive lipase expression and activity in relation to lipolysis in human fat cells. Journal of Lipid Research 39: 1688-1695.

247. Peffer, P. L., Lin, X. & Odle, J. (1518) Hepatic beta-oxidation and carnitine palmitoyltransferase I in neonatal pigs after dietary treatments of clofibric acid, isoproterenol, and medium-chain triglycerides. American Journal of Physiology Regulatory Integrative & Comparative Physiology 288.

248. Odle, J., Lin, X., van Kempen, T. A., Drackley, J. K. & Adams, S. H. (1995) Carnitine palmitoyltransferase modulation of hepatic fatty acid metabolism and radio-HPLC evidence for low ketogenesis in neonatal pigs. Journal of Nutrition 125: 2541-2549.

249. Smith SB, Mersmann HJ, Smith EO, Britain KG. (1999)Stearoyl-coenzyme A desaturase gene expression during growth in adipose tissue from obese and crossbred pigs. J Anim Sci. 77(7):1710-6.

250. Casimir DA, Ntambi JM. (1996). cAMP activates the expression of stearoyl-CoA desaturase gene 1 during early preadipocyte differentiation.
J Biol Chem. 271:29847-53.

251. Kaestner KH, Flores-Riveros JR, McLenithan JC, Janicot M, Lane MD. (1991). Transcriptional repression of the mouse insulin-responsive glucose transporter (GLUT4) gene by cAMP. Proc Natl Acad Sci U S A. 88(5):1933-7.

252. Vinals F, Ferre J, Fandos C, Santalucia T, Testar X, Palacin M, Zorzano A. (1997)Cyclic adenosine 3',5'-monophosphate regulates GLUT4 and GLUT1 glucose transporter expression and stimulates transcriptional activity of the GLUT1 promoter in muscle cells. Endocrinology. 138(6):2521-9.

253. Zhang, Y., Proenca, R., Maffei, M., Barone, M., Leopold, L. & Friedman, J. M. (1994) Positional cloning of the mouse obese gene and its human homologue Nature 372: 425-432.

254. Tartaglia, L. A. (1997) The leptin receptor. Journal of Biological Chemistry 272: 6093-6096.

255. Trayhurn, P. (2005) Endocrine and signalling role of adipose tissue: new perspectives on fat. Acta Physiologica Scandinavica 184: 285-293.

256. Harris, K. B., Cross, H. R., Pond, W. G. & Mersmann, H. J. (1993) Effect of dietary fat and cholesterol level on tissue cholesterol concentrations of growing pigs selected for high or low serum cholesterol. Journal of Animal Science 71: 807-810.

257. Unger, R. H. (2000) Leptin physiology: a second look. Regulatory Peptides 92: 87-95.

258. Van Gaal, L. F., Wauters, M. A., Mertens, I. L., Considine, R. V. & De Leeuw, I. H. (1999) Clinical endocrinology of human leptin. International Journal of Obesity & Related Metabolic Disorders: Journal of the International Association for the Study of Obesity 1: 29-36.

260. Wauters, M., Considine, R. V. & Van Gaal, L. F. (2000) Human leptin: from an adipocyte hormone to an endocrine mediator. European Journal of Endocrinology 143: 293-311.

261. Chuaqui, R. F., Bonner, R. F., Best, C. J., Gillespie, J. W., Flaig, M. J., Hewitt, S. M., Phillips, J. L., Krizman, D. B., Tangrea, M. A., Ahram, M., Linehan, W. M., Knezevic, V. & Emmert-Buck, M. R. (2002) Post-analysis follow-up and validation of microarray experiments. Nature Genetics 32: 509-514.

262. Cui, X., Hwang, J. T., Qiu, J., Blades, N. J. & Churchill, G. A. (2005) Improved statistical tests for differential gene expression by shrinking variance components estimates. Biostatistics 6: 59-75.

263. Hill, J. O. (1302) Preventing excessive weight gain.. Obesity Research 13.

264. Schrauwen-Hinderling, V. B., van Loon, L. J., Koopman, R., Nicolay, K., Saris, W. H. & Kooi, M. E. (2003) Intramyocellular lipid content is increased after exercise in nonexercising human skeletal muscle. Journal of Applied Physiology 95: 2328-2332.

265. Pettigrew and Moser in Miller et al, Swine Nutrition, Butterworth, 1991, Chapter 7

266. Tzameli, I., Fang, H., Ollero, M., Shi, H., Hamm, J. K., Kievit, P., Hollenberg, A. N. & Flier, J. S. (2004) Regulated production of a peroxisome proliferator-activated receptor-gamma ligand during an early phase of adipocyte differentiation in 3T3-L1 adipocytes. Journal of Biological Chemistry 279: 36093-36102.

267. Flier, J. S. & Hollenberg, A. N. (1999) ADD-1 provides major new insight into the mechanism of insulin action.[comment]. Proceedings of the National Academy of Sciences of the United States of America 96: 14191-14192.

268. Cohen, P., Zhao, C., Cai, X., Montez, J. M., Rohani, S. C., Feinstein, P., Mombaerts, P. & Friedman, J. M. (1113) Selective deletion of leptin receptor in neurons leads to obesity. Journal of Clinical Investigation 108: 1113-1121.

269. Brandt, J. M., Djouadi, F. & Kelly, D. P. (1998) Fatty acids activate transcription of the muscle carnitine palmitoyltransferase I gene in cardiac myocytes via the peroxisome proliferator-activated receptor alpha. Journal of Biological Chemistry 273: 23786-23792.

270. Bremer, J. (2001) The biochemistry of hypo- and hyperlipidemic fatty acid derivatives: metabolism and metabolic effects. Progress in Lipid Research 40: 231-268.

271. Reddy, J. K. & Mannaerts, G. P. (1994) Peroxisomal lipid metabolism. Annu. Rev. Nutr. 14:343-70.

272. Horton, J. D. & Shimomura, I. (1999) Sterol regulatory element-binding proteins: activators of cholesterol and fatty acid biosynthesis. Curr. Opin. Lipidol. 10:143-150.

273. Osborne, T. F. (2000) Sterol regulatory element-binding proteins (SREBPs): key regulators of nutritional homeostasis and insulin action. Journal of Biological Chemistry 275: 32379-32382.

274. Magana, M. M., Koo, S. H., Towle, H. C. & Osborne, T. F. (2000) Different sterol regulatory element-binding protein-1 isoforms utilize distinct co-regulatory factors to activate the promoter for fatty acid synthase. Journal of Biological Chemistry 275: 4726-4733.

275. Semenkovich, C. F. (1997) Regulation of fatty acid synthase (FAS). Progress in Lipid Research 36: 43-53.

276. Clarke, S. D. (1999) Nutrient regulation of gene and protein expression.Current Opinion in Clinical Nutrition & Metabolic Care 2: 287-289.

277. Yin, D., Clarke, S. D. & Etherton, T. D. (2001) Transcriptional regulation of fatty acid synthase gene by somatotropin in 3T3-F442A adipocytes. Journal of Animal Science 79: 2336-2345.

278. Pape, M. E., Lopez-Casillas, F. & Kim, K. H. (1988) Physiological regulation of acetyl-CoA carboxylase gene expression: effects of diet, diabetes, and lactation on acetyl-CoA carboxylase mRNA. Archives of Biochemistry & Biophysics 267: 104-109.

279. Pape, M. E., Schultz, P. A., Rea, T. J., DeMattos, R. B., Kieft, K., Bisgaier, C. L., Newton, R. S. & Krause, B. R. (1995) Tissue specific changes in acyl-CoA: cholesterol acyltransferase (ACAT) mRNA levels in rabbits. Journal of Lipid Research 36: 823-838.

280. Lee, K. N., Pariza, M.W. & Ntambi, J.M. (1998) Conjugated linoleic acid decreases hepatic strearoyl-CoA desaturase mRNA expression. Biochem Biophys Res Commun 248: 817-821

281. Glatz, J. F. & Storch, J. (2001) Unravelling the significance of cellular fatty acid-binding proteins. Current Opinion in Lipidology 12: 267-274.

282. Wolfrum, C., Borchers, T., Sacchettini, J. C. & Spener, F. (2000) Binding of fatty acids and peroxisome proliferators to orthologous fatty acid binding proteins from human, murine, and bovine liver. Biochemistry 39: 1469-1474.

283. McArthur, M. J., Atshaves, B. P., Frolov, A., Foxworth, W. D., Kier, A. B. & Schroeder, F. (1371) Cellular uptake and intracellular trafficking of long chain fatty acids. Journal of Lipid Research 40: 1371-1383.

284. Wolfrum, C., Borrmann, C. M., Borchers, T. & Spener, F. (2001) Fatty acids and hypolipidemic drugs regulate peroxisome proliferator-activated receptors alpha - and gamma-mediated gene expression via liver fatty acid binding protein: a signaling path to the nucleus. Proceedings of the National Academy of Sciences of the United States of America 98: 2323-2328.

285. Huang, H., Starodub, O., McIntosh, A., Kier, A. B. & Schroeder, F. (2002) Liver fatty acid-binding protein targets fatty acids to the nucleus. Real time confocal and multiphoton fluorescence imaging in living cells. Journal of Biological Chemistry 277: 29139-29151.

286. Tan, N. S., Shaw, N. S., Vinckenbosch, N., Liu, P., Yasmin, R., Desvergne, B., Wahli, W. & Noy, N. (2002) Selective cooperation between fatty acid binding proteins and peroxisome proliferator-activated receptors in regulating transcription.[erratum appears in Mol Cell Biol 2002 Sep;22(17):6318]. Molecular & Cellular Biology 22: 5114-5127.

287. Huang, H., Starodub, O., McIntosh, A., Atshaves, B. P., Woldegiorgis, G., Kier, A. B. & Schroeder, F. (2004) Liver fatty acid-binding protein colocalizes with

peroxisome proliferator activated receptor alpha and enhances ligand distribution to nuclei of living cells. Biochemistry 43: 2484-2500.

288. Erol, E., Kumar, L. S., Cline, G. W., Kelly, D. P. & Binas, B. (2004) Liver fatty acid binding protein is required for high rates of hepatic fatty acid oxidation but not for the action of PPARalpha in fasting mice. FASEB Journal 18:347-349.

289. Neschen, S., Moore, I., Regittnig, W., Yu, C. L., Wang, Y., Pypaert, M., Petersen, K. F. & Shulman, G. I. (2002) Contrasting effects of fish oil and safflower oil on hepatic peroxisomal and tissue lipid content. American Journal of Physiology Endocrinology & Metabolism 282.

290. Unger RH. (2002) Lipotoxic diseases. Annu Rev Med 53: 319-336.

291. Nehra V, Angulo P, Buchman A, Lindor KD. (2001) Nutritional and metabolic considerations in the etiology of nonalcoholic steatohepatitis. Dig Dis Sci 46: 2347-2352.

292. Guicciardi ME, Deussing J, Miyoshi H, Bronk SF, Svingen PA, Peters C, et al. (2000) Cathepsin B contributes to TNF-alpha-mediated hepatocyte apoptosis by promoting mitochondrial release of cytochrome c. J Clin Invest 106: 1127-1137.

293. Chiu, P. Y., Chaudhuri, S., Harding, P. A., Kopchick, J. J., Donkin, S. & Etherton, T. D. (1196) Cloning of a pig glucose transporter 4 cDNA fragment: use in developing a sensitive ribonuclease protection assay for quantifying low-abundance glucose transporter 4 mRNA in porcine adipose tissue. Journal of Animal Science 72: 1196-1203.

294. Waeber, G., Thompson, N., Haefliger, J.-A., and Nicod, P. (1994) Characterization of the murine high Km glucose transporter GLUT2 gene and its transcriptional regulation by glucose in a differentiated insulin-secreting cell line. J. Biol. Chem. 269, 26912-26916.

295. Gremlich S, Roduit R, Thorens B. (1997) Dexamethasone induces posttranslational degradation of GLUT2 and inhibition of insulin secretion in isolated pancreatic beta cells. J Biol Chem. 272(6):3216-22.

296. Vaulont, S., Vasseur-Cognet, M. & Kahn, A. (2000) Glucose regulation of gene transcription. Journal of Biological Chemistry 275: 31555-31558.

297. Abbot, E.L. et al. (2005). Diverging regulation of pyruvate dehydrogenase kinase isoform gene expression in cultured human muscle cells. *FEBS J.* 272:3004-3014

298. Clarke, S. D., Romsos, D. R. & Leveille, G. A. (1977) Influence of dietary fatty acids on liver and adipose tissue lipogenesis and on liver metabolites in meal-fed rats. Journal of Nutrition 107: 1277-1287.

299. Li, J., Yu, X., Pan, W. & Unger, R. H. (2002) Gene expression profile of rat adipose tissue at the onset of high-fat-diet obesity. Am J Physiol Endocrinol Metab. 282(6):E1334-41.

300. Al-Hasani, H. & Joost, H. G. (2005) Nutrition-/diet-induced changes in gene expression in white adipose tissue. Best Practice & Research Clinical Endocrinology & Metabolism 19: 589-603.

301. Dunshea, F. R., Suster, D., Kerton, D. J. & Leury, B. J. (2003) Exogenous porcine somatotropin administered to neonatal pigs at high doses can alter lifetime fat but not lean tissue deposition. British Journal of Nutrition 89: 795-801.

302. Ramsay, T. G., Yan, X. & Morrison, C. (1998) The obesity gene in swine: sequence and expression of porcine leptin. Journal of Animal Science 76: 484-490.

303. Hiltunen, J. K. & Qin, Y. (1484) beta-oxidation - strategies for the metabolism of a wide variety of acyl-CoA esters. Biochimica et Biophysica Acta: 12.

304. Latruffe, N., Cherkaoui Malki, M., Nicolas-Frances, V., Clemencet, M. C., Jannin, B. & Berlot, J. P. (1027) Regulation of the peroxisomal beta-oxidation-dependent pathway by peroxisome proliferator-activated receptor alpha and kinases. Biochemical Pharmacology 60: 1027-1032.

305. Margareto, J., Larrarte, E., Marti, A. & Martinez, J. A. (1471) Up-regulation of a thermogenesis-related gene (UCP1) and down-regulation of PPARgamma and aP2 genes in adipose tissue: possible features of the antiobesity effects of a beta3-adrenergic agonist. Biochemical Pharmacology 61: 1471-1478.

306. Houseknecht, K. L., Bidwell, C. A., Portocarrero, C. P. & Spurlock, M. E. (1998) Expression and cDNA cloning of porcine peroxisome proliferator-activated receptor gamma (PPARgamma). Gene 225: 89-96.

307. Klaus, S. (2005) Increasing the protein:carbohydrate ratio in a high-fat diet delays the development of adiposity and improves glucose homeostasis in mice. Journal of Nutrition 135: 1854-1858.

308. Vernon, R. G., Barber, M. C. & Travers, M. T. (1999) Present and future studies on lipogenesis in animals and human subjects. Proceedings of the Nutrition Society 58: 541-549.

309. Wang, M. Y., Lee, Y. & Unger, R. H. (1999) Novel form of lipolysis induced by leptin. Journal of Biological Chemistry 274: 17541-17544.

310. Zurlo, F., Larson, K., Bogardus, C. & Ravussin, E. (1423) Skeletal muscle metabolism is a major determinant of resting energy expenditure. Journal of Clinical Investigation 86: 1423-1427.

311. Dagenais, G. R., Tancredi, R. G. & Zierler, K. L. (1976) Free fatty acid oxidation by forearm muscle at rest, and evidence for an intramuscular lipid pool in the human forearm. Journal of Clinical Investigation 58: 421-431.

312. Kelley, D. E. (2004) Influence of weight loss and physical activity interventions upon muscle lipid content in relation to insulin resistance. Current Diabetes Reports 4: 165-168.

313. Corton, J. C., Anderson, S. P. & Stauber, A. (2000) Central role of peroxisome proliferator-activated receptors in the actions of peroxisome proliferators. Annual Review of Pharmacology & Toxicology 40: 491-518.

314. Ellis, B. A., Poynten, A., Lowy, A. J., Furler, S. M., Chisholm, D. J., Kraegen, E. W. & Cooney, G. J. (2000) Long-chain acyl-CoA esters as indicators of lipid metabolism and insulin sensitivity in rat and human muscle. American Journal of Physiology Endocrinology & Metabolism 279.

315. Kelley, D. E. (2002) Skeletal muscle triglycerides: an aspect of regional adiposity and insulin resistance. Annals of the New York Academy of Sciences 967: 135-145.

316. Randle, P. J. (1964) Fuel and power in the control of carbohydrate metabolism in mammalian muscle. Symposia of the Society for Experimental Biology 18: 129-155.

317. Romijn, J. A., Coyle, E. F., Sidossis, L. S., Gastaldelli, A., Horowitz, J. F., Endert, E. & Wolfe, R. R. (1993) Regulation of endogenous fat and carbohydrate

metabolism in relation to exercise intensity and duration. American Journal of Physiology 265.

318. Lowell, B. B., Ruderman, N. B. & Goodman, M. N. (1121) Regulation of myofibrillar protein degradation in rat skeletal muscle during brief and prolonged starvation. Metabolism: Clinical & Experimental 35: 1121-1127.

319. Saha, A. K., Vavvas, D., Kurowski, T. G., Apazidis, A., Witters, L. A., Shafrir, E. & Ruderman, N. B. (1997) Malonyl-CoA regulation in skeletal muscle: its link to cell citrate and the glucose-fatty acid cycle. American Journal of Physiology 272.

320. Berthon, P. M., Howlett, R. A., Heigenhauser, G. J. & Spriet, L. L. (1998) Human skeletal muscle carnitine palmitoyltransferase I activity determined in isolated intact mitochondria. Journal of Applied Physiology 85: 148-153.

321. Boden, G., Chen, X., Ruiz, J., White, J. V. & Rossetti, L. (1994) Mechanisms of fatty acid-induced inhibition of glucose uptake. Journal of Clinical Investigation 93: 2438-2446.

322. Hargreaves, M., Kiens, B. & Richter, E. A. (1991) Effect of increased plasma free fatty acid concentrations on muscle metabolism in exercising men. Journal of Applied Physiology 70: 194-201.

323. Wolfe, R. R. (1998) Metabolic interactions between glucose and fatty acids in humans. American Journal of Clinical Nutrition 67.

324. Wolfe, B. M., Klein, S., Peters, E. J., Schmidt, B. F. & Wolfe, R. R. (1988) Effect of elevated free fatty acids on glucose oxidation in normal humans. Metabolism: Clinical & Experimental 37: 323-329.

325. Sidossis, L. S. & Wolfe, R. R. (1996) Glucose and insulin-induced inhibition of fatty acid oxidation: the glucose-fatty acid cycle reversed. American Journal of Physiology 270.

326. Sidossis, L. S., Stuart, C. A., Shulman, G. I., Lopaschuk, G. D. & Wolfe, R. R. (1996) Glucose plus insulin regulate fat oxidation by controlling the rate of fatty acid entry into the mitochondria. Journal of Clinical Investigation 98: 2244-2250.

327. Cameron-smith, D., Burke, L. M., Angus, D. J., Tunstall, R. J., Cox, G. R., Bonen, A., Hawley, J. A. & Hargreaves, M. A. (2003) short-term, high fat diet up-regulates lipid metabolism and gene expression in human skeletal muscle. Am J Clin Nutr 77: 313-318.

328. Sparks, L. M., Xie, H., Koza, R. A., Mynatt, R., Hulver, M. W., Bray, G. A. & Smith, S. R. (1926) A high-fat diet coordinately downregulates genes required for mitochondrial oxidative phosphorylation in skeletal muscle. Diabetes 54: 1926-1933.

329. Ter Kuile, B. H. & Westerhoff, H. V. (2001) Transcriptome meets metabolome: hierarchical and metabolic regulation of the glycolytic pathway. FEBS Lett. 500(3):169-71.

330. Patsouris, D., Muller, M. & Kersten, S. (2005) Peroxisome proliferator activated receptor ligands for the treatment of insulin resistance. Current Opinion in Investigational Drugs 5: 1045-1050.

331. Hammond, J. (1932) Growth and Development of Mutton Qualities in the Sheep. Oliver and Boyd, Edinburgh, Scotland.

332. Mersmann, H. J. (1992) Regulation of porcine adipose tissue lipolytic activity by adrenergic agonists and antagonists. Comparative Biochemistry & Physiology. C, Comparative Pharmacology & Toxicology 102: 407-411.

333. Seerley, R. W., Foley, C. W., Williams, D. J., 3rd & Curtis, S. E. (1972) Hemoglobin concentration and thermostability in neonatal piglets. Journal of Animal Science 34: 82-84.

334. Sanger, F., Nicklen, S. & Coulson, A. R. (1977) DNA sequencing with chain-terminating inhibitors. Proceedings of the National Academy of Sciences of the United States of America 74: 5463-5467.

335. Information, N. C. f. B. (1997) BLASTn. In, National Center for Biotechnology Information, Bethesda, MD

336. Information, N. C. f. B. (1997) BLASTp. In, National Center for Biotechnology Information, Bethesda, MD

337. Meadus, W. J., MacInnis, R. & Dugan, M. E. (2002) Prolonged dietary treatment with conjugated linoleic acid stimulates porcine muscle peroxisome proliferator activated receptor gamma and glutamine-fructose aminotransferase gene expression in vivo. Journal of Molecular Endocrinology 28: 79-86.

338. Pape, M. E., Castle, C. K., Murray, R. W., Funk, G. M., Hunt, C. E., Marotti, K. R. & Melchior, G. W. (1997) Apo B metabolism in the cynomolgus monkey: evidence for post-transcriptional regulation. Biochimica et Biophysica Acta 3: 326-334.

339. Wang, A. B., Liu, D. P. & Liang, C. C. (2003) Regulation of human apolipoprotein B gene expression at multiple levels. Exp Cell Res. 290(1):1-12.

340. Dixon, J. L. & Ginsberg, H. N. (1992) Hepatic synthesis of lipoproteins and apolipoproteins. Seminars in Liver Disease 12: 364-372.

341. Cases, S., Smith, S. J., Zheng, Y. W., Myers, H. M., Lear, S. R., Sande, E., Novak, S., Collins, C., Welch, C. B., Lusis, A. J., Erickson, S. K. & Farese, R. V., Jr. (1998) Identification of a gene encoding an acyl CoA:diacylglycerol acyltransferase, a key enzyme in triacylglycerol synthesis. Proceedings of the National Academy of Sciences of the United States of America 95: 13018-13023.

342. Volpe, J. J. & Vagelos P. R. (1973) Saturated Fatty Acid Biosynthesis and its Regulation. Annual Review of Biochemistry 42:21-60.

343. Anderson, D. B., Kauffman, R. G. & Kastenschmidt, L. L. (1972) Lipogenic enzyme activities and cellularity of porcine adipose tissue from various anatomical locations. J Lipid Res 13: 593-599.

344. Mersmann, H. J. (1998) Lipoprotein and Hormone-sensitive Lipases in Porcine Adipose Tissue. J Anim Sci 76: 1396-1404

345. Deng, X., Elam, M. B., Wilcox, H. G., Cagen, L. M., Park, E. A., Raghow, R., Patel, D., Kumar, P., Sheybani, A. & Russell, J. C. (2004) Dietary olive oil and menhaden oil mitigate induction of lipogenesis in hyperinsulinemic corpulent JCR:LA-cp rats: microarray analysis of lipid-related gene expression. Endocrinology 145: 5847-5861.

346. Seo, T., Oelkers, P. M., Giattina, M. R., Worgall, T. S., Sturley, S. L. & Deckelbaum, R. J. (2001) Differential modulation of ACAT1 and ACAT2 transcription and activity by long chain free fatty acids in cultured cells. Biochemistry 40: 4756-4762.

347. Chang, T. Y., Chang, C. C. & Cheng, D. (1997) Acyl-coenzyme A:cholesterol acyltransferase. Annual Review of Biochemistry 66: 613-638.

348. Uelmen, P. J., Oka, K., Sullivan, M., Chang, C. C., Chang, T. Y. & Chan, L. (1995) Tissue-specific expression and cholesterol regulation of acylcoenzyme

A:cholesterol acyltransferase (ACAT) in mice. Journal of Biological Chemistry 270: 26192-26201.

349. Schaffer, J. E. (2003) Lipotoxicity: when tissues overeat. Current Opinion in Lipidology 14: 281-287.

350. Ottnad, E., Parthasarathy, S., Sambrano, G. R., Ramprasad, M. P., Quehenberger, O., Kondratenko, N., Green, S. & Steinberg, D. (1391) A macrophage receptor for oxidized low density lipoprotein distinct from the receptor for acetyl low density lipoprotein: partial purification and role in recognition of oxidatively damaged cells. Proceedings of the National Academy of Sciences of the United States of America 92: 1391-1395.

351. Kinnunen, P. K., Jackson, R. L., Smith, L. C., Gotto, A. M., Jr. & Sparrow, J. T. (1977) Activation of lipoprotein lipase by native and synthetic fragments of human plasma apolipoprotein C-II. Proceedings of the National Academy of Sciences of the United States of America 74: 4848-4851.

352. Maeda, N., Ebert, D. L., Doers, T. M., Newman, M., Hasler-Rapacz, J., Attie, A. D., Rapacz, J. & Smithies, O. (1988) Molecular genetics of the apolipoprotein B gene in pigs in relation to atherosclerosis. Gene 70: 213-229.

353. Richardson, P. E., Manchekar, M., Dashti, N., Jones, M. K., Beigneux, A., Young, S. G., Harvey, S. C. & Segrest, J. P. (2005) Assembly of lipoprotein particles containing apolipoprotein-B: structural model for the nascent lipoprotein particle. Biophysical Journal 88: 2789-2800.

354. Kane, J. P. (1983) Apolipoprotein B: structural and metabolic heterogeneity. Annual Review of Physiology 45: 637-650.

355. Dixon, J. L. & Ginsberg, H. N. (1993) Regulation of hepatic secretion of apolipoprotein B-containing lipoproteins: information obtained from cultured liver cells. Journal of Lipid Research 34: 167-179.

356. Fisher, E. A. & Ginsberg, H. N. (2002) Complexity in the secretory pathway: the assembly and secretion of apolipoprotein B-containing lipoproteins. Journal of Biological Chemistry 277: 17377-17380.

357. Semenkovich, C. F. (2004) Fatty acid metabolism and vascular disease. Trends in Cardiovascular Medicine 14: 72-76.

358. Hammond, J. (1947) Animal breeding in relation to nutrition and environmental conditions. Biological Reviews 22:195-213.

359. Steele, N. C. & Pursel, V. G. (1990) Nutrient Partitioning by Transgenic Animals. Annual Review of Nutrition, Vol. 10: 213-232.

360. Elliott, R. & Ong,TJ (2002). Nutritional genomics. BMJ 324, 1438-1442.

361. Roberts, M. A., Mutch, D. M. & German, J. B. (2001) Genomics: food and nutrition. Curr Opin Biotechnol. 12:516-522.

362. Ideker, T., Galitski, T. & Hood. L. (2001) A new approach to decoding life: systems biology. Annu Rev Genomics Hum Genet. 2:343-372.

363. Peregrin, T. (2001)The new frontier of nutrition science:. nutrigenomics. J. Am. Diet Assoc. 101, 1306.

Appendix A. Images of total RNA resolved on agarose gel (including RNA samples used in microarray analysis)

Fig 1-13. Integrity of the total RNA was evaluated by gel electrophoresis of ~1 μg RNA on an 1% agarose 0.5× tris(hydroxymethyl)aminomethane (Tris)-borate-EDTA buffer (TBE) gel containing ethidium bromide, at 120V for 30 minutes using 1× TBE as the running buffer. Images of the gels were taken under ultraviolet (UV) light using Polaroid instant film number 55 to generate printed image of the gel.

All RNAs were resoled and imaged using same electrophoresis and imaging methods. Fig 1-10 were images of RNA captured during the period of microarray analysis, and Fig 11-13 were images of RNA captures on April of 2006 after receiving comments and suggestion from the committees.

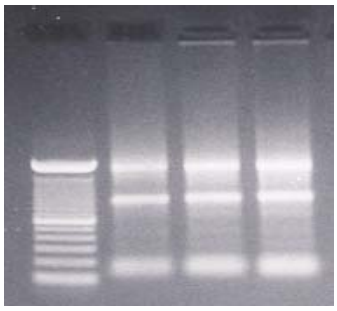

Fig 1. Images of RNAs developed on April 4, 2005. RNAs were isolated from liver tissue in sudden dietary shift study (Chapter 3). The lanes from left to right are: DNA marker, #5207, #5502, #6001.

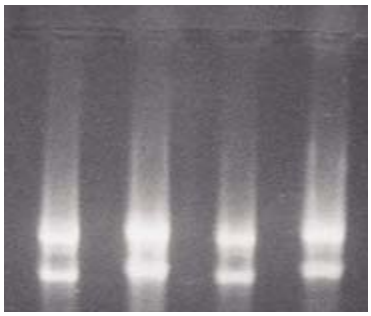

Fig 2. Images of RNAs developed on May 23, 2005. RNAs were isolated from liver tissue in sudden dietary shift study (Chapter 3). The lanes from left to right are: #4901, #6002, #5504, #4905.

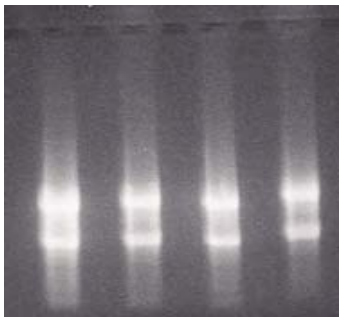

Fig 3. Images of DNase-treated RNAs developed on May 24, 2005. RNAs were isolated from liver tissue in sudden dietary shift study (Chapter 3). The lanes from left to right are: #6002, #5504, #4905, control pool RNA.

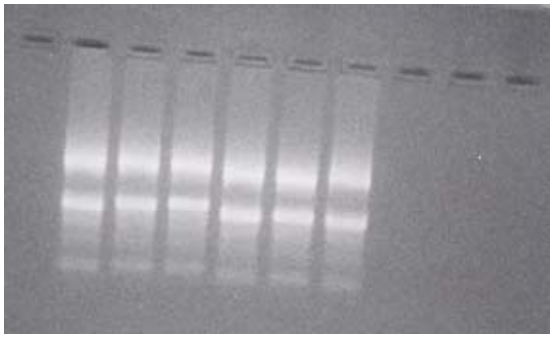

Fig 4. Images of RNAs developed on June 18, 2005. RNAs were isolated from liver tissue in sudden dietary shift study (Chapter 3). The lanes from left to right are: #4901, #6002, #5504, #5205, #4905.

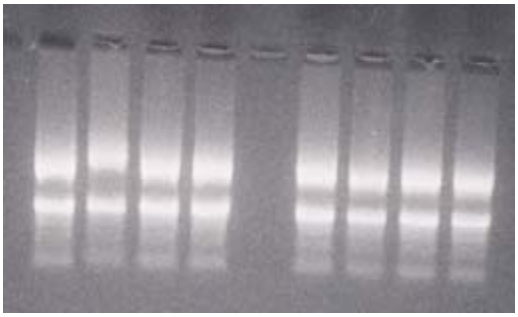

Fig 5. Images of RNAs developed on July 13, 2005. RNAs were isolated from liver tissue in sudden dietary shift study (Chapter 3). The lanes from left to right are: #4901, #6002, #5504, #5205, #5207, #4905, #5502, #6001.

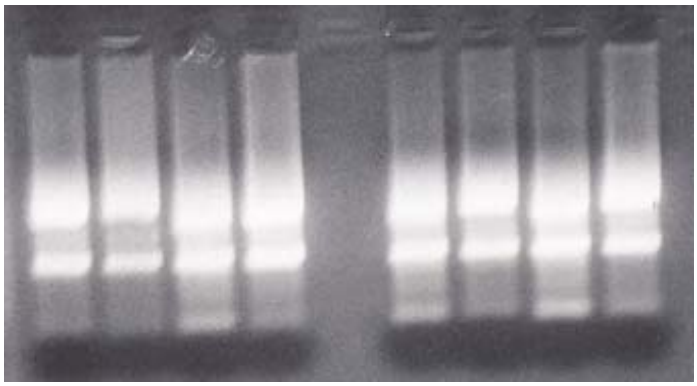

Fig 6. Images of RNAs developed on July 21, 2005. RNAs were isolated from adipose tissue in sudden dietary shift study (Chapter 3). The lanes from left to right are: #4901, #6002, #5504, #5205, #5207, #6001, #5502, #4905.

Fig 7. Images of RNAs developed on July 26, 2005. RNAs were isolated from adipose tissue in sudden dietary shift study (Chapter 3). The lanes from left to right are: #4901, #5205, #5504, #6002.

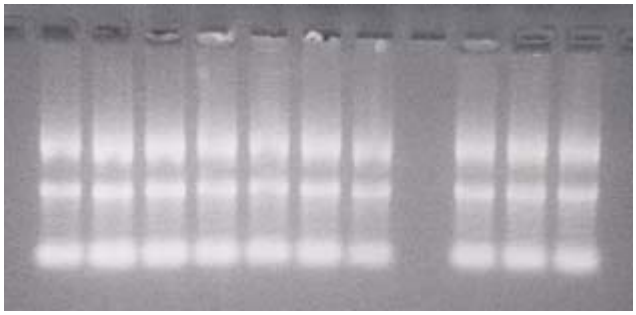

Fig 8. Images of RNAs developed on August 2, 2005. RNAs were isolated from adipose tissue in sudden dietary shift study (Chapter 3). The lanes from left to right are: #5502, #5207, #4905, #6001, #6002, #5205, #5504, #4901.

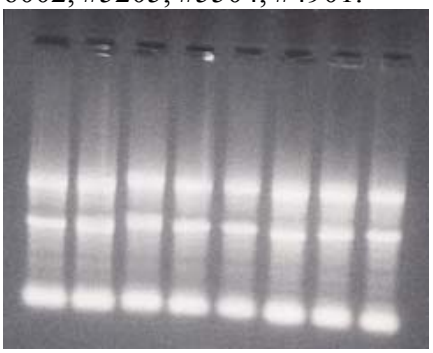

Fig 9. Images of RNAs developed on Sempter 13, 2005. RNAs were isolated from muscle tissue in sudden dietary shift study (Chapter 3). The lanes from left to right are: #4901, #5205, #5504, #6002, #4905, #5207, #5502, #6001.

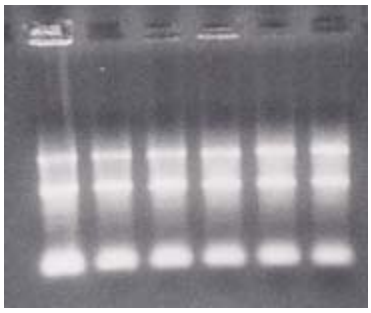

Fig 10. Images of RNAs developed on Sempter 13, 2005. RNAs were isolated from adipose tissue in Paylean study (Chapter 2). The lanes from left to right are: #787, #784, #779, #796, #807, #826.

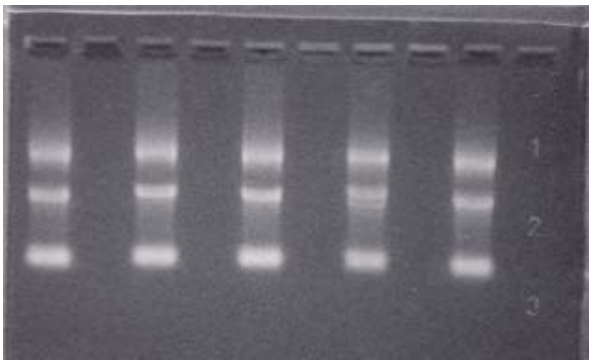

Fig 11. Images of RNAs developed on April 13, 2006. RNAs were isolated from adipose tissue in Paylean study (Chapter 2). The lanes from left to right are: #784, #796, #779, #826, #807.

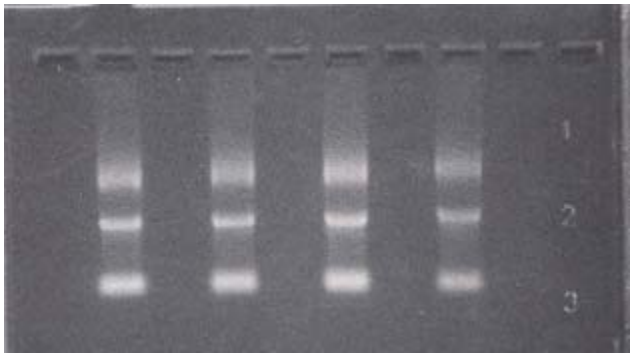

Fig 12. Images of RNAs developed on April 14, 2006. RNAs were isolated from liver tissue in sudden diet shift study (Chapter 3). The lanes from left to right are: #4901, #5207, #4905, #6002.

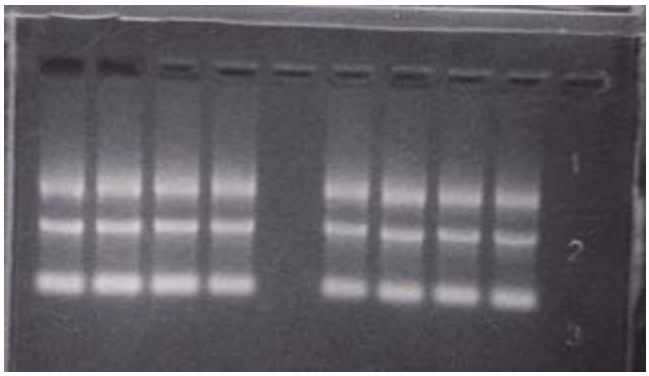

Fig 13. Images of RNAs developed on April 14, 2006. RNAs were isolated from muscle tissue in sudden diet shift study (Chapter 3). The lanes from left to right are: #5502, #5207, #4905, #6001, #4901, #5205,#6002,#5504.

Appendix B. Microarray Analysis Protocol

References: Amino Allyl Labeling of RNA for microarrays protocol. Functional Genomics Lab, W. M. Keck Center for Functional and Comparative Genomics, University of Illinois at Urbana-Champaign.

AMINOALLYL LABELING OF RNA FOR MICROARRAYS

1. PURPOSE

This protocol describes the labeling of eukaryotic RNA with aminoallyl labeled nucleotides via first strand cDNA synthesis followed by a coupling of the aminoallyl groups to either Cyanine 3 or 5 (Cy 3/Cy5) fluorescent molecules.

2. SCOPE

This procedural format is utilized by Human Colon Cancer and Mouse microarray projects under the supervision of within the Eukaryotic Genomics Dept. TIGR

3. MATERIALS

3.1 5-(3-aminoallyl)-2'deoxyuridine-5'-triphosphate (AA-dUTP) (Sigma; Cat # A0410)
3.2 100 mM dNTP Set PCR grade
3.3 Random Hexamer primers (3mg/mL) or polydT $_{18\text{-}22}$ oligo
3.4 SuperScript III RT (200U/uL) (Invitrogen Cat # 18080-044)
3.5 Cy Dye Post Labelling reactive dye pack (Amersham-GE RPN5661) or Invitrogen-Molecular Probes Alexa Fluor Dye Decapack A32755
3.7 QIAquick PCR Purification Kit (Qiagen; Cat # 28106)
3.8 RNeasy® Mini Kit (Qiagen; Cat # 74106)

4. REAGENT PREPARATION

4.1 Phosphate Buffers

4.1.1 Prepare 2 solutions: 1M K2HPO4 and 1M KH2PO4
4.1.2 To make a 1M Phosphate buffer (KPO4, pH 8.5-8.7) combine:
1M K2HPO4……..9.5 mL
1M KH2PO4……..0.5 mL
4.1.3 For 100 mL Phosphate wash buffer (5 mM KPO4, pH 8.0, 80% EtOH) mix:
1 M KPO4 pH 8.5…. 0.5 mL
MilliQ water……... 15.25 mL
95% ethanol……... 84.25 mL
Note: Wash buffer will be slightly cloudy.
4.1.4 Phosphate elution buffer is made by diluting 1 M KPO4, pH 8.5 to 4 mM with MilliQ water.

4.2 Aminoallyl dUTP

4.2.1 For a final concentration of 100mM add 19.1 µL of 0.1 M KPO4 buffer (pH 7.5) to a stock vial containing 1 mg of aa-dUTP. Gently vortex to mix and transfer the aa-dUTP solution into a new microfuge tube. Store at –20^{o}C.

4.2.2 Measure the concentration of the aa-dUTP solution by diluting an aliquot 1:5000 in 0.1 M KPO4 (pH 7.5) and measuring the OD289. (Stock concentration in mM = OD289 x 704)

4.3 Labeling Mix (50X) with 2:3 aa-dUTP: dTTP ratio

4.3.1 Mix the following reagents:

Final concentration

dATP (100 mM)……5µL….. (25 mM)
dCTP (100 mM)……5µL….. (25 mM)
dGTP (100 mM)……5µL….. (25 mM)
dTTP (100 mM)……3µL……(15 mM)
aa-dUTP (100 mM)…...2µL……(10 mM)
Total: 20µL

4.3.1 Store unused solution at –20°C.

4.4 Sodium Carbonate Buffer (Na2CO3): 1M, pH 9.0

4.4.1 Dissolve 2.7 gram sodium carbonate in 20 ml and adjust pH to 9.0 with 12N HCl. Fill to 25 ml.

4.4.2 To make a 0.1 M solution for the dye coupling reaction dilute 1:10 with water.

Note: Carbonate buffer changes composition over time; make it fresh each day when use.

4.5 Cy-dye esters

4.5.1 Cy3-ester and Cy5-ester are provided as a dried product in 5 tubes. Resuspend a tube of dye ester in 45 uL of DMSO before use.

4.5.2 Wrap all reaction tubes with foil and keep covered as much as possible in order to prevent photobleaching of the dyes.

Note: Dye esters must either be used immediately or aliquoted and stored at –80°C. Any introduced water to the dye esters will result in a lower coupling efficiency due to the hydrolysis of the dye esters. Since DMSO is hygroscopic (absorbs water from the atmosphere) store it well sealed in desiccant.

5. PROCEDURE

5.1 Aminoallyl Labeling

5.1.1 To 10 ug (10-20 ug) of total RNA (or 2 ug poly(A+) RNA) which has been DNase I-treated and Qiagen RNeasy purified, add 2 uL Random Hexamer primers (3mg/mL) (We use 3 ug of dT_{18} primer for total RNA), spiking controls (if desired), and bring the final volume up to 18.5 □L with RNase-free or DEPC treated water.

5.1.2 Mix well and incubate at 70°C for 10 minutes.

5.1.3 Place on ice for 30 seconds, centrifuge.

5.1.4 Add:

5X First Strand buffer…….. 6 uL
0.1 M DTT…….. 3 uL
50X aminoallyl-dNTP mix…….. 0.6 uL
SuperScript III RT (200U/uL)….. 2 uL

(We also add 0.5 ul or 20U RNAse inhibitor)

5.1.5 Mix and incubate at 46°C for 3 hours to overnight.

5.1.6 To hydrolyze RNA, add:

1 M NaOH 10 uL

0.5 M EDTA 10 uL

mix and incubate at 65°C for 15 minutes.

5.1.7 Add 10 uL of 1 M HCl to neutralize pH. Add 10 ul sodium acetate 3M.

5.2 Reaction Purification I: Removal of unincorporated aa-dUTP and free amines (Qiagen PCR Purification Kit)

Note: This purification protocol is modified from the Qiagen QIAquick PCR purification kit protocol. The phosphate wash and elution buffers (prepared in 4.1.3 & 4.1.4) are substituted for the Qiagen supplied buffers because the Qiagen buffers contain free amines which compete with the Cy dye coupling reaction.

5.2.1 Mix cDNA reaction with 300 uL (5X reaction volume) buffer PB (Qiagen supplied) and transfer to QIAquick column.

5.2.2 Place the column in a 2 ml collection tube (Qiagen supplied) and centrifuge at ~13,000 rpm (10,000g) for 1 minute. Empty collection tube.

5.2.3 To wash, add 750 uL phosphate wash buffer to the column and centrifuge at ~13,000 rpm (10,000g) for 1 minute.

5.2.4 Empty the collection tube and repeat the wash and centrifugation step (5.2.3).

5.2.5 Empty the collection tube and centrifuge column an additional 1 minute at maximum speed.

5.2.6 Transfer column to a new 1.5 mL microfuge tube and carefully add 30 uL phosphate elution buffer (*see 4.1.4*) to the center of the column membrane.

5.2.7 Incubate for 1 minute at room temperature.

5.2.8 Elute by centrifugation at ~13,000 rpm(10,000g) for 1 minute.

5.2.9 Elute a second time into the same tube by repeating steps 5.2.6-5.2.8. The final elution volume should be ~60 uL.

5.2.10 Dry sample in a speed vac. (about 1 hr.)

5.3 Coupling aa-cDNA to Cy Dye Ester.

5.3.1 Resuspend single pack of dye in 9.0 ul 0.1M sodium carbonate. Transfer dye to sample and mix.

Note: To prevent photobleaching of the Cy dyes wrap all reaction tubes in foil and keep them sequestered from light as much as possible.

5.3.3 Incubate the reaction for 1 hour in the dark at room temperature.

5.4 Reaction Purification II: Removal of uncoupled dye (Qiagen PCR Purification Kit)

5.4.1 To the reaction add 35 uL 3M NaOAc pH 5.2.

5.4.2 Add 250 uL (5X reaction volume) Buffer PB (Qiagen supplied).

5.4.3 Place a QIAquick spin column in a 2 mL collection tube (Qiagen supplied), apply the sample to the column, and centrifuge at 10,000 g for 1 minute. Empty collection tube.

5.4.4 To wash, add 0.75 mL Buffer PE (Qiagen supplied) to the column and centrifuge at ~13,000 rpm (10,000g) for 1 minute.
Note: Make sure Buffer PE has added ethanol before using (see label for correct volume).
5.4.5 Empty collection tube and centrifuge column for an additional 1 minute at maximum speed.
5.4.6 Place column in a clean 1.5 mL microfuge tube and carefully add 40 uL Buffer EB (Qiagen supplied) to the center of the column membrane.
5.4.7 Incubate for 1 minute at room temperature.
5.4.8 Elute by centrifugation at ~13,000 rpm (10,000g) for 1 minute.
5.4.9 Elute a second time into the same tube by repeating steps 5.4.6-5.4.8. The final elution volume should be ~80 uL.
Note: This protocol is modified from the Qiagen QIAquick Spin

5.5 Analysis of Labeling Reaction
5.5.1 Use an 80 uL Beckman quartz MicroCuvette to analyze the entire undiluted sample in a spectrophotometer.
5.5.2 Wash the cuvette with water and blow dry with compressed air duster.
5.5.3 Pipette sample into cuvette and place cuvette in spectrophotometer.
5.5.4 For each sample measure absorbance at 260 nm and either 550 nm for Cy3 or 650 nm for Cy5, as appropriate.
5.5.5 Pipette sample from cuvette back into the original sample tube.
5.5.6 For each sample calculate the total picomoles of cDNA synthesized using:

$$\text{pmol nucleotides} = \frac{[\text{OD260} * \text{volume (uL)} * 37\ \text{ng/uL} * 1000\ \text{pg/ng}]}{324.5\ \text{pg/pmol}}$$

Note: 1 OD260 = 37 ng/uL for cDNA; 324.5 pg/pmol average molecular weight of a dNTP)
5.5.7 For each sample calculate the total picomoles of dye incorporation (Cy3 or Cy5 accordingly) using:

pmol Cy3 = OD550 * volume (uL) /0.15
pmol Cy5 = OD650 * volume (uL) /0.25
nucleotides/dye ratio = pmol cDNA/pmol Cy dye

Note: >30 pmol of dye incorporation per sample and a ratio of less than 50 nucleotides/dye molecules is optimal for hybridizations.
5.5.9 Dry the Cy3/Cy5 probes to completion in a speed vac.

Hybridization (Corning GAPS II Aminosilane coated slides)

Prehybridization

1. Preheat prehybridization solution in 42C water bath. Place slides in Coplin jar with the array towards the bottom of the jar. Fill with prehyb solution until array is covered. Allow to incubate in 42C water bath for 45 min. shaking occasionally.
2. Wash in millipore water 5 times and then isopropanol. Spin dry. (Spin in 50 ml tube with kimwipe stuffed in the bottom in a swing bucket rotor. Place array side up)

3. Hybridize immediately (or as soon as possible).

TIGR Prehyb buffer

5 X SSC	25 ml 20 X SSC
0.1% SDS	1 ml 10% SDS
1% BSA	1 g BSA (Sigma A-9647)
fill to 100 ml.	

Alternative Prehyb Buffer: 250 ml. (This is a hybridization buffer that we traditionally used on membranes but works well on **Aminosilane coated slides** as well)

20% Formamide	50 ml Formamide
5X Denhardts	25 ml 50X Denhards
6X SSC	83 ml 20X SSC
0.1% SDS	2.5 ml 10% SDS
25 ug/ml tRNA	0.625 ml 10 mg/ml tRNA
H_2O	88.5 ml
	250 ml

Hybridization

1. For a 48 pin slide (22 x 60mm Lifterslip coverslip) add 20 ug COT-1, 20 ug PolyA to one probe and fill to 40ul with sterile water. Transfer solution to second probe and mix well with pipettor.
2. Probe is heated at 95^{o}C for 2-3 min.
3. Position slide in corning hyb chamber with Lifterslip covering array area.
4. Add 40 ul of 2X hybridization buffer preheated to 42 C and apply to slide.

2X Hybridization buffer:

50% Formamide	5 ml
10X SSC	5 ml 20X SSC
0.2% SDS	200 ul 10% SDS

5. Slide is placed in Corning Hybridization Chamber with 2 small pieces of tissue paper saturated with water on either end of the slide, and hybridized 16-20 hours (overnight) or longer at 42C. (It has been shown that 2 or 3 days gives even better results.)

Wash

1. First wash- 1X SSC, 0.2% SDS at 42C, coverslip is removed by agitation 5 min.
2. Second wash- 0.1%X SSC, 0.2% SDS at room temperature, agitation 5 min.
3. Third wash- 0.1X SSC, agitation 5 min. Repeat step 3 in wash 3 again.
4. An extra wash may be needed if high background is visible after scanning.
5. Spin dry immediately. Any droplet that dries on the surface of the slide will leave background haze.

Wash 1: 50 ml 20XSSC, 20 ml 10% SDS, fill to 1 liter
Wash 2: 5 ml 20XSSC, 20 ml 10% SDS, fill to 1 liter
Wash 3: 5 ml 20XSSC, fill to 1 liter

Appendix C. Images of fluorescent dye Cy-5 labeled cDNA probe for slides hybridization in microarray analysis

Fig 1-15. Cy5-labeled cDNA probe was resolved on a 2% agarose gel at 130V for 45 minutes, the gel was imaged on Typhoon 9410 (Amersham Pharmacia Biotech) at PMT 600 using emission filter for Cy5 (laser 633nm). All the probes were resoled and imaged using same electrophoresis and imaging condition. Fig 1-3 were images of probes used in Paylean study (Chapter 2) and Fig 4-15 were images of probes used in sudden dietary shift study (Chapter 3).

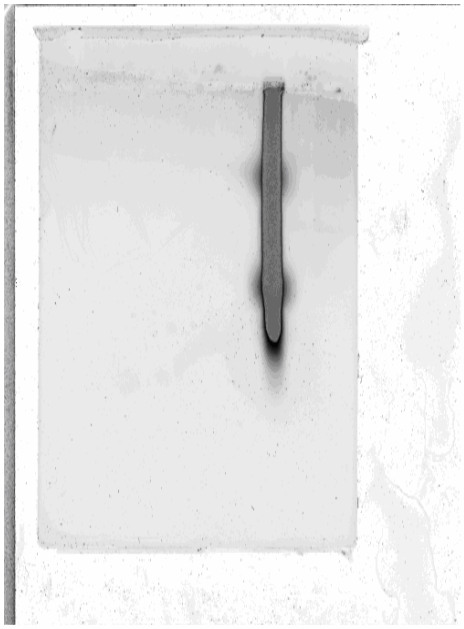

Fig 1. Image of Cy5 labeled cDNA probe developed from RNA preparation of adipose tissue (pig number: #784) in Paylean study (Chapter 2). The probe was prepared on November 3, 2005.

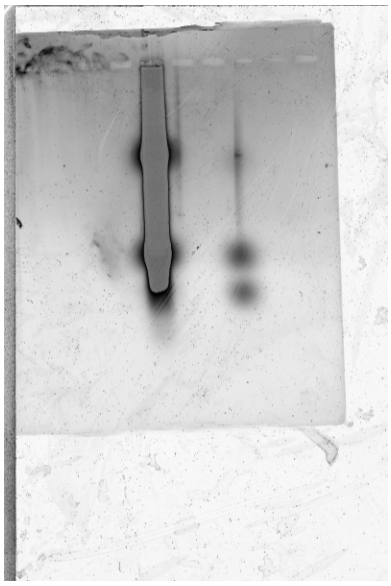

Fig 2. Image of Cy5 labeled cDNA probe developed from RNA preparation of adipose tissue (pig number: #796) in Paylean study (Chapter 2). The probe was prepared on November 8, 2005.

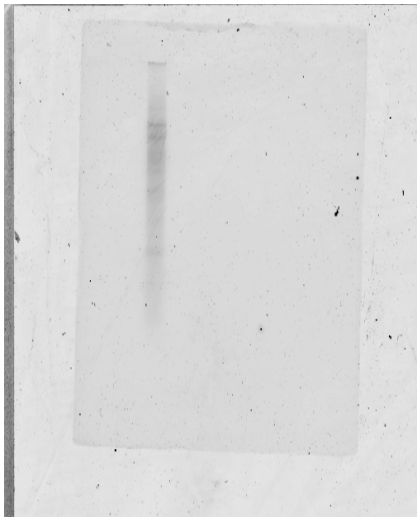

Fig 3. Image of Cy5 labeled cDNA probe developed from control pool RNA preparation of adipose tissue in Paylean study (Chapter 2). The probe was prepared on November 17, 2005.

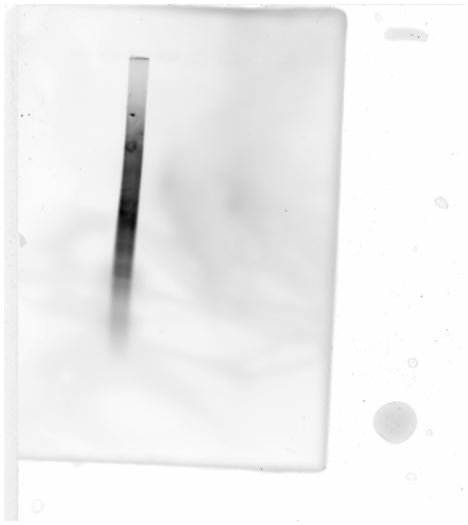

Fig 4. Image of Cy5 labeled cDNA probe developed from RNA preparation of liver tissue (pig number: #6001) in sudden dietary shift study (Chapter 3). The probe was prepared on July 11, 2005.

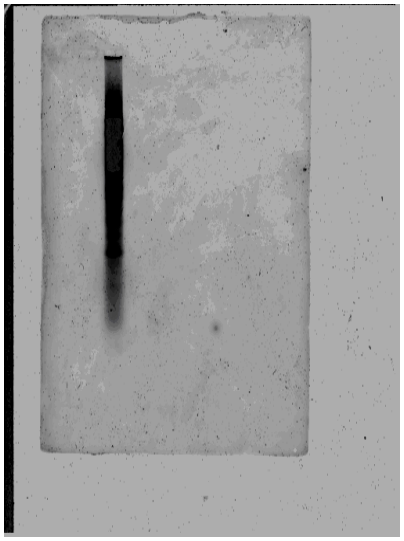

Fig 5. Image of Cy5 labeled cDNA probe developed from control pool RNA preparation of liver tissue in sudden dietary shift study (Chapter 3). The probe was prepared on July 18, 2005.

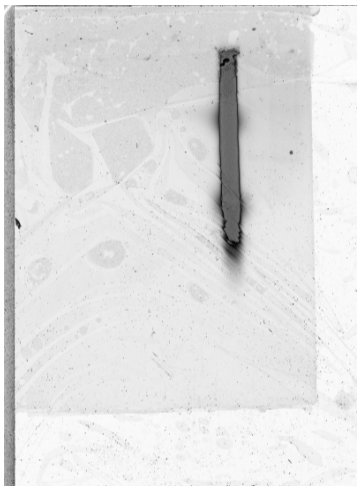

Fig 6. Image of Cy5 labeled cDNA probe developed from control pool RNA preparation of liver tissue in sudden dietary shift study (Chapter 3). The probe was prepared on July 24, 2005.

Fig 7. Image of Cy5 labeled cDNA probe developed from RNA preparation of liver tissue (pig number: #5207) in sudden dietary shift study (Chapter 3). The probe was prepared on July 27, 2005.

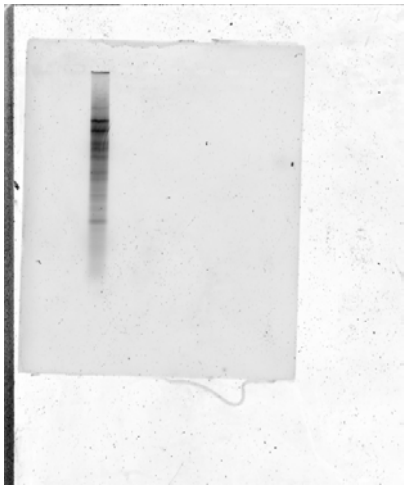

Fig 8. Image of Cy5 labeled cDNA probe developed from control pool RNA preparation of adipose tissue in sudden dietary shift study (Chapter 3).The probe was prepared on August 1, 2005.

Fig 9. Image of Cy5 labeled cDNA probe developed from RNA preparation of adipose tissue (pig number: #6001) in sudden dietary shift study (Chapter 3). The probe was prepared on August 5, 2005.

Fig 10. Image of Cy5 labeled cDNA probe developed from control pool RNA preparation of adipose tissue in sudden dietary shift study (Chapter 3). The probe was prepared on September 9, 2005.

Fig 11. Image of Cy5 labeled cDNA probe developed from RNA preparation of adipose tissue (pig number: #5502) in sudden dietary shift study (Chapter 3). The probe was prepared on Octorber10, 2005.

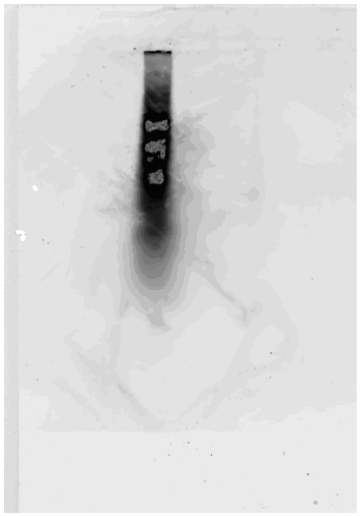

Fig 12. Image of Cy5 labeled cDNA probe developed from RNA preparation of muscle tissue (pig number: #4905) in sudden dietary shift study (Chapter 3). The probe was prepared on September 19, 2005.

Fig 13. Image of Cy5 labeled cDNA probe developed from control pool RNA preparation of muscle tissue in sudden dietary shift study (Chapter 3). The probe was prepared on September 26, 2005.

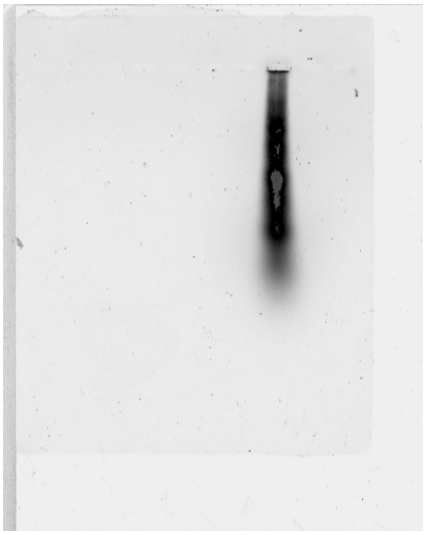

Fig 14. Image of Cy5 labeled cDNA probe developed from control pool RNA preparation of muscle tissue in sudden dietary shift study (Chapter 3). The probe was prepared on September 30, 2005.

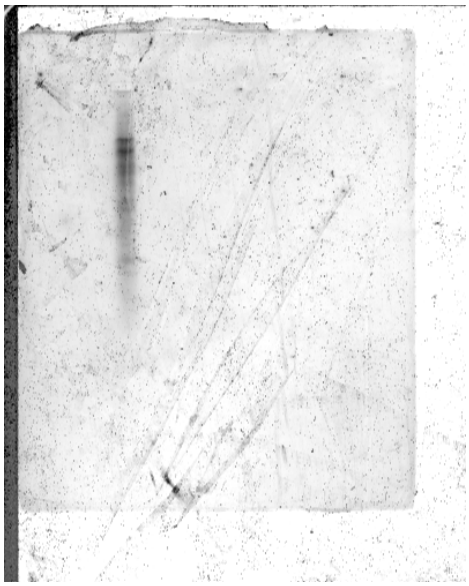

Fig 15. Image of Cy5 labeled cDNA probe developed from RNA preparation of muscle tissue (pig number: #5207) in sudden dietary shift study (Chapter 3). The probe was prepared on October 3, 2005.

Appendix D. Pig Genome Oligo Set and Pig Genome Oligo Extension Set 1.0

Reference: QIAGEN Array-Ready Oligo Sets™ for the Pig Genome and the Pig Genome Oligo Extension Set, Version 1.0.

Gene sequence source and selection

All probes are designed from The Institute of Genome Research (TIGR) Gene Index Database SsGI Release5.0, released on Octable 1, 2002. (http://www.tigr.org/tdb/tgi/ssgi/). SsGI Release 5.0 contains a total of 49,201 unique sequences including 17,354 tentative consensus sequences (TCs), singleton 494 expressed transcripts (ETs), and 31.353 singleton ESTs. ETs represent mature transcripts.

Table1. Gene sequence source of Pig Genome Oligo Set and Extension Set Version 1.0

TIGR Pig SsGI Release 5.0 Database	Number of sequences in SsGI Release 5.0	Pig Genome Oligo Set Version 1.0	Pig Genome Oligo Extension Set Version 1.0
TCs	17,354	10,313	2632
Singleton ETs	494	352	0
Singleton ESTS	31,353	0	0
Total	49,201	10,665	2632

Pig Genome Oligo Set sequence selection

All TCs and singleton ETs were aligned using BLAST versus known gene transcripts for human, mouse, and pig. These TCs and singleton ETs were aligned to 27,628 known human gene trancripts from ENSEMBL, 28,097 known mouse gene trancripts, and 1897 known pig gene transcripts from the Pig UniGene Build #10 (http://www.ncbi.nlm.nih.gov). Both the human and mouse ENSEMBL database are from January 2003 and were obtained from http://www.ensembl.org. All TCs and singleton ETs with a >75% identity over at least 100 bases to a known human, mouse, or pig gene transcript and yielding a designed probe <=70 crosshybridization identity is included in this set.

Pig Genome Oligo Extension Set sequence selection

All component ESTs used to make the TCs were obtained from GenBank at http://www.ncbi.nlm.nih.gov. All ESTs with the keyword 3', denoting a 3 primer EST, were marked. A total of 7739 TCs were found at least one 3' EST. The TCs that contain at least one 3' EST and are not present in the Pig Genome Oligo Set are included in the Pig Genome Oligo Extension Set.

Table 2. Oligo sequence selection Pig Genome Oligo Set and Extension Set Version 1.0

	Pig Genome Oligo Set Version 1.0	Pig Genome Oligo Extension Set Version 1.0
Number of oligos designed from a TC with at least one 3' EST	5005	2632
Number of oligos designed from a sequence with a hit to a known human, mouse, or pig gene transcript	10,665	172
Numer of oligos that have a <=70% crosshybridization identity to another sequence	10,665	2538
Total	10,665	2632

Sequence orientation

TIGR obtains and predicts orientation for all the tentative consensus sequences and singletons based on various techniques including alignments to known proteins and poly A trimming. After SsGI 5.0 was released, TIGR later updated orientation of 7218 of the sequences in this database. A total of 628 of these are TCs and the rest are singleton ESTs. Probes for these 628 TCs that appear in the sets are therefore designed in the updated orientation. In the gene list, a column indicates the orientation of the probe to the original TC sequence. All probes are designed in the sense strand as given by TIGR.

Table 3. Probe design and selection rules for Pig Genome Oligo Set and Extension Set 1.0

Oligo selection criteria	Criteria values	Number of oligos in the Pig Genome Oligo Set Version 1.0 satisfying these criteria	Number of oligos in the Pig Genome Extension Set Version 1.0 satisfying these criteria
Length	70mer	10,607	2418
Melting temperature	78 ^{o}C ± 5^{o}C		
Location from 3' end	<=1000		
Poly(N) tract length	<8		
Stem length in protein hairpin	<9		
Cross-hybridization identity to all other sequences	<=70%		
Contiguous base match to any other sequence	<=20		
Total number of oligos not satisfying one or more of the above criteria		58	214
Length	50mer	27*	10†
Location from 3' end	>1000	31*	6†
Contiguous base match to any other sequence	>20	0*	176†
Cross-hybridization to all other sequences	>70%	0*	94†
Total		10,665	2632

*Out of 58 probes
†Out of 214 probes

Quality check of probe design specification

Once the final oligo set has been selected to represent a gene, each oligo undergoes design specifications quality control where we use an independent method to confirm that

all oligos have met the specified design specifications. The table below summarizes data from Qiagen quality check for probe design specifications for all probes.

Table 4. Qiagen quality check for probe design specifications

Probe design specification	Expected value	Verified range	Number of oligos pig genome oligo set version 1.0	Number of oligos pig genome extension set version 1.0
Melting temperature (^{o}C)	78 ^{o}C ± 5^{o}C	73.6-82.9	10,665	2632
Cross-hybridization identity (%)	<=70	31-70	10,665	2538
Cross-hybridization identity (%)	>70	71-100	0	94

The following graphs and illustrations show the distribution of all 10,665 oligos representing the Pig Genome Oligo Set Version 1.0 followed by the 2632 oligos from the Pig Genome Oligo Extension Set for the melting temperature, GC content, location from 3' end, and longest stem length, and cross-hybridization identity.

Fig1. Melting temperature-Pig genome oligo set

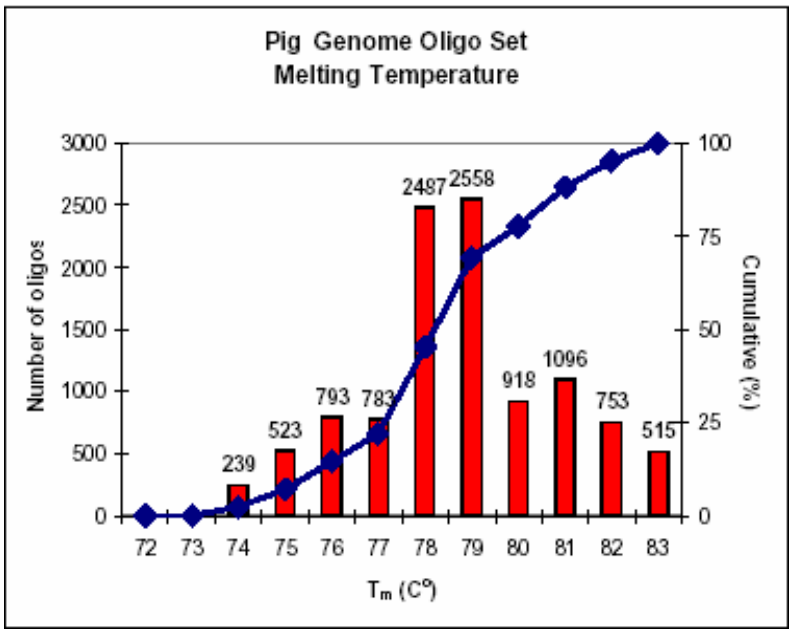

Fig2. GC content-Pig genome oligo set

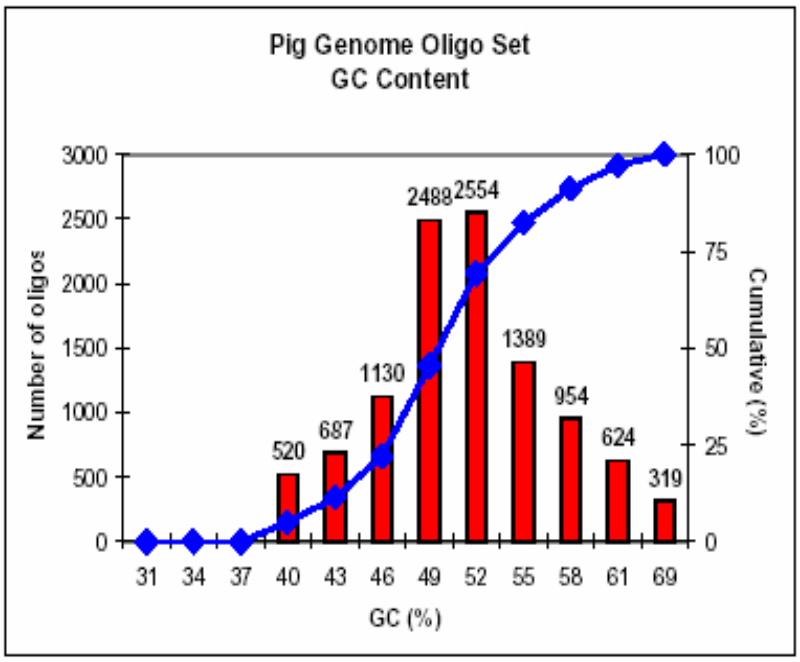

Fig3. Location from 3' end-Pig genome oligo set

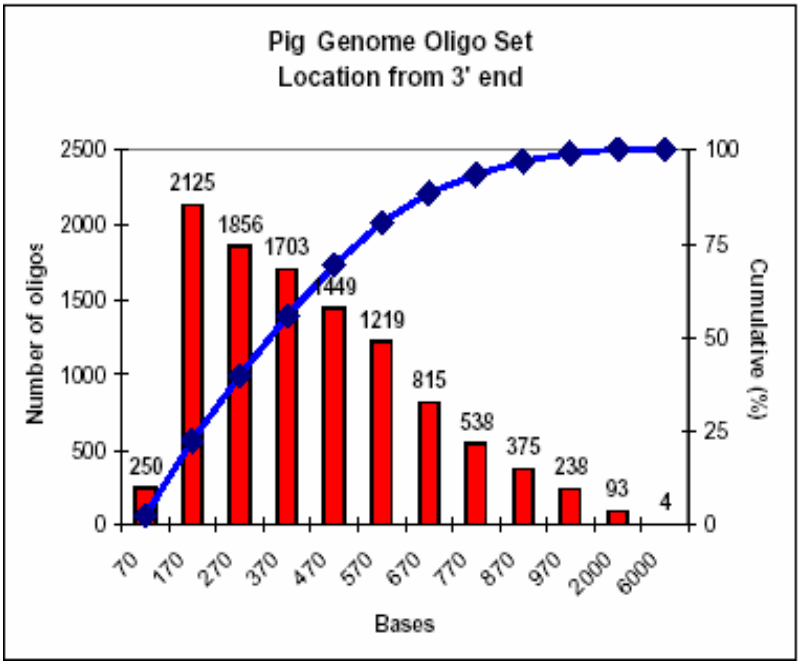

Fig4. Longest hairpin stem length-Pig genome oligo set

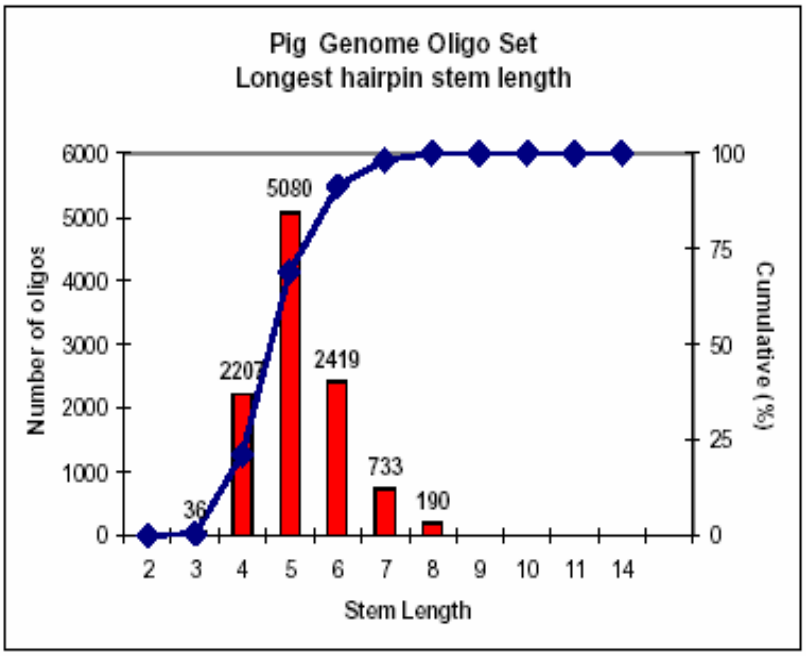

Fig5. Cross-hybridization identity-Pig genome oligo set

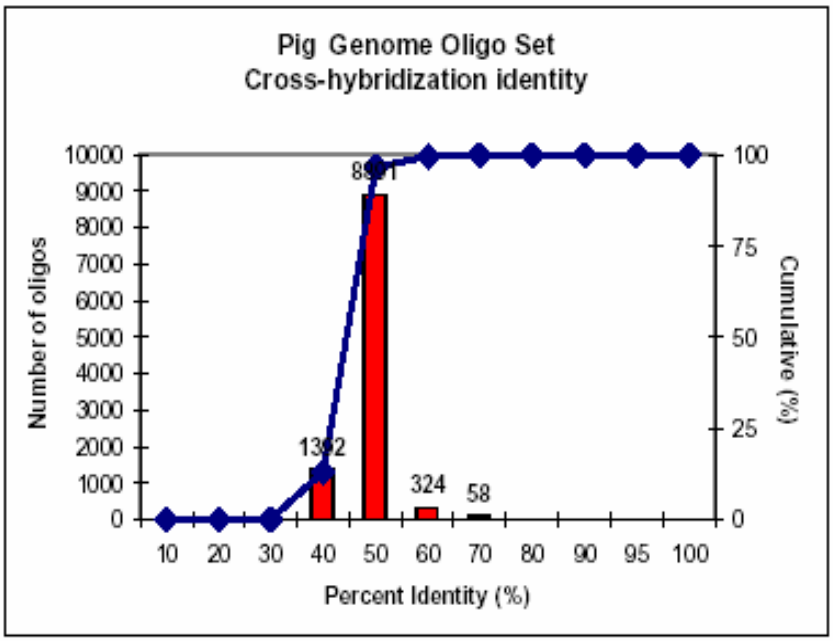

Fig6. Melting temperature-Pig genome oligo set

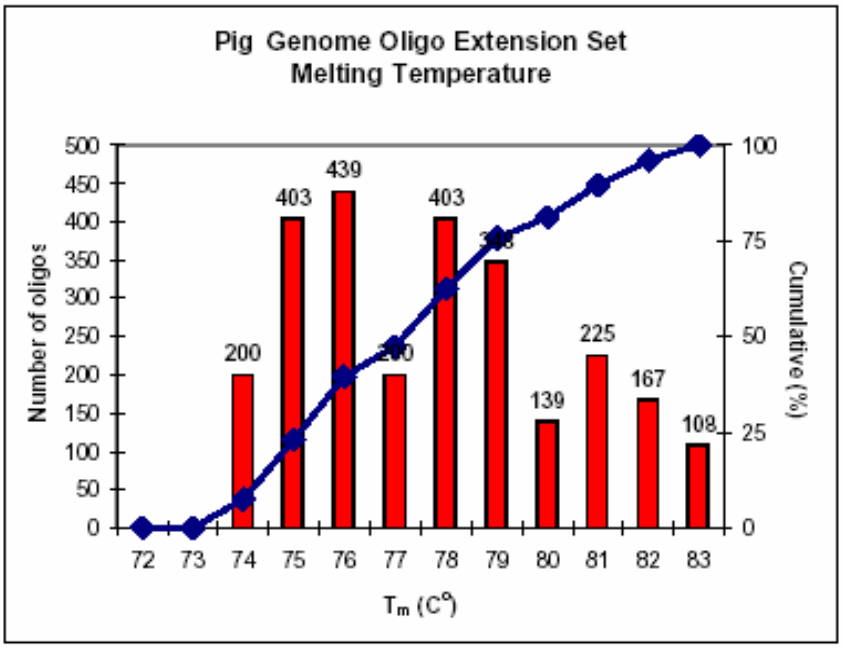

Fig7. GC content-pig genome oligo extension set

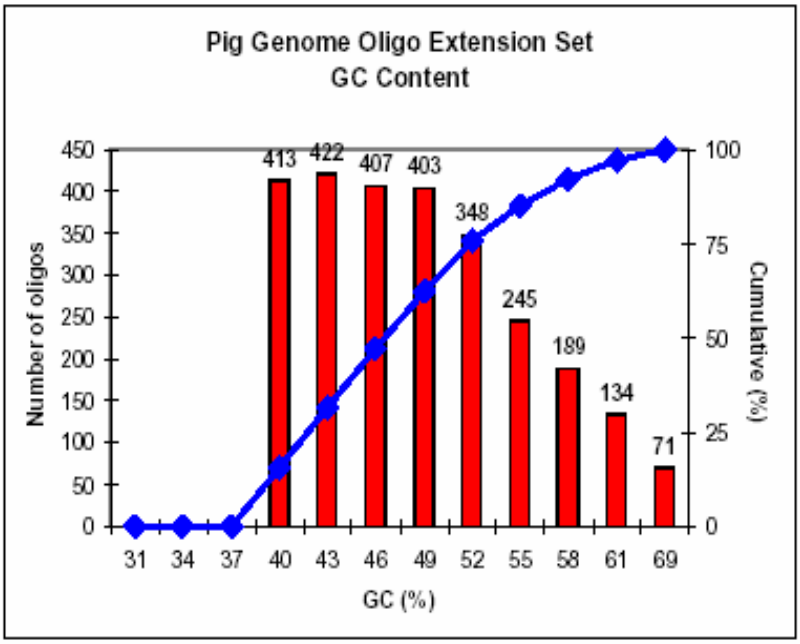

Fig8. Location from 3’ end-pig genome oligo extension set

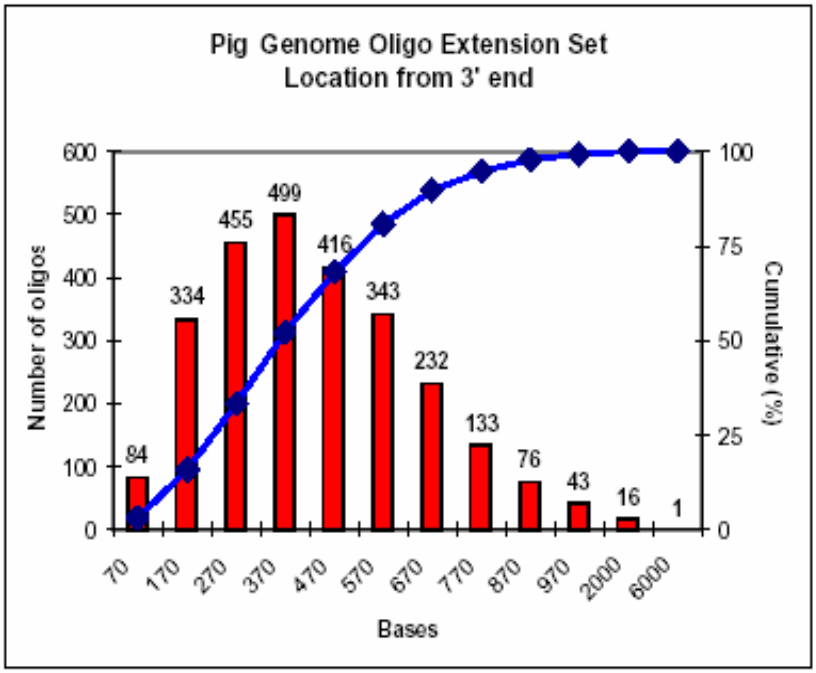

Fig9. Longest hairpin stem length-Pig genome oligo extension set

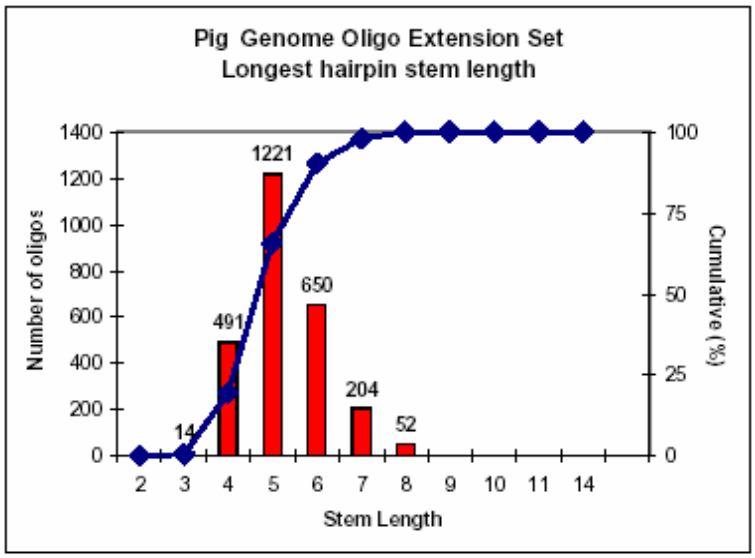

Fig10. Cross-hybridization identity-pig genome oligo extension set

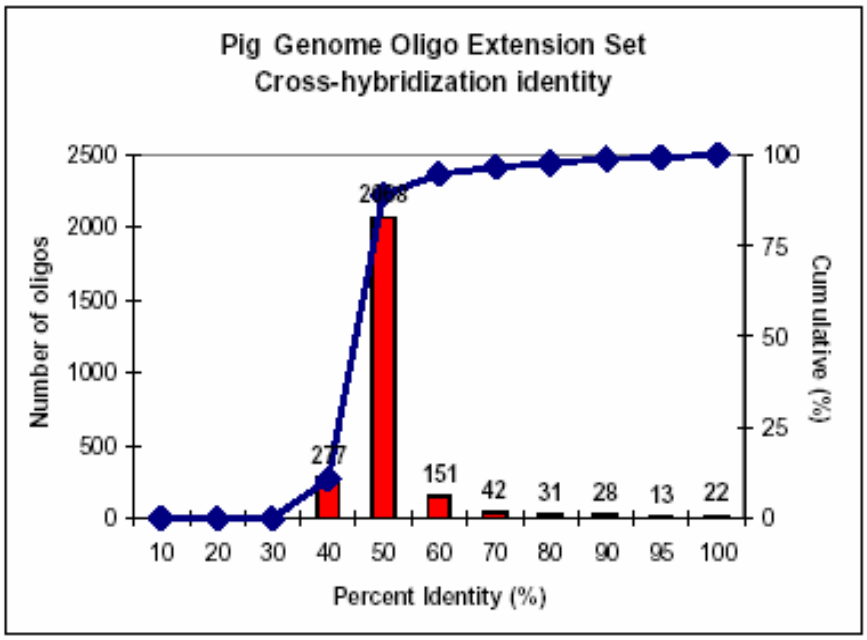

Appendix E. Microarray images of Ractopamine experiment (Chapter 2)

Fig 1. Ratio image of hybridization of adipose tissue RNAs from control pool RNA labeled by Cy5 and RNA from pig #779 labeled by Cy3. The image was obtained when scanning channels 532nm and 635 nm together by AXON 4000B laser scanner, and shown as ratio imaging (635/532). Detail scanning method was described in Materials and Methods in Chapter 2.

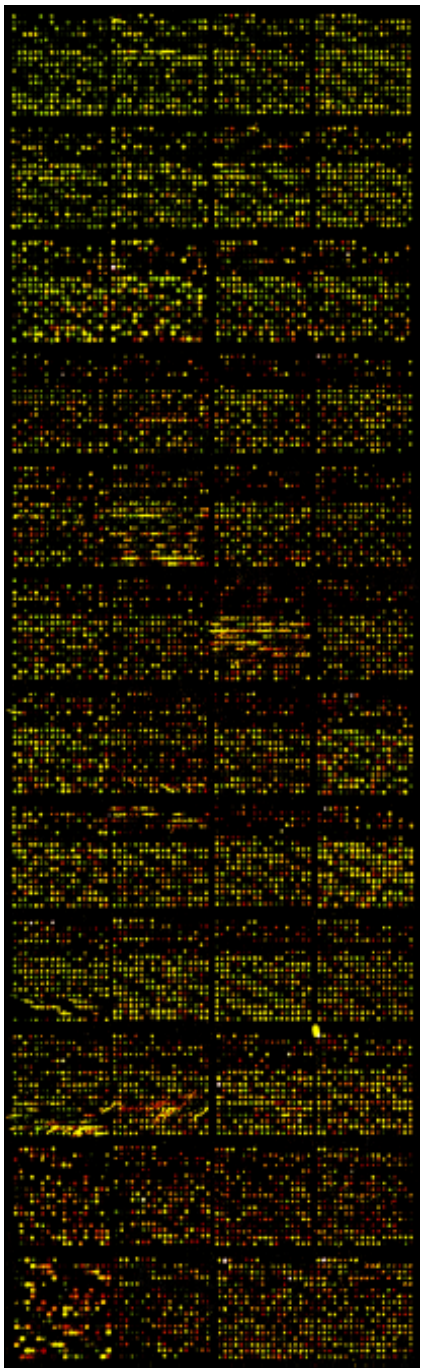

Fig 2. Ratio image of hybridization of adipose tissue RNAs from control pool RNA labeled by Cy3 and RNA from pig #796 labeled by Cy5. The image was obtained when scanning channels 532nm and 635 nm together by AXON 4000B laser scanner, and shown as ratio imaging (635/532). Detail scanning method was described in Materials and Methods in Chapter 2.

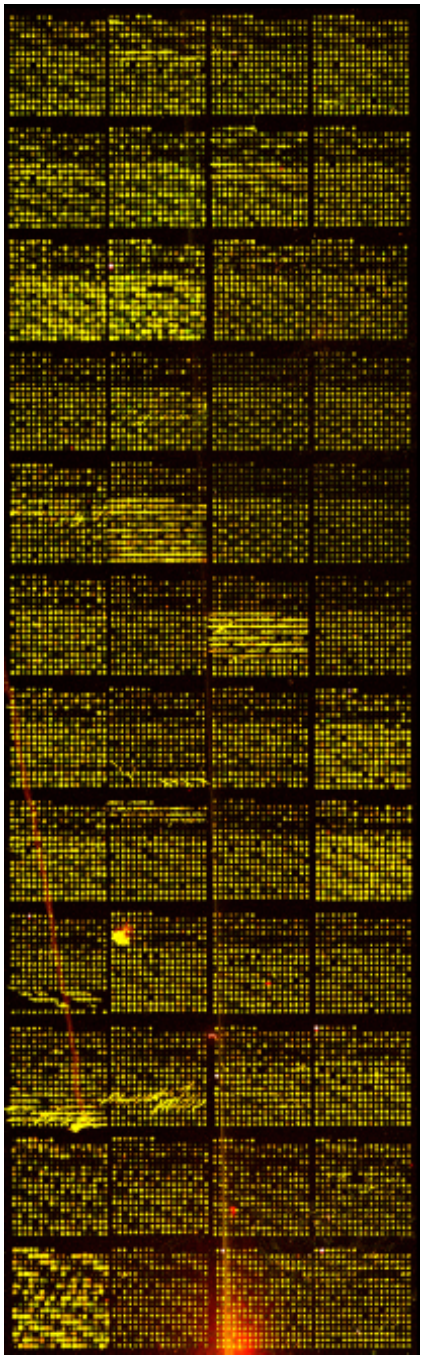

Fig 3. Ratio image of hybridization of adipose tissue RNAs from control pool RNA labeled by Cy3 and RNA from pig #784 labeled by Cy5. The image was obtained when scanning channels 532nm and 635 nm together by AXON 4000B laser scanner, and shown as ratio imaging (635/532). Detail scanning method was described in Materials and Methods in Chapter 2.

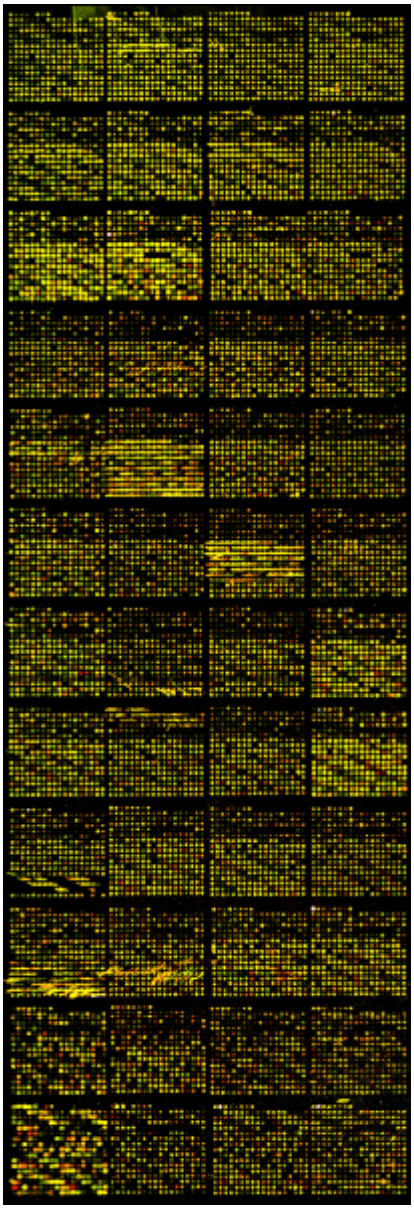

Appendix F. M-A plots of pro- and post- LOWESS normalization for Ractopamine experiment (Chapter 2)

Fig 1. Median pixel intensities from adipose tissue of #779 (T) Cy3 labeled RNA and control pool (C) Cy5 labeled RNA hybridized to pig array presented as scatter plots of $M = \log_2(T/C)$ vs. $A = \log_2(T*C)/2$.
(A) before (pro-) normalization, (B) after (post-) LOWESS normalization
(A)

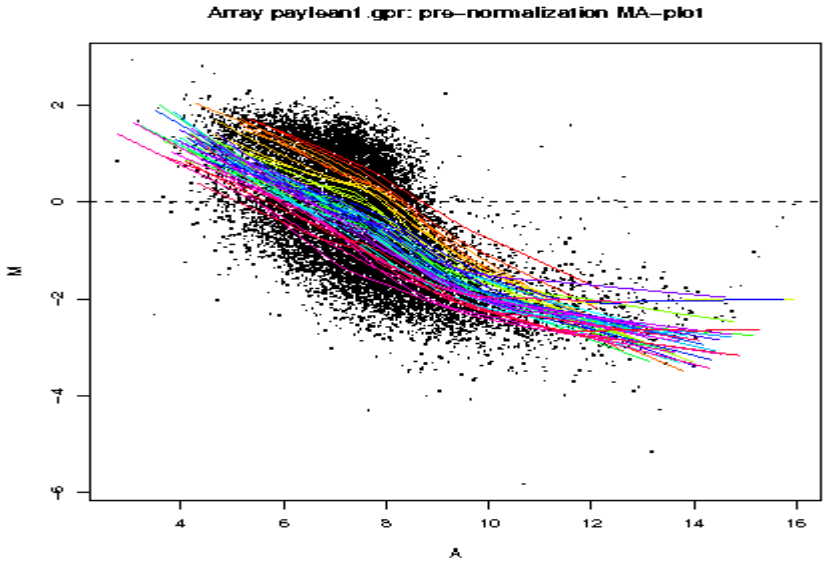

(B)
Post-LOWESS-normalization

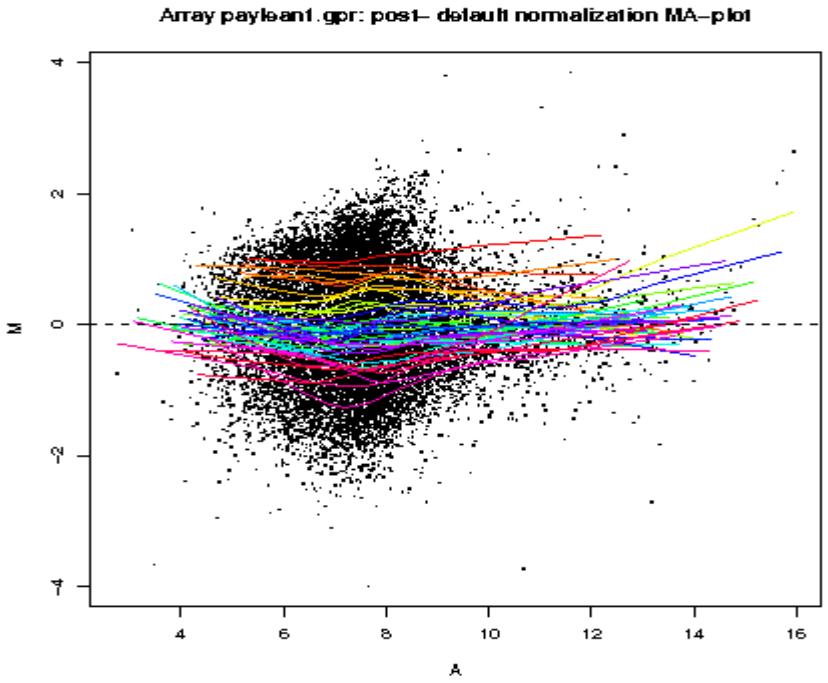

Fig 2. Median pixel intensities from adipose tissue of #796 (T) Cy5 labeled RNA and control pool (C) Cy3 labeled RNA hybridized to pig array presented as scatter plots of $M = \log_2(T/C)$ vs. $A = \log_2(T*C)/2$.
(A) before (pro-) normalization, (B) after (post-) LOWESS normalization

(A)

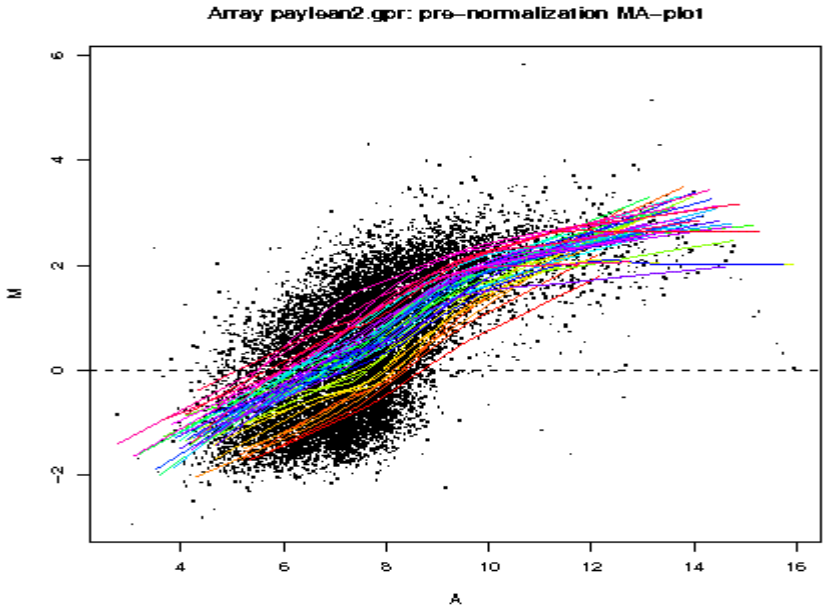

(B)

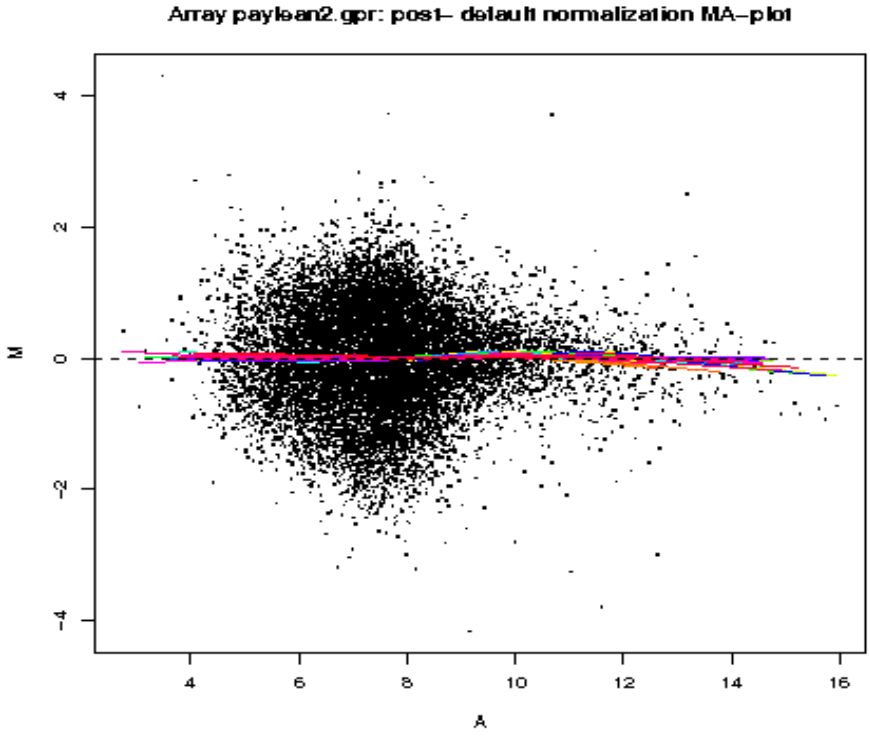

Fig 3. Median pixel intensities from adipose tissue of #784 (T) Cy5 labeled RNA and control pool (C) Cy3 labeled RNA hybridized to pig array presented as scatter plots of $M = \log_2(T/C)$ vs. $A = \log_2(T*C)/2$.
(A) before (pro-) normalization, (B) after (post-) LOWESS normalization
(A)

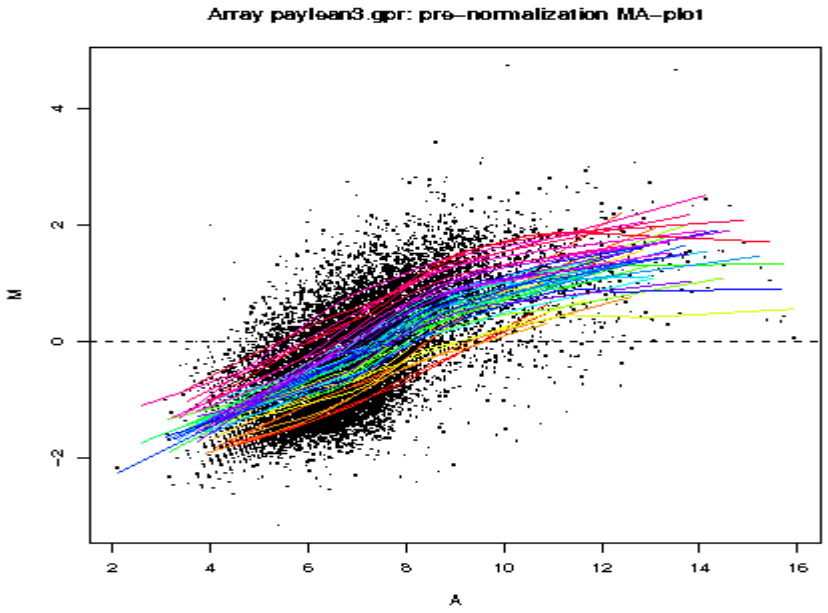

(B)

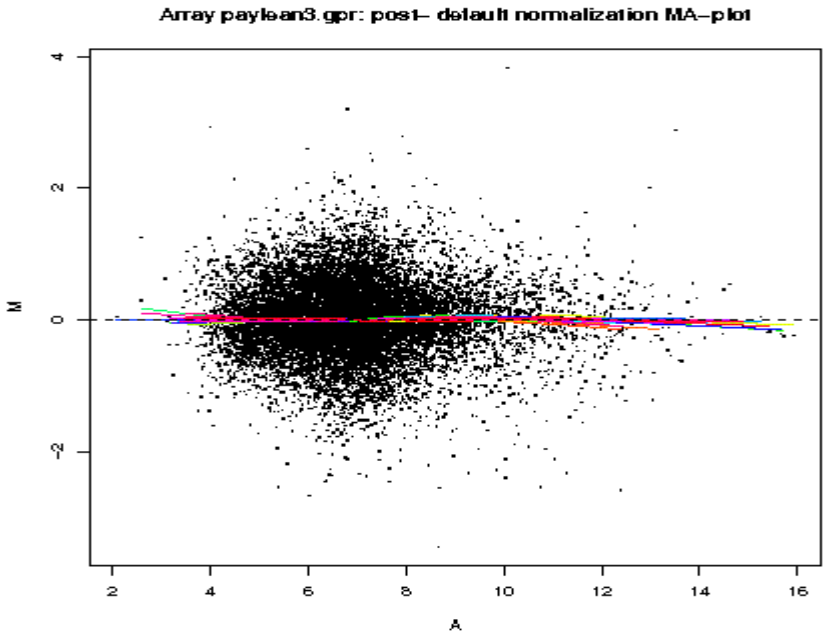

Appendix G. Microarray images of diet shifting experiment (Chapter 3)

Fig 1. Ratio image of hybridization of liver tissue RNAs from control pool RNA labeled by Cy5 and RNA from pig #4905 labeled by Cy3. The image was obtained when scanning channels 532nm and 635 nm together by AXON 4000B laser scanner, and shown as ratio imaging (635/532). Detail scanning method was described in Materials and Methods in Chapter 2.

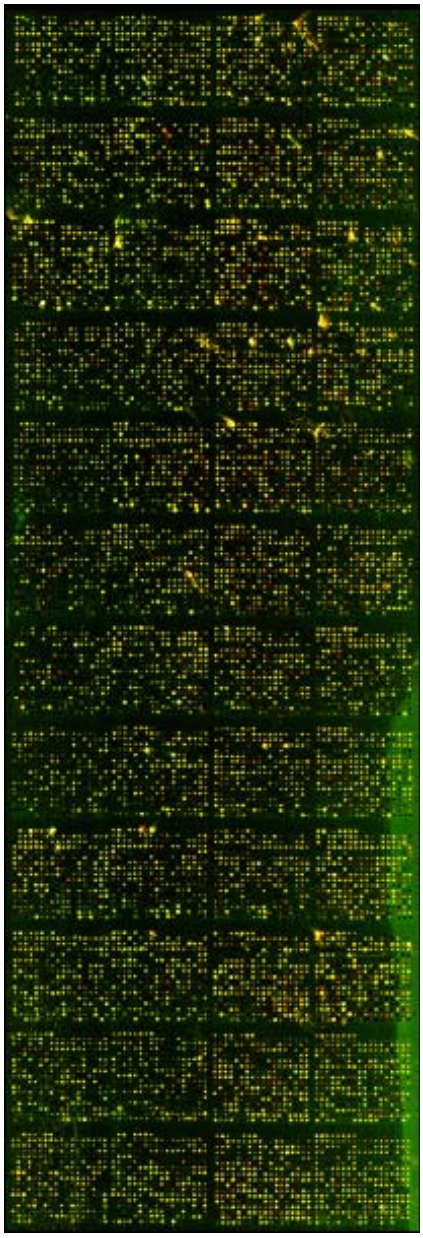

Fig 2. Ratio image of hybridization of liver tissue RNAs from control pool RNA labeled by Cy3 and RNA from pig #5207 labeled by Cy5. The image was obtained when scanning channels 532nm and 635 nm together by AXON 4000B laser scanner, and shown as ratio imaging (635/532). Detail scanning method was described in Materials and Methods in Chapter 2.

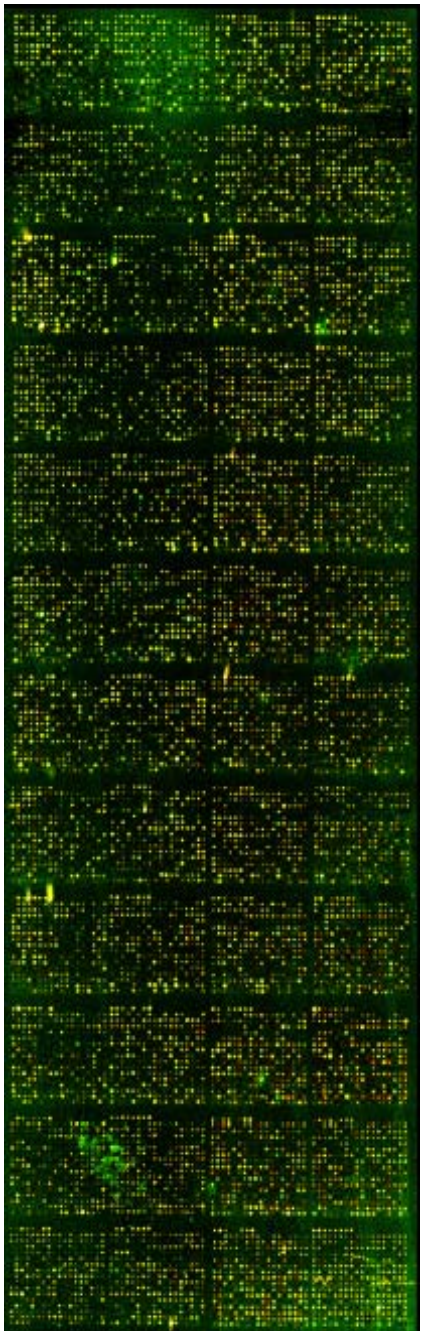

Fig 3. Ratio image of hybridization of liver tissue RNAs from control pool RNA labeled by Cy5 and RNA from pig #5502 labeled by Cy3. The image was obtained when scanning channels 532nm and 635 nm together by AXON 4000B laser scanner, and shown as ratio imaging (635/532). Detail scanning method was described in Materials and Methods in Chapter 2.

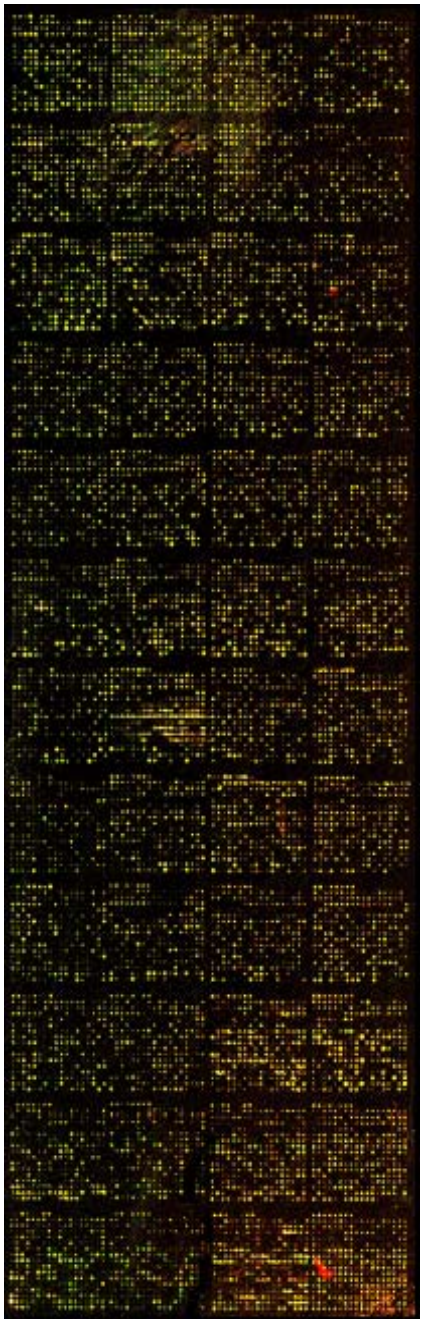

Fig 4. Ratio image of hybridization of liver tissue RNAs from control pool RNA labeled by Cy3 and RNA from pig #6001 labeled by Cy5. The image was obtained when scanning channels 532nm and 635 nm together by AXON 4000B laser scanner, and shown as ratio imaging (635/532). Detail scanning method was described in Materials and Methods in Chapter 2.

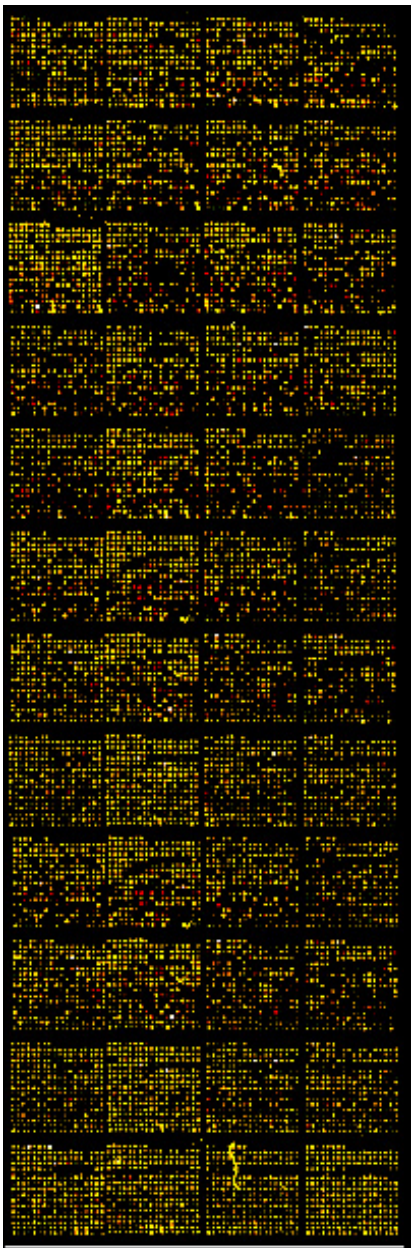

Fig 5. Ratio image of hybridization of adipose tissue RNAs from control pool RNA labeled by Cy5 and RNA from pig #4905 labeled by Cy3. The image was obtained when scanning channels 532nm and 635 nm together by AXON 4000B laser scanner, and shown as ratio imaging (635/532). Detail scanning method was described in Materials and Methods in Chapter 2.

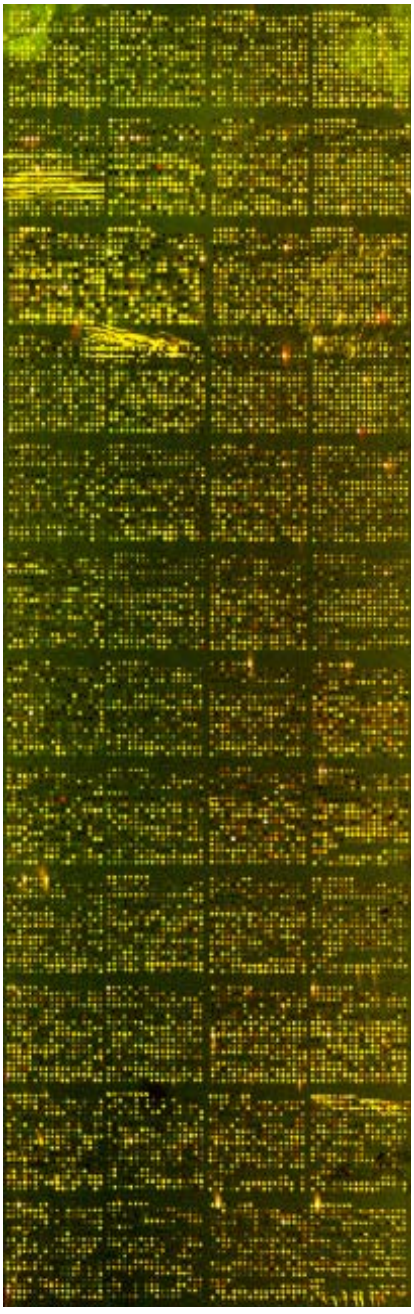

Fig 6. Ratio image of hybridization of adipsoe tissue RNAs from control pool RNA labeled by Cy5 and RNA from pig #5207 labeled by Cy3. The image was obtained when scanning channels 532nm and 635 nm together by AXON 4000B laser scanner, and shown as ratio imaging (635/532). Detail scanning method was described in Materials and Methods in Chapter 2.

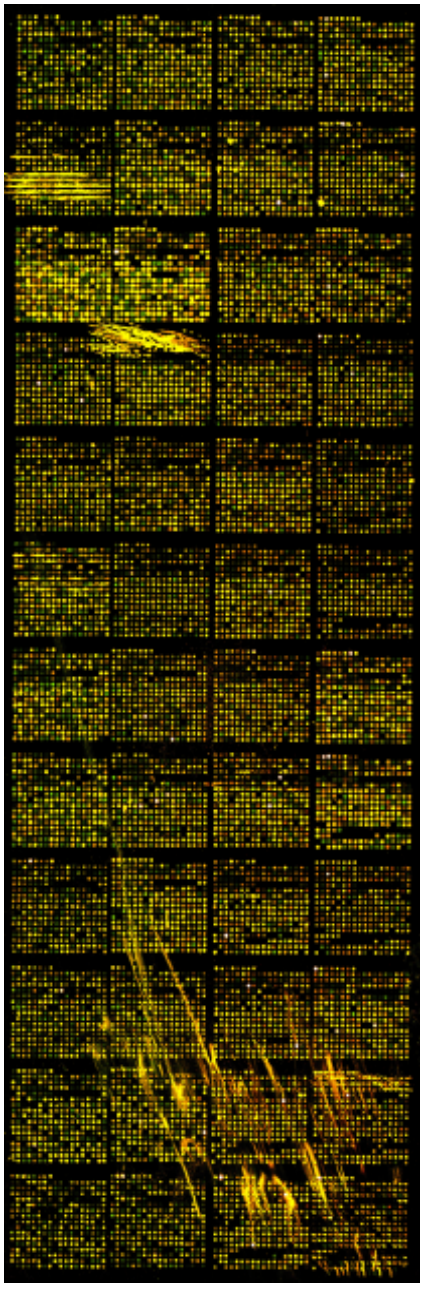

Fig 7. Ratio image of hybridization of adipsoe tissue RNAs from control pool RNA labeled by Cy3 and RNA from pig #5502 labeled by Cy5. The image was obtained when scanning channels 532nm and 635 nm together by AXON 4000B laser scanner, and shown as ratio imaging (635/532). Detail scanning method was described in Materials and Methods in Chapter 2.

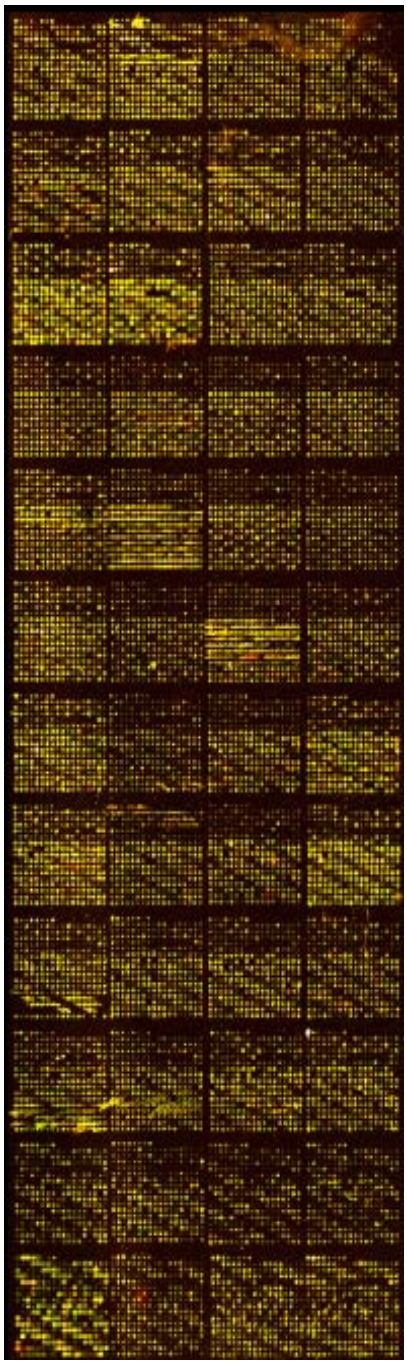

Fig 8. Ratio image of hybridization of adipose tissue RNAs from control pool RNA labeled by Cy3 and RNA from pig #6001 labeled by Cy5. The image was obtained when scanning channels 532nm and 635 nm together by AXON 4000B laser scanner, and shown as ratio imaging (635/532). Detail scanning method was described in Materials and Methods in Chapter 2.

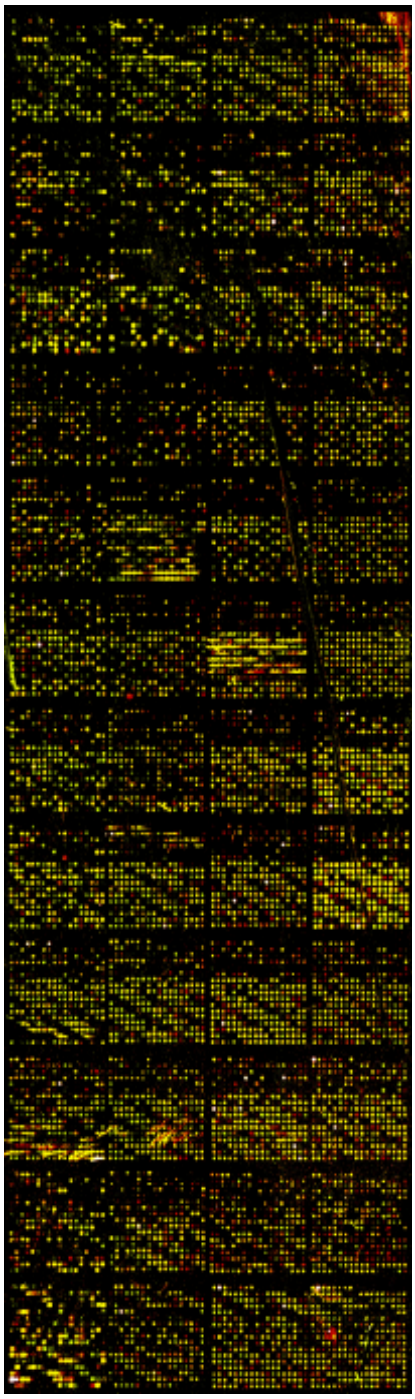

Fig 9. Ratio image of hybridization of muscle tissue RNAs from control pool RNA labeled by Cy3 and RNA from pig #5207 labeled by Cy5. The image was obtained when scanning channels 532nm and 635 nm together by AXON 4000B laser scanner, and shown as ratio imaging (635/532). Detail scanning method was described in Materials and Methods in Chapter 2.

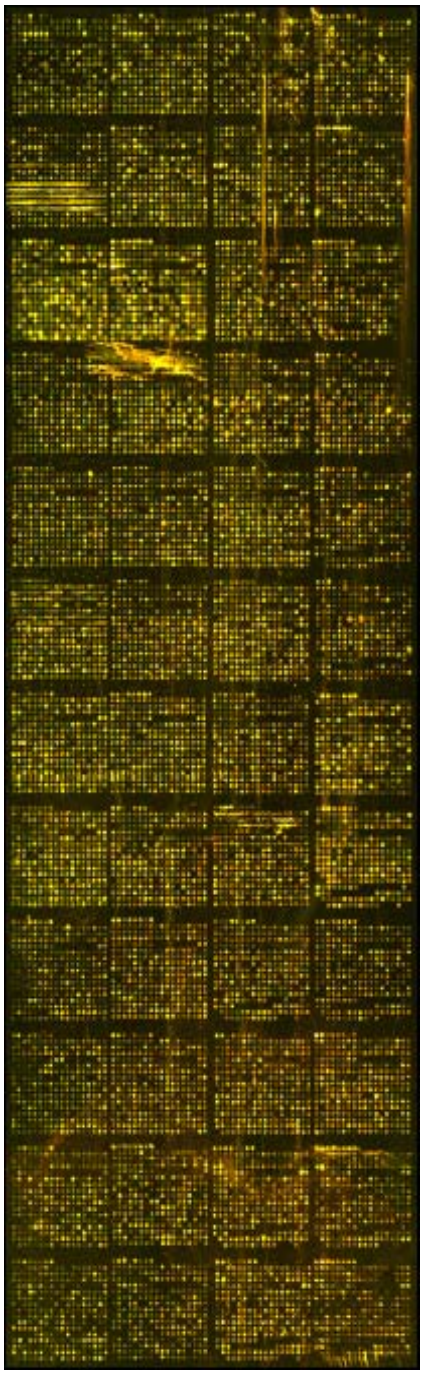

Fig 10. Ratio image of hybridization of muscle tissue RNAs from control pool RNA labeled by Cy5 and RNA from pig #5502 labeled by Cy3. The image was obtained when scanning channels 532nm and 635 nm together by AXON 4000B laser scanner, and shown as ratio imaging (635/532). Detail scanning method was described in Materials and Methods in Chapter 2.

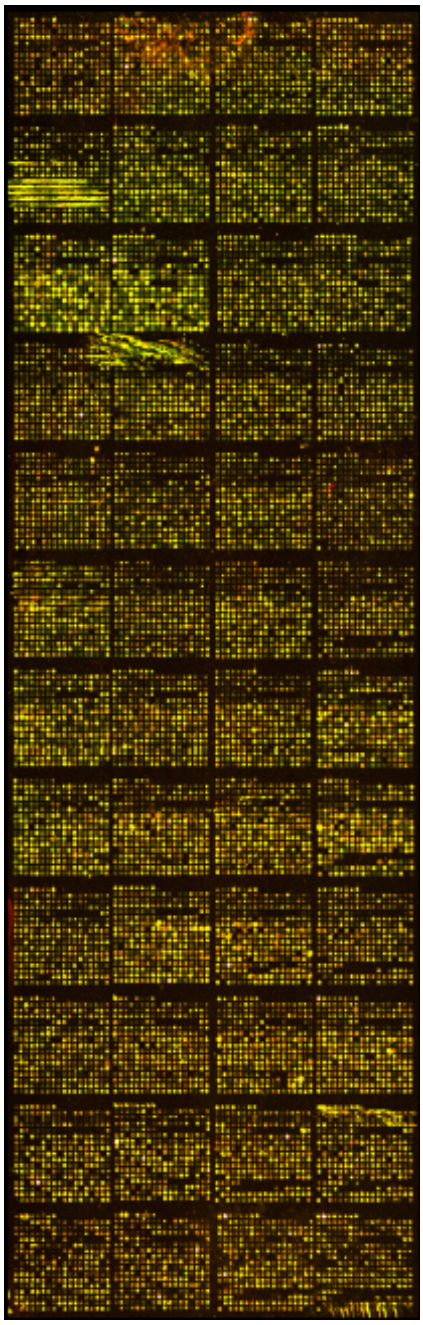

Fig 11. Ratio image of hybridization of muscle tissue RNAs from control pool RNA labeled by Cy3 and RNA from pig #4905 labeled by Cy5. The image was obtained when scanning channels 532nm and 635 nm together by AXON 4000B laser scanner, and shown as ratio imaging (635/532). Detail scanning method was described in Materials and Methods in Chapter 2.

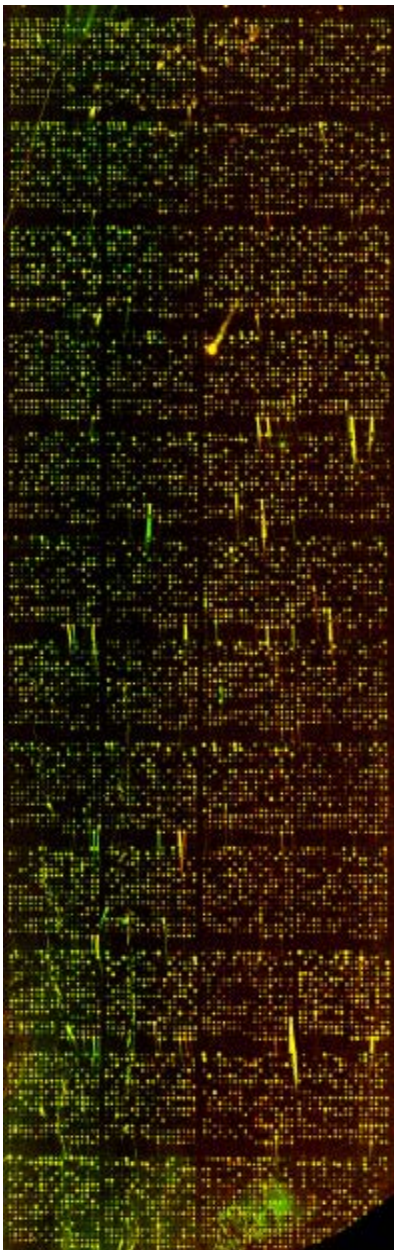

Fig 12. Ratio image of hybridization of muscle tissue RNAs from control pool RNA labeled by Cy5 and RNA from pig #6001 labeled by Cy3. The image was obtained when scanning channels 532nm and 635 nm together by AXON 4000B laser scanner, and shown as ratio imaging (635/532). Detail scanning method was described in Materials and Methods in Chapter 2.

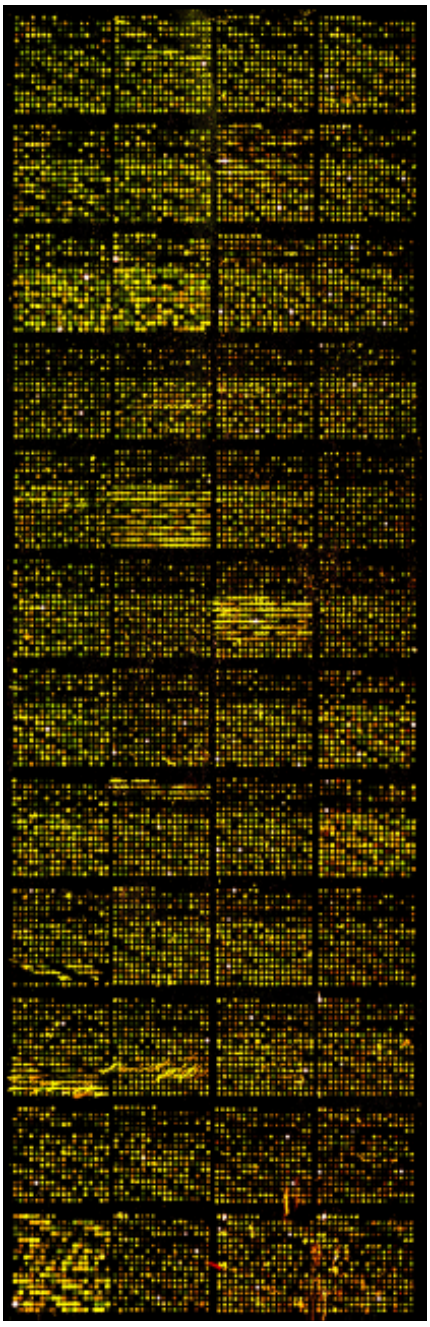

Appendix H. M-A plots of pro- and post- LOWESS normalization for diet shifting experiment (Chapter 3)

Fig 1. Median pixel intensities from liver tissue of #4905 (T) Cy3 labeled RNA and control pool (C) Cy5 labeled RNA hybridized to pig array presented as scatter plots of $M=\log_2(T/C)$ vs. $A= \log_2 (T*C)/2$.
(A) before (pro-) normalization, (B) after (post-) LOWESS normalization
(A)

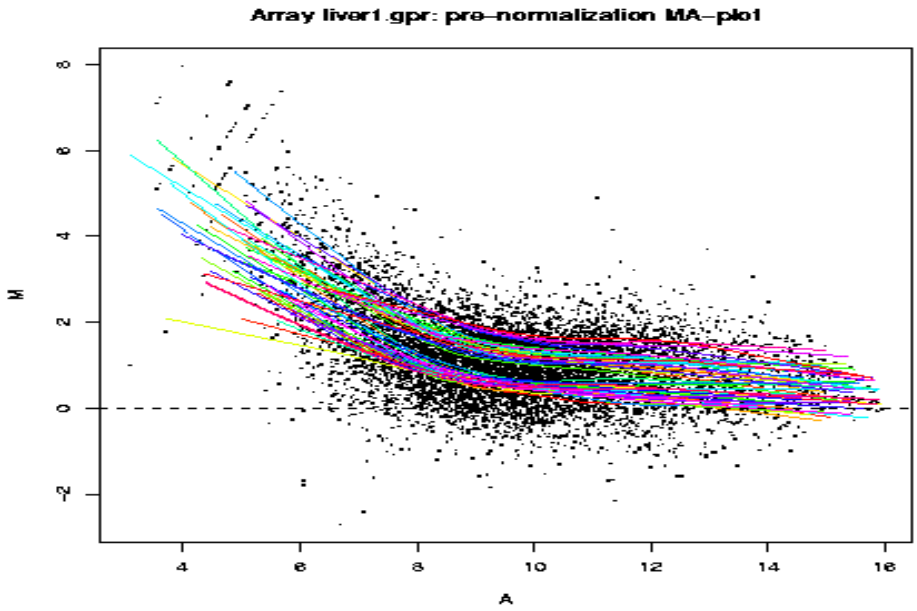

(B)

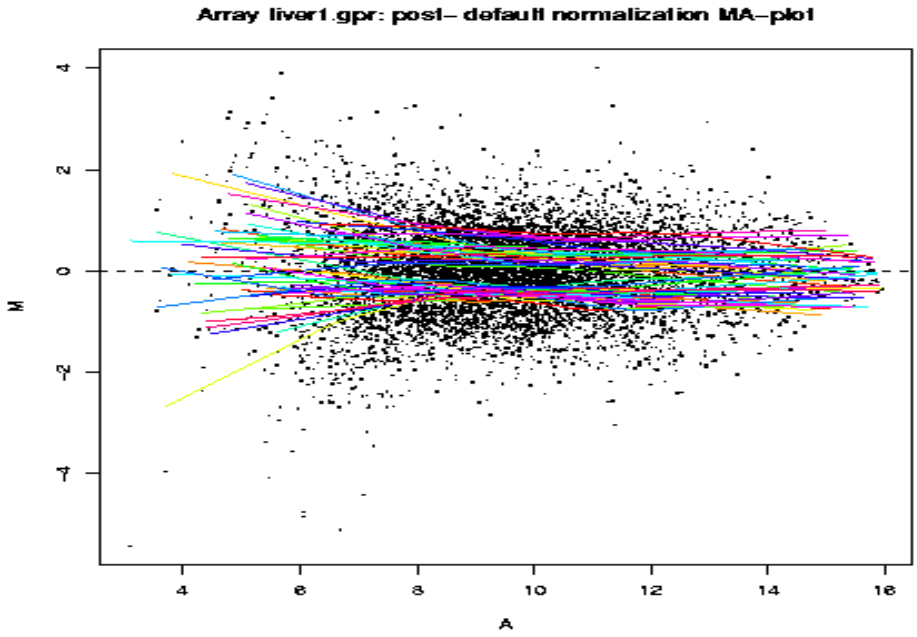

Fig 2 Median pixel intensities from liver tissue of #5207 (T) Cy5 labeled RNA and control pool (C) Cy3 labeled RNA hybridized to pig array presented as scatter plots of $M = \log_2(T/C)$ vs. $A = \log_2(T*C)/2$.
(A) before (pro-) normalization, (B) after (post-) LOWESS normalization
(A)

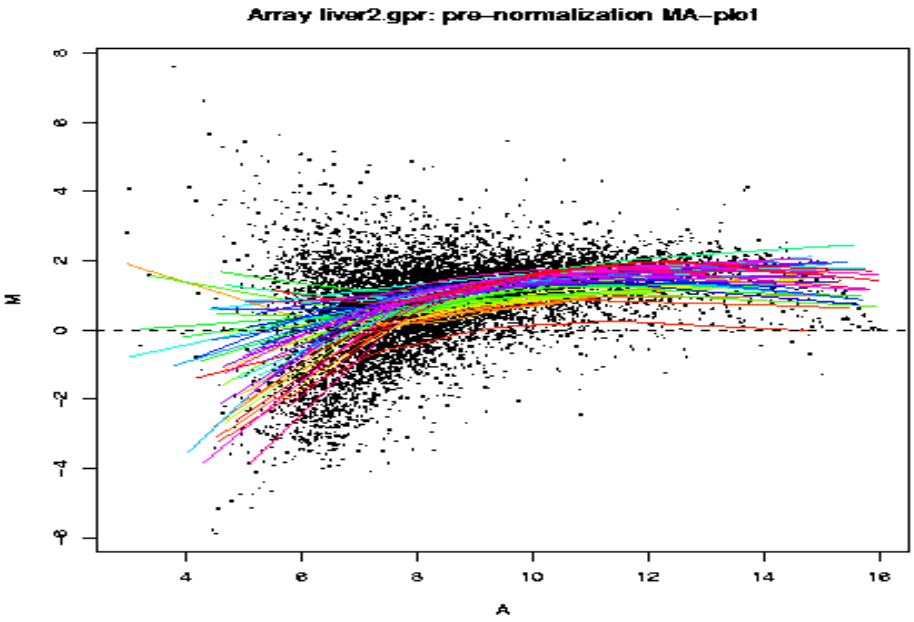

(B)

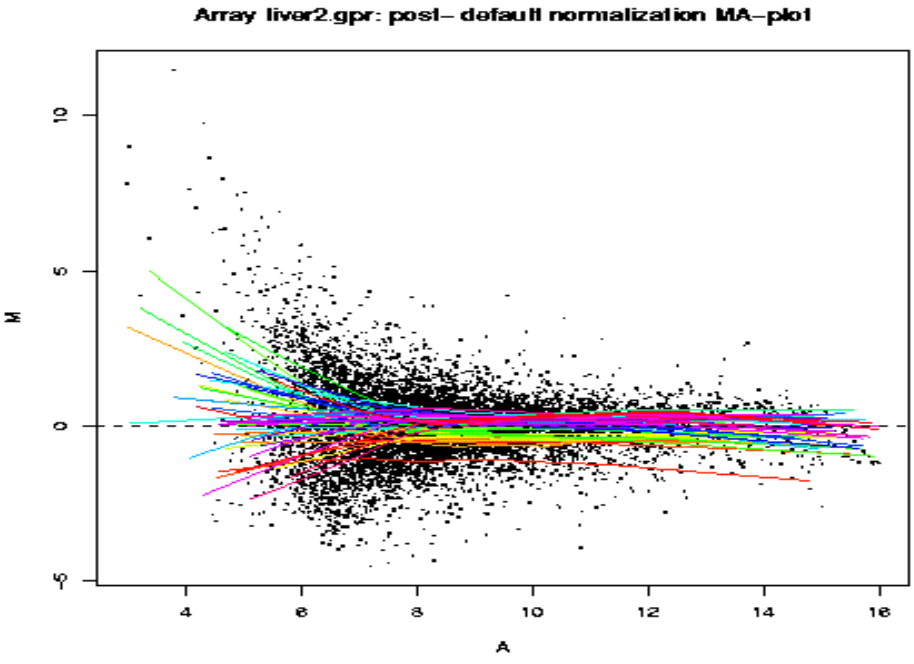

Fig 3 Median pixel intensities from liver tissue of #5502 (T) Cy3 labeled RNA and control pool (C) Cy5 labeled RNA hybridized to pig array presented as scatter plots of $M = \log_2(T/C)$ vs. $A = \log_2(T*C)/2$.
(A) before (pro-) normalization, (B) after (post-) LOWESS normalization
(A)

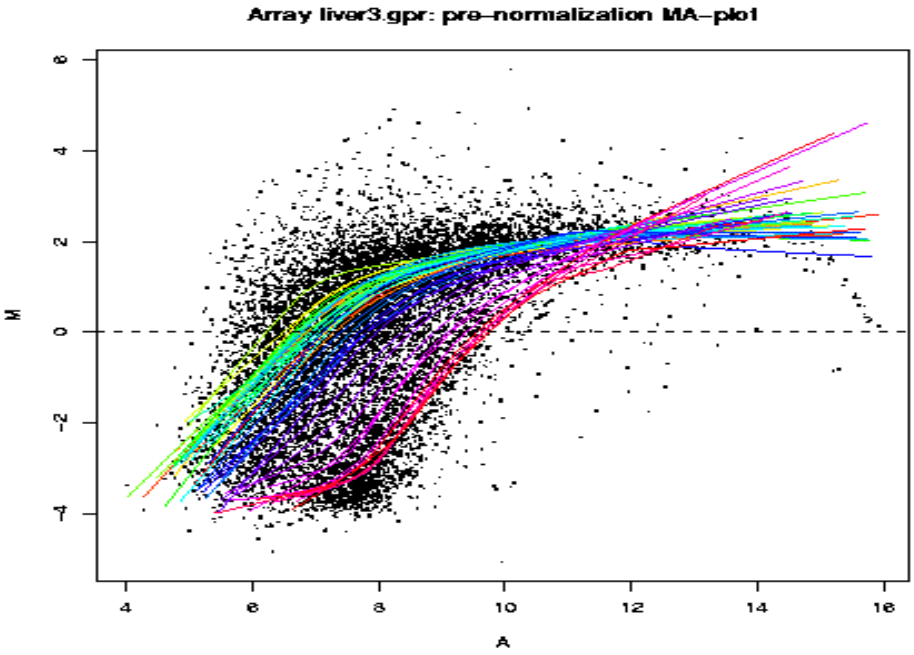

(B)

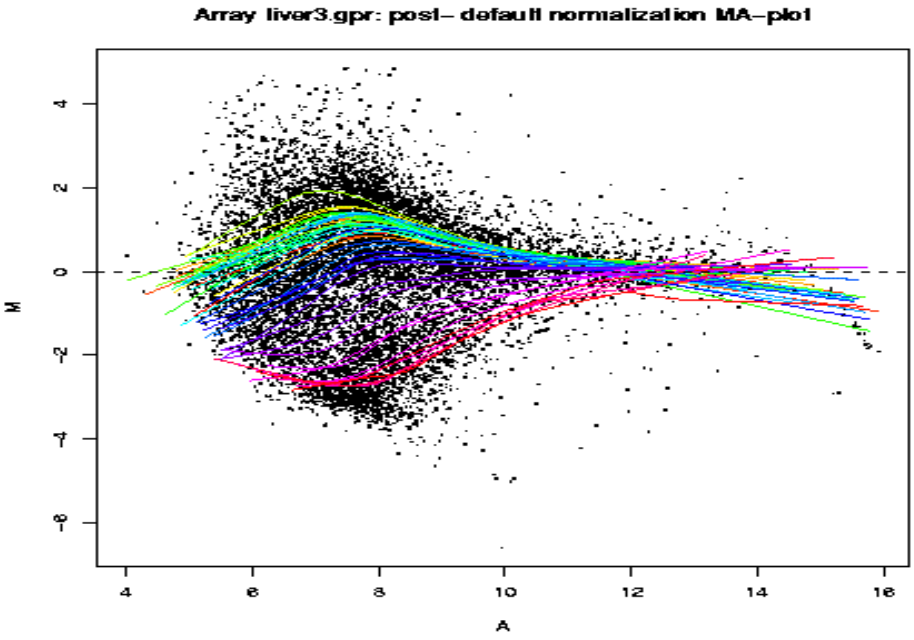

Fig 4. Median pixel intensities from liver tissue of #6001 (T) Cy5 labeled RNA and control pool (C) Cy3 labeled RNA hybridized to pig array presented as scatter plots of $M = \log_2(T/C)$ vs. $A = \log_2(T*C)/2$.
(A) before (pro-) normalization, (B) after (post-) LOWESS normalization
(A)

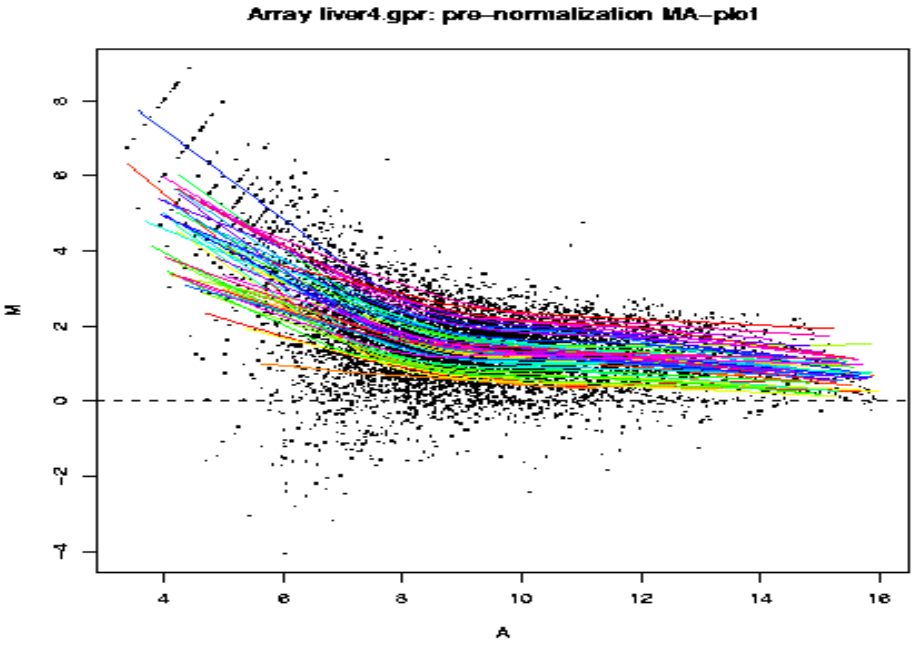

(B)

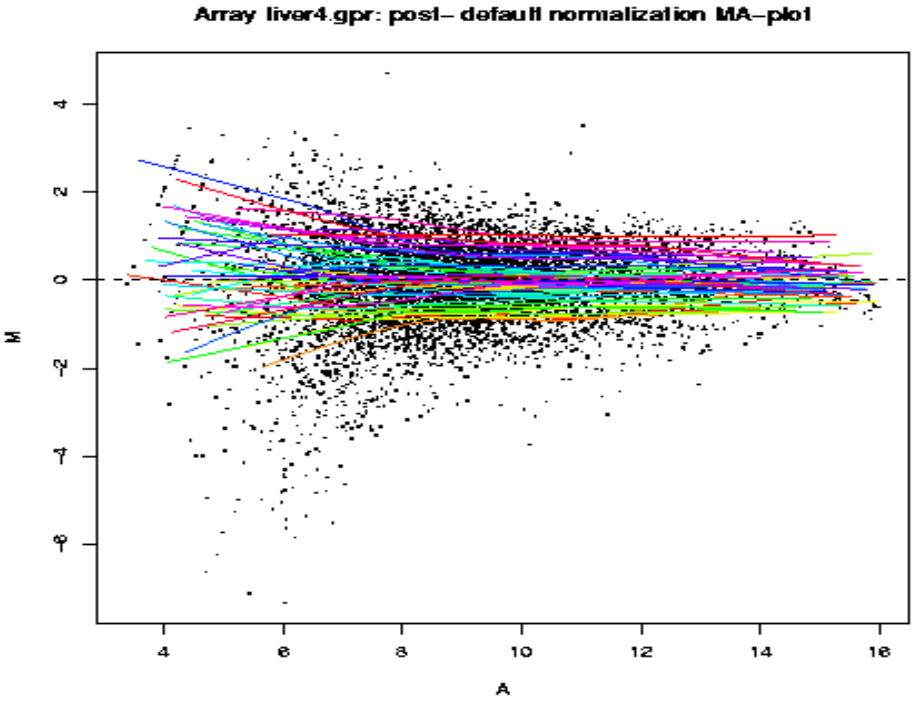

Fig 5 Median pixel intensities from adipose tissue of #4905 (T) Cy3 labeled RNA and control pool (C) Cy5 labeled RNA hybridized to pig array presented as scatter plots of $M = \log_2(T/C)$ vs. $A = \log_2(T*C)/2$.
(A) before (pro-) normalization, (B) after (post-) LOWESS normalization

(A)

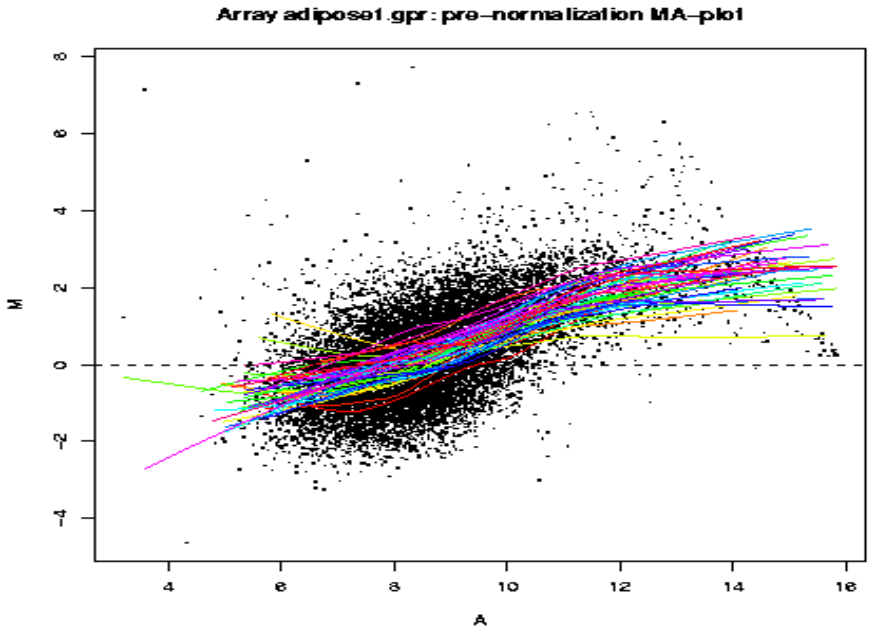

(B)

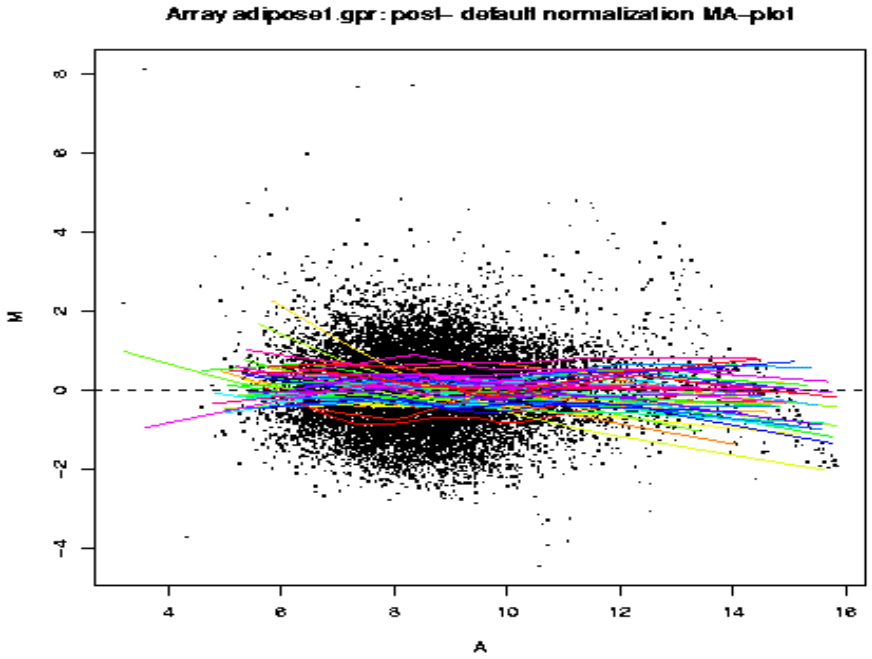

Fig 6. Median pixel intensities from adipose tissue of #5207 (T) Cy3 labeled RNA and control pool (C) Cy5 labeled RNA hybridized to pig array presented as scatter plots of $M = \log_2(T/C)$ vs. $A = \log_2(T*C)/2$.
(A) before (pro-) normalization, (B) after (post-) LOWESS normalization

(A)

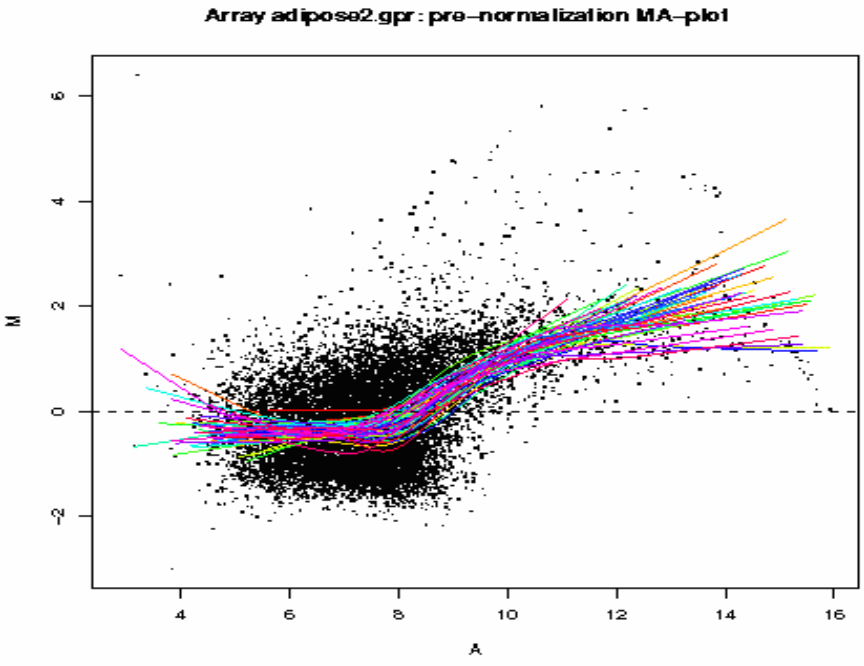

(B)

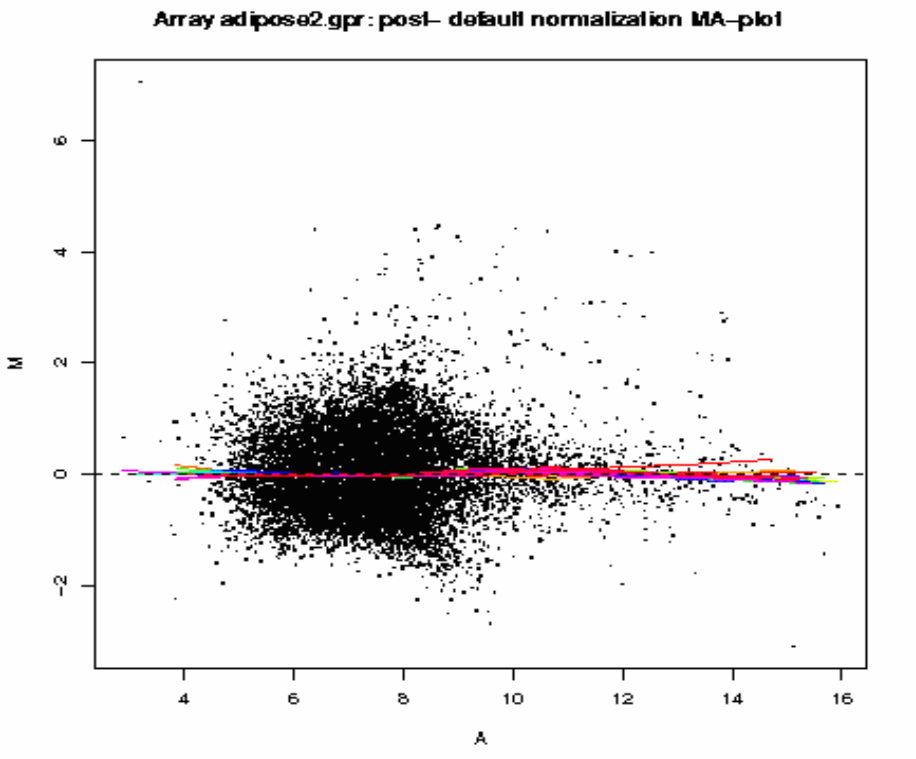

Fig 7. Median pixel intensities from adipose tissue of #5502 (T) Cy5 labeled RNA and control pool (C) Cy3 labeled RNA hybridized to pig array presented as scatter plots of $M = \log_2(T/C)$ vs. $A = \log_2(T*C)/2$.
(A) before (pro-) normalization, (B) after (post-) LOWESS normalization
(A)

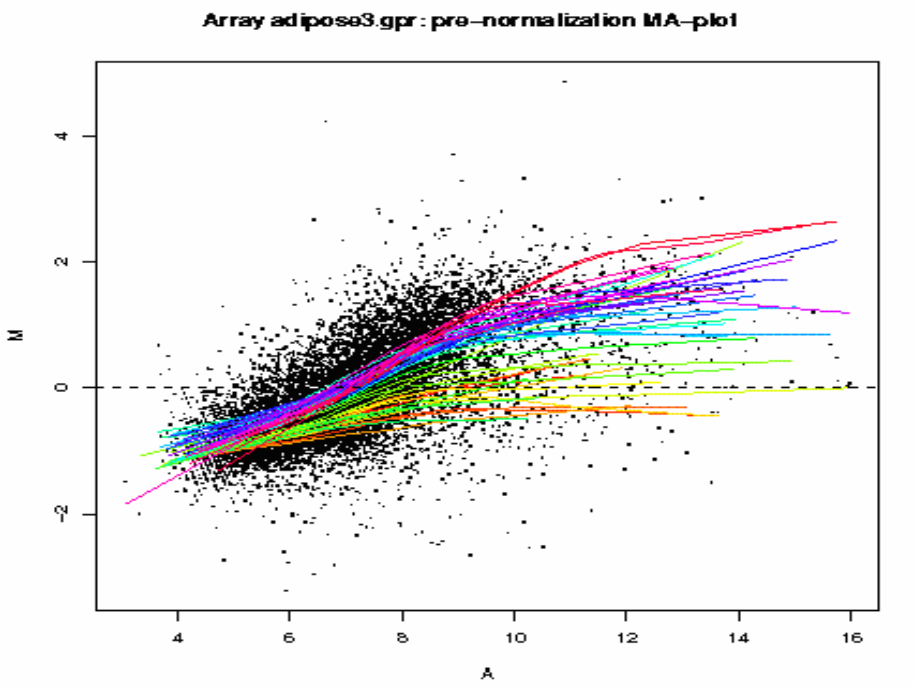

(B)

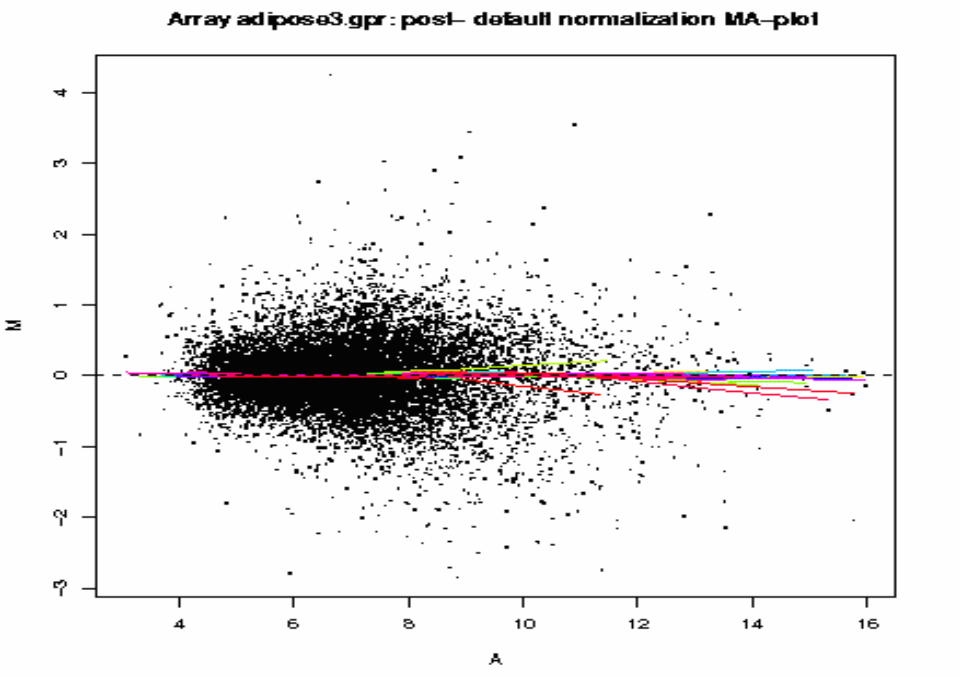

Fig 8. Median pixel intensities from adipose tissue of #6001 (T) Cy5 labeled RNA and control pool (C) Cy3 labeled RNA hybridized to pig array presented as scatter plots of $M = \log_2(T/C)$ vs. $A = \log_2(T*C)/2$.
(A) before (pro-) normalization, (B) after (post-) LOWESS normalization
(A)

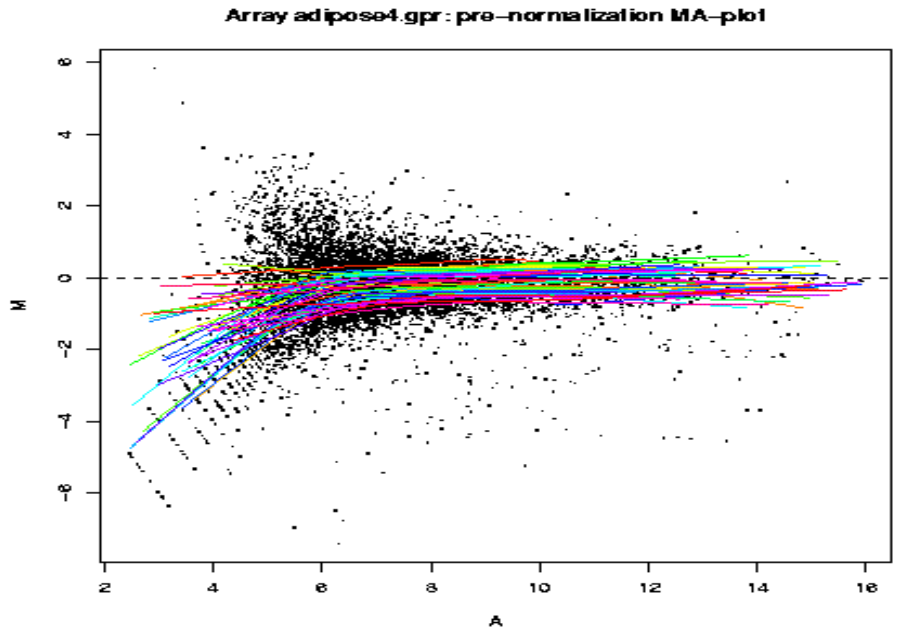

(B)

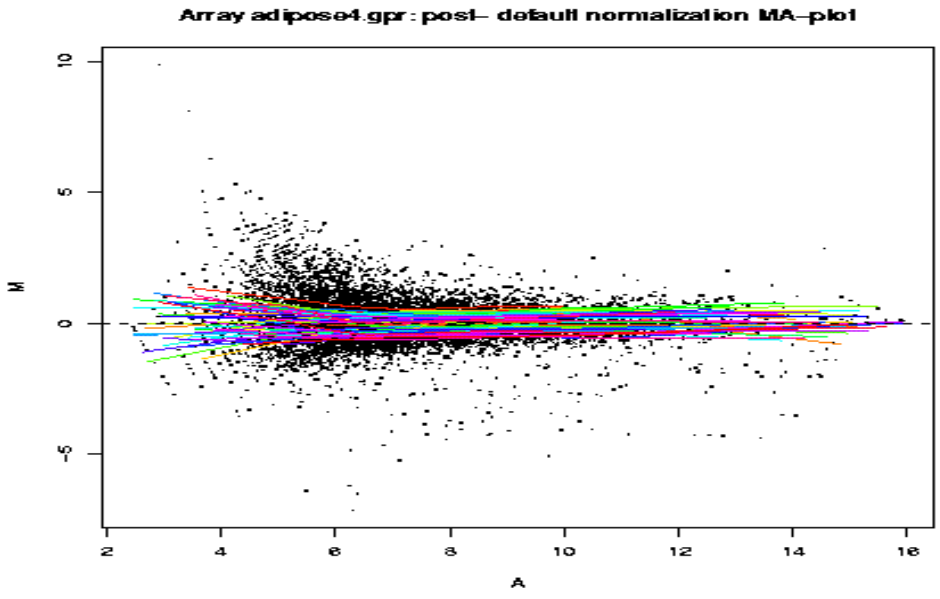

Fig9. Median pixel intensities from muscle tissue of #4905 (T) Cy5 labeled RNA and control pool (C) Cy3 labeled RNA hybridized to pig array presented as scatter plots of $M = \log_2(T/C)$ vs. $A = \log_2(T*C)/2$.
(A) before (pro-) normalization, (B) after (post-) LOWESS normalization
(A)

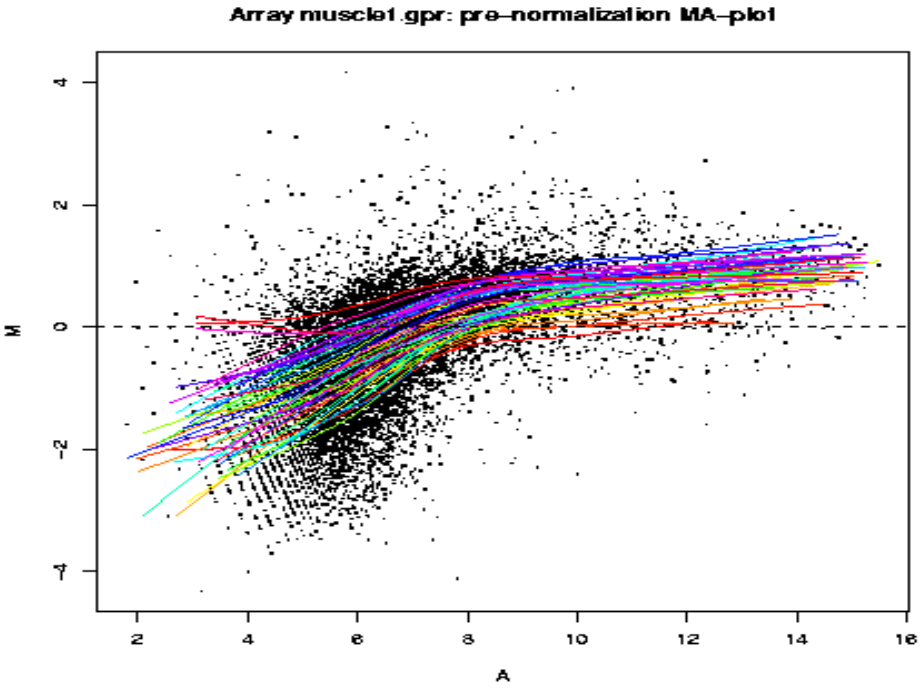

(B)

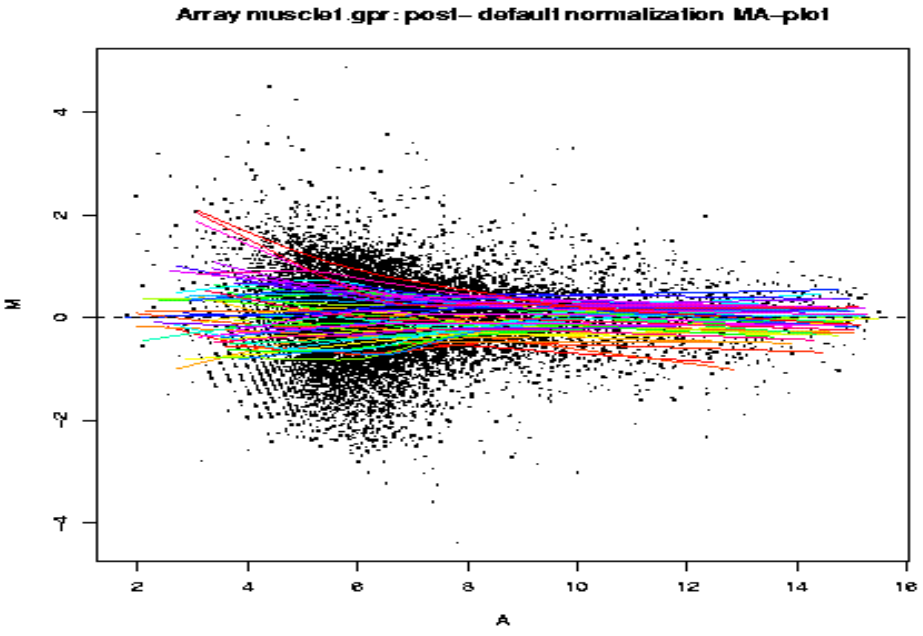

Fig 10. Median pixel intensities from muscle tissue of #5207 (T) Cy5 labeled RNA and control pool (C) Cy3 labeled RNA hybridized to pig array presented as scatter plots of $M = \log_2(T/C)$ vs. $A = \log_2(T*C)/2$.
(A) before (pro-) normalization, (B) after (post-) LOWESS normalization
(A)

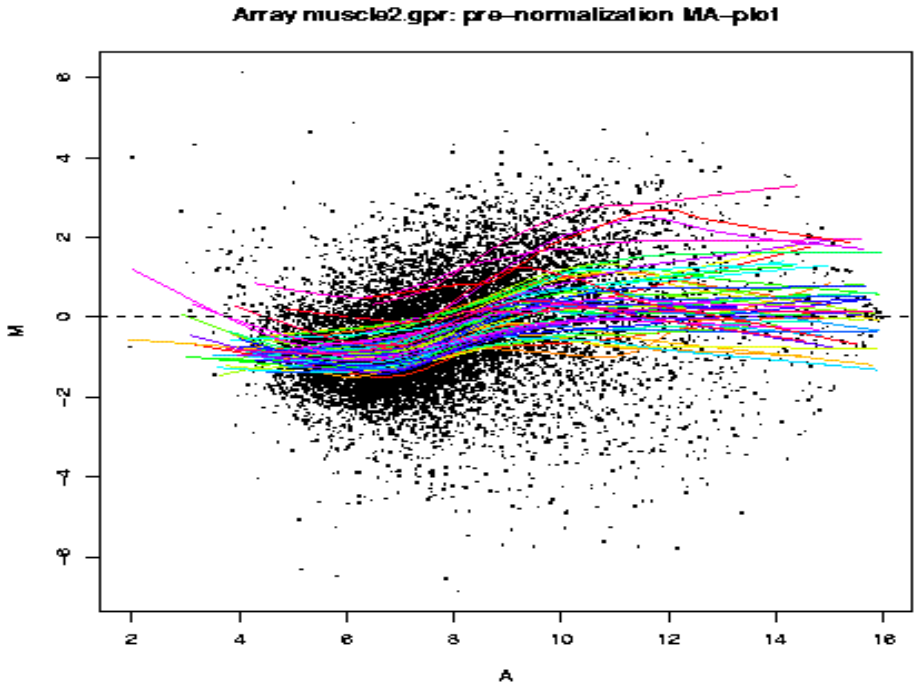

(B)

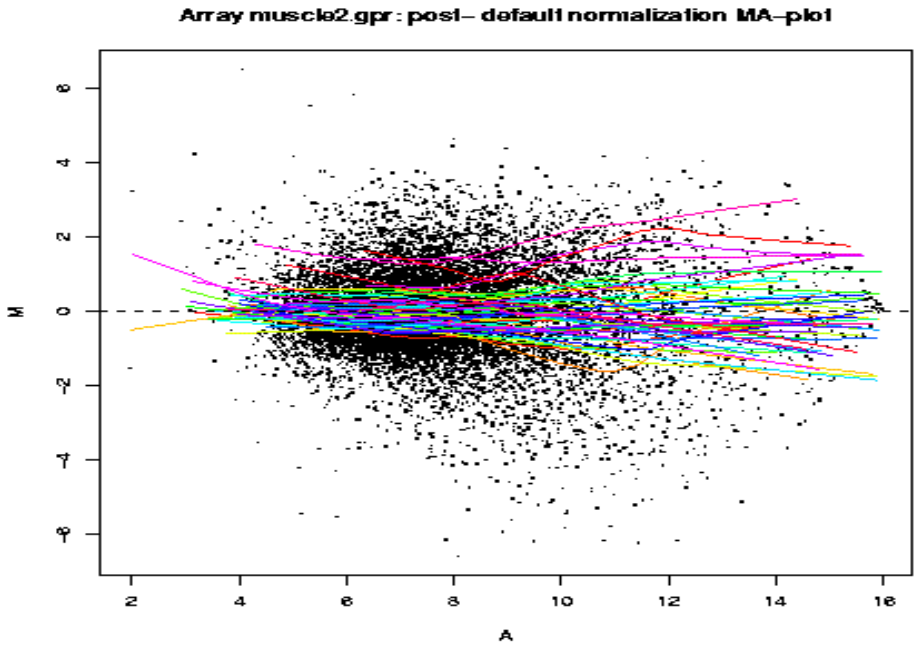

Fig 11 Median pixel intensities from muscle tissue of #5502 (T) Cy3 labeled RNA and control pool (C) Cy5 labeled RNA hybridized to pig array presented as scatter plots of $M = \log_2(T/C)$ vs. $A = \log_2(T*C)/2$.
(A) before (pro-) normalization, (B) after (post-) LOWESS normalization
(A)

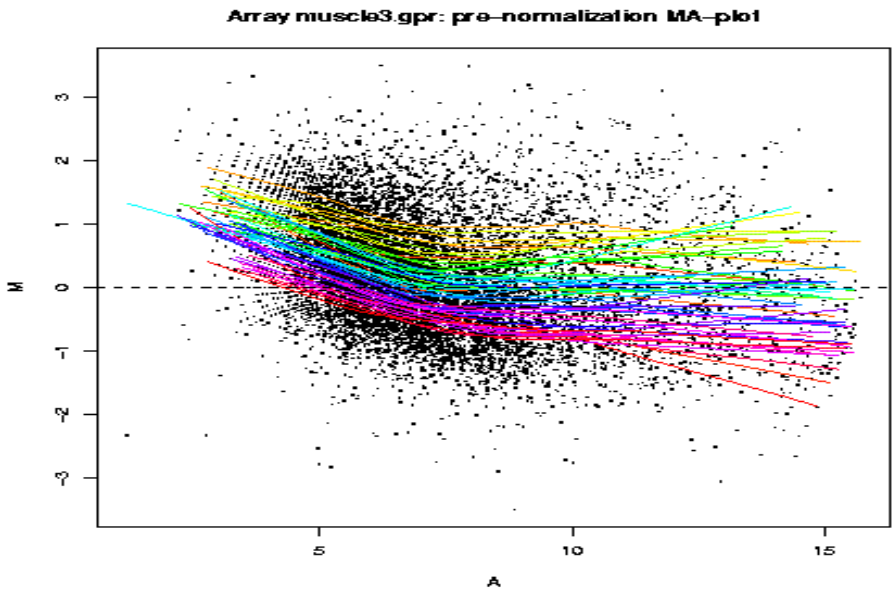

(B)

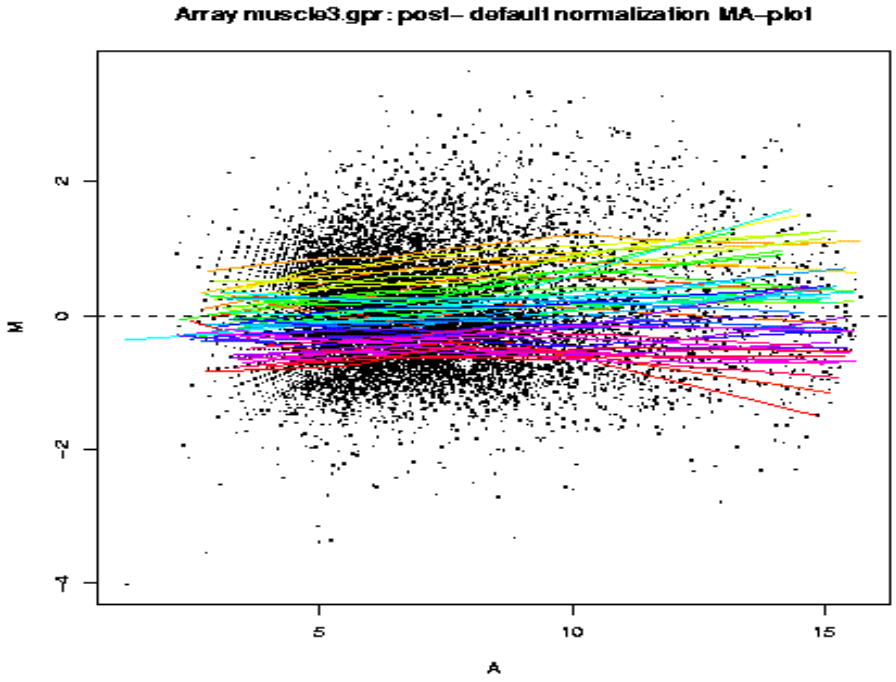

Fig 12 Median pixel intensities from muscle tissue of #6001 (T) Cy3 labeled RNA and control pool (C) Cy5 labeled RNA hybridized to pig array presented as scatter plots of $M = \log_2(T/C)$ vs. $A = \log_2(T*C)/2$.
(A) before (pro-) normalization, (B) after (post-) LOWESS normalization
(A)

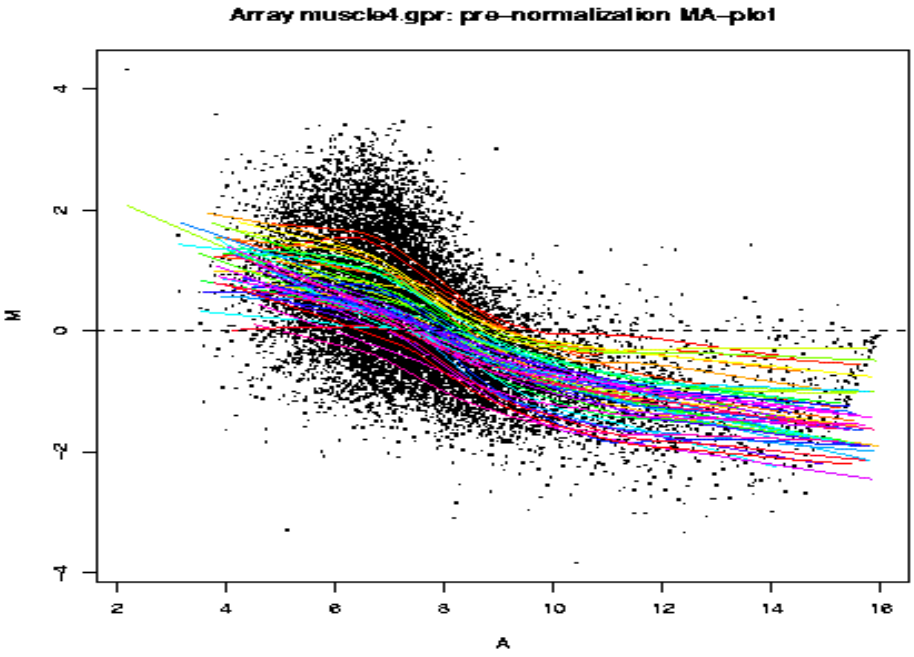

(B)

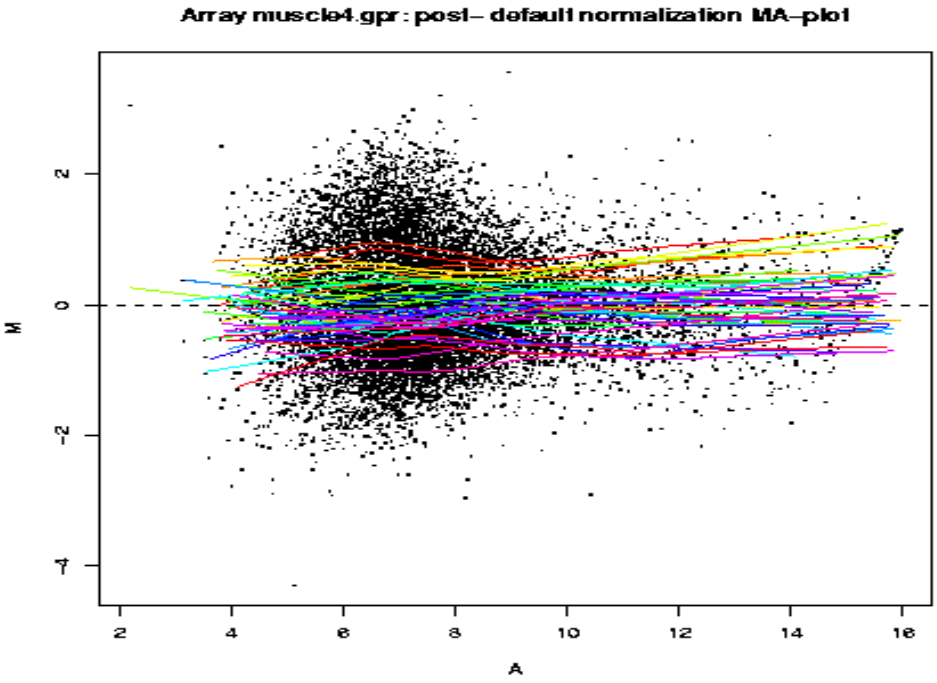

Appendix I. List of transcripts up/down regulated (top 200 highest/lowest Log_2ratio value) by dietary ractopamine supplement or dietary shifting (including Log_2ratio of each microarray analysis for biological replications)

Table 1. Transcripts highly up/down regulated determined by oligo-array in the adipose tissue by dietary supplement of Paylean^T (60ppm) (Chapter 2). For each transcript, log_2ratio=log_2(Paylean^T treated/ no Paylean^T treated).The positive value means higher mRNA abundance in Paylean^T treated pigs; negative value means lower mRNA abundance in Paylean^T treated pigs

Gene name	Log_2(R1/ G1)	Log_2(G2/ R2)	Log_2(G3/ R3)	Average
NADH/NADPHthyroidoxidasep138-tox[Susscrofa]	1.7701	2.7176	3.7438	2.7438
unknown	2.0000	1.0875	4.5437	2.5437
unknown	0.0825	2.5236	4.3030	2.3030
unknown	1.7814	1.5236	3.1525	2.1525
unknown	2.2095	0.8845	3.0470	2.0470
homologuetoGP2828068gbAAB99978.1BRCA1-associatedRINGdomainprotein{Homosapiens}.partial(15%)	1.1623	0.8826	4.0225	2.0225
surfactantproteinB[Susscrofa]	1.2224	1.8074	3.0149	2.0149
unknown	1.6699	1.3219	2.9959	1.9959
unknown	0.8365	1.0875	3.9620	1.9620
similartoGP15594005embCAC69823.p373c6.1(novelC2H2typezincfingerprotein){Homosapiens}.partial(19%)	1.6699	1.2479	2.9589	1.9589
25-hydroxyvitaminD31alpha-hydroxylase[Susscrofa]	1.6521	1.2630	2.9576	1.9576
unknown	1.3847	1.5146	2.9496	1.9496
homologuetoGP4235275gbAAD13152.1talin{Homosapiens}.partial(5%)	1.3890	1.4406	2.9148	1.9148
similartoSPP51690ARSE_HUMANArylsulfataseEprecursor(EC3.1.6.-)(ASE).[Human]{Homosapiens}.partial(38%)	1.2044	0.6245	3.9144	1.9144
unknown	1.8875	0.9349	2.9112	1.9112
butyrophilin[Susscrofa]	1.8845	0.9260	2.9053	1.9053
GP2224539dbjBAA20759.1KIAA0299{Homosapiens}.partial(9%)	1.1375	1.6699	2.9037	1.9037
porcineInterleukin2[Susscrofa]interleukin-2[Susscrofa]interleukin2precursor[Susscrofa]	1.3049	1.7948	2.5998	1.8998
unknown	1.6245	1.8699	2.1972	1.8972
unknown	1.6699	1.3155	2.6927	1.8927
pituitarytranscriptionfactor1beta[Susscrofa]	1.2505	1.8236	2.5871	1.8871
VLA-2[Susscrofa]	0.4150	2.0219	3.1685	1.8685
unknown	1.3536	1.3785	2.8661	1.8661
unknown	1.6130	1.3155	2.6642	1.8642
unknown	1.3626	1.4388	2.7507	1.8507
unknown	1.4919	1.7016	2.3467	1.8467
unknown	1.8182	0.6745	3.0463	1.8463
unknown	1.2016	1.8739	2.4378	1.8378
unknown	1.8231	1.2074	2.4152	1.8152
pot.ORF1(aa1-44)[Susscrofa]pot.ORF2(aa1-19)[Susscrofa]mAChR(aa1-460)[Susscrofa]	2.0000	0.9215	2.5107	1.8107
h2-calponin[Susscrofa]	1.7801	1.3219	2.3010	1.8010
estradiolreceptorbeta[Susscrofa]estrogenreceptorbeta[Susscrofa]estrogenreceptorbeta[Susscrofa]	1.1605	1.9150	2.2878	1.7878

matrixmetalloproteinase3precursor[Susscrofa]	1.1876	1.5656	2.5766	1.7766
similartoGP1684843gbAAB48302.1pinin{Bostaurus}.partial(19%)	1.0593	1.9686	2.2639	1.7639
unknown	1.0431	1.6507	2.5469	1.7469
unknown	0.9069	1.5850	2.7459	1.7459
Na+/H+exchangerisoform4[Susscrofa]	0.5525	1.4386	3.2456	1.7456
weaklysimilartoPIRI38488I38488trophinin-human.partial(37%)	1.4493	1.3297	2.4395	1.7395
homologuetoGP1054873gbAAA80977.1alpha-2IXcollagen{Homosapiens}.partial(31%)	1.2663	1.2876	2.6270	1.7270
homologuetoGP6331022dbjBAA86578.1KIAA1264protein{Homosapiens}.partial(9%)	1.3074	0.9375	2.9225	1.7225
unknown	0.8406	2.0000	2.3203	1.7203
homologuetoGP16444660gbAAL16407.1muscleatrophyF-boxprotein{Homosapiens}.partial(80%)	1.2630	1.4592	2.4111	1.7111
similartoSPO15375MOT6_HUMANMonocarboxylatetransporter6(MCT6)(MCT5).[Human]{Homosapiens}.partial(62%)	1.5677	1.2509	2.3093	1.7093
interleukin12receptorbeta2chain[Susscrofa]interleukin-12receptorbeta2[Susscrofa]	1.5224	1.0931	2.5078	1.7078
weaklysimilartoGP15082550gbAAH12183.1Unknown(proteinforMGC:20470){Homosapiens}.partial(34%)	1.3049	1.1069	2.7059	1.7059
unknown	1.1864	1.7224	2.2044	1.7044
unknown	1.2756	1.2325	2.6040	1.7040
unknown	1.9370	0.6699	2.5034	1.7034
homologuetoGP11693028gbAAG38938.1calcineurin-bindingproteincalsarcin-1{Homosapiens}.partial(49%)	1.5850	0.7140	2.7995	1.6995
DNA-directedRNApolymeraseIIpolypeptideB;POLR2B[Susscrofa]	1.3283	1.3677	2.3980	1.6980
unknown	1.0641	1.0219	2.9930	1.6930
unknown	1.5025	0.8814	2.6919	1.6919
unknown	0.8785	2.0000	2.1893	1.6893
myoglobin	1.4996	0.8745	2.6870	1.6870
unknown	1.5850	1.2802	2.1826	1.6826
steroidogenicfactor-1SF-1[Susscrofa]	1.5110	1.1541	2.3826	1.6826
weaklysimilartoSPQ14690RRP5_HUMANRRP5proteinhomolog(Fragment).[Human]{Homosapiens}.partial(13%)	1.4964	1.0601	2.4783	1.6783
unknown	1.3081	1.0484	2.6782	1.6782
unknown	1.3923	0.9635	2.6779	1.6779
unknown	0.7536	2.0000	2.2768	1.6768
voltage-dependentKchannel[Susscrofa]	1.0000	3.3505	0.6752	1.6752
unknown	2.5443	1.7975	0.6709	1.6709
unknown	2.4044	1.9260	0.6652	1.6652
homologuetoGP14017779dbjBAB47410.MEGF11protein(KIAA1781){Homosapiens}.partial(25%)	1.8679	2.0546	1.0612	1.6612
unknown	1.7162	2.6049	0.6605	1.6605
unknown	1.2388	2.6809	1.0599	1.6599
unknown	1.3985	0.8981	2.6483	1.6483
homologuetoGP17384624embCAC81020.kainatereceptorsubunit{Homosapiens}.partial(22%)	1.5146	1.1814	2.2480	1.6480
homologuetoGP13276649embCAB66508.hypotheticalprotein{Homosapiens}.partial(32%)	0.8625	1.4021	2.6323	1.6323
unknown	1.5146	2.1500	1.2323	1.6323
unknown	1.0000	1.7563	2.1282	1.6282
similartoSPQ9Y4L1OXRP_HUMAN150kDaoxygen-regulatedproteinprecursor(Orp150).[Human]{Homosapiens}.partial(17%)	1.1979	1.3506	2.3243	1.6243
enamelinprecursor[Susscrofa]	1.3479	0.8931	2.6205	1.6205

homologuetoGP11138034dbjBAB17758.KIAA1173protein{Homosapiens}.partial(31%)	1.3440	2.3931	1.1185	1.6185
sarcoendoplasmicreticulumcalciumATPase[Susscrofa]	1.2701	0.9668	2.6185	1.6185
homologuetoGP15559571gbAAH14146.1Unknown(proteinforMGC:20704){Homosapiens}.partial(57%)	0.9345	2.0000	1.9172	1.6172
unknown	0.7370	1.3854	2.7112	1.6112
myosinlightchain[Susscrofa]fastmyosinlightchain1F[Susscrofa]	1.3785	0.8413	2.6099	1.6099
weaklysimilartoGP7671629embCAB89275.2bA145L22.2(novelKRABboxcontainingC2H2typezincfingerprotein){Homosapiens}.partial(27%)	1.3344	1.0835	2.4090	1.6090
similartoPIRA45771A457712-5A-dependentRNAase-human.partial(23%)	1.1454	1.4653	2.2054	1.6054
similartoGP8574032embCAB94769.1b24o18.4(proteaseserine16(thymus)){Homosapiens}.partial(26%)	1.3668	0.8433	2.6050	1.6050
unknown	1.1926	1.3150	2.3038	1.6038
unknown	1.2439	0.9635	2.6037	1.6037
alpha-lactalbumin	0.6031	2.0000	2.2015	1.6015
unknown	0.9220	1.0768	2.7994	1.5994
homologuetoGP1665809dbjBAA13401.1SimilartoC.eleganshypothetical37.7kDprotein{Homosapiens}.partial(21%)	1.6130	0.5850	2.5990	1.5990
unknown	1.2288	0.9658	2.5973	1.5973
unknown	1.3561	1.0365	2.3963	1.5963
GP13905302gbAAH06949.1SimilartoATPaseclassIItype9A{Musmusculus}.partial(19%)	1.4150	0.7776	2.5963	1.5963
similartoGP13279167gbAAH04300.1Similartovillin-like{Homosapiens}.partial(18%)	0.7427	0.7004	3.3357	1.5929
similartoGP10438776dbjBAB15338.unnamedproteinproduct{Homosapiens}.partial(22%)	1.2630	1.9228	1.5929	1.5929
unknown	1.0153	1.7699	1.9926	1.5926
unknown	1.1864	0.9936	2.5900	1.5900
opticin[Susscrofa]	1.4330	1.2254	2.1092	1.5892
unknown	1.8657	0.7105	2.1881	1.5881
unknown	1.2563	0.9175	2.5869	1.5869
L-gulono-gamma-lactoneoxidase[Susscrofa]	1.0923	1.3809	2.2866	1.5866
unknown	1.6101	0.9607	2.1854	1.5854
similartoGP12840537dbjBAB24873.putative{Musmusculus}.partial(80%)	0.7313	1.9359	2.0836	1.5836
unknown	1.1283	1.0381	2.5832	1.5832
interleukin-13[Susscrofa]interleukin-13[Susscrofa]	1.7162	0.6406	2.3784	1.5784
GP1145789gbAAA97870.1neuroligin2{Rattusnorvegicus}.partial(21%)	1.1844	1.2696	2.2770	1.5770
unknown	1.3520	2.0000	1.3760	1.5760
unknown	1.0919	1.0566	2.5743	1.5743
weaklysimilartoGP8896138gbAAF81254.1pregnancy-associatedglycoprotein4{Susscrofa}.partial(25%)	0.8375	2.0000	1.8688	1.5688
unknown	1.0395	0.2969	3.3682	1.5682
unknown	0.8667	0.9685	2.8676	1.5676
albumin[Susscrofa]	1.3312	2.0000	1.3656	1.5656
apolipoproteinB	0.9069	0.8224	2.9646	1.5646
unknown	0.7271	2.0000	1.9636	1.5636
ART5protein[Susscrofa]	1.0105	1.7166	1.9635	1.5635
unknown	1.2479	0.8745	2.5612	1.5612
homologuetoGP1373169gbAAC50520.1autosomaldominantpolycystickidneydiseasetypeII{Homosapiens}.partial(19%)	1.1319	1.2875	2.2597	1.5597
unknown	1.2323	1.4854	1.9588	1.5588

unknown	1.3692	1.0454	2.2573	1.5573
unknown	1.2345	0.8745	2.5545	1.5545
homologuetoGP3114828embCAA06754.1JM5{Homosapiens}.partial(31%)	1.4044	1.0004	2.2524	1.5524
similartoGP13324451gbAAK18752.1putativeGprotein-coupledreceptorGPCR1precursor{Homosapiens}.partial(64%)	1.5475	0.8525	2.2500	1.5500
unknown	0.9386	1.3575	2.3481	1.5481
weaklysimilartoGP12859945dbjBAB31821.putative{Musmusculus}.partial(56%)	1.3458	1.2485	2.0471	1.5471
unknown	1.3785	1.0127	2.2456	1.5456
unknown	0.9831	1.6054	2.0442	1.5442
unknown	1.2410	1.3413	2.0412	1.5412
Tcellreceptorbeta-chain[Susscrofa]Tcellreceptorbeta-chain[Susscrofa]	1.1970	1.0826	2.3398	1.5398
unknown	1.3720	0.7063	2.5391	1.5391
unknown	1.0000	1.2753	2.3376	1.5376
unknown	1.1699	1.1931	2.2315	1.5315
homologuetoGP9651081dbjBAB03553.1hypotheticalprotein{Macacafascicularis}.partial(58%)	1.1979	1.3551	2.0265	1.5265
transmembraneleptinreceptor[Susscrofa]	1.1069	1.1411	2.3240	1.5240
similartoGP13183568gbAAK15262.1GTRGEO22{Musmusculus}.partial(60%)	0.6903	2.0565	1.8234	1.5234
homologuetoGP3003021gbAAC08996.1acetylcholinesteraseglycophospholipid-anchoredformprecursor{Feliscatus}.partial(19%)	1.3505	0.9939	2.2222	1.5222
unknown	0.7444	2.0000	1.8222	1.5222
erythropoietinreceptor[Susscrofa]	0.9280	1.4150	2.2215	1.5215
unknown	1.0661	1.2758	2.2209	1.5209
unknown	1.5339	2.0000	1.0170	1.5170
voltage-dependentpotassiumchannel[Susscrofa]potassiumvoltage-gatedchannel[Susscrofa]	1.6479	1.7843	1.1161	1.5161
weaklysimilartoGP16550968dbjBAB71080.unnamedproteinproduct{Homosapiens}.partial(46%)	0.7776	1.8538	1.9157	1.5157
unknown	0.9260	1.4043	2.2152	1.5152
unknown	1.2928	1.2370	2.0149	1.5149
GP9501803dbjBAB03308.1potassiumchannelinteractingprotein1{Rattusnorvegicus}.partial(37%)	1.1699	1.9587	1.4143	1.5143
unknown	1.3104	2.0144	1.2124	1.5124
unknown	1.6571	1.6656	1.2114	1.5114
homologuetoPIRT00390T00390KIAA0614protein-human(fragment).partial(7%)	1.0304	0.9912	2.5108	1.5108
unknown	1.5546	1.8634	1.1090	1.5090
homologuetoGP7637906gbAAF65253.1Ralguaninenucleotideexchangefactor RalGPS1A{Homosapiens}.partial(55%)	1.0785	1.6374	1.8080	1.5080
similartoGP13249297gbAAK16734.1bicarbonatetransporter-relatedproteinBTR1{Homosapiens}.partial(14%)	0.9456	1.2704	2.3080	1.5080
similartoGP12833761dbjBAB22654.putative{Musmusculus}.complete	1.0614	1.1511	2.3062	1.5062
unknown	0.8260	1.5844	2.1052	1.5052
SPQ9NP90RB9L_HUMANRas-relatedproteinRab-9L(RAB9-likeprotein).[Human]{Homosapiens}.partial(46%)	0.9220	1.3875	2.2047	1.5047
unknown	1.0850	1.4245	2.0047	1.5047
similartoGP16923707gbAAL31549.1glutathionetransferaseT1-1{Homosapiens}.complete	1.2996	1.0090	2.2043	1.5043
homologuetoGP7022449dbjBAA91602.1unnamedproteinproduct{Homosapiens}.partial(86%)	1.0614	0.9449	2.5031	1.5031
homologuetoSPP48443RXRG_HUMANRetinoicacidreceptorRXR-gamma.[Human]{Homosapiens}.partial(30%)	1.2479	1.2549	2.0014	1.5014

unknown	1.2395	1.9615	1.3005	1.5005
growthdifferentiationfactor9B[Susscrofa]	1.0375	1.0635	2.4005	1.5005
unknown	0.8921	1.3060	2.2991	1.4991
unknown	1.3329	1.1615	1.9972	1.4972
unknown	1.5505	1.6405	1.2955	1.4955
unknown	0.9098	1.3797	2.1948	1.4948
unknown	1.0211	1.2674	2.1942	1.4942
unknown	1.2854	1.3004	1.8929	1.4929
unknown	1.0271	1.0578	2.3925	1.4925
apolipoproteinC-III	1.2713	1.4078	1.7896	1.4896
somatostatin	1.4594	1.8194	1.1894	1.4894
weaklysimilartoSPQ05588UPAR_BOVINUrokinaseplasminogenactivatorsurfacereceptorprecursor(U-PAR)(CD87).[Bovine]{Bostaurus}.partial(46%)	0.8047	1.1699	2.4873	1.4873
brain-derivedneurotrophicfactorprecursor(AA-18to234)[Susscrofa]brain-derivedneurotrophicfactor[Susscrofa]	1.1769	1.2975	1.9872	1.4872
unknown	1.5333	1.8382	1.0858	1.4858
homologuetoGP12833806dbjBAB22670.putative{Musmusculus}.partial(43%)	1.0261	1.4406	1.9833	1.4833
homologuetoGP17226390gbAAL37760.1ventricularmyosinlightchain2{Canisfamiliaris}.partial(85%)	1.3388	1.8262	1.2825	1.4825
unknown	1.5288	1.6262	1.2925	1.4825
transforminggrowthfactor-betatypeIIIreceptor	0.8962	1.0677	2.4820	1.4820
homologuetoGP14669471gbAAK71934.1lysyloxidase-relatedproteinC{Homosapiens}.partial(14%)	1.4245	1.2377	1.7811	1.4811
homologuetoGP12803161gbAAH02384.1methionine-tRNAsynthetase{Homosapiens}.partial(12%)	1.0297	1.2316	2.1807	1.4807
unknown	0.7063	2.5538	1.1800	1.4800
unknown	1.3480	2.1085	0.9783	1.4783
unknown	1.5219	1.6301	1.2760	1.4760
unknown	0.9749	1.3765	2.0757	1.4757
similartoGP12654233gbAAH00936.1Similartohypotheticalproteinclone1-2{Homosapiens}.partial(30%)	1.5146	1.0361	1.8753	1.4753
weaklysimilartoGP15020653embCAC44536.hypotheticalprotein{Homosapiens}.partial(14%)	1.2801	1.2699	1.8750	1.4750
unknown	1.0000	1.3475	2.0738	1.4738
Tcellreceptorbeta-chain[Susscrofa]TCRbetachainV-beta-T13Vregion[Susscrofa]	1.4058	1.8408	1.1733	1.4733
unknown	1.6395	1.9069	0.8732	1.4732
unknown	0.9773	1.2678	2.1725	1.4725
unknown	1.6147	1.5219	1.2683	1.4683
unknown	1.1321	1.6045	1.6683	1.4683
unknown	1.0780	1.3580	1.9680	1.4680
similartoGP5911433gbAAD55791.1putativephosphate/phosphoenolpyruvatetranslocator{Rattusnorvegicus}.partial(33%)	1.7232	1.5090	1.1661	1.4661
homologuetoSPO88413TUL3_MOUSETubbyrelatedprotein3(Tubby-likeprotein3).[Mouse]{Musmusculus}.partial(44%)	1.2630	1.0674	2.0652	1.4652
homologuetoGP7020121dbjBAA91002.1unnamedproteinproduct{Homosapiens}.partial(58%)	1.1623	1.2672	1.9647	1.4647
unknown	1.3699	1.7574	1.2637	1.4637
unknown	1.3410	1.2850	1.7630	1.4630
unknown	1.4515	1.6730	1.2622	1.4622
homologuetoGP12846941dbjBAB27371.putative{Musmusculus}.partial(84%)	1.1561	1.2682	1.9622	1.4622

interleukin-7[Susscrofa]interleukin7precursor[Susscrofa]interleukin7[Susscrofa]	1.1882	1.7332	1.4607	1.4607
unknown	1.6743	1.7451	0.9597	1.4597
similartoGP177107gbAAA51533.1arachidonate12-lipoxygenase{Homosapiens}.partial(13%)	1.2451	1.8724	1.2587	1.4587
similartoGP12833402dbjBAB22510.putative{Musmusculus}.complete	0.9723	1.2438	2.1581	1.4581
homologuetoGP1239957gbAAB17015.1estrogenreceptor-relatedprotein{Homosapiens}.partial(17%)	-1.3255	-2.0660	-2.5208	-1.9708
unknown	-1.5035	-2.4689	-1.9412	-1.9712
unknown	-1.4224	-2.3212	-2.1868	-1.9768
unknown	-1.5392	-2.1456	-2.2474	-1.9774
unknown	-1.7202	-2.5352	-1.6777	-1.9777
homologuetoSPP05386RLA1_HUMAN60SacidicribosomalproteinP1.[Human]{Homosapiens}.complete	-1.5211	-2.7257	-1.6884	-1.9784
homologuetoGP15559423gbAAH14079.1Unknown(proteinforMGC:20582){Homosapiens}.partial(48%)	-1.5067	-2.5428	-1.8898	-1.9798
weaklysimilartoGP2072963gbAAC51270.1p40{Homosapiens}.partial(35%)	-1.5593	-2.6037	-1.7815	-1.9815
unknown	-1.7952	-2.5115	-1.6433	-1.9833
SPP43331SMD3_HUMANSmallnuclearribonucleoproteinSmD3(snRNPcoreproteinD3)(Sm-D3).[Human]{Homosapiens}.complete	-1.3167	-2.5626	-2.0746	-1.9846
SPP02383RS26_HUMAN40SribosomalproteinS26.[Rat]{Rattusnorvegicus}.complete	-1.3618	-2.2981	-2.2949	-1.9849
unknown	-1.5287	-2.0630	-2.3659	-1.9859
unknown	-1.6356	-2.6808	-1.6482	-1.9882
unknown	-1.3952	-2.8515	-1.7184	-1.9884
similartoSPO18778PAHX_BOVINPhytanoyl-CoAdioxygenaseperoxisomalprecursor(EC1.14.11.18)(Phytanoyl-CoAalpha-hydroxylase).partial(34%)	-1.6731	-2.1330	-2.1731	-1.9931
homologuetoSPP48201AT93_HUMANATPsynthaselipid-bindingproteinmitochondrialprecursor(EC3.6.1.34).complete	-1.5888	-2.0404	-2.3546	-1.9946
unknown	-1.1893	-2.3631	-2.4362	-1.9962
unknown	-1.4708	-2.1326	-2.3867	-1.9967
unknown	-1.6850	-2.1302	-2.1776	-1.9976
unknown	-1.4604	-2.6504	-1.8904	-2.0004
unknown	-1.4105	-2.4621	-2.1313	-2.0013
GP13542790gbAAH05598.1Similartodendriticcellprotein{Musmusculus}.partial(54%)	-1.2386	-2.4611	-2.3149	-2.0049
homologuetoSPQ9Z2U0PSA7_MOUSEProteasomesubunitalphatype7(EC3.4.25.1)(ProteasomesubunitRC6-1).[Mouse]{Musmusculus}.complete	-1.7126	-2.7463	-1.5694	-2.0094
unknown	-1.8745	-2.0309	-2.1327	-2.0127
similartoGP13569612gbAAK31162.1ubiquitinA-52residueribosomalproteinfusionproduct1{Homosapiens}.partial(73%)	-1.7062	-2.5392	-1.7927	-2.0127
homologuetoGP12847259dbjBAB27498.putative{Musmusculus}.partial(51%)	-1.2436	-2.4694	-2.3365	-2.0165
homologuetoGP13274518gbAAK17960.1complement-c1qtumornecrosisfactor-relatedprotein{Homosapiens}.partial(78%)	-1.4663	-2.6573	-1.9268	-2.0168
unknown	-1.7457	-2.0390	-2.2674	-2.0174
GP12654655gbAAH01165.1N-ethylmaleimide-sensitivefactorattachmentproteinalpha{Homosapiens}.partial(56%)	-1.4053	-2.7307	-1.9180	-2.0180
unknown	-1.6773	-2.1301	-2.2487	-2.0187
unknown	-0.9711	-3.1709	-1.9210	-2.0210
homologuetoGP13325337gbAAH04480.1Unknown(proteinforMGC:10520){Homosapiens}.partial(38%)	-0.9636	-2.4803	-2.6219	-2.0219
GP15929961gbAAH15405.1ribosomalproteinS5{Homosapiens}.complete	-1.6558	-2.4389	-1.9729	-2.0225
rig-analogDNA-bindingprotein[Susscrofa]	-1.5339	-2.1577	-2.3858	-2.0258

unknown	-1.3786	-2.8659	-1.8373	-2.0273
unknown	-1.6446	-2.0443	-2.3995	-2.0295
unknown	-1.5881	-2.3114	-2.1898	-2.0298
PIRJC2329JC2329translationinitiationfactoreIF-2betachain-rabbit.partial(36%)	-1.0037	-2.9479	-2.1408	-2.0308
unknown	-1.5104	-2.8649	-1.7227	-2.0327
GP15824485gbAAL09365.1DiGeorgesyndrome-relatedproteinFKSG5{Homosapiens}.complete	-0.9937	-2.8760	-2.2349	-2.0349
unknown	-1.6038	-2.1364	-2.3651	-2.0351
cystatinB[Susscrofa]	-1.4337	-2.7633	-1.9185	-2.0385
similartoPIRS11021S1102124-dienoyl-CoAreductase(NADPH)(EC1.3.1.34)-rat.partial(20%)	-1.4304	-2.4676	-2.2190	-2.0390
homologuetoGP15080078gbAAH11819.1DEAD/H(Asp-Glu-Ala-Asp/His)boxpolypeptide3{Homosapiens}.partial(19%)	-1.6332	-2.5422	-1.9527	-2.0427
unknown	-1.6715	-2.2190	-2.2452	-2.0452
unknown	-1.6011	-2.9412	-1.5962	-2.0462
SPP01252THYA_BOVINProthymosinalpha.[Bovine]{Bostaurus}.complete	-1.4431	-2.5628	-2.1380	-2.0480
homologuetoSPP37980IPYR_BOVINInorganicpyrophosphatase(EC3.6.1.1)(Pyrophosphatephospho-hydrolase)(PPase).[Bovine].partial(49%)	-1.6521	-2.6740	-1.8180	-2.0480
unknown	-1.7909	-2.6572	-1.6991	-2.0491
unknown	-1.6012	-2.7828	-1.7720	-2.0520
homologuetoGP3986482gbAAC84044.1translationinitiationfactoreIF3p40subunit;eIF3p40{Homosapiens}.partial(44%)	-1.6177	-2.3145	-2.2361	-2.0561
unknown	-1.6634	-2.6468	-1.8851	-2.0651
unknown	-1.3015	-2.3801	-2.5158	-2.0658
unknown	-1.3151	-2.2811	-2.6081	-2.0681
unknown	-1.2508	-2.3485	-2.6096	-2.0696
unknown	-1.5582	-2.2420	-2.4101	-2.0701
]NADH2[Susscrofa]NADHdehydrogenasesubunit2[Susscrofa]NADHdehydrogenasesubunit2[Susscrofa]	-1.5597	-2.8514	-1.8005	-2.0705
homologuetoSPQ02375NUYM_BOVINNADH-ubiquinoneoxidoreductase18kDasubunitmitochondrialprecursor(EC1.6.5.3)(EC1.6.99.3).complete	-1.6727	-2.7615	-1.7821	-2.0721
unknown	-1.6269	-2.8750	-1.7260	-2.0760
similartoGP14290496gbAAH09016.1Similartocomplementcomponent1qsubcomponentcpolypeptide{Homosapiens}.complete	-1.4862	-2.3459	-2.3961	-2.0761
unknown	-1.2846	-3.1695	-1.7771	-2.0771
similartoSPP28268TBA_EUPVATubulinalphachain.{Euplotesvannus}.partial(39%)	-1.2640	-2.6705	-2.3123	-2.0823
unknown	-1.7512	-3.4136	-1.0824	-2.0824
PIRS42409S42409proteintranslocationcomplexSec61betachainendoplasmicreticulum-dog.complete	-1.9453	-2.0631	-2.2442	-2.0842
PIRS08228S08228ribosomalproteinS2cytosolic-human(fragment).partial(94%)	-1.5355	-2.7670	-1.9562	-2.0862
unknown	-1.3967	-2.4920	-2.3793	-2.0893
unknown	-1.6358	-2.6898	-1.9528	-2.0928
homologuetoGP4929553gbAAD34037.1CGI-41protein{Homosapiens}.partial(44%)	-1.6054	-2.3822	-2.2938	-2.0938
cytochromeb5[Susscrofa]	-1.9852	-2.6529	-1.6440	-2.0940
homologuetoPIRB54211B54211H+-transportingATPsynthase(EC3.6.1.34)chaing-bovine.complete	-1.7981	-2.1604	-2.3242	-2.0942
unknown	-1.6053	-2.7134	-1.9643	-2.0943
unknown	-1.7935	-2.6881	-1.8058	-2.0958
similartoGP13093775embCAC29495.hypotheticalprotein{Homosapie	-1.3951	-2.2853	-2.6502	-2.1102

ns}.partial(61%)				
unknown	-1.6818	-2.3407	-2.3263	-2.1163
unknown	-1.5866	-2.4693	-2.2979	-2.1179
unknown	-1.0593	-3.3267	-1.9680	-2.1180
preprocathepsinH[Susscrofa]	-1.3166	-2.9811	-2.0588	-2.1188
unknown	-1.7721	-2.3517	-2.2569	-2.1269
unknown	-1.7421	-2.8345	-1.8083	-2.1283
homologuetoSPP27952RS2_RAT40SribosomalproteinS2.[Rat]{Rattusnorvegicus}.partial(91%)	-1.2222	-2.7869	-2.3795	-2.1295
unknown	-1.6887	-2.7542	-1.9515	-2.1315
unknown	-1.7285	-2.4573	-2.2279	-2.1379
tropomyosin4[Susscrofa]	-1.5159	-2.8729	-2.0294	-2.1394
unknown	-1.4850	-2.6167	-2.3209	-2.1409
cytolytictriggermoleculeG7CD16A.c[Susscrofa]	-1.8050	-2.8470	-1.7860	-2.1460
unknown	-1.6393	-2.4566	-2.3479	-2.1479
decorin[Susscrofa]	-1.6619	-2.8898	-1.9009	-2.1509
PIRA22632UQHUR7ubiquitin/ribosomalproteinS27acytosolic[validated]-human.complete	-1.7489	-2.4233	-2.2811	-2.1511
40SribosomalproteinS12[Susscrofa]	-1.9041	-2.7892	-1.7617	-2.1517
unknown	-1.1594	-3.4360	-1.8777	-2.1577
apolipoproteinRprecursor[Susscrofa]apolipoproteinRprecursor[Susscrofa]	-1.9525	-2.6341	-1.8883	-2.1583
homologuetoPIRD53737D53737phosphatecarrierproteinprecursormitochodrialspliceformB-bovine.partial(69%)	-1.7823	-2.3560	-2.3391	-2.1591
unknown	-1.5135	-2.3774	-2.5904	-2.1604
homologuetoGP5106998gbAAD39918.1HSPC040protein{Homosapiens}.complete	-1.6951	-2.8689	-1.9220	-2.1620
similartoSPP14622COXR_BOVINCytochromecoxidasepolypeptideVIII-livermitochondrialprecursor(EC1.9.3.1)(IX).[Bovine].complete	-1.7873	-2.7675	-1.9324	-2.1624
unknown	-0.3628	-3.5660	-2.5644	-2.1644
unknown	-1.8910	-3.0859	-1.5175	-2.1648
unknown	-1.6164	-2.1783	-2.7074	-2.1674
homologuetoPIRS11696A29170phosphopyruvatehydratase(EC4.2.1.11)alpha-human.complete	-1.8712	-2.9757	-1.6584	-2.1684
hyaluronansynthase2[Susscrofa]	-1.6703	-2.4731	-2.3717	-2.1717
unknown	-1.6929	-3.1517	-1.6723	-2.1723
SPP12947RL31_HUMAN60SribosomalproteinL31.[Pig]{Susscrofa}.complete	-1.5726	-2.9856	-1.9641	-2.1741
similartoSPP42929HS27_CANFAHeatshock27kDaprotein(HSP27).[Dog]{Canisfamiliaris}.complete	-1.4851	-2.7896	-2.2724	-2.1824
unknown	-2.0000	-2.6352	-1.9126	-2.1826
SPP18621RL17_HUMAN60SribosomalproteinL17(L23).[Human]{Homosapiens}.complete	-1.7138	-2.4646	-2.3742	-2.1842
SPP38663RL24_HUMAN60SribosomalproteinL24(L30).[Bovine]{Bostaurus}.complete	-1.9013	-2.7468	-1.9191	-2.1891
similartoGP3126984gbAAC16021.1CAG-isl7{Homosapiens}.complete	-1.6517	-2.3731	-2.5524	-2.1924
SPQ9C005DP30_HUMANDpy-30-likeprotein.[Human]{Homosapiens}.complete	-1.7751	-2.4289	-2.4020	-2.2020
PIRG01229G01229cappingproteinalpha-human(fragment).partial(25%)	-1.4773	-2.2999	-2.8336	-2.2036
homologuetoGP12843076dbjBAB25849.putative{Musmusculus}.partial(85%)	-1.3065	-2.9674	-2.3469	-2.2069
PIRS55913S55913ribosomalproteinL21cytosolic-human.complete	-1.8416	-2.7528	-2.0272	-2.2072
unknown	-1.5838	-2.3854	-2.6596	-2.2096

unknown	-1.8738	-2.8696	-1.8917	-2.2117
unknown	-1.3306	-3.5409	-1.7757	-2.2157
homologuetoSPQ95140RLA0_BOVIN60SacidicribosomalproteinP0(L10E)(Fragment).[Bovine]{Bostaurus}.complete	-2.0490	-2.9203	-1.6896	-2.2196
SPP05209TBA1_CRIGRTubulinalpha-1chain.[Chinesehamster]{Cricetulusgriseus}.partial(42%)	-1.6812	-2.1309	-2.8511	-2.2211
GP17932958dbjBAB79470.ribosomalproteinL34{Homosapiens}.complete	-1.8143	-2.3622	-2.4932	-2.2232
cytoplasmiclight-chaindynein[Susscrofa]	-1.8473	-2.7941	-2.0357	-2.2257
unknown	-1.8339	-2.1644	-2.6891	-2.2291
similartoGP16197488dbjBAB69947.legumain{Bostaurus}.complete	-2.0236	-2.3476	-2.3206	-2.2306
homologuetoPIRS18294EFHU2translationelongationfactoreEF-2-human.partial(19%)	-1.6235	-2.1689	-2.9012	-2.2312
unknown	-1.5823	-2.5354	-2.5839	-2.2339
homologuetoPIRI51803I51803TAXREB107-human.partial(88%)	-2.0782	-2.8705	-1.7693	-2.2393
weaklysimilartoGP2648023embCAB09994.1cICF0811.6(chromosome6openreadingframe11(BING4)){Homosapiens}.partial(49%)	-1.7698	-2.1737	-2.7817	-2.2417
unknown	-1.0183	-3.7430	-1.9756	-2.2456
PIRS38962S38962serpin-pig.partial(64%)	-1.5418	-3.2145	-1.9882	-2.2482
unknown	-1.8697	-2.4605	-2.4351	-2.2551
similartoGP14250636gbAAH08782.1nuclearfactorofkappalightpolypeptidegeneenhancerinB-cellsinhibitor-like2{Homosapiens}.partial(24%)	-1.7898	-2.2719	-2.7059	-2.2559
unknown	-1.0286	-3.8500	-1.8993	-2.2593
weaklysimilartoGP11345388gbAAG34681.1lysosomalthiolreductaseprecursor{Musmusculus}.complete	-1.7908	-2.3406	-2.6507	-2.2607
homologuetoSPP13272UCRI_BOVINUbiquinol-cytochromeCreductaseiron-sulfursubunitmitochondrialprecursor(EC1.10.2.2).partial(49%)	-2.1490	-2.6899	-1.9995	-2.2795
similartoGP15779050gbAAH14597.1SimilartoRIKENcDNA1700052K15gene{Homosapiens}.partial(28%)	-1.5267	-3.4388	-1.8828	-2.2828
homologuetoPIRA26437UQHUBpolyubiquitin3-human.partial(85%)	-1.8709	-2.1356	-2.8432	-2.2832
unknown	-1.3980	-2.6921	-2.7800	-2.2900
PIRS49326S49326nascentpolypeptide-associatedcomplexalphachain-human.complete	-1.8686	-2.9801	-2.0344	-2.2944
GP14719845gbAAD20460.3ribosomalproteinL11{Homosapiens}.complete	-1.7992	-2.9785	-2.1188	-2.2988
PIRS34755S3475514-3-3protein(clone1054)-human.complete	-1.5856	-3.6472	-1.7014	-2.3114
unknown	-1.7802	-2.9802	-2.1852	-2.3152
GP7688693gbAAF67487.130kDaprotein{Homosapiens}.partial(63%)	-1.8751	-2.3442	-2.7547	-2.3247
unknown	-2.0421	-3.0284	-1.9352	-2.3352
homologuetoGP15186717dbjBAB62888.TdTbindingprotein{Homosapiens}.partial(50%)	-1.0900	-3.6706	-2.2453	-2.3353
unknown	-2.0587	-3.0932	-1.8560	-2.3360
homologuetoSPO88322NID2_MOUSENidogen-2precursor(NID-2)(Entactin-2).[Mouse]{Musmusculus}.partial(9%)	-2.0179	-2.3137	-2.7058	-2.3458
GP6624731embCAB63859.1putativenonclassicalMHCclassIantigen{Susscrofa}.complete	-1.7254	-2.8693	-2.4474	-2.3474
dihydrolipoamideacetyltransferase[Susscrofa]	-1.9272	-2.0611	-3.0592	-2.3492
unknown	-2.2722	-2.7953	-1.9938	-2.3538
unknown	-2.0615	-2.4976	-2.5046	-2.3546
PIRJC4662JC4662ribosomalproteinS3acytosolic-human.complete	-2.0549	-3.2136	-1.8542	-2.3742
SPP23131RL23_HUMAN60SribosomalproteinL23(L17).[Pig]{Susscrofa}.complete	-2.1121	-2.3681	-2.6451	-2.3751
unknown	-1.4334	-3.6848	-2.0341	-2.3841
malatedehydrogenasedecarboxylase(NADP+)[Susscrofa]	-1.8353	-2.4937	-2.8395	-2.3895

unknown	-2.2063	-2.3490	-2.6527	-2.4027
homologuetoSPQ9DBS5KLC3_MOUSEProbablekinesinlightchain3(KLC3).[Mouse]{Musmusculus}.partial(37%)	-1.5627	-3.9234	-1.7981	-2.4281
similartoGP12654605gbAAH01138.1SimilartohexosaminidaseA(alph apolypeptide){Homosapiens}.partial(40%)	-1.8925	-3.2687	-2.1456	-2.4356
Igkappachain	-1.5681	-3.6811	-2.0846	-2.4446
homologuetoGP12804601gbAAH01722.1CGI-99protein{Homosapiens}.complete	-2.2066	-2.3516	-2.7891	-2.4491
fibrillin-1precursor[Susscrofa]	-2.2117	-3.2714	-1.8716	-2.4516
unknown	-1.9590	-2.4565	-2.9577	-2.4577
homologuetoGP14286220gbAAH08906.1enoylCoenzymeAhydratase shortchain1mitochondrial{Homosapiens}.partial(50%)	-1.7922	-3.6168	-2.0295	-2.4795
unknown	-1.4482	-3.6817	-2.3550	-2.4950
similartoGP29539embCAA28407.1precursorofC1r(AA-17to688){Homosapiens}.partial(10%)	-1.8083	-3.6475	-2.0529	-2.5029
unknown	-2.0807	-2.3916	-3.0462	-2.5062
unknown	-1.7158	-3.8660	-1.9809	-2.5209
homologuetoSPQ9UL46PSE2_HUMANProteasomeactivatorcomplex subunit2(Proteasomeactivator28-betasubunit)(PA28beta)(PA28b).complete	-2.0141	-2.9879	-2.6210	-2.5410
similartoGP558908gbAAA67727.1reversetranscriptase{Musmusculus}.partial(10%)	-1.8824	-2.6948	-3.0836	-2.5536
unknown	-1.6446	-3.2375	-2.8010	-2.5610
similartoGP12833323dbjBAB22481.putative{Musmusculus}.complete	-2.1386	-2.4848	-3.0617	-2.5617
homologuetoSPP17665COXO_MOUSECytochromecoxidasepolypeptideVIIcmitochondrialprecursor(EC1.9.3.1).[Mouse]{Musmusculus}.complete	-2.2571	-2.3134	-3.1702	-2.5802
S100Cprotein[Susscrofa]S100C[Susscrofa]	-1.8383	-2.8750	-3.0317	-2.5817
similartoGP14279576gbAAK58638.1interferon-inducedprotein1-8U{Bostaurus}.partial(89%)	-2.1011	-3.5838	-2.1074	-2.5974
MHCclassIIDR-alpha	-2.2021	-3.6807	-1.9214	-2.6014
homologuetoSPO95445APOM_HUMANApolipoproteinM(ApoM)(G3a)(HSPC336).[Human]{Homosapiens}.complete	-1.5496	-3.3457	-2.9127	-2.6027
Ca2+ATPaseoffasttwitch1skeletalmusclesarcoplasmicreticulum[Susscrofa]	-2.5535	-2.0683	-3.2109	-2.6109
unknown	-2.4346	-2.6497	-2.7522	-2.6122
homologuetoGP10717134gbAAG22029.1carbonicanhydraseIII{Musmusculus}.complete	-1.5791	-2.6975	-3.7133	-2.6633
unknown	-1.8741	-3.9888	-2.1965	-2.6865
unknown	-2.1522	-3.1928	-2.8075	-2.7175
unknown	-2.3915	-3.8634	-1.9125	-2.7225
homologuetoPIRT14797T14797hypotheticalproteinDKFZp564B167.1-human.complete	-2.0901	-2.6139	-3.4770	-2.7270
unknown	-2.7707	-2.3274	-3.1041	-2.7341
homologuetoGP12835239dbjBAB23198.putative{Musmusculus}.partial(24%)	-2.6937	-3.6766	-1.8652	-2.7452
homologuetoGP13879314gbAAH06632.1Unknown(proteinforIMAGE:3481996){Musmusculus}.partial(23%)	-2.6148	-3.8678	-1.7563	-2.7463
stearyl-CoAdesaturase[Susscrofa]	-2.3930	-3.6949	-2.2040	-2.7640
MHCclassIantigen[Susscrofa]MHCclassIantigen[Susscrofa]	-2.1832	-2.9851	-3.1691	-2.7791
similartoGP18139943gbAAL60202.1X-boxbindingproteinprocessedisoform{Musmusculus}.partial(47%)	-3.9642	-2.8622	-1.5532	-2.7932
homologuetoPIRA40119SNHUINinsulysin(EC3.4.24.56)[validated]-human.partial(16%)	-1.8098	-3.1682	-3.7640	-2.9140
SLA-DR1beta1domain[Susscrofa]	-2.4055	-4.2679	-2.1817	-2.9517
immunoglobulinlambda-chainimmunoglobulinlambdachain[Susscrofa]	-1.4962	-4.8754	-2.5708	-2.9808
similartoSPQ28022MGP2_BOVINMicrofibril-associatedglycoprotein2precursor(MAGP-	-2.7404	-2.6714	-3.5309	-2.9809

2)(MP25).[Bovine]{Bostaurus}.partial(85%)				
SLA-DQbeta1domain[Susscrofa]SLA-DQbeta1domain[Susscrofa]	-2.4513	-3.6160	-2.9586	-3.0086
putativeolfactoryreceptor-likeprotein[Susscrofa]	-2.7296	-3.6798	-2.6497	-3.0197
unknown	-2.9464	-3.5569	-2.8466	-3.1166
beta2-microglobulinbeta-2-microglobulinprotein[Susscrofa]	-2.3536	-3.0963	-3.9849	-3.1449
similartoGP443671gbAAB59537.1complementcomponentC4A{Homo sapiens}.partial(6%)	-2.3474	-3.6868	-3.5271	-3.1871
unknown	-3.1231	-3.9207	-2.9819	-3.3419
unknown	-3.3282	-3.8706	-3.7944	-3.6644
salivarylipocalin[Susscrofa]	-4.9285	-5.0744	-6.1415	-5.3815

Table 2. Transcripts highly up/down regulated determined by oligo-array in the liver tissue by the dietary shifting from LFD to HFD (Chapter 3). For each transcript, $\log_2$ratio=$\log_2$(HFD/LFD).The positive value means higher mRNA abundance in HFD pigs; negative value means lower mRNA abundance in HFD pigs

Gene Name	$\log_2$(R1/G1)	$\log_2$(R2/G2)	$\log_2$(G3/R3)	$\log_2$(G4/R4)	Average
unknown	3.2084	5.8379	6.8249	2.2214	4.5232
unknown	3.1699	5.3576	5.2436	3.2839	4.2637
unknown	3.8387	4.1352	1.8144	6.1594	3.9869
homologue to GP|6331022|dbj|BAA86578.1 KIAA1264 protein {Homo sapiens}, partial (9%)	3.5748	4.2365	1.6245	6.1868	3.9057
unknown	3.6472	4.1085	2.1203	5.6355	3.8779
unknown	3.3400	4.2245	2.9696	4.5949	3.7823
unknown	2.4150	5.0255	3.8188	3.6218	3.7203
unknown	2.7975	4.4897	3.6209	3.6663	3.6436
unknown	3.7197	3.5560	2.0196	5.2562	3.6379
homologue to SP|Q62813|LAMP_RAT Limbic system-associated membrane protein precursor (LSAMP). [Rat] {Rattus norvegicus}, partial (37%)	3.4072	3.8480	1.3269	5.9283	3.6276
unknown	3.6483	3.5826	2.2303	5.0005	3.6154
endothelin receptor subtype A, ETA receptor [swine, lung, Peptide, 427 aa]	3.8000	3.3808	4.6049	2.5759	3.5904
unknown	3.3385	3.7318	4.5850	2.4853	3.5351
unknown	3.6537	3.2745	2.6731	4.2551	3.4641
unknown	4.1906	2.7205	1.2668	5.6442	3.4555
unknown	4.3155	2.5104	1.9701	4.8558	3.4129
unknown	3.7761	2.9871	1.6781	5.0851	3.3816
homologue to PIR|A38096|A38096 perlecan precursor - human, partial (4%)	3.2693	3.4650	0.2382	6.4961	3.3671
unknown	3.4842	3.2364	1.4994	5.2212	3.3603
unknown	3.4941	3.2042	1.2763	5.4220	3.3491
unknown	3.9152	2.6759	0.3551	6.2360	3.2956
unknown	3.4692	3.0506	1.0000	5.5199	3.2599
unknown	3.0211	3.4849	0.1389	6.3671	3.2530
homologue to GP|8100510|gb|AAF72335.1| Y-box protein ZONAB-A {Canis familiaris}, partial (26%)	3.6153	2.8407	1.4085	5.0475	3.2280
unknown	3.4936	2.9617	0.9155	5.5398	3.2277
unknown	3.3663	3.0184	0.7119	5.6728	3.1924
unknown	3.1608	3.1933	1.8569	4.4972	3.1770
unknown	3.4429	2.9005	0.4171	5.9263	3.1717

unknown	3.2224	3.1085	0.0995	6.2314	3.1655
unknown	3.1375	3.0205	0.8553	5.3027	3.0790
unknown	2.7987	3.2835	-0.2774	6.3596	3.0411
unknown	3.7445	2.2722	0.6138	5.4029	3.0083
unknown	3.2920	2.7225	0.7551	5.2594	3.0072
unknown	3.0433	2.9053	-0.1585	6.1071	2.9743
unknown	3.0255	2.8698	1.3956	4.4997	2.9477
unknown	2.6135	3.2345	1.1024	4.7456	2.9240
unknown	3.7442	1.9929	0.2360	5.5011	2.8685
unknown	3.4948	2.2332	-0.3699	6.0979	2.8640
unknown	3.5236	2.2029	1.1255	4.6010	2.8633
unknown	3.2730	2.4485	0.5372	5.1843	2.8607
unknown	2.8560	2.8138	0.0970	5.5727	2.8349
homologue to GP|12860213|dbj|BAB31879. putative {Mus musculus}, partial (65%)	3.2386	2.4046	2.0386	3.6046	2.8216
unknown	3.1651	2.4525	0.4985	5.1191	2.8088
unknown	2.7389	2.8402	1.1497	4.4294	2.7896
unknown	3.1797	2.3863	0.7029	4.8631	2.7830
homologue to GP|16306782|gb|AAH01585.1 ligatin {Homo sapiens}, partial (30%)	3.2854	2.1753	0.3930	5.0677	2.7304
unknown	3.5327	1.9031	1.0112	4.4246	2.7179
unknown	2.8309	2.5900	0.6651	4.7558	2.7105
unknown	3.2957	2.0979	0.7092	4.6844	2.6968
unknown	2.6189	2.6909	0.5450	4.7648	2.6549
unknown	2.9417	2.3635	2.0959	3.2093	2.6526
unknown	2.8770	2.3959	0.9773	4.2956	2.6365
unknown	2.8284	2.3890	1.0568	4.1606	2.6087
unknown	3.1009	2.0894	1.5783	3.6120	2.5951
unknown	3.2536	1.9160	1.3813	3.7882	2.5848
unknown	2.3612	2.7803	1.4150	3.7264	2.5707
homologue to GP|1389694|gb|AAB02905.1| FX-induced thymoma transcript {Mus musculus}, partial (43%)	3.9854	1.1375	1.0173	4.1056	2.5614
unknown	2.1615	2.9329	0.8646	4.2298	2.5472
unknown	2.7225	2.3154	1.2402	3.7976	2.5189
unknown	2.4245	2.6122	1.3740	3.6627	2.5183
unknown	3.2056	1.8282	1.7370	3.2969	2.5169
unknown	3.0334	1.9728	1.6781	3.3282	2.5031
unknown	3.3278	1.6632	1.4477	3.5434	2.4955
unknown	1.8948	3.0875	1.0904	3.8919	2.4911
unknown	2.2161	2.7646	0.2730	4.7076	2.4903
unknown	2.0199	2.9584	1.5590	3.4194	2.4892
unknown	2.6677	2.3029	2.1525	2.8181	2.4853
unknown	2.6705	2.2876	1.9955	2.9626	2.4791
homologue to GP|12803695|gb|AAH02683.1 neuritin {Homo sapiens}, partial (88%)	1.3312	3.6245	2.0810	2.8747	2.4778
unknown	1.7843	3.1699	-0.3440	5.2982	2.4771
unknown	2.9190	2.0293	1.8604	3.0879	2.4742
unknown	3.3817	1.5361	1.0012	3.9166	2.4589
unknown	3.1775	1.7056	1.6960	3.1870	2.4415

unknown	1.7708	3.1085	0.1255	4.7538	2.4397
calcineurin catalytic subunit delta isoform [Sus scrofa]	3.1528	1.6861	0.4393	4.3996	2.4195
unknown	2.3376	2.4935	1.7952	3.0359	2.4156
unknown	2.6845	2.1113	1.4594	3.3363	2.3979
homologue to GP|12655231|gb|AAH01474.1 Unknown (protein for IMAGE:3138844) {Homo sapiens}, partial (13%)	3.2283	1.5375	1.8211	2.9447	2.3829
similar to GP|7329074|gb|AAF59902.1| collagen type V alpha 3 chain {Homo sapiens}, partial (4%)	2.9936	1.7667	0.6586	4.1018	2.3802
unknown	3.3124	1.4374	0.6249	4.1249	2.3749
unknown	2.6695	2.0461	1.0364	3.6792	2.3578
unknown	3.3397	1.3735	0.1239	4.5893	2.3566
unknown	1.8981	2.8142	2.6951	2.0172	2.3562
unknown	2.7446	1.9542	0.9637	3.7351	2.3494
unknown	1.7472	2.9307	1.7081	2.9699	2.3390
similar to GP|6467994|gb|AAF13271.1| CBL-B {Rattus norvegicus}, partial (49%)	1.2350	3.3923	1.7675	2.8599	2.3137
unknown	2.5797	2.0381	0.2469	4.3709	2.3089
unknown	2.3428	2.2521	1.0984	3.4965	2.2975
unknown	2.2184	2.3717	1.4406	3.1495	2.2951
unknown	2.9404	1.6384	1.0189	3.5600	2.2894
unknown	1.8398	2.7235	0.9704	3.5929	2.2817
unknown	2.4530	2.1037	1.7821	2.7746	2.2783
unknown	2.7959	1.7608	2.3453	2.2114	2.2783
unknown	1.8346	2.7199	1.1484	3.4061	2.2772
unknown	1.8931	2.6521	1.5715	2.9736	2.2726
unknown	3.0190	1.5070	1.1754	3.3505	2.2630
unknown	2.7588	1.7442	0.7272	3.7758	2.2515
unknown	2.4561	2.0388	1.4222	3.0727	2.2474
unknown	3.7521	0.7182	0.9272	3.5431	2.2352
unknown	2.1893	2.2801	-0.2073	4.6768	2.2347
unknown	3.1849	1.2551	2.2166	2.2234	2.2200
unknown	2.2455	2.1926	0.9133	3.5249	2.2191
unknown	3.1085	1.3293	0.8850	3.5529	2.2189
unknown	2.9165	1.5045	1.0636	3.3574	2.2105
similar to SP|Q16790|CAH9_HUMAN Carbonic anhydrase IX precursor (EC 4.2.1.1) (Carbonate dehydratase IX) (CA-IX) (CAIX), partial (56%)	3.2088	1.2099	1.1262	3.2924	2.2093
unknown	2.1788	2.2168	0.6384	3.7572	2.1978
unknown	2.9747	1.4099	0.8497	3.5349	2.1923
unknown	2.8219	1.5552	1.2687	3.1084	2.1886
unknown	2.3440	2.0258	0.2009	4.1689	2.1849
homologue to GP|16550722|dbj|BAB71035. unnamed protein product {Homo sapiens}, partial (34%)	3.1864	1.1725	0.8881	3.4708	2.1794
unknown	3.3337	0.9907	0.9069	3.4175	2.1622
unknown	2.6551	1.6473	0.9334	3.3690	2.1512
sarcoendoplasmic reticulum calcium ATPase [Sus scrofa]	1.8835	2.4150	0.6394	3.6591	2.1493
unknown	2.6280	1.6666	1.0191	3.2755	2.1473
unknown	2.4631	1.8257	0.8564	3.4323	2.1444
weakly similar to SP|O95661|RHOI_HUMAN Rho-related GTP-binding protein RhoI. [Human] {Homo sapiens}, partial	2.7349	1.5431	0.4034	3.8747	2.1390

(79%)					
homologue to SP|P13213|SPRC_BOVIN SPARC precursor (Secreted protein acidic and rich in cysteine) (Osteonectin) (ON), partial (50%)	1.0000	3.2538	1.3491	2.9046	2.1269
unknown	2.0718	2.1809	0.9310	3.3218	2.1264
unknown	2.9075	1.3405	0.7768	3.4713	2.1240
unknown	2.4868	1.7517	1.1553	3.0832	2.1193
unknown	2.4874	1.7304	0.2208	3.9970	2.1089
unknown	2.7442	1.4481	1.0935	3.0987	2.0961
unknown	2.8931	1.2987	1.1279	3.0638	2.0959
homologue to GP|6634025|dbj|BAA20833.2 KIAA0379 protein {Homo sapiens}, partial (21%)	3.7127	0.4780	1.1354	3.0553	2.0954
unknown	2.7142	1.4496	1.1066	3.0573	2.0819
unknown	2.1240	2.0092	1.3692	2.7640	2.0666
unknown	2.3410	1.7625	0.8480	3.2555	2.0518
unknown	2.2479	1.8532	1.2778	2.8233	2.0505
unknown	3.2888	0.8074	1.7147	2.3814	2.0481
unknown	3.0361	1.0521	0.4594	3.6288	2.0441
unknown	2.8103	1.2587	1.2337	2.8354	2.0345
immunoglobulin heavy chain [Sus scrofa]	2.6229	1.4395	0.5956	3.4669	2.0312
unknown	1.3219	2.7291	0.4263	3.6248	2.0255
unknown	1.9475	2.0623	0.9622	3.0476	2.0049
unknown	2.6689	1.3012	1.2787	2.6914	1.9850
unknown	2.6963	1.2704	0.7049	3.2618	1.9834
unknown	3.0306	0.9018	0.7012	3.2312	1.9662
unknown	3.2224	0.7078	0.2559	3.6743	1.9651
unknown	2.2801	1.6101	0.6250	3.2652	1.9451
unknown	3.2388	0.6439	-2.9579	6.8406	1.9413
unknown	1.9087	1.9260	2.0000	1.8347	1.9174
unknown	2.5078	1.3219	1.1069	2.7228	1.9149
unknown	1.7955	2.0202	1.3962	2.4195	1.9079
unknown	2.6660	1.1410	1.1708	2.6361	1.9035
homologue to GP|11041489|dbj|BAB17282. hypothetical protein {Macaca fascicularis}, partial (58%)	1.5361	2.2679	0.5257	3.2783	1.9020
unknown	2.6393	1.1634	0.0137	3.7891	1.9014
unknown	2.1520	1.6464	0.7144	3.0839	1.8992
unknown	2.5142	1.2812	2.2082	1.5872	1.8977
unknown	2.5632	1.2317	1.3877	2.4072	1.8975
GP|15489242|gb|AAH13725.1 Unknown (protein for IMAGE:3859726) {Homo sapiens}, partial (52%)	2.8415	0.9438	2.5321	1.2532	1.8927
unknown	1.7718	2.0000	0.2990	3.4729	1.8859
homologue to GP|12060855|gb|AAG48269.1 serologically defined breast cancer antigen NY-BR-96 {Homo sapiens}, partial (24%)	3.2987	0.4581	0.9329	2.8240	1.8784
unknown	2.7618	0.9903	2.1451	1.6070	1.8761
unknown	1.6848	2.0611	1.7817	1.9642	1.8730
unknown	2.1988	1.5429	1.6004	2.1413	1.8708
unknown	2.8319	0.8981	2.0166	1.7134	1.8650
unknown	3.1155	0.6114	2.0129	1.7140	1.8635
unknown	1.5146	2.2016	1.8305	1.8857	1.8581

unknown	2.6893	1.0194	1.6362	2.0725	1.8543
galanin-like peptide precursor [Sus scrofa]	1.2400	2.4628	1.8631	1.8397	1.8514
unknown	2.2216	1.4809	0.6701	3.0324	1.8512
homologue to SP|P47240|PX8A_CANFA Paired box protein PAX-8 isoform 8A. [Dog] {Canis familiaris}, partial (26%)	3.2793	0.4072	1.3265	2.3601	1.8433
unknown	2.7340	0.9471	0.3857	3.2954	1.8405
unknown	2.6387	1.0421	0.8596	2.8211	1.8404
CD11b	2.8352	0.8455	1.7236	1.9571	1.8403
unknown	2.0310	1.6208	0.2970	3.3549	1.8259
unknown	1.7521	1.8838	1.0753	2.5606	1.8179
homologue to PIR|JC5952|JC5952 mitogen-activated protein kinase-activated protein kinase (EC 2.7.-.-) 5 - mouse, partial (29%)	2.3896	1.2395	0.0056	3.6234	1.8145
unknown	2.5816	1.0459	1.1433	2.4843	1.8138
unknown	2.7937	0.8237	1.7326	1.8849	1.8087
unknown	2.4984	1.1161	1.2642	2.3502	1.8072
unknown	2.4010	1.2025	1.3396	2.2639	1.8017
homologue to GP|11907601|gb|AAG41237.1 protein kinase HIPK2 {Mus musculus}, partial (7%)	3.3509	0.2515	1.5417	2.0608	1.8012
unknown	2.5699	1.0086	1.8729	1.7055	1.7892
unknown	3.1859	0.3812	0.5923	2.9748	1.7836
homologue to GP|12654557|gb|AAH01113.1 U3 snoRNP-associated 55-kDa protein {Homo sapiens}, partial (21%)	3.2040	0.3463	2.1657	1.3846	1.7752
unknown	1.5626	1.9758	1.4499	2.0884	1.7692
homologue to GP|4337109|gb|AAD18085.1| BAT3 {Homo sapiens}, partial (12%)	2.9355	0.6020	1.2655	2.2720	1.7687
unknown	1.4199	2.0969	0.2876	3.2292	1.7584
unknown	1.5850	1.9220	1.2964	2.2106	1.7535
unknown	2.1399	1.3646	0.7585	2.7460	1.7523
unknown	2.1532	1.3365	0.7885	2.7013	1.7449
homologue to GP|7959345|dbj|BAA96063.1 KIAA1539 protein {Homo sapiens}, partial (29%)	2.9048	0.5798	2.0690	1.4155	1.7423
unknown	2.4466	1.0344	2.4075	1.0735	1.7405
unknown	2.8655	0.5905	0.4663	2.9897	1.7280
precursor protein (partial) (AA -24 to 392) [Sus scrofa]	2.3906	1.0638	0.1680	3.2864	1.7272
unknown	2.0000	1.4415	2.1320	1.3095	1.7208
GP|14272235|emb|CAC39629. bA183L8.1 (lipoma HMGIC fusion partner) {Homo sapiens}, partial (53%)	2.8645	0.5749	1.7287	1.7107	1.7197
unknown	2.5006	0.9260	3.0224	0.4042	1.7133
unknown	3.3879	0.0208	3.0219	0.3868	1.7043
unknown	2.4442	0.9635	0.8904	2.5173	1.7038
unknown	3.1370	0.2641	0.5067	2.8943	1.7005
unknown	1.8593	1.5380	0.2473	3.1499	1.6986
unknown	3.2763	0.0966	1.7975	1.5754	1.6864
unknown	1.8142	1.5568	1.0314	2.3397	1.6855
unknown	1.5525	1.8125	0.8178	2.5472	1.6825
unknown	2.4386	0.9199	1.1497	2.2088	1.6793
unknown	2.2736	1.0728	1.5230	1.8234	1.6732
homologue to GP|17511743|gb|AAH18727.1 Unknown (protein for MGC:3183) {Homo sapiens}, partial (15%)	1.7776	1.5686	1.3553	1.9909	1.6731
unknown	2.1940	1.1352	0.6594	2.6698	1.6646

unknown	1.7943	1.5255	1.0163	2.3034	1.6599
unknown	1.7792	1.5138	1.7830	1.5100	1.6465
similar to SP|O15228|DAPT_HUMAN Dihydroxyacetone phosphate acyltransferase (EC 2.3.1.42) (DHAP-AT) (DAP-AT), partial (27%)	3.2244	0.0611	1.5638	1.7217	1.6428
unknown	1.3847	1.8937	0.6821	2.5963	1.6392
unknown	1.8931	1.3626	1.2279	2.0278	1.6278
unknown	-2.9319	-2.2091	-1.7044	-3.4366	**-2.5705**
fibrinogen A-alpha-chain [Sus scrofa]	-0.3862	-4.7639	-1.2507	-3.8994	**-2.5750**
unknown	-1.9651	-3.1942	-1.4173	-3.7420	**-2.5797**
unknown	-3.9596	-1.2169	-2.4301	-2.7464	**-2.5882**
unknown	-2.5494	-2.6474	-2.4874	-2.7094	**-2.5984**
PIR|S38962|S38962 serpin - pig, partial (64%)	-0.7701	-4.4314	-1.7929	-3.4086	**-2.6008**
homologue to SP|P15586|GL6S_HUMAN N-acetylglucosamine-6-sulfatase precursor (EC 3.1.6.14) (G6S) (Glucosamine-6-sulfatase). [Human], partial (34%)	-3.1503	-2.0533	-1.8919	-3.3117	**-2.6018**
similar to GP|7582395|gb|AAF64308.1| class mu glutathione S-transferase {Bos taurus}, partial (55%)	-3.4719	-1.7440	-2.1642	-3.0517	**-2.6080**
unknown	-3.3982	-1.8184	-1.9872	-3.2294	**-2.6083**
unknown	-3.5059	-1.7135	-1.4397	-3.7797	**-2.6097**
homologue to SP|P35227|ME18_HUMAN DNA-binding protein Mel-18 (Zinc finger protein 144). [Human] {Homo sapiens}, partial (61%)	-2.9457	-2.2776	-1.3583	-3.8649	**-2.6116**
unknown	-2.6234	-2.6129	-1.3358	-3.9005	**-2.6182**
similar to GP|14602473|gb|AAH09742.1 ladinin 1 {Homo sapiens}, partial (21%)	-2.4974	-2.7510	-3.3424	-1.9060	**-2.6242**
unknown	-3.0718	-2.1826	-1.2948	-3.9595	**-2.6272**
homologue to GP|1730288|gb|AAC50934.1| acetolactate synthase homolog {Homo sapiens}, partial (61%)	-4.3899	-0.8648	-1.6598	-3.5948	**-2.6273**
unknown	-2.5369	-2.7218	-1.9194	-3.3394	**-2.6294**
similar to GP|1311661|gb|AAC50471.1| hepatocyte growth factor-like protein {Homo sapiens}, partial (36%)	-3.9958	-1.2715	-3.1755	-2.0919	**-2.6337**
similar to GP|16552719|dbj|BAB71368. unnamed protein product {Homo sapiens}, partial (80%)	-2.7323	-2.5387	-1.7370	-3.5341	**-2.6355**
similar to GP|3687387|emb|CAA69957.1 ranbp3 {Homo sapiens}, partial (26%)	-1.7630	-3.5110	-2.2692	-3.0047	**-2.6370**
GP|14495652|gb|AAH09434.1 Unknown (protein for MGC:15765) {Homo sapiens}, partial (4%)	-2.5294	-2.7617	-1.8910	-3.4000	**-2.6455**
unknown	-2.5449	-2.7530	-1.4220	-3.8759	**-2.6489**
unknown	-3.4073	-1.9010	-1.5578	-3.7505	**-2.6542**
unknown	-2.8305	-2.4812	-0.7994	-4.5123	**-2.6558**
similar to SP|P06681|CO2_HUMAN Complement C2 precursor (EC 3.4.21.43) (C3/C5 convertase). [Human] {Homo sapiens}, partial (26%)	-2.7072	-2.6071	-1.5634	-3.7509	**-2.6572**
SP|P29053|TF2B_RAT Transcription initiation factor IIB (TFIIB) (RNA polymerase II alpha initiation factor). [Rat], partial (80%)	-2.0740	-3.2479	-2.4249	-2.8971	**-2.6610**
homologue to SP|P53007|TXTP_HUMAN Tricarboxylate transport protein mitochondrial precursor (Citrate transport protein) (CTP), partial (86%)	-2.5373	-2.8010	-1.9130	-3.4253	**-2.6692**
unknown	-3.2091	-2.1434	-2.5603	-2.7922	**-2.6763**
similar to GP|12802994|gb|AAH01099.1 Unknown (protein for IMAGE:3510317) {Homo sapiens}, partial (71%)	-3.6818	-1.7067	-3.1313	-2.2572	**-2.6943**
SP|Q00380|A2S1_MOUSE Clathrin coat assembly protein AP17 (Clathrin coat associated protein AP17), partial (59%)	-2.3172	-3.0753	-2.2709	-3.1216	**-2.6963**
unknown	-2.6465	-2.7612	-2.3873	-3.0204	**-2.7039**

similar to GP|12852439|dbj|BAB29412. putative {Mus musculus}, partial (18%)	-3.7987	-1.6090	-1.8268	-3.5809	**-2.7039**
weakly similar to GP|16878257|gb|AAH17327.1 Unknown (protein for MGC:29726) {Homo sapiens}, partial (23%)	-1.5740	-3.8448	-2.7423	-2.6766	**-2.7094**
unknown	-3.3015	-2.1316	-2.4386	-2.9945	**-2.7165**
homologue to GP|8515870|gb|AAF76218.1| bridging integrator-3 {Homo sapiens}, partial (67%)	-3.4191	-2.0150	-2.3873	-3.0467	**-2.7170**
similar to SP|P21195|PDI_RABIT Protein disulfide isomerase precursor (PDI) (EC 5.3.4.1) (Prolyl 4-hydroxylase beta subunit), partial (46%)	-3.0709	-2.3691	-1.7676	-3.6724	**-2.7200**
similar to GP|15080110|gb|AAH11831.1 Unknown (protein for MGC:20496) {Homo sapiens}, partial (72%)	-2.5744	-2.8669	-2.6535	-2.7878	**-2.7206**
endothelin-converting enzyme 1 [Sus scrofa]	-2.7067	-2.7380	-2.4240	-3.0206	**-2.7223**
homologue to GP|12653059|gb|AAH00294.1 Unknown (protein for IMAGE:2819455) {Homo sapiens}, complete	-1.5438	-3.8887	-2.3752	-3.0821	**-2.7224**
homologue to GP|13279068|gb|AAH04266.1 Unknown (protein for IMAGE:3613103) {Homo sapiens}, partial (45%)	-2.5481	-2.9040	-2.5180	-2.9341	**-2.7261**
homologue to GP|14290607|gb|AAH09084.1 Similar to selenium binding protein 1 {Homo sapiens}, partial (30%)	-3.1525	-2.3121	-3.3243	-2.1402	**-2.7323**
vascular endothelial growth factor	-2.9024	-2.5685	-2.1981	-3.2729	**-2.7355**
homologue to SP|O60907|TBL1_HUMAN Transducin beta-like 1 protein. [Human] {Homo sapiens}, partial (47%)	-2.6931	-2.8027	-2.1375	-3.3583	**-2.7479**
similar to GP|2645879|gb|AAB87523.1| molybdenum cofactor biosynthesis protein A {Homo sapiens}, partial (46%)	-1.9311	-3.5757	-2.2697	-3.2370	**-2.7534**
similar to GP|2224569|dbj|BAA20773.1 KIAA0314 {Homo sapiens}, partial (22%)	-3.0078	-2.5025	-2.4854	-3.0249	**-2.7552**
cytochorme P450 2A19 [Sus scrofa]	-3.3379	-2.1767	-2.2105	-3.3041	**-2.7573**
homologue to GP|11275667|gb|AAG33699.1 oxidized-LDL responsive gene 2 {Homo sapiens}, partial (36%)	-2.9915	-2.5240	-1.1441	-4.3714	**-2.7577**
similar to GP|16516591|emb|CAD10242. unnamed protein product {Homo sapiens}, partial (56%)	-3.4348	-2.0865	-0.6715	-4.8498	**-2.7607**
homologue to SP|P02469|LMB1_MOUSE Laminin beta-1 chain precursor (Laminin B1 chain). [Mouse] {Mus musculus}, partial (15%)	0.0931	-5.6147	-3.6221	-1.8995	**-2.7608**
metallothionein isoform [Sus scrofa]metallothionein isoform [Sus scrofa]metallothionein isoform [Sus scrofa]metallothionein isoform [Sus scrofa]metallothionein isoform [Sus scrofa]metallothionein isoform [Sus scrofa]metallothionein isoform [S	-4.1415	-1.3899	-2.7291	-2.8023	**-2.7657**
homologue to GP|14336773|gb|AAK61300.1 annexin A2 like - ? : selenoprotein X {Homo sapiens}, complete	-3.2463	-2.2891	-2.1356	-3.3998	**-2.7677**
homologue to GP|1840045|gb|AAB47236.1| transporter protein {Homo sapiens}, partial (27%)	-3.1409	-2.3955	-1.0699	-4.4665	**-2.7682**
unknown	-2.3780	-3.1621	-1.2742	-4.2658	**-2.7700**
gag protein [Sus scrofa]pol protein [Sus scrofa]env protein [Sus scrofa]gag-pol precursor [Sus scrofa domestica]protease [Sus scrofa]protease [Sus scrofa]protease [Sus scrofa]protease [Sus scrofa]protease [Sus scrofa]polyprotein [Sus sc	-0.9403	-4.6098	-1.6868	-3.8633	**-2.7750**
homologue to GP|14043628|gb|AAH07788.1 Similar to eukaryotic translation initiation factor 4 gamma 1 {Homo sapiens}, partial (35%)	-2.9371	-2.6162	-1.6998	-3.8536	**-2.7767**
unknown	-3.0365	-2.5271	-4.4150	-1.1485	**-2.7818**
homologue to GP|12804417|gb|AAH01611.1 Similar to bromodomain-containing 7 {Homo sapiens}, partial (32%)	-2.6049	-2.9830	-1.3419	-4.2459	**-2.7939**
complement component C1s [Sus scrofa]	-2.7853	-2.8118	-1.3415	-4.2556	**-2.7986**
GP|567053|gb|AAA56751.1|| beta 5 tubulin {Xenopus laevis}, partial (22%)	-4.6795	-0.9783	-2.5973	-3.0605	**-2.8289**
unknown	-2.7875	-2.8739	-0.8875	-4.7739	**-2.8307**
unknown	-2.9519	-2.7134	-0.8495	-4.8158	**-2.8326**

homologue to GP|12832716|dbj|BAB22226. putative {Mus musculus}, partial (30%)	-3.8374	-1.8291	-1.2025	-4.4639	**-2.8332**
similar to SP|P58058|PPNK_MOUSE Putative inorganic polyphosphate/ATP-NAD kinase (EC 2.7.1.23) (Poly(P)/ATP NAD kinase). [Mouse], partial (55%)	-2.8913	-2.7767	-1.3164	-4.3516	**-2.8340**
mature porcine factor I	-2.4647	-3.2060	-2.1344	-3.5363	**-2.8353**
unknown	-3.0822	-2.5984	-2.9882	-2.6924	**-2.8403**
similar to GP|13477137|gb|AAH05025.1 Similar to metalloprotease 1 (pitrilysin family) {Homo sapiens}, partial (20%)	-3.2389	-2.4490	-1.9511	-3.7369	**-2.8440**
matricin	-2.0796	-3.6400	-3.0965	-2.6230	**-2.8598**
polypyrimidine tract-binding protein [Sus scrofa]	-3.1578	-2.5674	-2.2410	-3.4842	**-2.8626**
similar to GP|3882165|dbj|BAA34442.1 KIAA0722 protein {Homo sapiens}, partial (9%)	-2.6613	-3.0902	-2.6416	-3.1099	**-2.8758**
acyl-CoA oxidase [Sus scrofa]	-3.1852	-2.5802	-1.9946	-3.7708	**-2.8827**
similar to GP|17512170|gb|AAH19069.1 Unknown (protein for MGC:29596) {Homo sapiens}, partial (29%)	-2.7710	-2.9982	-1.6339	-4.1354	**-2.8846**
GP|12803403|gb|AAH02524.1 KIAA0064 gene product {Homo sapiens}, partial (81%)	-2.9709	-2.8004	-3.4968	-2.2744	**-2.8856**
similar to GP|14602654|gb|AAH09849.1 Unknown (protein for MGC:15400) {Homo sapiens}, partial (56%)	-3.4883	-2.2898	-2.3806	-3.3975	**-2.8891**
similar to SP|Q9XT77|SL56_RABIT Sodium-dependent multivitamin transporter (Na(+)-dependent multivitamin transporter). [Rabbit], partial (17%)	-1.7521	-4.0279	-1.7143	-4.0657	**-2.8900**
unknown	-3.0350	-2.7714	-1.4303	-4.3761	**-2.9032**
unknown	-3.8885	-1.9257	-1.8609	-3.9533	**-2.9071**
homologue to GP|15929704|gb|AAH15276.1 inter-alpha trypsin inhibitor heavy chain 3 {Mus musculus}, partial (21%)	-3.3755	-2.4548	-1.5124	-4.3179	**-2.9151**
similar to SP|O43615|IM44_HUMAN Import inner membrane translocase subunit TIM44 mitochondrial precursor. [Human] {Homo sapiens}, partial (38%)	-0.4780	-5.3707	-3.2487	-2.6000	**-2.9244**
similar to GP|37996|emb|CAA46158.1|| Xeroderma Pigmentosum Group C Complementing factor {Homo sapiens}, partial (23%)	-2.3902	-3.4725	-1.9368	-3.9259	**-2.9314**
SP|P42891|ECE1_BOVIN Endothelin-converting enzyme 1 (EC 3.4.24.71) (ECE-1). [Bovine] {Bos taurus}, partial (14%)	-3.7493	-2.1140	-1.6683	-4.1950	**-2.9317**
vascular endothelial growth factor [Sus scrofa]	-2.9890	-2.8953	-2.1244	-3.7598	**-2.9421**
glucose-6-phosphatase catalytic subunit [Sus scrofa]	-3.1862	-2.7024	-0.8747	-5.0138	**-2.9443**
unknown	-3.2909	-2.6204	-1.9983	-3.9130	**-2.9557**
similar to SP|P15169|CBPN_HUMAN Carboxypeptidase N catalytic chain precursor (EC 3.4.17.3) (Arginine carboxypeptidase) (Kininase 1), partial (32%)	-2.7057	-3.2089	-1.3984	-4.5161	**-2.9573**
homologue to GP|3800742|gb|AAC68839.1| RGC-32 {Rattus norvegicus}, partial (90%)	-2.7942	-3.1340	-2.1017	-3.8265	**-2.9641**
similar to GP|12658433|gb|AAK01138.1 interferon regulatory factor 1 {Ovis aries}, partial (61%)	-2.4690	-3.4594	-2.5584	-3.3701	**-2.9642**
similar to SP|Q92484|AS3A_HUMAN Acid sphingomyelinase-like phosphodiesterase 3a (EC 3.1.4.-) (ASM-like phosphodiesterase 3a), partial (49%)	-2.8748	-3.0666	-1.7651	-4.1763	**-2.9707**
similar to GP|12803319|gb|AAH02477.1 Unknown (protein for MGC:3090) {Homo sapiens}, partial (7%)	-2.8516	-3.1035	-0.5678	-5.3872	**-2.9775**
gal beta-1,3 GalNAc alpha-2,3 sialyltransferase	-0.1526	-5.8159	-1.6941	-4.2745	**-2.9843**
similar to GP|7644350|gb|AAF65550.1| golgi matrix protein GM130 {Homo sapiens}, partial (9%)	-3.5180	-2.4665	-0.6118	-5.3727	**-2.9922**
GP|12654655|gb|AAH01165.1 N-ethylmaleimide-sensitive factor attachment protein alpha {Homo sapiens}, partial (56%)	-3.3293	-2.6581	-0.4894	-5.4980	**-2.9937**
homologue to GP|2285790|dbj|BAA21659.1 p47 {Rattus norvegicus}, partial (76%)	-2.7822	-3.2072	-1.7340	-4.2554	**-2.9947**

homologue to GP|15341753|gb|AAH12406.1 Unknown (protein for MGC:7221) {Mus musculus}, partial (41%)	-3.0480	-2.9512	-0.5729	-5.4263	**-2.9996**
homologue to GP|2624718|pdb|1RGP| Gtpase-Activation Domain From Rhogap, partial (88%)	-2.7109	-3.2955	-0.9057	-5.1007	**-3.0032**
similar to GP|10441934|gb|AAG17244.1 unknown {Homo sapiens}, partial (29%)	-3.4183	-2.5897	-4.0602	-1.9478	**-3.0040**
homologue to GP|13559033|emb|CAC36008. bA11M20.3.1 (novel protein similar to Pleurodeles waltlii RAP55 protein isoform 1) {Homo sapiens}, partial (48%)	-2.3330	-3.6818	-2.3814	-3.6334	**-3.0074**
homologue to GP|13785926|gb|AAK39520.1 BTB domain protein {Homo sapiens}, partial (34%)	-2.8387	-3.2072	-0.4954	-5.5505	**-3.0229**
homologue to SP|P22234|PUR6_HUMAN Multifunctional protein ADE2, partial (54%)	-2.5758	-3.4720	-0.8815	-5.1663	**-3.0239**
unknown	-3.3773	-2.7031	-1.3742	-4.7063	**-3.0402**
similar to GP|3372677|gb|AAC29066.1| tumorous imaginal discs protein Tid56 homolog {Homo sapiens}, partial (35%)	-2.8217	-3.2617	-0.7370	-5.3464	**-3.0417**
similar to GP|15214665|gb|AAH12461.1 Similar to RIKEN cDNA 2310061O04 gene {Homo sapiens}, partial (63%)	-0.5450	-5.5546	-1.3717	-4.7278	**-3.0498**
similar to PIR|A31870|A31870 amine oxidase (flavin-containing) (EC 1.4.3.4) B - rat, partial (32%)	-3.3733	-2.7538	-2.2373	-3.8898	**-3.0635**
homologue to GP|10440073|dbj|BAB15639. unnamed protein product {Homo sapiens}, partial (29%)	-2.4378	-3.7188	-1.5054	-4.6513	**-3.0783**
similar to PIR|T12469|T12469 hypothetical protein DKFZp564C1940.1 - human (fragment), partial (93%)	-4.1196	-2.0395	-1.3194	-4.8396	**-3.0795**
unknown	-4.0080	-2.1583	-1.6560	-4.5103	**-3.0832**
homologue to GP|14486422|gb|AAK61367.1 retina ubiquilin {Bos taurus}, partial (38%)	-2.2398	-3.9542	-0.9016	-5.2924	**-3.0970**
homologue to SP|Q07954|LRP1_HUMAN Low-density lipoprotein receptor-related protein 1 precursor (LRP) (Alpha-2-macroglobulin receptor), partial (5%)	-3.7630	-2.4454	-0.5451	-5.6633	**-3.1042**
homologue to GP|12653075|gb|AAH00303.1 phosphoglycerate dehydrogenase {Homo sapiens}, partial (31%)	-4.0861	-2.1504	-1.1034	-5.1331	**-3.1182**
homologue to GP|10717134|gb|AAG22029.1 carbonic anhydrase III {Mus musculus}, complete	-3.2913	-2.9463	-0.9393	-5.2983	**-3.1188**
similar to GP|18089178|gb|AAH20844.1 Unknown (protein for MGC:23971) {Homo sapiens}, partial (84%)	-1.9437	-4.3143	-2.3109	-3.9471	**-3.1290**
MHC class I antigen [Sus scrofa]MHC PD1 major transplantation antigenMHC PD1a major transplantation antigenMHC class I antigen heavy chain [Sus scrofa]	-2.0010	-4.2753	-4.8067	-1.4696	**-3.1382**
similar to GP|13477197|gb|AAH05060.1 Similar to quinolinate phosphoribosyltransferase, partial (58%)	-3.9014	-2.4673	-1.9480	-4.4207	**-3.1843**
homologue to GP|8925838|gb|AAF81636.1| acidic alpha-glucosidase {Bos taurus}, partial (23%)	-3.7638	-2.6496	-0.6636	-5.7498	**-3.2067**
similar to GP|12652817|gb|AAH00161.1 secretory carrier membrane protein 3 {Homo sapiens}, partial (35%)	-3.3108	-3.2254	-1.2670	-5.2692	**-3.2681**
similar to GP|15209782|emb|CAC51180. unnamed protein product {Homo sapiens}, complete	-3.7078	-2.8719	-2.4695	-4.1103	**-3.2899**
similar to SP|P98153|IDD_HUMAN Integral membrane protein DGCR2/IDD precursor. [Human] {Homo sapiens}, partial (94%)	-3.0263	-3.5850	-2.3824	-4.2288	**-3.3056**
homologue to GP|4590328|gb|AAD26531.1| valyl-tRNA synthetase {Mus musculus}, partial (16%)	-2.9069	-3.7188	-1.0547	-5.5710	**-3.3129**
similar to EGAD|88612|96537 lysophosphatidic {Homo sapiens}, partial (37%)	-4.2724	-2.4102	-0.8945	-5.7881	**-3.3413**
similar to GP|12858330|dbj|BAB31278. putative {Mus musculus}, partial (37%)	-3.5317	-3.2333	-3.3609	-3.4040	**-3.3825**
unknown	-3.1455	-3.6727	-1.8301	-4.9881	**-3.4091**
unknown	-3.4700	-3.3916	-2.1400	-4.7216	**-3.4308**
GP|12654775|gb|AAH01230.1 Similar to CGI-78 protein {Homo sapiens}, partial (53%)	-4.0867	-2.8314	-1.9796	-4.9386	**-3.4591**
sialyltransferase [Sus scrofa]	-1.8864	-5.0490	-1.6261	-5.3094	**-3.4677**
homologue to PIR|I39174|I39174 seven trans-membrane domain protein AD3LP/AD5 - human, partial (61%)	-3.8841	-3.0952	-0.9941	-5.9852	**-3.4896**

similar to SP|P17177|CP27_RABIT Cytochrome P450 27 mitochondrial precursor (EC 1.14.-.-) (Cytochrome P-450C27/25), partial (34%)	-4.2203	-2.7629	-0.2183	-6.7650	**-3.4916**
similar to SP|P35292|RB17_MOUSE Ras-related protein Rab-17. [Mouse] {Mus musculus}, partial (68%)	-4.1898	-2.8138	-2.3385	-4.6652	**-3.5018**
similar to GP|3273228|dbj|BAA29057.1 very-long-chain acyl-CoA dehydrogenase {Homo sapiens}, partial (27%)	-3.6789	-3.4065	-1.6499	-5.4356	**-3.5427**
homologue to GP|6319138|gb|AAF07179.1| ALG-2 interacting protein 1 {Rattus norvegicus}, partial (38%)	-3.3612	-3.7694	-2.7249	-4.4057	**-3.5653**
homologue to EGAD|136325|145398 neutral and basic amino acid transporter protein {Sus scrofa}, complete	-2.3267	-4.8142	-4.7970	-2.3439	**-3.5705**
similar to GP|4826565|emb|CAB42884.1 cathepsin F {Mus musculus}, partial (63%)	-2.8979	-4.2576	-1.3684	-5.7871	**-3.5777**
homologue to PIR|G01236|G01236 enhancer of split m9/m10 (groucho protein) - human, partial (92%)	-2.2910	-4.8899	-1.8802	-5.3007	**-3.5904**
similar to SP|P23588|IF4B_HUMAN Eukaryotic translation initiation factor 4B (eIF-4B). [Human] {Homo sapiens}, partial (33%)	-3.5004	-3.7213	-3.1055	-4.1162	**-3.6108**
GP|14550508|gb|AAH09504.1 Similar to CG8974 gene product {Homo sapiens}, partial (66%)	-2.9194	-4.3607	-1.6157	-5.6645	**-3.6401**
immunoglobulin kappa light chain VJ region [Sus scrofa]immunoglobulin kappa light chain VJ region [Sus scrofa]	-3.5288	-3.7567	-2.8242	-4.4614	**-3.6428**
acid-labile subunit [Sus scrofa]	-3.7897	-3.5591	-2.7039	-4.6450	**-3.6744**
similar to GP|12652617|gb|AAH00054.1 7-dehydrocholesterol reductase {Homo sapiens}, complete	-3.7207	-3.7808	-1.5133	-5.9882	**-3.7508**
similar to GP|12655193|gb|AAH01454.1 phosphoenolpyruvate carboxykinase 2 (mitochondrial) {Homo sapiens}, partial (23%)	-5.8303	-1.6752	-5.0303	-2.4753	**-3.7528**
weakly similar to GP|881921|gb|AAC50161.1|| interferon-inducible peptide precursor {Homo sapiens}, partial (95%)	-3.9620	-3.6104	-4.0468	-3.5256	**-3.7862**
unknown	-4.2590	-3.3177	-2.1305	-5.4462	**-3.7884**
similar to GP|5596693|emb|CAB51405.1 hypothetical protein {Homo sapiens}, partial (43%)	-3.0494	-4.5427	-1.0710	-6.5211	**-3.7961**
similar to GP|12654625|gb|AAH01149.1 Similar to KIAA0266 gene product {Homo sapiens}, partial (21%)	-3.5990	-4.0224	-3.4185	-4.2029	**-3.8107**
homologue to SP|P34897|GLYM_HUMAN Serine hydroxymethyltransferase mitochondrial precursor (EC 2.1.2.1) (Serine methylase), partial (31%)	-4.0647	-3.6516	-4.3602	-3.3561	**-3.8581**
homologue to GP|6330847|dbj|BAA86562.1 KIAA1248 protein {Homo sapiens}, partial (50%)	-4.6183	-3.1515	-3.1856	-4.5843	**-3.8849**
homologue to SP|Q98TR3|RNT1_FUGRU Putative regulator of nonsense transcripts 1. [Japanese pufferfish Takifugu rubripes], partial (14%)	-2.5366	-5.2854	-4.1544	-3.6676	**-3.9110**
similar to GP|17511927|gb|AAH18918.1 Unknown (protein for MGC:12603) {Homo sapiens}, complete	-5.5236	-2.4537	-3.5483	-4.4290	**-3.9886**
homologue to GP|7022137|dbj|BAA91499.1 unnamed protein product {Homo sapiens}, partial (48%)	-2.2416	-5.7495	-5.4242	-2.5670	**-3.9956**
GP|11514162|pdb|1FKN|A Chain A Structure Of Beta-Secretase Complexed With Inhibitor, partial (66%)	-1.4101	-6.5925	-2.2818	-5.7208	**-4.0013**
homologue to GP|12857441|dbj|BAB31012. putative {Mus musculus}, partial (36%)	-4.2044	-3.8563	-4.4581	-3.6027	**-4.0304**
homologue to SP|Q9NSE2|CISH_HUMAN Cytokine-inducible SH2-containing protein (Suppressor of cytokine signaling) (SOCS) (CIS1) (G18)., partial (54%)	-2.1398	-6.1579	-3.2977	-5.0000	**-4.1488**
similar to SP|P28800|A2AP_BOVIN Alpha-2-antiplasmin precursor (Alpha-2-plasmin inhibitor) (Alpha-2-PI) (Alpha-2-AP). [Bovine], partial (50%)	-4.7630	-3.5694	-3.2089	-5.1235	**-4.1662**
SP|O55096|DPP3_RAT Dipeptidyl-peptidase III (EC 3.4.14.4) (DPP III) (Dipeptidyl aminopeptidase III), partial (21%)	-3.8515	-4.4998	-3.1655	-5.1859	**-4.1757**
homologue to GP|13543295|gb|AAH05811.1 pyruvate dehydrogenase kinase isoenzyme 2 {Homo sapiens}, partial (53%)	-4.9206	-3.5308	-3.8883	-4.5631	**-4.2257**
similar to GP|12003293|gb|AAG43523.1 organic anion	-5.0924	-3.4217	-3.0395	-5.4746	**-4.2571**

transporter 2 {Homo sapiens}, partial (28%)					
similar to PIR|I56095|C4HU complement C4A precursor [validated] - human, partial (9%)	-5.7787	-2.8958	-4.8162	-3.8584	**-4.3373**
similar to PIR|A56619|A56619 female sterile homeotic (fsh) homolog RING3 - human, partial (27%)	-4.4403	-4.2919	-3.6348	-5.0974	**-4.3661**
homologue to GP|4938304|emb|CAA07619.2 lysine-ketoglutarate reductase /saccharopine dehydrogenase {Homo sapiens}, partial (15%)	-0.8021	-7.9530	-4.4003	-4.3548	**-4.3775**
similar to GP|467528|dbj|BAA01185.1| alanine aminotransferase {Rattus norvegicus}, partial (24%)	-4.5250	-4.2790	-3.2394	-5.5645	**-4.4020**
similar to GP|3327162|dbj|BAA31649.1 KIAA0674 protein {Homo sapiens}, partial (14%)	-3.6082	-5.2854	-3.7888	-5.1048	**-4.4468**
similar to SP|P30519|HO2_HUMAN Heme oxygenase 2 (EC 1.14.99.3) (HO-2). [Human] {Homo sapiens}, complete	-4.7502	-4.2364	-5.0230	-3.9636	**-4.4933**
similar to GP|14789873|gb|AAH10812.1 Unknown (protein for IMAGE:4211034) {Mus musculus}, partial (50%)	-4.8527	-4.5506	-4.3326	-5.0706	**-4.7016**
similar to SP|O75891|FTDH_HUMAN 10-formyltetrahydrofolate dehydrogenase (EC 1.5.1.6) (10-FTHFDH). [Human] {Homo sapiens}, partial (18%)	-5.0176	-4.4480	6.2603	-15.7258	**-4.7328**
similar to GP|14603281|gb|AAH10100.1 Unknown (protein for MGC:19693) {Homo sapiens}, partial (22%)	-3.7384	-5.8159	-5.6939	-3.8604	**-4.7771**
similar to GP|17389278|gb|AAH17692.1 Similar to quiescin Q6 {Homo sapiens}, partial (30%)	-4.4499	-5.4378	-3.6599	-6.2277	**-4.9438**
alpha-2,6-sialyltransferase [Sus scrofa]	**-4.8471**	**-5.6660**	**-3.7079**	**-6.8052**	**-5.2565**

Table 3. Transcripts highly up/down regulated determined by oligo-array in the adipose tissue by the dietary shifting from LFD to HFD (Chapter 3). For each transcript, $\log_2$ratio=$\log_2$(HFD/LFD).The positive value means higher mRNA abundance in HFD pigs; negative value means lower mRNA abundance in HFD pigs

Gene name	$\log_2$(R1/G1)	$\log_2$(R2/G2)	$\log_2$(G3/R3)	$\log_2$(G4/R4)	Average
similartoGP13810568dbjBAB43955.Toll-likereceptor5{Homosapiens}.partial(19%)	3.5025	4.4811	4.3977	3.5859	3.9918
DNA-directedRNApolymeraseIIpolypeptideB;POLR2B[Susscrofa]	2.1876	5.3576	2.2878	5.2574	3.7726
unknown	2.1769	5.3129	1.8452	5.6445	3.7449
alpha-1-antichymotrypsin3[Susscrofa]	2.8413	5.3672	2.4207	3.9059	3.6338
homologuetoGP12805589gbAAH02274.1Unknown(proteinforMGC:7676){Musmusculus}.complete	1.4150	6.3750	1.7276	4.0624	3.3950
AMP-activatedproteinkinasegammasubunit[Susscrofa]AMPKgammasubunit[Susscrofa]	2.8875	3.3219	2.1494	4.0601	3.1047
unknown	3.9069	2.0544	1.1019	4.8595	2.9807
unknown	0.6280	5.3219	0.5070	5.4430	2.9750
similartoGP7981270embCAB91983.1hypotheticalprotein{Homosapiens}.partial(56%)	0.9434	4.9189	2.2912	3.5710	2.9311
homologuetoGP3327126dbjBAA31631.1KIAA0656protein{Homosapiens}.partial(22%)	2.0000	3.8413	2.3383	3.5030	2.9207
unknown	0.2137	6.0444	1.2617	4.1415	2.9153
unknown	0.5305	5.2095	0.1959	5.5440	2.8700
homologuetoGP2828149gbAAC00006.1cyclophilin-33A{Homosapiens}.partial(72%)	0.5850	5.1293	0.1507	5.5636	2.8571
weaklysimilartoGP13623713gbAAH06486.1Unknown(proteinforMGC:771){Homosapiens}.partial(61%)	1.9069	3.6724	1.6980	3.8813	2.7897
unknown	0.5146	5.0444	2.0780	3.4810	2.7795
similartoGP17389636gbAAH17843.1cholesterol25-	1.1127	5.4263	0.9189	3.6201	2.7695

hydroxylase{Homosapiens}.partial(60%)					
similartoGP12803737gbAAH02705.1chromosome22openreadingframe3{Homosapiens}.partial(84%)	1.3692	4.1155	1.1699	4.3148	2.7424
unknown	0.2801	5.1699	0.4005	5.0495	2.7250
similartoGP183997gbAAA58640.1heregulin-beta2{Homosapiens}.partial(17%)	2.1699	3.2095	2.2473	3.1320	2.6897
unknown	0.8480	4.4919	1.1234	4.2165	2.6699
unknown	0.7370	4.5850	1.1629	4.1590	2.6610
unknown	10.2041	5.4919	1.6479	-6.7683	2.6439
unknown	0.0875	5.1293	0.5580	4.6588	2.6084
unknown	0.2801	4.8413	1.3866	3.7348	2.5607
unknown	0.4657	4.5850	0.7590	4.2916	2.5253
unknown	0.5771	4.4150	0.6558	4.3362	2.4960
unknown	0.2479	4.6439	1.6923	3.1995	2.4459
unknown	1.0182	3.8413	0.7628	4.0967	2.4298
similartoGP10435722dbjBAB14652.unnamedproteinproduct{Homosapiens}.partial(81%)	1.9296	2.9069	2.3923	2.4442	2.4183
unknown	2.0419	2.7655	0.8766	3.9308	2.4037
similartoGP10438452dbjBAB15247.unnamedproteinproduct{Homosapiens}.partial(42%)	1.7645	3.0356	2.3079	2.4923	2.4001
unknown	0.4475	5.2095	1.2462	2.6209	2.3810
similartoGP1770426embCAA66469.1G-proteincoupledreceptorkinase{Homosapiens}.partial(75%)	3.1699	1.5850	0.7977	3.9572	2.3774
GP13938376gbAAH07321.1Unknown(proteinforMGC:1346){Homosapiens}.complete	0.4639	4.2801	0.8417	3.9023	2.3720
similartoGP1732422gbAAB51326.1C3f{Homosapiens}.partial(20%)	0.3626	4.3576	0.4500	4.2701	2.3601
unknown	0.1159	4.4919	1.2613	3.3465	2.3039
unknown	2.4594	2.0809	1.8729	2.6674	2.2702
unknown	0.5850	3.9542	2.3862	2.1530	2.2696
unknown	1.2458	3.2801	4.0608	0.4651	2.2629
unknown	1.0704	4.5850	0.0907	3.2831	2.2573
weaklysimilartoGP16306780gbAAH01584.1Unknown(proteinforIMAGE:3461401){Homosapiens}.partial(54%)	1.0378	3.4594	1.9316	2.5656	2.2486
CCAAT/enhancerbindingproteinbeta[Susscrofa]	1.3301	3.1375	0.8598	3.6078	2.2338
homologuetoSPQ15329E2F5_HUMANTranscriptionfactorE2F5(E2F-5).[Human]{Homosapiens}.partial(40%)	1.5384	2.9175	2.1716	2.2843	2.2280
SPP29053TF2B_RATTranscriptioninitiationfactorIIB(TFIIB)(RNApolymeraseIIalphainitiationfactor).[Rat].partial(80%)	0.8074	3.6439	0.1683	4.2829	2.2256
similartoGP13591537embCAC36352.dJ1033H22.2(breastcanceranti-estrogenresistance3){Homosapiens}.partial(50%)	1.4150	2.9798	0.4386	3.9563	2.1974
unknown	0.6134	3.7814	2.3299	2.0648	2.1974
homologuetoSPO14493CLD4_HUMANClaudin-4(Clostridiumperfringensenterotoxinreceptor)(CPE-receptor)(CPE-R).[Human].complete	1.8480	2.4831	1.7989	2.5322	2.1655
unknown	0.9260	3.3576	0.0674	4.2162	2.1418
unknown	0.3219	4.5850	1.0972	2.5220	2.1315
unknown	0.5361	3.7004	0.1660	4.0705	2.1182
similartoGP13751639embCAC37285.C367G8.1(melanomaantigenP15){Homosapiens}.partial(88%)	1.0473	3.1832	2.2684	1.9621	2.1153
intermediate-conductancecalcium-activatedpotassiumchannel[Susscrofa]	0.6705	3.5361	1.6613	2.5452	2.1033
unknown	1.4910	2.7004	1.4443	2.7471	2.0957
homologuetoPIRJC5392JC5392zincfingerproteinKF-	2.4594	1.7253	1.8519	2.3328	2.0924

1precursor-human.partial(42%)					
unknown	1.5824	4.3458	0.5652	1.7534	2.0617
unknown	-0.5619	4.6439	3.0972	0.9847	2.0410
cyclin-dependentkinaseinhibitor.p16[Susscrofa]cyclindependantkinaseinhibitor[Susscrofa]cyclindependantkinaseinhibitor[Susscrofa]	2.0000	2.0780	1.1405	2.9375	2.0390
unknown	0.6101	3.4594	0.3660	3.7035	2.0347
unknown	0.1155	4.1699	0.2370	3.5865	2.0272
weaklysimilartoGP17315166gbAAH14156.1Unknown(proteinforMGC:20834){Homosapiens}.partial(62%)	-0.0893	4.1247	2.3231	1.7123	2.0177
homologuetoGP11527783dbjBAB18652.ubiquitin-conjyugatingenzymeE2{Homosapiens}.partial(59%)	2.0477	1.9676	1.4617	2.5535	2.0076
unknown	0.5703	3.4429	0.2630	3.7502	2.0066
unknown	1.0000	3.0000	1.0658	2.9342	2.0000
unknown	0.3720	3.5607	0.9977	2.9350	1.9663
unknown	0.9411	2.9819	2.4517	1.4713	1.9615
similartoSPP30519HO2_HUMANHemeoxygenase2(EC1.14.99.3)(HO-2).[Human]{Homosapiens}.complete	2.0324	1.8745	0.5017	3.4052	1.9534
similartoGP17736920gbAAL41029.1asparaginase-likespermautoantigen{Rattusnorvegicus}.partial(42%)	0.3626	3.5443	1.1050	2.8019	1.9534
similartoGP12654233gbAAH00936.1Similartohypotheticalproteinclone1-2{Homosapiens}.partial(86%)	1.3847	2.5146	1.2104	2.6889	1.9496
unknown	1.9386	1.9434	0.8573	3.0248	1.9410
unknown	1.7549	2.0926	0.6642	3.1833	1.9238
homologuetoGP1054835embCAA63313.1ICA105{Rattusnorvegicus}.partial(14%)	1.0375	2.8074	0.8604	2.9844	1.9224
homologuetoGP496887embCAA56071.1betatubulin{Homosapiens}.partial(56%)	-0.0931	3.9307	0.7457	3.0919	1.9188
homologuetoGP207008gbAAA42158.1smallnuclearribonucleoparticle-associatedprotein{Rattusnorvegicus}.partial(56%)	1.8074	2.0000	2.2515	1.5558	1.9037
unknown	0.3175	3.4854	1.9916	1.8114	1.9015
unknown	1.7004	2.0995	1.5294	2.2705	1.9000
similartoSPP20132SDHL_HUMANL-serinedehydratase(EC4.2.1.13)(L-serinedeaminase).[Human]{Homosapiens}.partial(37%)	0.6139	3.1699	1.0203	2.7635	1.8919
homologuetoGP12231878gbAAG49297.1copineI{Homosapiens}.partial(83%)	0.8074	2.9386	1.2746	2.4713	1.8730
GP12746394gbAAK07475.1CUG-BPandETR-3likefactor4{Homosapiens}.partial(21%)	1.0661	3.8074	0.6868	1.9222	1.8706
similartoGP16878298gbAAH17344.1Similartohypotheticalprotein FLJ23469{Homosapiens}.complete	1.5850	2.1520	2.3281	1.4089	1.8685
homologuetoGP4521249dbjBAA76297.1DNAhelicase{Musmusculus}.partial(31%)	0.5850	3.1375	1.4788	2.2436	1.8612
unknown	2.2928	1.4288	1.4797	2.2420	1.8608
unknown	0.4374	3.2801	1.6828	2.0347	1.8588
unknown	0.7370	2.9798	1.0740	2.6428	1.8584
unknown	0.4361	3.2801	1.1716	2.5446	1.8581
homologuetoGP6729336dbjBAA89782.1seventransmembranedomainorphanreceptor{Homosapiens}.partial(58%)	0.3626	3.3219	0.2288	3.4557	1.8422
similartoGP13277562gbAAH03690.1SimilartoRIKENcDNA8430408O15gene{Homosapiens}.partial(35%)	0.7574	2.9260	0.1191	3.5644	1.8417
unknown	2.3388	1.3093	1.5445	2.1036	1.8241
unknown	0.3959	3.2479	1.6987	1.9452	1.8219
similartoPIRT08771T08771hypotheticalproteinDKFZp586L151.1-human(fragment).partial(35%)	0.9260	2.7162	0.8845	2.7577	1.8211
homologuetoSPQ9ULW2FZ10_HUMANFrizzled10precursor(Frizzled-10)(Fz-	0.7687	2.8413	-2.4780	6.0880	1.8050

10)(hFz10)(FzE7).[Human]{Homosapiens}.partial(27%)					
unknown	0.6374	2.9635	1.9820	1.6189	1.8005
unknown	0.1612	3.4263	1.4363	2.1511	1.7937
GP13436092gbAAH04869.1Unknown(proteinforIMAGE:3834272){Homosapiens}.partial(47%)	0.0000	3.5850	1.6680	1.9170	1.7925
unknown	0.6521	2.9260	0.3565	3.2216	1.7890
unknown	0.5206	4.0875	1.0540	1.4718	1.7834
unknown	1.5146	2.0211	1.9980	1.5376	1.7678
unknown	0.5721	2.9594	0.9686	2.5629	1.7657
homologuetoGP15930203gbAAH15534.1Unknown(proteinforMGC:9474){Homosapiens}.partial(50%)	0.2895	3.8074	1.7359	1.2030	1.7589
unknown	0.5850	2.9307	0.7922	2.7235	1.7578
unknown	0.1420	2.3692	1.1546	3.3567	1.7556
similartoGP16198523gbAAH15943.1Unknown(proteinforMGC:9325){Homosapiens}.partial(84%)	0.7279	2.7655	1.4666	2.0269	1.7467
homologuetoGP603953dbjBAA07893.1Thisgeneisnovel.{Homosapiens}.partial(18%)	2.5361	0.9438	1.4416	2.0383	1.7399
unknown	0.6215	2.8524	1.9243	1.5496	1.7370
interleukin-15[Susscrofa]	1.7162	1.7432	1.5878	1.8716	1.7297
unknown	1.1575	2.2928	0.5792	2.8712	1.7252
unknown	0.4854	2.9635	1.3326	2.1163	1.7245
similartoGP14714476gbAAH10364.1mitochondrialribosomalproteinS18A{Homosapiens}.complete	1.3994	3.8220	0.6874	0.9365	1.7113
similartoPIRA42912A429123alpha(or20beta)-hydroxysteroiddehydrogenase(EC1.1.1.53)-pig.complete	0.5305	2.8679	0.7199	2.6785	1.6992
unknown	0.3858	2.9635	2.4069	0.9424	1.6746
unknown	0.5261	2.8202	1.0921	2.2541	1.6731
homologuetoGP11141704gbAAG32038.1SIR2L2{Musmusculus}.partial(50%)	0.4330	2.9069	0.0931	3.2467	1.6699
unknown	1.5850	1.7549	0.5679	2.7720	1.6699
unknown	0.6630	2.6738	1.8005	1.5362	1.6684
similartoGP12406680embCAC24973.unnamedproteinproduct{Homosapiens}.partial(65%)	0.8737	2.4429	2.4001	0.9166	1.6583
homologuetoGP13938463gbAAH07375.1Similartotumordifferentiallyexpressed1{Homosapiens}.partial(56%)	1.5208	1.7935	0.2196	3.0948	1.6572
unknown	0.7004	2.6114	1.3337	1.9782	1.6559
homologuetoSPP48443RXRG_HUMANRetinoicacidreceptorRXR-gamma.[Human]{Homosapiens}.partial(41%)	0.1699	3.1293	1.9361	1.3631	1.6496
GP16041715gbAAH15733.1Unknown(proteinforMGC:22977){Homosapiens}.partial(31%)	-0.2988	3.5850	0.1415	3.1446	1.6431
unknown	2.1155	1.1699	1.1678	2.1176	1.6427
unknown	0.7814	1.4975	2.3803	1.8986	1.6394
homologuetoGP15919176gbAAL10712.1buddinguninhibitedbybenzimidazoles1beta{Homosapiens}.partial(16%)	0.5097	2.7655	1.1021	2.1731	1.6376
unknown	0.6101	2.6605	1.9502	1.3204	1.6353
similartoGP1469205dbjBAA09490.1TheKIAA0141geneproductisnovel.{Homosapiens}.partial(36%)	1.0589	3.3219	0.2847	1.8606	1.6315
similartoGP12652921gbAAH00217.1Similartohypotheticalprotein{Homosapiens}.complete	1.4094	1.8398	0.9104	2.3389	1.6246
unknown	0.4150	2.8301	1.0835	2.1616	1.6226
unknown	1.2451	1.4594	1.6848	2.0393	1.6072
homologuetoGP12053249embCAB66806.hypotheticalprotein{Homosapiens}.complete	0.3785	2.8301	0.8257	2.3828	1.6043
unknown	0.5305	2.6699	1.2873	1.9130	1.6002
similartoSPO75031HBP2_HUMANHeatshockfactor2bindingprotein.[Human]{Homosapiens}.partial(73%)	1.3969	1.5850	2.0354	1.3589	1.5940

homologuetoGP12655091gbAAH01396.1AD-003protein{Homosapiens}.partial(62%)	1.3281	3.5110	0.7245	0.8021	1.5914
similartoGP13177635gbAAK14906.1phospholipaseCbeta-3{Rattusnorvegicus}.partial(28%)	0.1069	3.0661	0.7427	2.4303	1.5865
unknown	0.5850	2.5850	0.3799	2.7900	1.5850
SPP52433RPB7_HUMANDNA-directedRNApolymeraseII19kDapolypeptide(EC2.7.7.6)(RPB7).[Rat]{Rattusnorvegicus}.complete	1.6323	1.5311	1.5334	1.6299	1.5817
unknown	2.1699	0.9922	1.1210	2.0411	1.5811
homologuetoSPP55931ETFD_PIGElectrontransferflavoprotein-ubiquinoneoxidoreductasemitochondrialprecursor(EC1.5.5.1).partial(22%)	1.8931	1.2666	1.8083	1.3514	1.5799
weaklysimilartoGP6841340gbAAF29023.1HSPC051{Homosapiens}.partial(86%)	1.6049	1.5493	2.7632	0.3910	1.5771
homologuetoGP13625170gbAAK34944.1NDR3{Homosapiens}.partial(67%)	0.6374	2.5166	1.5406	1.6134	1.5770
unknown	1.0995	2.0531	1.8455	1.3072	1.5763
unknown	0.0000	3.1468	1.0106	2.1363	1.5734
unknown	1.6571	1.4780	1.6234	1.5117	1.5676
homologuetoGP10441970gbAAG17262.1unknown{Homosapiens}.partial(20%)	1.0000	2.1346	1.6650	1.4697	1.5673
homologuetoGP17223689gbAAK77940.1F-boxproteinFBG3{Homosapiens}.partial(74%)	0.6414	2.4919	1.8489	1.2843	1.5666
similartoGP12653567gbAAH00557.1phosphatidylethanolamineN-methyltransferase{Homosapiens}.partial(86%)	0.1031	3.0297	0.3037	2.8292	1.5664
homologuetoGP17224454gbAAL36982.1nanos{Homosapiens}.partial(78%)	0.6668	2.4594	2.3667	0.7595	1.5631
unknown	1.1491	1.2730	2.2821	1.5434	1.5619
GP12652557gbAAH00018.1Similartoactinrelatedprotein2/3complexsubunit5(16kD){Homosapiens}.complete	0.7885	2.3219	1.8734	1.2371	1.5552
unknown	0.6630	2.4475	0.5995	2.5110	1.5552
unknown	1.4330	1.6738	1.4599	1.6468	1.5534
unknown	0.5117	2.5850	0.5406	2.5561	1.5483
unknown	1.3219	1.7726	1.4010	1.6935	1.5473
GP13540389gbAAK29448.1ceramideglucosyltransferase{Cricetulusgriseus}.partial(25%)	1.5850	1.5070	0.0625	3.0294	1.5460
unknown	1.1979	1.8931	1.4527	1.6383	1.5455
unknown	0.9386	2.1520	1.1944	1.8962	1.5453
homologuetoGP1523871embCAA65861.1cofactorA{Bostaurus}.complete	0.7965	2.2912	1.8723	1.2154	1.5438
unknown	1.5850	1.5025	0.7262	2.3612	1.5437
unknown	0.1394	2.9475	1.5171	1.5699	1.5435
SPP38384S61G_HUMANProteintransportproteinSEC61gammasubunit.[Dog]{Canisfamiliaris}.complete	1.7419	1.3426	1.4014	1.6830	1.5422
similartoPIRA53028A53028isopentenyl-diphosphateDelta-isomerase(EC5.3.3.2)homolog-human.complete	1.2861	1.7979	0.8402	2.2437	1.5420
homologuetoSPQ9NPD3RR41_HUMANExosomecomplexexonucleaseRRP41(EC3.1.13.-)(RibosomalRNAprocessingprotein41).[Human].partial(77%)	1.5850	1.4919	1.0111	2.0658	1.5384
similartoGP3789868gbAAC67525.1signaltransducerandactivatoroftranscription6{Homosapiens}.partial(30%)	0.9329	2.1375	0.7578	2.3126	1.5352
GP12803667gbAAH02669.1nuclearreceptorsubfamily2groupFmember6{Homosapiens}.partial(50%)	0.6477	2.4215	1.3731	1.6961	1.5346
myosinregulatorylightchainventricularisoform[Susscrofa]myosinlightchain2[Susscrofa]	1.4935	1.4279	1.7475	1.4624	1.5328
unknown	1.3112	1.7506	0.5146	2.5473	1.5309
unknown	1.1699	1.8894	1.7649	1.2945	1.5297

homologuetoGP14250686gbAAH08809.1Similartoangio-associatedmigratorycellprotein{Homosapiens}.partial(80%)	0.1806	2.8745	1.3219	1.7331	1.5275
voltage-dependentanionchannel2[Susscrofa]	1.5471	1.4932	2.9776	0.0627	1.5201
unknown	1.2274	1.2605	1.0060	2.5723	1.5166
homologuetoSPQ00013EM55_HUMAN55kDaerythrocytemembraneprotein(P55).[Human]{Homosapiens}.partial(23%)	0.6183	2.4126	2.5056	0.5252	1.5154
unknown	-0.1013	3.1265	1.8059	1.2193	1.5126
similartoSPQ9Y3Q8TIZ2_HUMANTSC22-relatedinducibleleucinezipperprotein2(Tsc-22-likeproteinTHG-1).[Human]{Homosapiens}.partial(35%)	0.8688	2.1468	0.8278	2.1878	1.5078
unknown	0.0352	2.9798	1.5395	1.4755	1.5075
unknown	1.3219	1.6859	0.7203	2.2875	1.5039
unknown	0.7935	2.2115	1.5328	1.4723	1.5025
unknown	1.3591	1.6408	1.4545	1.5454	1.4999
similartoGP17512436gbAAH19177.1Similartoalveolarsoftpartsarcomachromosomeregioncandidate1{Musmusculus}.partial(44%)	0.3870	2.6088	1.1641	1.8318	1.4979
homologuetoGP13374079embCAC34475.TAFII140protein{Homosapiens}.partial(20%)	1.3576	1.6374	1.7812	1.2138	1.4975
similartoGP16740625gbAAH16196.1Unknown(proteinforMGC:27580){Musmusculus}.partial(56%)	-0.0544	3.0484	1.9482	1.0457	1.4970
unknown	0.3440	2.6394	2.4658	0.5175	1.4917
similartoGP12839167dbjBAB24454.putative{Musmusculus}.partial(58%)	0.3049	2.6781	0.9845	1.9984	1.4915
similartoGP9930614gbAAG02116.1steroidreceptorRNAactivatorisoform3{Homosapiens}.partial(73%)	1.1155	1.8667	1.0208	1.9615	1.4911
unknown	1.0614	2.9069	0.7549	1.2134	1.4841
unknown	0.5850	2.3785	1.4542	1.5093	1.4817
similartoGP13097537gbAAH03494.1Unknown(proteinforMGC:6943){Musmusculus}.partial(75%)	0.8886	2.0671	1.5022	1.4535	1.4778
homologuetoGP493132gbAAC41688.1creatinetransporter{Homosapiens}.partial(27%)	-1.8373	-0.6744	-0.4606	-2.0511	-1.2558
tissueinhibitorofmetalloproteinase-3[Susscrofa]	-0.3219	-2.1979	-1.2856	-1.2343	-1.2599
unknown	-1.0916	-1.4384	-1.2830	-1.2470	-1.2650
hyaluronidase	-1.0845	-1.4475	-0.6053	-1.9267	-1.2660
unknown	-1.1473	-1.3923	-1.3851	-1.1545	-1.2698
weaklysimilartoPIRS68191S68191triadin-human.partial(19%)	-1.5424	-1.0909	-2.0107	-0.4530	-1.2742
unknown	-1.6812	-0.8780	-0.0328	-2.5264	-1.2796
homologuetoGP5821375dbjBAA83793.1MTH1b(p22)MTH1c(p21)MTH1d(p18){Homosapiens}.partial(72%)	-1.2482	-1.3152	-0.1880	-2.3754	-1.2817
5-HT1Dreceptor[Susscrofa]serotoninreceptor1D[Susscrofa]	-0.6674	-1.2310	-1.8894	-1.3393	-1.2818
homologuetoSPQ13887KLF5_HUMANKrueppel-likefactor5(Intestinal-enrichedkrueppel-likefactor)(Colonkrueppel-likefactor).partial(52%)	-0.7453	-1.8210	-1.5146	-1.0517	-1.2831
weaklysimilartoSPP23606TGLK_RATProtein-glutaminegamma-glutamyltransferaseK(EC2.3.2.13)(TransglutaminaseK)(TGaseK)(TGK).partial(20%)	-0.1587	-2.7402	-1.3186	-0.9456	-1.2908
unknown	-0.7400	-1.6595	-1.2614	-1.5101	-1.2928
homologuetoSPO18751PHS2_SHEEPGlycogenphosphorylasemuscleform(EC2.4.1.1)(Myophosphorylase).[Sheep]{Ovisaries}.partial(26%)	-0.6206	-1.9683	-1.4211	-1.1678	-1.2944
similartoGP16359275gbAAH16100.1Unknown(proteinforMGC:27672){Musmusculus}.partial(35%)	-1.7631	-0.8277	-1.6362	-0.9546	-1.2954
similartoPIRB34087B34087hypotheticalprotein(L1H3'reg	-1.1279	-2.7225	-0.3859	-0.9529	-1.2973

ion)-human.partial(11%)					
aminopeptidaseN.[Susscrofa]aminopeptidaseN[Susscrofa]aminopeptidase[Susscrofa]	-1.1806	-1.4150	-0.6975	-1.8981	-1.2978
unknown	-0.2065	-2.3923	-1.4766	-1.1222	-1.2994
unknown	-0.4019	-2.1987	-1.1022	-1.4984	-1.3003
beta-tropomyosin[Susscrofa]beta-tropomyosin[Susscrofa]	-0.4656	-3.0692	-1.5866	-0.0858	-1.3018
unknown	-1.1609	-1.4435	-1.4080	-1.1964	-1.3022
similartoGP11385352gbAAG34759.1aminoacidtransporterSLC3A1{Canisfamiliaris}.partial(20%)	-0.7590	-1.3646	-1.0701	-2.0175	-1.3028
unknown	-0.1312	-2.4780	-0.9236	-1.6857	-1.3046
insulin-likegrowthfactorbindingprotein2[Susscrofa]IGFbindingprotein-2	-1.0701	-1.5425	-1.8340	-0.7787	-1.3063
similartoGP14424509gbAAH09274.1Unknown(proteinforMGC:10681){Homosapiens}.partial(53%)	-1.6039	-1.0224	-0.7960	-1.8303	-1.3131
unknown	-0.3049	-2.3219	-0.1608	-2.4660	-1.3134
unknown	-1.6660	-0.9621	-1.6950	-0.9331	-1.3140
unknown	0.0000	-2.6521	-1.9486	-0.7035	-1.3260
homologuetoGP13177775gbAAH03656.1minichromosomemaintenancedeficient(S.cerevisiae)5(celldivisioncycle46){Homosapiens}.partial(48%)	-1.3588	-1.2971	-1.2035	-1.4524	-1.3279
unknown	-0.8352	-1.8257	-0.8234	-1.8375	-1.3305
homologuetoGP1430783embCAA65075.1X-linkedmentalretardationcandidategene{Homosapiens}.partial(11%)	-1.5850	-1.2479	-1.6325	-0.8605	-1.3315
similartoPIRT12462T12462hypotheticalproteinDKFZp564I122.1-human(fragment).partial(97%)	-0.6125	-2.0506	-1.6442	-1.0190	-1.3316
homologuetoSPO46392CA21_CANFACollagenalpha2(I)chainprecursor.[Dog]{Canisfamiliaris}.partial(12%)	-1.5459	-1.1493	-0.7951	-1.9000	-1.3476
heparin-bindingepidermalgrowthfactor-likegrowthfactor[Susscrofa]Heparin-bindingepidemialgrowthfactor[Susscrofa]	-0.0791	-2.7753	-1.0372	-1.5009	-1.3481
unknown	-1.5472	-1.1492	-0.9429	-1.7535	-1.3482
unknown	-0.4044	-1.1043	-2.0044	-1.8867	-1.3500
similartoGP15862322embCAC88591.unnamedproteinproduct{Homosapiens}.partial(52%)	-0.4971	-2.2130	-1.2213	-1.4888	-1.3550
similartoGP14714906gbAAH10609.1hypotheticalproteinFLJ22167{Homosapiens}.partial(37%)	-1.1844	-1.8972	-1.1108	-1.2331	-1.3564
homologuetoSPP27706EF12_MOUSEElongationfactor1-alpha2(EF-1-alpha-2)(Elongationfactor1A-2)(eEF1A-2)(StatinS1).[Rat].partial(15%)	0.1830	-2.8970	-1.6056	-1.1084	-1.3570
unknown	-1.7004	-2.4263	-0.5992	-0.7258	-1.3629
unknown	-1.4737	-1.2575	-0.4418	-2.2894	-1.3656
homologuetoGP10438696dbjBAB15314.unnamedproteinproduct{Homosapiens}.partial(30%)	-1.3612	-1.3735	-0.2825	-2.4521	-1.3673
similartoGP14160858gbAAK07671.1ADP-ribosepyrosphosphataseNUDT9{Homosapiens}.partial(28%)	-0.8684	-1.8707	-1.5075	-1.2316	-1.3695
ART5protein[Susscrofa]	-1.6114	-2.0176	-1.8153	-0.0479	-1.3731
unknown	-0.9733	-1.7776	-1.1133	-1.6376	-1.3755
similartoPIRT18522T18522tubulin-foldingcofactorD-bovine.partial(15%)	-0.2266	-2.5361	-0.1139	-2.6487	-1.3813
titin[Susscrofa]	-0.8091	-1.5959	-1.8917	-1.2769	-1.3934
unknown	-0.0544	-2.7327	-1.1455	-1.6417	-1.3936
unknown	-1.0356	-1.8379	-2.3991	-0.3319	-1.4012
unknown	-1.3395	-1.4671	-2.3992	-0.4074	-1.4033
homologuetoSPP23588IF4B_HUMANEukaryotictranslationinitiationfactor4B(eIF-	-0.1444	-2.6651	-0.8293	-1.9802	-1.4048

4B).[Human]{Homosapiens}.partial(27%)					
homologuetoGP15862466embCAC88632.unnamedproteinproduct{Homosapiens}.partial(79%)	-0.3609	-2.4594	-1.3070	-1.5134	-1.4102
Igkappachain	-0.7583	-2.0641	-0.2524	-2.5700	-1.4112
similartoGP10438524dbjBAB15267.unnamedproteinproduct{Homosapiens}.partial(82%)	-0.3752	-2.4478	-0.2870	-2.5360	-1.4115
homologuetoGP18027794gbAAL55858.1unknown{Homosapiens}.partial(11%)	-1.6697	-1.1623	-1.1283	-1.7037	-1.4160
unknown	-1.4150	-1.2479	-1.3421	-1.6607	-1.4164
unknown	-0.7555	-2.0921	-0.8444	-2.0032	-1.4238
homologuetoSPQ9P2W9STXH_HUMANSyntaxin18.[Human]{Homosapiens}.partial(28%)	-1.1575	-1.0156	-0.5696	-2.9733	-1.4290
homologuetoGP1800225gbAAC50950.1JAK3{Homosapiens}.partial(6%)	-0.6501	-2.2121	-1.1329	-1.7293	-1.4311
unknown	-1.6677	-1.1983	-0.4986	-2.3674	-1.4330
GP15929669gbAAH15264.1sialyltransferase5{Musmusculus}.partial(42%)	-0.0458	-2.8346	-0.4919	-2.3885	-1.4402
similartoSPP10074HKR3_HUMANKrueppel-relatedzincfingerprotein3(HKR3protein).[Human]{Homosapiens}.partial(33%)	-1.6630	-1.5443	-1.4721	-1.0833	-1.4407
unknown	-1.1405	-1.0444	-2.3305	-1.2925	-1.4520
weaklysimilartoGP3218467embCAA07090.1putativephosphatase{Gallusgallus}.partial(66%)	-0.1715	-2.7370	-0.6228	-2.2856	-1.4542
cartilageaggregatingproteoglycan[Susscrofa]aggrecanCS2domain[Susscrofa]	-1.3219	-1.2479	-2.4056	-0.8765	-1.4630
readingframe[Susscrofa]	-2.2668	-1.2224	-1.6481	-0.7739	-1.4778
similartoGP2564320dbjBAA22955.1KIAA0286{Homosapiens}.partial(26%)	-0.2392	-1.1964	-1.5967	-2.8821	-1.4786
homologuetoSPQ92176CO1A_BOVINCoronin-likeproteinp57(Coronin1A).[Bovine]{Bostaurus}.partial(27%)	-0.6420	-2.3219	-1.3894	-1.5745	-1.4819
homologuetoPIRA28442TPRBCStroponinCfastskeletalmuscle-rabbit.complete	-0.2808	-1.2504	-2.0127	-2.3952	-1.4848
unknown	-1.4561	-1.4263	-1.8284	-1.2296	-1.4851
similartoGP6683128dbjBAA20800.2KIAA0342protein{Homosapiens}.partial(13%)	-1.4721	-1.4854	-0.8215	-2.2477	-1.5067
similartoGP6179932gbAAF05716.1tektin{Canisfamiliaris}.partial(32%)	-0.0618	-1.9696	-2.3955	-1.6359	-1.5157
unknown	-1.1444	-1.1876	-1.4240	-2.3305	-1.5216
GP14250798gbAAH08869.1hypotheticalproteinF17127_1{Homosapiens}.partial(41%)	-1.0193	-2.0324	-0.4529	-2.5988	-1.5259
triadin[Susscrofa]	-0.4448	-1.5110	-2.3896	-1.7870	-1.5331
unknown	-2.0056	-1.0744	-1.4050	-1.6526	-1.5344
mineralocorticoidreceptor[Susscrofa]	-0.5753	-2.5025	-1.4373	-1.6405	-1.5389
unknown	-0.8470	-2.2327	-1.9130	-1.1666	-1.5398
similartoGP12854557dbjBAB30070.putative{Musmusculus}.partial(83%)	-1.4150	-1.5025	-1.9980	-1.2594	-1.5437
similartoGP8896138gbAAF81254.1pregnancy-associatedglycoprotein4{Susscrofa}.partial(34%)	-0.9386	-2.1619	-0.7975	-2.3030	-1.5502
similartoGP2351683gbAAB68608.1nucleolarfibrillarcenterprotein{Homosapiens}.partial(31%)	-0.8301	-1.9542	-1.6761	-1.7879	-1.5621
ubiquitousTPRmotifproteinubiquitousTPRmotifproteinUTY[Susscrofa]ubiquitousTPRmotifproteinUTX[Susscrofa]	-0.4321	-1.5677	-1.3440	-2.9274	-1.5678
Gprotein-coupledreceptor	-1.0815	-2.2200	-1.6981	-1.2773	-1.5693
homologuetoGP10437164dbjBAB15001.unnamedproteinproduct{Homosapiens}.partial(16%)	-1.4930	-1.6550	-0.7757	-2.3723	-1.5740
unknown	-2.8074	-1.9658	-0.2471	-1.2967	-1.5792
unknown	-0.6521	-2.5081	-1.4372	-1.7229	-1.5801
similartoGP3327808gbAAC39879.1latenttransforminggrowthfactor-	-1.3036	-1.8581	-1.5202	-1.6415	-1.5809

betabindingprotein4S{Homosapiens}.partial(13%)					
similartoSPQ9H9D4PRDH_HUMANPR-domainzincfingerprotein17.[Human]{Homosapiens}.partial(18%)	-0.5519	-2.6280	-1.3073	-1.8726	-1.5900
unknown	-0.6406	-2.5465	-1.7507	-1.4364	-1.5935
unknown	-1.8074	-1.0297	-1.1294	-2.4783	-1.6112
unknown	-1.6439	-1.8704	-0.8019	-2.1369	-1.6133
homologuetoGP13184897embCAC33267.unnamedproteinproduct{Homosapiens}.partial(18%)	-1.9594	-1.2288	-1.9952	-1.3555	-1.6347
unknown	-1.3219	-1.6049	-0.2884	-3.3507	-1.6415
homologuetoGP4325215gbAAD17301.1single-strandselectivemonofunctionaluracilDNAglycosylase{Homosapiens}.partial(77%)	-0.6868	-1.9790	-1.9578	-1.9607	-1.6461
skeletalmusclespecificcalpain;Ca2+-dependentcysteineprotinase[Susscrofa]skeletalmuscle-specificcalpaincalpainlargepolypeptideL3[	-0.4019	-2.8938	-0.8864	-2.4093	-1.6478
smallproline-richprotein	-1.4739	-2.7866	-2.3012	-0.0636	-1.6563
homologuetoGP5689525dbjBAA83046.1KIAA1094protein{Homosapiens}.partial(42%)	-0.9285	-2.3923	-2.5461	-0.7747	-1.6604
typeIIcollagenalpha1[Susscrofa]	-1.6665	-1.6557	-0.1148	-3.2075	-1.6611
similartoSPQ9Z262CLD6_MOUSEClaudin-6.[Mouse]{Musmusculus}.complete	-0.2854	-3.6245	-0.9223	-1.8460	-1.6695
homologuetoGP11139720gbAAG31814.1polyadenylationproteinCSTF64{Musmusculus}.partial(17%)	-1.1756	-2.1743	-0.7256	-2.6242	-1.6749
similartoGP16552606dbjBAB71352.unnamedproteinproduct{Homosapiens}.partial(35%)	-0.1363	-3.2224	-0.9856	-2.3731	-1.6794
similartoGP12840019dbjBAB24733.putative{Musmusculus}.partial(52%)	-1.3833	-1.7549	-0.7992	-2.8057	-1.6858
unknown	-0.6699	-2.7090	-1.2224	-2.1564	-1.6894
homologuetoGP17900927embCAD19357.unnamedproteinproduct{Homosapiens}.partial(9%)	-0.6292	-2.0128	-2.0693	-2.0560	-1.6918
homologuetoGP9651109dbjBAB03567.1TTYH1{Macacafascicularis}.partial(30%)	-0.4109	-3.0000	-1.9461	-1.4648	-1.7054
unknown	-0.4748	-2.9386	-1.4043	-2.0091	-1.7067
apoptosisinhibitorsurvivin[Susscrofa]	-1.3458	-2.1043	-1.1935	-2.2566	-1.7251
homologuetoSPP29562IF41_RABITEukaryoticinitiationfactor4A-I(eIF-4A-I)(eIF4A-I)(Fragment).[Rabbit]{Oryctolaguscuniculus}.partial(18%)	-1.9175	-1.3750	-2.1098	-1.5126	-1.7288
similartoGP12407338gbAAG53461.1proteinO-mannosyltransferase1{Rattusnorvegicus}.partial(27%)	-1.3476	-2.1184	-1.8292	-1.6369	-1.7330
unknown	-0.1150	-3.3646	-2.5025	-0.9771	-1.7398
similartoSPP28667MRP_MOUSEMARCKS-relatedprotein(MAC-MARCKS)(BrainproteinF52).[Mouse]{Musmusculus}.partial(78%)	-1.7935	-1.7391	-2.3743	-1.1582	-1.7663
alpha2A-adrenergicreceptor(PORA2AR)alpha-2Aadrenergicreceptor[Susscrofa]	-0.7899	-2.7608	-2.4065	-1.1442	-1.7754
unknown	-0.9055	-2.6462	-1.4869	-2.0647	-1.7758
homologuetoGP5081463gbAAD39394.1bigMAPkinase1a{Musmusculus}.partial(14%)	-1.4637	-2.0952	-0.6167	-2.9421	-1.7794
unknown	-0.9069	-2.6650	-0.6193	-2.9526	-1.7859
unknown	-0.7776	-2.8074	-0.8195	-2.7655	-1.7925
typeIcollagenalpha1[Susscrofa]	-0.4978	-3.0999	-2.1502	-1.4474	-1.7988
homologuetoGP12804735gbAAH01799.1Unknown(proteinforIMAGE:3354600){Homosapiens}.partial(35%)	-1.4657	-2.0661	-1.9750	-1.6941	-1.8002
weaklysimilartoGP1196432gbAAA88037.1unknownprotein{Homosapiens}.partial(10%)	-0.3479	-2.2530	-1.2484	-3.3525	-1.8005
dipeptidaseprecursor[Susscrofa]dipeptidase[Susscrofa]	-1.3103	-1.9260	-1.5431	-2.4518	-1.8078
similartoSPQ9Y2B2PIGL_HUMANN-acetylglucosaminyl-phosphatidylinositolde-N-acetylase(EC3.5.1.-	-1.0000	-2.6630	-1.5932	-2.0698	-1.8315

).partial(34%)					
similartoGP6841522gbAAF29114.1HSPC150{Homosapiens}.partial(40%)	-1.1545	-2.8413	-1.3650	-2.0128	-1.8434
unknown	-1.6167	-2.0969	-0.8418	-2.8718	-1.8568
homologuetoGP6329074dbjBAA86388.1UDP-GlcNAc:a-13-D-mannosideb-14-N-acetylglucosaminyltransferaseIV{Homosapiens}.partial(34%)	-2.3923	-2.1085	-2.0335	-0.8981	-1.8581
weaklysimilartoGP37996embCAA46158.1XerodermaPigmentosumGroupCComplementingfactor{Homosapiens}.partial(18%)	-1.0314	-1.7597	-1.4426	-3.2230	-1.8642
homologuetoSPP24140GPT_CRIGRUDP-N-acetylglucosamine--dolichyl-phosphateN-acetylglucosaminephosphotransferase(EC2.7.8.15).partial(42%)	-1.6200	-2.1257	-1.6356	-2.1101	-1.8729
unknown	-0.7014	-3.0495	-1.5733	-2.1776	-1.8755
unknown	-1.8114	-2.5859	-1.0075	-2.1442	-1.8873
similartoGP9367763embCAB97494.1zincfingerproteinCezanne{Homosapiens}.partial(25%)	-1.7608	-1.5443	-1.0695	-3.1923	-1.8918
unknown	-0.9042	-2.9292	-0.8336	-2.9999	-1.9167
similartoGP18089247gbAAH20966.1Unknown(proteinforMGC:9127){Homosapiens}.partial(19%)	-0.3923	-3.2395	-1.7530	-2.3095	-1.9236
homologuetoGP3721838dbjBAA33714.1NIK{Homosapiens}.partial(29%)	-0.6575	-3.2197	-1.1283	-2.7488	-1.9386
unknown	-2.3626	-1.2479	-1.7912	-2.3690	-1.9427
unknown	-1.0913	-3.9819	-1.1915	-1.5164	-1.9453
homologuetoGP12804537gbAAH01679.1Unknown(proteinforMGC:2722){Homosapiens}.partial(49%)	-0.3771	-3.5850	-1.5429	-2.4192	-1.9810
unknown	-1.1520	-2.1155	-1.5504	-3.1091	-1.9817
Ca2+ATPaseoffasttwitch1skeletalmusclesarcoplasmicreticulum[Susscrofa]	-0.3460	-3.3113	-2.1326	-2.1407	-1.9826
unknown	-1.6854	-3.2873	-0.9303	-2.0424	-1.9863
unknown	-1.1225	-2.8580	-1.3578	-2.6227	-1.9902
homologuetoGP434775dbjBAA04946.1KIAA0014{Homosapiens}.partial(36%)	-1.4530	-2.5406	-1.9845	-2.0091	-1.9968
homologuetoGP6330597dbjBAA86534.1KIAA1220protein{Homosapiens}.partial(24%)	-1.4448	-2.4485	-1.6566	-2.4575	-2.0018
matrixmetalloproteinase	-1.0265	-2.0000	-1.8395	-3.1869	-2.0132
similartoGP1684843gbAAB48302.1pinin{Bostaurus}.partial(19%)	-1.0506	-3.0875	-2.0151	-1.9205	-2.0184
weaklysimilartoPIRG01880G01880fatty-acidsynthase(EC2.3.1.85)(version2)-human.partial(7%)	-1.4838	-2.5914	-1.4604	-2.6148	-2.0376
melanocortintype4receptor[Susscrofa]melanocortin4receptor[Susscrofa]melanocortin-4receptorMC4R[Susscrofa]	-1.7241	-2.4739	-1.0626	-3.1354	-2.0990
unknown	-0.4868	-3.7188	-1.3956	-2.8100	-2.1028
similartoGP15823629dbjBAB69011.ALS2CR4{Homosapiens}.partial(21%)	-0.5096	-3.7391	-2.0698	-2.1789	-2.1243
unknown	-1.3155	-2.5831	-1.5394	-3.0972	-2.1338
homologuetoGP12856351dbjBAB30641.putative{Musmusculus}.complete	-2.0400	-1.2449	-2.2090	-3.0759	-2.1425
unknown	-2.3169	-2.6245	-1.7190	-1.9550	-2.1538
similartoSPQ92636FAN_HUMANProteinFAN(FactorassociatedwithN-SMaseactivation).partial(22%)	-1.6280	-2.9542	-1.7468	-2.3233	-2.1631
similartoGP1669621dbjBAA13700.1latexin{Musmusculus}.partial(36%)	-1.3049	-4.7549	-1.4522	-1.3882	-2.2250
unknown	-1.5443	-3.0444	-1.8908	-2.5207	-2.2500
preproacrosin[Susscrofa]acrosinprecursor(EC3.4.21.10)	-2.1069	-2.6439	-1.3536	-2.9695	-2.2685
homologuetoEGAD2653127372discs-largehomologg3{Homosapiens}.partial(27%)	-0.5761	-3.9696	-1.3654	-3.1803	-2.2729
gagprotein[Susscrofa]polprotein[	-2.5850	-3.9765	-1.2091	-1.3524	-2.2808

similartoSPO43246CTR4_HUMANCationicaminoacidtransporter-4(CAT-4)(CAT4).[Human]{Homosapiens}.partial(62%)	-2.4815	-2.0875	-0.8999	-3.6691	-2.2845
homologuetoGP12314190embCAC16281.dJ445H2.2(novelprotein){Homosapiens}.partial(30%)	-1.6101	-2.1898	-1.7970	-3.5627	-2.2899
unknown	-1.5077	-4.0931	-1.7061	-1.8947	-2.3004
homologuetoSPP50461CSR3_HUMANLIMdomainproteincardiac(MuscleLIMprotein)(Cysteine-richprotein3)(CRP3).[Human].partial(76%)	-1.6940	-2.9260	-2.8826	-1.7374	-2.3100
similartoSPP35605COPP_BOVINCoatomerbeta'subunit(Beta'-coatprotein)(Beta'-COP)(p102).[Bovine]{Bostaurus}.partial(8%)	-2.0000	-2.7004	-0.9733	-3.7272	-2.3502
unknown	-1.8074	-3.5236	-2.5192	-1.5823	-2.3581
homologuetoSPP15407FRA1_HUMANFOS-relatedantigen1.[Human]{Homosapiens}.partial(31%)	-1.7127	-3.4919	-1.8177	-2.5360	-2.3896
unknown	-1.3985	-4.3837	-1.2012	-2.5811	-2.3911
unknown	-1.4381	-3.2533	-2.6152	-2.3238	-2.4076
similartoPIRA44128A44128(N-acetylneuraminyl)-galactosylglucosylceramideN-acetylgalactosaminyltransferase(EC2.4.1.92)-.partial(46%)	-2.3219	-2.5648	-1.9772	-2.9095	-2.4434
homologuetoGP8515870gbAAF76218.1bridgingintegrator-3{Homosapiens}.partial(67%)	-2.3665	-2.5317	-3.4693	-1.4289	-2.4491
homologuetoPIRS04090S04090myosinheavychain3skeletalmuscleembryonic-human.partial(4%)	-2.2738	-3.6684	-1.2549	-2.6873	-2.4711
unknown	-2.0238	-3.9674	-1.3740	-2.6173	-2.4956
fattyacidsynthase[Susscrofa]	-1.7643	-4.3325	-2.4084	-1.6885	-2.5484
unknown	-2.5305	-5.8074	-0.8235	-1.3923	-2.6384
weaklysimilartoGP7671629embCAB89275.2bA145L22.2(novelKRABboxcontainingC2H2typezincfingerprotein){Homosapiens}.partial(27%)	-2.4721	-3.0000	-2.8841	-2.6997	-2.7640
titin[Susscrofa]	-3.0307	-2.9505	-3.5721	-2.4091	-2.9906
unknown	-4.3141	-2.6147	-1.9807	-3.6917	-3.1503
unknown	-4.0643	-2.2368	-3.5633	-2.7378	-3.1506
unknown	-3.0729	-2.4896	-3.1690	-4.1018	-3.2083
unknow	-1.8826	-5.4094	-1.9647	-3.7968	-3.2634

Table 4. Transcripts highly up/down regulated determined by oligo-array in the muscle tissue by the dietary shifting from LFD to HFD (Chapter 3). For each transcript, $\log_2$ratio=$\log_2$(HFD/LFD).The positive value means higher mRNA abundance in HFD pigs; negative value means lower mRNA abundance in HFD pigs

Gene name	Log_2(R1/G1)	Log_2(G2/R2)	Log_2(R3/G3)	Log_2(G4/R4)	Avrage
unknown	2.6663	1.8616	2.7270	1.8010	2.2640
ribosomalproteinL19[Susscrofa]	2.5662	1.8995	2.0796	2.3861	2.2328
homologuetoPIR|S71405|S71405helix-loop-helixproteinID3longspliceform-human.partial(65%)	1.4332	2.9359	3.0173	1.3518	2.1845
similartoSP|O00212|RHOD_HUMANRho-relatedGTP-bindingproteinRhoD(Rho-relatedproteinHP1)(RhoHP1).[Human]{Homosapiens}.partial(91%)	3.2661	0.9472	2.1781	2.0352	2.1067
homologuetoSP|P55931|ETFD_PIGElectrontransferflavoprotein-ubiquinoneoxidoreductasemitochondrialprecursor(EC1.5.5.1).partial(22%)	2.1843	1.9564	2.5663	1.5744	2.0704
homologuetoSP|P22392|NDKB_HUMANNucleosidediphosphatekinaseB(EC2.7.4.6)(NDKB)(NDPkinaseB)(nm23-H2).complete	2.7958	1.2525	2.3009	1.7475	2.0242

unknown	2.7031	1.2880	2.9856	1.0056	1.9956
unknown	2.8269	1.1632	1.8722	2.1178	1.9950
PIR|A48045|A48045ribosomalproteinS27cytosolic-human.complete	2.6471	1.8754	1.7109	1.6117	1.9613
homologuetoGP|12833968|dbj|BAB22732.putative{Musmusculus}.partial(23%)	2.1672	1.7244	2.2182	1.6733	1.9458
homologuetoGP|5531805|gb|AAD44477.1|16.7Kdprotein{Homosapiens}.complete	3.2370	0.6302	2.0132	1.8540	1.9336
unknown	2.3772	1.4493	1.6647	2.1618	1.9132
medium-chainacyl-CoAdehydrogenase	2.6677	1.0346	1.2100	2.4923	1.8511
homologuetoSP|P82664|RT10_HUMANMitochondrial28SribosomalproteinS10(MRP-S10)(MSTP040).[Human]{Homosapiens}.partial(30%)	2.2430	1.4406	2.0695	1.6140	1.8418
unknown	3.2359	0.4258	2.0773	1.5843	1.8308
unknown	2.5573	1.0780	2.5619	1.0735	1.8177
90-kDaheatshockprotein[Susscrofa]	2.4052	1.0389	1.8896	1.5545	1.7220
homologuetoSP|P07471|COXD_BOVINCytochromecoxidasepolypeptideVIa-heartmitochondrialprecursor(COXVIAH).partial(75%)	2.3281	1.1100	1.7416	1.6965	1.7190
homologuetoGP|2547076|dbj|BAA22860.1A+U-richelementRNAbindingfactor{Homosapiens}.partial(33%)	2.5399	0.8919	1.4815	1.9502	1.7159
unknown	1.9664	1.4185	1.0646	2.3203	1.6924
unknown	2.6746	0.6738	1.3466	2.0018	1.6742
similartoGP|12407437|gb|AAG53507.1tripartitemotifproteinTRIM16{Musmusculus}.partial(66%)	2.3643	0.9590	1.3274	1.9960	1.6617
homologuetoSP|P29350|PTN6_HUMANProtein-tyrosinephosphatasenon-receptortype6(EC3.1.3.48)(Protein-tyrosinephosphatase1C).partial(63%)	2.2657	1.0541	1.7946	1.5252	1.6599
homologuetoGP|12843392|dbj|BAB25965.putative{Musmusculus}.complete	0.9076	2.4103	1.3579	1.9600	1.6589
unknown	1.5768	1.7370	2.0641	1.2497	1.6569
similartoGP|12053165|emb|CAB66762.hypotheticalprotein{Homosapiens}.partial(19%)	1.5670	1.7404	1.9786	1.3287	1.6537
weaklysimilartoGP|14336751|gb|AAK61280.1unknown{Homosapiens}.partial(27%)	2.2877	1.0000	1.6845	1.6032	1.6438
unknown	2.3820	0.8963	1.1022	2.1761	1.6391
beta2-microglobulinbeta-2-microglobulinprotein[Susscrofa]	2.2755	0.9919	1.0502	2.2171	1.6337
unknown	2.5115	0.7498	1.2974	1.9639	1.6306
unknown	2.3909	0.8425	1.2039	2.0294	1.6167
similartoSP|Q13283|G3BP_HUMANRas-GTPase-activatingproteinbindingprotein1(GAPSH3-domainbindingprotein1)(G3BP-).[Human].partial(54%)	2.4975	0.7291	2.2798	0.9468	1.6133
homologuetoGP|15072481|gb|AAK71328.1LOH1CR12{Homosapiens}.partial(83%)	1.7751	1.4429	0.7618	2.4562	1.6090
heatshockprotein70[Susscrofa]heatshockprotein70.hsp70	2.3166	0.8931	1.3994	1.8103	1.6048
similartoGP|6573163|gb|AAF17574.1|ubiquitinspecificprocessingprotease{Rattusnorvegicus}.partial(43%)	1.6300	1.5729	2.1155	1.0874	1.6014
unknown	2.7362	0.4594	1.4070	1.7886	1.5978
homologuetoGP|286011|dbj|BAA02792.1|KIAA0002{Homosapiens}.partial(20%)	2.4962	0.6969	0.5958	2.5974	1.5966
homologuetoGP|12804349|gb|AAH03035.1Unknown(proteinforMGC:4355){Homosapiens}.partial(38%)	1.1237	2.0156	1.7370	1.4024	1.5697
homologuetoGP|3282771|gb|AAC33845.1|actin-bindingproteinhomologABP-278{Homosapiens}.partial(9%)	2.1387	1.0000	1.0682	2.0706	1.5694
unknown	1.9225	1.1907	0.3723	2.7408	1.5566

unknown	2.6843	0.4208	1.2242	1.8809	1.5526
GP|12654423|gb|AAH01037.1ribosomalproteinL35a{Homosapiens}.complete	1.8096	1.2918	1.3009	1.8005	1.5507
similartoGP|6624920|emb|CAB63941.1DMBT1prototype{Homosapiens}.partial(10%)	1.8891	1.2033	0.0929	2.9996	1.5462
homologuetoPIR|I38191|I38191nucleicacidbindingprotein-human(fragment).partial(96%)	2.6905	0.3612	1.4150	1.6367	1.5258
unknown	1.6820	1.3692	0.9086	2.1427	1.5256
unknown	2.2230	0.8274	1.1103	1.9401	1.5252
unknown	1.7776	1.2706	1.3862	1.6621	1.5241
homologuetoGP|4929617|gb|AAD34069.1|CGI-74protein{Homosapiens}.partial(78%)	2.4470	0.5850	1.0969	1.9351	1.5160
homologuetoGP|11138955|gb|AAG31556.115kDaselenoprotein{Homosapiens}.complete	2.3346	0.6878	1.2224	1.7999	1.5112
similartoSP|P32019|I5P2_HUMANTypeIIinositol-145-trisphosphate5-phosphataseprecursor(EC3.1.3.56)(5PTASE)(Fragment)..partial(22%)	1.7489	1.2701	1.7225	1.2965	1.5095
homologuetoSP|P00819|ACYM_PIGAcylphosphatasemuscletypeisozyme(EC3.6.1.7)(Acylphosphatephosphohydrolase).[Pig].complete	2.1315	0.8823	2.0952	0.9186	1.5069
homologuetoGP|13940506|gb|AAK50397.1GDP-fucosetransporter{Homosapiens}.partial(92%)	0.9860	2.0247	1.7232	1.2875	1.5053
homologuetoSP|P70698|PYRG_MOUSECTPsynthase(EC6.3.4.2)(UTP--ammonialigase)(CTPsynthetase).[Mouse]{Musmusculus}.partial(20%)	1.3408	1.6684	1.6542	1.3550	1.5046
unknown	0.4548	2.5538	1.6807	1.3279	1.5043
unknown	2.3942	0.5726	1.6158	1.3510	1.4834
homologuetoGP|10439498|dbj|BAB15508.unnamedproteinproduct{Homosapiens}.partial(75%)	1.6067	1.3579	1.8057	1.1589	1.4823
unknown	1.1184	1.8407	2.0458	0.9133	1.4795
ATPsynthasegammasubunit1[Susscrofa]	2.6754	0.2828	1.3895	1.5687	1.4791
unknown	1.9361	1.0199	1.0354	1.9206	1.4780
unknown	3.2049	0.2580	1.2885	1.1424	1.4735
unknown	1.4671	1.4739	1.1137	1.8274	1.4705
SP|P23821|RS7_HUMAN40SribosomalproteinS7(S8).[Rat]{Rattusnorvegicus}.complete	2.5080	0.4241	1.3388	1.5933	1.4660
similartoGP|12845654|dbj|BAB26840.putative{Musmusculus}.complete	2.5002	0.4288	1.2323	1.6967	1.4645
unknown	2.7203	0.2027	1.0555	1.8675	1.4615
unknown	2.9003	1.0117	0.9831	0.9290	1.4560
SP|P33552|CKS2_HUMANCyclin-dependentkinasesregulatorysubunit2(CKS-2).[Human]{Homosapiens}.complete	2.1028	0.8074	1.3108	1.5994	1.4551
homologuetoGP|15524116|emb|CAC69312.unnamedproteinproduct{Homosapiens}.partial(25%)	2.2926	0.6117	1.3845	1.5198	1.4522
unknown	2.3703	0.5305	2.0721	0.8287	1.4504
homologuetoGP|7321168|emb|CAB82246.1dJ860F19.3(metallocarboxypeptidaseCPX-1){Homosapiens}.partial(54%)	1.8884	1.0092	1.3462	1.5515	1.4488
homologuetoEGAD|45512|479773-hydroxyisobutyryl-coenzymeAhydrolase{Homosapiens}.partial(49%)	1.3072	1.5850	1.9569	0.9352	1.4461
unknown	2.3914	0.4975	2.2890	0.5999	1.4444
homologuetoSP|P18067|RAB7_CANFARas-relatedproteinRab-7.[Dog]{Canisfamiliaris}.complete	2.3868	0.4902	1.0643	1.8127	1.4385
similartoEGAD|3524|3493collagentypeVIalpha3{Homosapiens}.partial(18%)	1.5267	1.3499	2.2718	0.6048	1.4383
unknown	2.0756	0.7907	1.8549	1.0113	1.4331
similartoSP|O75185|ATC4_HUMANProbablecalcium-	1.6494	1.2115	1.3714	1.4896	1.4305

transportingATPaseKIAA0703(EC3.6.3.8).[Human]{Homosapiens}.partial(40%)					
homologuetoGP|15012167|gb|AAH10991.1hypothetic alproteinFLJ21977{Homosapiens}.partial(56%)	0.5637	2.2946	1.2655	1.5929	1.4292
arachidonate12-lipoxygenase(EC1.13.11.31)arachidonate12-lipoxygenase[Susscrofa]	0.1354	2.7178	1.2572	1.5960	1.4266
SP|P00829|ATPB_BOVINATPsynthasebetachainmitochondrialprecursor(EC3.6.3.14).[Bovine]{Bostaurus}.partial(48%)	2.7907	0.0501	1.8585	0.9824	1.4204
dihydropyrimidinedehydrogenase	1.5025	1.3219	1.4996	1.3249	1.4122
homologuetoGP|14250712|gb|AAH08825.1DEAD/H(Asp-Glu-Ala-Asp/His)boxpolypeptide16{Homosapiens}.partial(19%)	1.6095	1.2100	1.2455	1.5740	1.4097
unknown	2.2605	0.5539	1.1926	1.6218	1.4072
unknown	1.4516	1.3567	1.7567	1.0516	1.4041
similartoSP|P27213|PTPS_RAT6-pyruvoyltetrahydrobiopterinsynthaseprecursor(EC4.6.1.10)(PTPS)(PTPsynthase).[Rat].partial(93%)	2.1546	0.6521	0.4586	2.3480	1.4033
similartoGP|9864062|gb|AAG01291.1|MOG1isoformB{Homosapiens}.complete	1.9074	0.8974	0.2604	2.5444	1.4024
GP|13172662|gb|AAK14178.1ubiquitin-like5protein{Homosapiens}.complete	2.4691	0.3334	1.8402	0.9623	1.4012
unknown	1.9894	0.8045	1.0641	1.7298	1.3970
unknown	2.0977	1.3053	1.0635	1.1183	1.3962
PIR|S05014|R5RT37ribosomalproteinL37acytosolic[validated]-rat.complete	1.3136	1.4772	1.5563	1.2346	1.3954
unknown	1.5677	1.2168	0.0943	2.6902	1.3922
metallothionein-III[Susscrofa]	0.6833	2.0959	1.1777	1.6015	1.3896
unknown	1.0596	1.7137	1.7797	0.9936	1.3867
homologuetoPIR|S60062|S60062hevinprecursor-human.partial(21%)	1.3229	1.4301	1.2122	1.5409	1.3765
neuron-derivedorphanreceptor-1beta[Susscrofa]neuron-derivedorphanreceptor-1alfa[Susscrofa]	1.5236	1.2224	1.8679	0.8781	1.3730
similartoGP|13279278|gb|AAH04341.1SimilartoRIKENcDNA5730568A12gene{Homosapiens}.partial(32%)	0.3940	2.3472	1.1676	1.5736	1.3706
unknown	1.4285	1.3093	1.4060	1.3318	1.3689
unknown	0.4231	2.3108	0.7894	1.9444	1.3669
homologuetoGP|13177724|gb|AAH03639.1Unknown(proteinforIMAGE:3346359){Homosapiens}.partial(95%)	0.7410	1.9894	0.3800	2.3503	1.3652
c-Fosprotein[Susscrofa]earlyimmediategeneexpression[Susscrofa]	1.9784	0.7498	1.3758	1.3524	1.3641
unknown	1.8426	0.8711	0.1729	2.5407	1.3568
unknown	1.7774	0.9319	1.7339	0.9754	1.3546
long-chainacyl-CoAdehydrogenase[Susscrofa]	1.8144	0.8713	0.0491	2.6366	1.3429
unknown	2.1063	0.5778	0.4578	2.2263	1.3420
unknown	2.2496	0.4316	1.6481	1.0331	1.3406
unknown	1.2729	1.3883	1.6426	1.0187	1.3306
SP|Q28151|OZF_BOVINZincfingerproteinOZF.[Bovine]{Bostaurus}.partial(19%)	1.8324	0.8220	0.8306	1.8238	1.3272
proteinphosphatase2Aalphasubunit	2.0760	0.5702	1.3930	1.2532	1.3231
GP|18043683|gb|AAH20043.1Unknown(proteinforMGC:28311){Musmusculus}.partial(45%)	-0.7370	3.3798	1.3699	1.2729	1.3214
similartoGP|2935442|gb|AAC78563.1|ribonucleaseH1{Homosapiens}.partial(46%)	2.0729	0.5590	1.1057	1.5262	1.3159
unknown	1.9571	0.6658	1.3375	1.2855	1.3115

unknown	1.1707	1.4365	1.4429	1.1642	1.3036
unknown	0.9254	1.6738	1.4552	1.1439	1.2996
homologuetoGP|10439230|dbj|BAB15467.unnamedproteinproduct{Homosapiens}.partial(32%)	2.5688	0.0159	1.3252	1.2596	1.2924
unknown	1.3164	1.2645	0.5811	1.9998	1.2905
SP|P41276|ARL1_RATADP-ribosylationfactor-likeprotein1.[Rat]{Rattusnorvegicus}.partial(56%)	2.2327	0.3479	0.2990	2.2817	1.2903
similartoGP|13325194|gb|AAH04415.1hypotheticalproteinFLJ13154{Homosapiens}.partial(87%)	1.5787	1.0000	1.5003	1.0784	1.2894
GP|12834526|dbj|BAB22945.putative{Musmusculus}.complete	0.9494	1.6268	1.6663	0.9100	1.2881
fattyacid-bindingprotein[Susscrofa]heartfattyacid-bindingprotein[Susscrofa]	1.2023	1.3732	0.7592	1.8162	1.2877
similartoGP|12382294|gb|AAG53094.13-methylcrotonyl-CoAcarboxylasebetasubunit{Homosapiens}.partial(19%)	1.3809	1.1915	0.5000	2.0724	1.2862
homologuetoGP|14603084|gb|AAH10013.1SimilartoputativeDNAbindingprotein{Homosapiens}.partial(29%)	0.9125	1.6592	1.3677	1.2040	1.2859
similartoGP|12654491|gb|AAH01075.1mitochondrialuncouplingprotein1{Homosapiens}.partial(43%)	1.4829	1.0875	1.5850	0.9854	1.2852
similartoPIR|T12474|T12474hypotheticalproteinDKFZp564K2062.1-human(fragment).complete	0.5521	2.0078	1.2082	1.3517	1.2800
similartoGP|15530220|gb|AAH13889.1Unknown(proteinforMGC:11192){Homosapiens}.partial(23%)	0.5300	2.0297	0.5236	2.0362	1.2799
unknown	1.3581	1.1993	0.2893	2.2682	1.2787
similartoGP|14035880|emb|CAC38536.unnamedproteinproduct{Homosapiens}.partial(47%)	1.6339	0.9228	0.3008	2.2560	1.2784
unknown	2.6826	0.1309	0.7580	1.5319	1.2758
homologuetoGP|10432840|dbj|BAB13857.unnamedproteinproduct{Homosapiens}.partial(30%)	0.6946	1.8516	1.0625	1.4837	1.2731
similartoSP|Q02380|NISM_BOVINNADH-ubiquinoneoxidoreductaseSGDHsubunitmitochondrialprecursor(EC1.6.5.3)(EC1.6.99.3).complete	2.3257	0.2153	1.4924	1.0486	1.2705
unknown	2.2955	0.2439	1.2008	1.3385	1.2697
beta-globin[Susscrofa]	0.1162	2.6487	1.1197	1.1803	1.2662
similartoGP|12751447|gb|AAK07659.1minorhistocompatibilityantigenprecursor{Musmusculus}.complete	1.2390	1.2876	0.1715	2.3551	1.2633
unknown	1.2619	1.2640	0.3714	2.1546	1.2630
heatshockprotein70.2[Susscrofa]	1.7897	0.7357	1.1511	1.3744	1.2627
unknown	1.2571	1.2563	0.1712	2.3423	1.2567
homologuetoGP|12314036|emb|CAC10469.dJ383J4.1(AKelchmotif-containingprotein){Homosapiens}.partial(22%)	1.0866	1.4263	1.5850	0.9279	1.2564
unknown	1.5971	0.9143	0.0693	2.4421	1.2557
MADH4protein[Susscrofa]Smad4	0.8724	1.6386	0.6130	1.8981	1.2555
unknown	0.9942	1.5164	0.4824	2.0283	1.2553
unknown	1.5237	0.9851	1.1896	1.3192	1.2544
homologuetoGP|3043720|dbj|BAA25524.1KIAA0598protein{Homosapiens}.partial(54%)	1.7586	0.7323	0.7822	1.7087	1.2454
PIR|S11393|R5HU32ribosomalproteinL32-human.complete	2.5469	-0.0613	0.9744	1.5112	1.2428
weaklysimilartoGP|15489209|gb|AAH13712.1Unknown(proteinforIMAGE:3155889){Musmusculus}.partial(55%)	1.1490	1.3350	0.7834	1.7006	1.2420
homologuetoPIR|I51803|I51803TAXREB107-human.partial(88%)	2.8150	0.3325	0.9458	0.8719	1.2413
homologuetoGP|18088472|gb|AAH20773.1Unknown(proteinforMGC:22685){Homosapiens}.partial(48%)	1.6374	0.8433	0.1293	2.3514	1.2404
unknown	2.2440	0.2333	1.1017	1.3756	1.2387

homologuetoGP|4406524|gb|AAD20016.1|tip-associatedproteinTAP{Homosapiens}.partial(45%)	0.8539	1.6215	1.3491	1.1262	1.2377
unknown	1.0213	1.4525	0.3000	2.1738	1.2369
homologuetoGP|6435831|gb|AAC25580.2|bithoraxoid-likeprotein{Rattusnorvegicus}.complete	2.0257	0.4475	1.0931	1.3801	1.2366
unknown	2.6684	0.2015	0.9179	1.1460	1.2335
unknown	0.5983	1.8667	0.9582	1.5068	1.2325
SP|Q93068|SM33_HUMANUbiquitin-likeproteinSMT3Cprecursor).complete	1.3495	1.1155	0.7182	1.7467	1.2325
unknown	1.1724	1.2801	0.9044	1.5481	1.2262
homologuetoGP|13097153|gb|AAH03350.1SimilartoGproteinpathwaysuppressor1{Musmusculus}.partial	0.9748	1.4698	0.6818	1.7628	1.2223
unknown	0.5297	1.9069	1.4643	0.9723	1.2183
unknown	0.3920	2.0403	0.5755	1.8568	1.2161
unknown	1.9154	0.4969	0.4799	1.9324	1.2062
preproSPAI-2[Susscrofa]SPAI-2[Susscrofa]SPAI-2[Susscrofa]	1.2722	1.1375	0.1349	2.2747	1.2048
homologuetoSP|P47197|AKT2_RATRAC-betaserine/threonineproteinkinase(EC2.7.1.-)(RAC-PK-beta)(ProteinkinaseAkt-2).partial(25%)	1.6449	0.7593	0.3118	2.0924	1.2021
homologuetoGP|183227|gb|AAB59563.1||glucokinase{Homosapiens}.partial(40%)	2.1928	0.1908	1.5149	0.8688	1.1918
similartoGP|14035956|emb|CAC38574.unnamedproteinproduct{Homosapiens}.partial(46%)	1.3219	1.0589	1.0627	1.3181	1.1904
adipocytefattyacidbindingprotein[Susscrofa]	0.8330	2.2115	1.2792	0.4333	1.1893
unknown	0.7876	1.5850	0.4172	1.9553	1.1863
CD40ligand[Susscrofa]CD40L[Susscrofa]	1.3978	0.9676	0.5100	1.8553	1.1827
unknown	1.6732	0.6840	1.2577	1.0995	1.1786
unknown	1.6815	0.6741	0.0602	2.2953	1.1778
GP|4689156|gb|AAD27787.1|unrprotein{Homosapiens}.partial(36%)	0.6693	1.6781	0.8310	1.5164	1.1737
unknown	2.3238	1.0225	0.7713	0.5749	1.1731
unknown	0.7853	1.5449	0.1569	2.1733	1.1651
unknown	1.7321	0.5963	1.3281	1.0003	1.1642
homologuetoSP|Q9Y2X7|GIT1_HUMANARFGTPase-activatingproteinGIT1(Gprotein-coupledreceptorkinase-interactor1).[Human].partial(53%)	-2.7726	-1.4150	-0.8260	-1.3617	-1.5938
homologuetoGP|12804745|gb|AAH01808.1nucleosidediphosphatekinasetype6(inhibitorofp53-inducedapoptosis-alpha){Homosapiens}.partial(38%)	-1.5220	-2.6684	-0.5773	-1.6130	-1.5952
similartoSP|P30519|HO2_HUMANHemeoxygenase2(EC1.14.99.3)(HO-2).[Human]{Homosapiens}.complete	-1.5397	-1.3458	-0.5220	-2.9805	-1.5970
GP|6463679|dbj|BAA86954.1Fzr1{Homosapiens}.partial(47%)	-2.6521	-1.4557	-1.1293	-1.1558	-1.5982
homologuetoEGAD|45385|47850envoplakin{Homosapiens}.partial(10%)	-2.3692	-1.1709	-0.3997	-2.4567	-1.5992
GP|4679028|gb|AAD27002.1|HSPC021{Homosapiens}.partial(44%)	-1.1474	-1.0525	-2.0121	-2.1878	-1.5999
homologuetoGP|14043628|gb|AAH07788.1Similartoeukaryotictranslationinitiationfactor4gamma1{Homosapiens}.partial(35%)	-1.2900	-1.0866	-1.0529	-2.9773	-1.6017
unknown	-1.5031	-1.2980	-1.3427	-2.2664	-1.6025
similartoGP|16306850|gb|AAH06548.1hypotheticalproteinFLJ22637{Homosapiens}.partial(24%)	-1.9806	-1.7751	-0.5968	-2.0585	-1.6028
homologuetoEGAD|31767|32837T1/ST2receptor-bindingprotein{Homosapiens}.complete	-2.1198	-1.9110	-1.8583	-0.5284	-1.6044
homologuetoGP|10438296|dbj|BAB15220.unnamedproteinproduct{Homosapiens}.partial(40%)	-2.1553	-1.0540	-0.4403	-2.7689	-1.6046

homologuetoSP|P78537|GC5L_HUMANGCN5-likeprotein1(RT14protein).[Human]{Homosapiens}.complete	-2.5699	-1.3581	-1.3458	-1.1498	-1.6059
collagenVIIIalpha1[Susscrofa]	-2.3390	-2.1193	-0.8836	-1.0975	-1.6099
homologuetoEGAD|140573|149904pyruvatekinaseM2{Susscrofa}.complete	-1.7650	-1.5392	-1.3851	-1.7624	-1.6129
unknown	-1.5353	-1.3046	-0.7719	-2.8496	-1.6154
homologuetoSP|O43826|G6PU_HUMANGlucose6-phosphatetranslocase(Glucose5-phosphatetransporter)(PRO0685).[Human]{Homosapiens}.complete	-2.1187	-0.8789	-1.6042	-1.8778	-1.6199
similartoGP|11177148|gb|AAG32154.1mitoribosomalproteinL12{Homosapiens}.complete	-2.3219	-1.0677	-0.4519	-2.6668	-1.6271
similartoSP|Q95108|THI2_BOVINThioredoxinmitochondrialprecursor(MT-TRX).[Bovine]{Bostaurus}.complete	-2.1898	-0.9307	-1.4588	-1.9388	-1.6295
unknown	-1.9208	-1.6610	-2.4915	-0.4462	-1.6299
homologuetoGP|17224454|gb|AAL36982.1nanos{Homosapiens}.partial(78%)	-2.6033	-1.3429	-0.4977	-2.0770	-1.6302
unknown	-2.0806	-1.1973	-1.5159	-1.7620	-1.6390
homologuetoPIR|JE0086|JE0086SH3-domainbindingproteinSab-human.partial(42%)	-2.9511	-1.3272	-0.5907	-1.6875	-1.6391
homologuetoGP|3449362|gb|AAC32546.1|slowskeletalmuscletroponinT{Musmusculus}.partial(51%)	-2.8819	-1.4012	-0.4495	-1.8336	-1.6415
similartoGP|10438452|dbj|BAB15247.unnamedproteinproduct{Homosapiens}.partial(42%)	-2.2132	-1.0723	-0.4027	-2.8828	-1.6427
unknown	-1.6746	-1.6267	-2.5215	-0.7797	-1.6506
homologuetoEGAD|3033|3004collagentypeIValpha2{Homosapiens}.partial(35%)	-2.0463	-1.2630	-1.0000	-2.3093	-1.6547
unknown	-2.8791	-1.4327	-1.1672	-1.1447	-1.6559
homologuetoGP|11611554|dbj|BAB18991.hypothetical protein{Macacafascicularis}.partial(43%)	-2.3750	-1.0612	-1.9903	-1.2012	-1.6569
PIR|B31486|FIHUAtranslationinitiationfactoreIF-5A[validated]-human.complete	-2.2427	-1.0737	-1.2508	-2.0656	-1.6582
unknown	-2.2033	-1.1155	-1.9866	-1.3322	-1.6594
unknown	-2.6630	-1.3440	-1.2157	-1.4154	-1.6595
similartoGP|14336708|gb|AAK61240.1similartoAK001902{Homosapiens}.partial(53%)	-1.3399	-2.0180	-1.6666	-1.6192	-1.6609
unknown	-2.2625	-1.0635	-1.0891	-2.2368	-1.6630
similartoSP|P51449|RORG_HUMANNuclearreceptorROR-gamma(NuclearreceptorRZR-gamma).[Human]{Homosapiens}.partial(16%)	-2.1420	-1.1846	-0.6746	-2.6520	-1.6633
similartoGP|11559826|gb|AAG38105.1hepatopoietinprotein{Homosapiens}.complete	-2.2946	-1.0447	-1.5646	-1.7747	-1.6696
unknown	-2.0238	-1.3219	-1.0468	-2.2990	-1.6729
similartoGP|12652989|gb|AAH00255.1Unknown(proteinforMGC:2495){Homosapiens}.complete	-1.8981	-1.4499	-1.2785	-2.0695	-1.6740
homologuetoGP|12653265|gb|AAH00401.1splicingfactor3bsubunit2145kD{Homosapiens}.partial(18%)	-2.4813	-0.8707	-0.8989	-2.4531	-1.6760
calcium-sensingreceptor[Susscrofa]	-2.5988	-1.2414	-1.5850	-1.2895	-1.6787
homologuetoGP|5442038|gb|AAD43218.1|stromalcell-derivedreceptor-1alpha{Homosapiens}.partial(81%)	-2.1806	-1.1846	-0.0196	-3.3456	-1.6826
unknown	-1.9069	-1.4710	-1.5909	-1.7870	-1.6889
unknown	-2.2161	-1.8369	-1.2994	-1.4060	-1.6896
unknown	-1.7405	-1.6423	-2.0118	-1.3710	-1.6914
similartoPIR|S27962|S27962modulatorrecognitionfactor1-human(fragment).partial(23%)	-1.7175	-2.3296	-1.3385	-1.3902	-1.6940
homologuetoGP|12654907|gb|AAH01299.1putativetransmembraneprotein;homologofyeastGolgimembraneproteinYif1p.partial(52%)	-1.5115	-1.1155	-1.6293	-2.5357	-1.6980

homologuetoGP|16041122|dbj|BAB69728.hypotheticalprotein{Macacafascicularis}.partial(32%)	-2.0517	-1.3502	-0.9926	-2.4093	-1.7010
GP|2791680|gb|AAC26843.1|26SproteasomeATPasesubunit{Homosapiens}.partial(39%)	-2.7682	-1.3604	-2.1242	-0.5628	-1.7039
homologuetoSP|P79334|PHS2_BOVINGlycogenphosphorylasemuscleform(EC2.4.1.1)(Myophosphorylase).[Bovine]{Bostaurus}.partial(22%)	-2.1562	-1.2521	-1.9779	-1.4304	-1.7041
homologuetoGP|3327044|dbj|BAA31590.1KIAA0615protein{Homosapiens}.partial(15%)	-1.9740	-1.5657	-2.0643	-1.2125	-1.7041
similartoGP|2914185|pdb|1FSU|4-Sulfatase(Human).partial(52%)	-2.1024	-1.3072	-1.6674	-1.7422	-1.7048
caspase-3[Susscrofa]	-2.4594	-1.0418	-1.0339	-2.3000	-1.7088
weaklysimilartoGP|463552|gb|AAA16956.1||AF-1{Homosapiens}.partial(69%)	-3.1346	-1.2930	-0.9364	-1.4913	-1.7138
homologuetoSP|P53620|COPG_BOVINCoatomergammasubunit(Gamma-coatprotein)(Gamma-COP).[Bovine]{Bostaurus}.partial(10%)	-2.7312	-0.7004	-1.1085	-2.3231	-1.7158
unknown	-2.1515	-1.2968	-1.9574	-1.4909	-1.7241
unknown	-2.3999	-2.0566	-0.5850	-1.8716	-1.7283
GP|551606|gb|AAA67650.1||RNApolymeaseIIelongationfactorSIIIp15subunit{Homosapiens}.complete	-2.7395	-1.2735	-1.2925	-1.6266	-1.7330
homologuetoGP|833776|emb|CAA32002.1|adrenodoxinreductase(338AA){Bostaurus}.partial(65%)	-2.0830	-1.3851	-0.8235	-2.6446	-1.7340
unknown	-2.9449	-0.5305	-1.0209	-2.4545	-1.7377
GP|2102696|gb|AAC51317.1|karyopherinbeta3{Homosapiens}.partial(21%)	-3.1315	-0.3491	-1.0870	-2.3935	-1.7403
homologuetoSP|Q92785|REQU_HUMANZinc-fingerproteinubi-d4(Requiem)(Apoptosisresponsezincfingerprotein).[Human].partial(43%)	-1.9849	-1.5004	-1.2366	-2.2470	-1.7422
homologuetoGP|14715064|gb|AAH10696.1proproteinconvertasesubtilisin/kexintype7{Homosapiens}.partial(79%)	-1.5363	-1.0480	-2.5700	-1.8224	-1.7442
heparin-bindingepidermalgrowthfactor-likegrowthfactor[Susscrofa]Heparin-bindingepidemialgrowthfactor[Susscrofa]	-2.3337	-1.1649	-2.0852	-1.4134	-1.7493
similartoGP|12858123|dbj|BAB31206.putative{Musmusculus}.partial(20%)	-2.0875	-1.5850	-1.7590	-1.5736	-1.7513
weaklysimilartoGP|12839600|dbj|BAB24608.putative{Musmusculus}.partial(33%)	-1.2226	-2.2801	-1.0713	-2.4313	-1.7513
similartoSP|Q13588|GRAP_HUMANGRB2-relatedadaptorprotein.[Human]{Homosapiens}.complete	-1.9228	-1.4154	-0.8603	-2.8164	-1.7537
homologuetoGP|12845499|dbj|BAB26774.putative{Musmusculus}.partial(43%)	-1.6491	-1.1350	-1.5081	-2.7361	-1.7571
fourandahalfLIMdomains1protein.isoformCskeletalmuscleLIMprotein[Susscrofa]	-3.1099	-0.4158	-1.2156	-2.3101	-1.7628
similartoGP|17512422|gb|AAH19171.1SimilartoRIKENcDNA2310010G13gene{Musmusculus}.partial(53%)	-2.6622	-1.1098	-1.8069	-1.5259	-1.7762
TATAboxbindingprotein(TBP)associatedfactor[Susscrofa]	-2.5952	-0.9870	-1.5511	-2.0310	-1.7911
unknown	-2.7726	-1.1844	-1.4001	-1.8192	-1.7941
homologuetoGP|13785926|gb|AAK39520.1BTBdomainprotein{Homosapiens}.partial(34%)	-2.5496	-2.0422	-1.4031	-1.1887	-1.7959
homologuetoSP|P17844|DDX5_HUMANProbableRNA-dependenthelicasep68(DEAD-boxproteinp68)(DEAD-boxprotein5).[Human].partial(13%)	-2.1076	-1.5096	-0.9890	-2.5897	-1.7990
unknown	-2.4851	-1.1166	-0.6742	-2.9275	-1.8009
similartoGP|10047355|dbj|BAB13465.KIAA1639protein{Homosapiens}.partial(9%)	-2.1463	-2.4669	-0.5530	-2.0602	-1.8066
similartoGP|2463531|dbj|BAA22541.1Fln29{Homosapiens}.partial(24%)	-2.9009	-1.7126	-1.2648	-1.3487	-1.8067

homologuetoSP|P00883|ALFA_RABITFructose-bisphosphatealdolaseA(EC4.1.2.13)(Muscle-typealdolase).[Rabbit].partial(24%)	-2.7379	-0.8856	-1.6784	-1.9451	-1.8117
unknown	-1.3324	-1.2916	-2.2985	-2.3255	-1.8120
unknown	-2.9696	-1.3410	-1.4671	-1.4794	-1.8143
similartoGP|1694954|dbj|BAA13745.1Neuroblastoma{Homosapiens}.partial(87%)	-2.2033	-1.4339	-1.3896	-2.2476	-1.8186
olfactoryreceptor[Susscrofa]	-2.4946	-1.1468	-1.5600	-2.0814	-1.8207
unknown	-2.5546	-1.1255	-1.2355	-2.4446	-1.8401
similartoSP|Q04857|CA16_MOUSECollagenalpha1(VI)chainprecursor.[Mouse]{Musmusculus}.partial(13%)	-2.6743	-1.9783	-1.4598	-1.2796	-1.8480
sodium/hydrogenexchangerisoform3[Susscrofa]	-2.6994	-1.0066	-1.0916	-2.6145	-1.8530
unknown	-2.7407	-1.0148	-1.2252	-2.4711	-1.8630
unknown	-1.6553	-2.0774	-1.5302	-2.2025	-1.8663
similartoGP|13182763|gb|AAK14927.1CDA03{Homosapiens}.partial(60%)	-2.7885	-0.9477	-1.6599	-2.0763	-1.8681
similartoSP|P52758|UK14_HUMAN14.5kDatranslationalinhibitorprotein(p14.5)(UK114antigenhomolog).[Human]{Homosapiens}.partial(75%)	-2.9069	-1.1220	-2.0000	-1.5409	-1.8925
similartoSP|P58058|PPNK_MOUSEPutativeinorganic polyphosphate/ATP-NADkinase(EC2.7.1.23)(Poly(P)/ATPNADkinase).[Mouse].partial(55%)	-3.6781	-1.1198	-1.5510	-1.2469	-1.8990
homologuetoSP|P42208|SEP2_MOUSESeptin2(NED D5protein).[Mouse]{Musmusculus}.partial(54%)	-3.0444	-1.2303	-1.0457	-2.3078	-1.9070
unknown	-2.8413	-1.0234	-2.2303	-1.5409	-1.9090
PIR|JC4949|JC4949ADP-ribosylationfactor5-mouse.partial(97%)	-2.2896	-1.4610	-0.8480	-3.0586	-1.9143
unknown	-2.0100	-2.1740	-1.8639	-1.6240	-1.9180
similartoGP|16605472|emb|CAC82744.acyl-malonylcondensingenzyme{Homosapiens}.partial(53%)	-2.1448	-2.3080	-1.8665	-1.3543	-1.9184
long-chainenoyl-CoAhydratase:3-hydroxyacyl-CoAdehydrogenaseprecursor[Susscrofa]gastrin-bindingprotein	-2.3969	-1.5484	-2.0291	-1.7224	-1.9242
homologuetoGP|11527783|dbj|BAB18652.ubiquitin-conjyugatingenzymeE2{Homosapiens}.partial(59%)	-2.6821	-1.8237	-0.9750	-2.2360	-1.9292
weaklysimilartoGP|12848483|dbj|BAB27972.putative{Musmusculus}.partial(78%)	-2.5169	-1.3473	-0.7494	-3.1148	-1.9321
homologuetoSP|Q9XSJ7|CA11_CANFACollagenalpha1(I)chainprecursor.[Dog]{Canisfamiliaris}.partial(5%)	-2.1026	-2.2174	-1.7998	-1.6505	-1.9426
homologuetoGP|7020143|dbj|BAA91010.1unnamedproteinproduct{Homosapiens}.partial(37%)	-2.4444	-1.5591	-1.3021	-2.4650	-1.9426
homologuetoGP|17390440|gb|AAH18197.1Similartohypotheticalprotein{Musmusculus}.partial(23%)	-3.5341	-0.3704	-1.3070	-2.5976	-1.9523
homologuetoGP|12832202|dbj|BAB22006.putative{Musmusculus}.partial(85%)	-2.5105	-1.6051	-1.7652	-1.9302	-1.9527
similartoSP|O94833|ACFX_HUMANTrabeculin-beta(Fragment).[Human]{Homosapiens}.partial(11%)	-1.5742	-2.3443	-1.1998	-2.7187	-1.9593
similartoGP|14250483|gb|AAH08682.1actin-relatedprotein3-beta{Homosapiens}.partial(45%)	-1.9189	-2.0000	-1.3399	-2.5790	-1.9594
unknown	-2.2730	-2.3479	-1.7799	-1.4494	-1.9625
GP|12654649|gb|AAH01162.1signalrecognitionparticlereceptor('dockingprotein'){Homosapiens}.partial(22%)	-2.1403	-1.8025	-1.5555	-2.3872	-1.9714
similartoGP|7020512|dbj|BAA91159.1unnamedproteinproduct{Homosapiens}.partial(22%)	-2.9079	-1.0503	-1.6773	-2.2809	-1.9791
unknown	-1.7509	-2.2377	-1.8106	-2.1780	-1.9943
homologuetoSP|P18754|RCC1_HUMANRegulatorofchromosomecondensation(Cellcycleregulatoryprotein).[Human]{Homosapiens}.partial(41%)	-2.8213	-1.1727	-1.0113	-2.9827	-1.9970
5-hydroxytryptaminereceptor2c[Susscrofa]	-2.0000	-1.8695	-2.5247	-1.6058	-2.0000

eag-relatedgene[Susscrofa]	-2.1964	-1.1844	-1.6554	-2.9878	-2.0060
similartoGP|12804145|gb|AAH02927.1HSCARGprotein{Homosapiens}.partial(53%)	-2.1699	-2.1579	-1.3226	-2.3735	-2.0060
homologuetoPIR|A26711|A26711translationinitiationfactoreIF-2alphachain-rat.partial(29%)	-1.5572	-1.5396	-2.2249	-2.7135	-2.0088
similartoGP|15430292|gb|AAK95951.1musclealpha-kinase{Homosapiens}.partial(5%)	-2.1085	-2.0825	-1.0641	-2.7970	-2.0130
homologuetoGP|13506235|gb|AAG24463.1ST7proteinform3splicevariantb{Musmusculus}.partial(57%)	-2.7814	-1.7270	-1.7370	-1.8634	-2.0272
similartoPIR|T08778|T08778hypotheticalproteinDKFZp586I1520.1-human(fragment).partial(12%)	-2.6245	-1.5682	-1.4444	-2.4755	-2.0281
homologuetoGP|12654907|gb|AAH01299.1putativetransmembraneprotein;homologofyeastGolgimembraneproteinYif1p.partial(52%)	-2.2446	-1.1672	-1.8507	-2.8922	-2.0387
unknown	-1.9668	-1.8889	-2.3930	-1.9071	-2.0390
similartoGP|13477137|gb|AAH05025.1Similartometalloprotease1(pitrilysinfamily){Homosapiens}.partial(20%)	-1.6163	-1.5280	-2.4213	-2.6109	-2.0441
GP|10280562|gb|AAG15419.1eukaryotictranslationinitiationfactor3subunitp42/p44{Homosapiens}.complete	-2.3399	-2.2479	-1.4929	-2.1032	-2.0460
homologuetoGP|179830|gb|AAA35636.1||caldesmon{Homosapiens}.partial(33%)	-1.7310	-1.3901	-2.3898	-2.7313	-2.0605
homologuetoGP|13430408|gb|AAK25826.1BTBD2protein{Homosapiens}.partial(37%)	-1.6196	-1.5295	-2.4433	-2.7058	-2.0745
unknown	-2.0297	-2.1283	-1.6229	-2.5351	-2.0790
homologuetoSP|O46392|CA21_CANFACollagenalpha2(I)chainprecursor.[Dog]{Canisfamiliaris}.partial(12%)	-2.0798	-2.0937	-1.3513	-2.8222	-2.0867
unknown	-2.2883	-2.0988	-1.4884	-2.5034	-2.0947
homologuetoPIR|T47177|T47177hypotheticalproteinDKFZp762H157.1-human(fragment).partial(43%)	-2.0224	-1.7997	-2.4150	-2.2082	-2.1113
weaklysimilartoGP|2981631|dbj|BAA25253.1ORF2{Canisfamiliaris}.partial(26%)	-2.3063	-1.9231	-0.4364	-3.7930	-2.1147
PIR|T50638|T50638synapticglycoproteinSC2[imported]-human.complete	-2.2967	-2.0640	-1.0425	-3.0621	-2.1163
similartoPIR|B34087|B34087hypotheticalprotein(L1H3'region)-human.partial(11%)	-2.4030	-1.8340	-1.3133	-2.9237	-2.1185
homologuetoGP|4071321|gb|AAC98673.1|Y-boxproteinMSY2{Musmusculus}.partial(47%)	-3.1729	-1.0745	-1.6032	-2.6442	-2.1237
GP|567053|gb|AAA56751.1||beta5tubulin{Xenopuslaevis}.partial(22%)	-2.3294	-2.0780	-1.0995	-2.9958	-2.1257
homologuetoSP|O95716|RB3D_HUMANRas-relatedproteinRab-3D.[Human]{Homosapiens}.partial(83%)	-2.0790	-2.1785	-1.9131	-2.3443	-2.1287
SP|Q14449|GRBE_HUMANGrowthfactorreceptor-boundprotein14(GRB14adapterprotein).[Human]{Homosapiens}.partial(30%)	-1.9707	-2.3041	-1.7285	-2.5463	-2.1374
fibroblastgrowthfactor9[Susscrofa]	-2.5850	-2.2224	-1.8301	-2.0877	-2.1813
homologuetoPIR|JC5252|JC5252mitogen-activatedproteinkinase(EC2.7.1.-)p38gamma-human.partial(61%)	-2.1665	-2.2204	-1.4342	-2.9528	-2.1935
homologuetoGP|1000746|gb|AAC50214.1|Pro-a2(XI){Homosapiens}.partial(12%)	-2.9387	-1.4789	-2.3429	-2.1591	-2.2299
gagprotein[Susscrofa]polprotein[Susscrofa]	-2.2384	-2.2261	-1.9760	-2.4885	-2.2322
similartoPIR|A55050|A55050enigma-human.partial(32%)	-2.5618	-1.9211	-2.2940	-2.1889	-2.2414
homologuetoSP|Q92830|GCL2_HUMANGeneralcontrolofaminoacidsynthesisprotein5-like2(EC2.3.1.-).partial(26%)	-3.5041	-0.9938	-2.8034	-1.6945	-2.2489
unknown	-3.4321	-1.1070	-1.1882	-3.3508	-2.2695
homologuetoGP|11141704|gb|AAG32038.1SIR2L2{Musmusculus}.partial(50%)	-2.7549	-2.1993	-1.6599	-2.4970	-2.2778
Ca2+ATPaseoffasttwitch1skeletalmusclesarcoplasmicreticulum[Susscrofa]	-2.7532	-2.1902	-1.4926	-2.6902	-2.2815

homologuetoGP|5821375|dbj|BAA83793.1MTH1b(p22)MTH1c(p21)MTH1d(p18){Homosapiens}.partial(72%)	-2.7915	-1.2266	-2.0855	-3.0263	-2.2825
homologuetoGP|7959283|dbj|BAA96035.1KIAA1511protein{Homosapiens}.partial(10%)	-2.6147	-2.0107	-2.2268	-2.3558	-2.3020
similartoGP|14272678|emb|CAC39777.unnamedproteinproduct{Homosapiens}.partial(28%)	-2.8541	-1.7843	-2.0418	-2.5966	-2.3192
unknown	-2.3374	-1.6894	-2.2811	-2.9880	-2.3240
homologuetoSP|P24140|GPT_CRIGRUDP-N-acetylglucosamine--dolichyl-phosphateN-acetylglucosaminephosphotransferase(EC2.7.8.15).partial(42%)	-2.1207	-2.4725	-2.4833	-2.2199	-2.3241
cytosolicglycerol-3-phosphatedehydrogenase[Susscrofa]	-2.2630	-2.4019	-2.5453	-2.1197	-2.3325
PIR|A24156|BCBOIAS-100proteinalphachain-bovine.partial(85%)	-2.1458	-2.5299	-1.7774	-2.8984	-2.3379
homologuetoSP|O18751|PHS2_SHEEPGlycogenphosphorylasemuscleform(EC2.4.1.1)(Myophosphorylase).[Sheep]{Ovisaries}.partial(26%)	-2.7762	-1.9125	-2.3896	-2.2990	-2.3443
unknown	-2.9069	-1.7984	-2.4330	-2.2724	-2.3527
similartoGP|13540827|gb|AAF15294.2LRP16{Homosapiens}.complete	-2.8912	-2.1606	-1.1350	-3.2743	-2.3653
homologuetoGP|2145060|gb|AAB58413.1|TTF-Iinteractingpeptide20;TIP20;TranscriptionTerminationFactorIInteractingPeptide20.partial(33%)	-3.2029	-2.3954	-1.1179	-2.8988	-2.4038
homologuetoGP|493132|gb|AAC41688.1||creatinetransporter{Homosapiens}.partial(27%)	-2.9203	-3.0588	-1.4981	-2.2460	-2.4308
similartoGP|13397120|emb|CAC34689.unnamedproteinproduct{Homosapiens}.partial(6%)	-3.5064	-2.4663	-1.8694	-2.1033	-2.4863
unknown	-3.0284	-2.0310	-2.6483	-2.2872	-2.4987
unknown	-3.2184	-1.8331	-1.4501	-3.6014	-2.5258
homologuetoSP|Q15113|PCO1_HUMANProcollagenC-proteinaseenhancerproteinprecursor(PCPE).partial(41%)	-1.6724	-2.5757	-3.2398	-2.7055	-2.5484
homologuetoGP|3413926|dbj|BAA32327.1KIAA0483protein{Homosapiens}.partial(54%)	-1.9069	-2.3515	-2.8365	-3.4219	-2.6292
KCNE4[Susscrofa]	-3.1793	-3.1080	-1.6995	-2.5878	-2.6436
similartoGP|6330358|dbj|BAA86507.1KIAA1193protein{Homosapiens}.partial(68%)	-2.3576	-4.0080	-3.5387	-0.7949	-2.6748
homologuetoGP|9931474|gb|AAG02184.1|RNAbindingproteinMCG10{Homosapiens}.partial(33%)	-2.7857	-3.4236	-1.8986	-2.6163	-2.6811
homologuetoSP|Q14324|MYPF_HUMANMyosin-bindingproteinCfast-type(FastMyBP-C)(C-proteinskeletalmusclefast-isoform).[Human].partial(11%)	-3.1693	-2.5337	-2.1753	-3.3928	-2.8178
GP|10438718|dbj|BAB15321.unnamedproteinproduct{Homosapiens}.partial(92%)	-3.4079	-3.1286	-3.1198	-2.9023	-3.1396
immunoglobulinmuheavychainconstantregion[swine.spleen.PeptidePartial.403aa]immunoglobulinmuchainch4andsecretedomainsofswineIgM[Susscrofa]	-4.8284	-2.5642	-2.3685	-3.0241	-3.1963
SP|P06366|RS14_HUMAN40SribosomalproteinS14(ProteinPRO2640).[Chinesehamster]{Cricetulusgriseus}.complete	-2.9971	-2.6899	-3.7448	-3.9422	-3.3435
typeIIcollagenalpha1[Susscrofa]	-4.7687	-2.9978	-2.7636	-3.0029	-3.3833

Appendix J. An example of searching tentative biological information for one unknown transcript (gene)

In the result of adipose tissue, transcription of an unknown gene was significantly increased with the average normalized $\log_2$ratio of 2.98. Tracking the GenePix Array List (GAL) file, the oligo ID of the unknown gene was SS0009090. Then searching the pig array Axon Text File (ATF) and the probe sequence was CGCGTCCGGTCTCGGATAAAAGTCCTGGATTTTCCATTGGTTTTCATAATGGG TGTTTATATAAAACTAC . Then, the sequence was submitted to TIGR Gene Index Database (SsGI 5.0) (http://www.tigr.org/tigr-scripts/tgi/T_index.cgi?species=pig). It returned the gene ID of TC60740. Then, the sequence information of TC60740 was recruited from SsGI, and the information was presented in the Fig 1.

Results showed four open reading frames were included by the sequence; each of them corresponds to an expression sequence tag (EST). The accession numbers of the four ESTs were CF179926, AW785390, BF711816 and BM659677 respectively. Since the ESTs provided limited biological information about the unknown gene, the tentative consensus sequence of the unknown gene was aligned against GenBank by running BLASTn (Stephen, F. et al, 1997). BLASTn returned 128 hits (Fig 2). Further research may be designed to characterize the unknown gene based on the result with highest BLAST percent identity score and the knowledge in the pig biology.

Fig 1: Recruiting information of TC60740 by searching TIGR Porcine (Sus scrofa) Gene Index (SsGI). (http://www.tigr.org/tigr-scripts/tgi/T_index.cgi?species=pig)

SsGI TC Report: TC60740

EST IDs are linked to SsGI EST reports. ET#s are linked to EGAD ET reports. GB#s are linked to GenBank accessions.

```
>TC209354 TC121063 TC14954 TC152291 TC171191 TC27064 TC46118 TC60740 TC75388 TC87084
GAAGTGCTGCGCTATAGTAACTGCCTTAGCAACTGTAGATGTCTCGGATAAAAGTCCTGGATTTTCCATTGGTTTTCATA
ATGGGTGTTTATATAAAACTACTAAAGACTTTTTAAATGGCTTGATGTAGCAGTCATAGCAAGTTTGTAAATAGCATCTA
TGTCACACTCTCCTAGAGTATAAAATGTGAATGTTTTTGTAGCTAAATTGTGATTTGAAACTGGCTCATTCCAGTTTATT
GATTTCACAATAGGGGTTAAATTGGCAAACATTCATATTTTTACTTCATTTTTAAAACAACTGACTAATAGTTCTATATT
TTCAAAATATTTGGAAAAAAAAAGTATTCCCAAATGATTTTAATTTAAAAACAAATTGGCTTTGTCTCATTGATCAGACA
AAAAGAAACTAGTATGAAGGGAAGCGCAAACACGTTTATTTTGTACTGCAGAAAAATTGCTTTTTTGTATCACTTTTTGT
GTAATGGTTAGTAATTGTCATTTAAGTCCTTTTATGTATAAAACTGCCAAATGCTTACCTGGTATTTTATTAGATGCAGA
AACAGATTGGAAACAGCTAAATTATAACCTTTACATACAGCTCTGTATTATGGTTTCTTCATACTGTGTCTGTATTTAAT
CTTTTTTTATGGAATCTGTTGCGCCTATTTATGAAATAATAAATATAGGTGTTTGTAAGTAAATTTGTTAGTATTTGGCA
AAAA
1==========Open Reading Frames==========724

                                    ==========          +1
                                                        +2
_                                                       +3
_
          ==========                                    -3
                                          ==========    -2
                                                        -1
_
                                              =======   ESTScan(-)

    ========                                            framefinder(+)
_____________________________________________________
1==========TC209354==========724
<----------1
     ----------2---------->
          <----------3
               <----------4
```

#	Src	EST Id	GB#	Clone/Protein	left	right	Library/Protein name
1	IOOB	814966	CF179926		1	724	MARC 3PIG
2	IOOB	116406	AW785390		41	412	MARC 1PIG
3	IOOF	MI-P-E6-acy-b-11-1-UM.s1	BF711816	MI-P-E6-acy-b-11-1-UM	105	700	MI-P-E6
4	IO19	IKU602768923.R1	BM659677		267	703	CSEQFXL40 pig thymus

Sequence source codes:

IOOB USDA ARS US Meat Animal Research Center,
IOOF Iowa State University, Molecular Genetics Laboratory, Department of Animal Science
IO19 Texas A&M University, Animal Breeding and Genetics

TC sequence strand: *coding strand*

		Evidence for coding strand		Evidence for reverse complement		Inconclusive evidence
ESTs	5' ESTs	*(used as +)*	1	*(used as -)*	-	*(5'/3' source not known)*
	3' ESTs	*(used as -)*	2	*(used as +)*	-	
	total		3		-	1
Expressed transcripts			-		-	
Predicted genes			-		-	
Protein hits			-		-	
Trimmed polyA/T			-		-	

Fig 2. Result of aligning tentative consensus sequence of the unknown gene against GenBank by BLASTn

Sequences producing significant alignments:	(Bits)	Value	
gi|51477724|ref|NM_014729.2| Homo sapiens thymus high mobilit...	1176	0.0	U E G
gi|50491910|emb|CR611103.1| full-length cDNA clone CSODJ015YC...	1176	0.0	U
gi|17530764|gb|AC091195.6| Homo sapiens chromosome 8, clone RP11	1176	0.0	
gi|17047091|gb|AC084837.4| Homo sapiens chromosome 8, clone CTD-	1176	0.0	
gi|3882336|dbj|AB018351.1| Homo sapiens mRNA for KIAA0808 protei	1176	0.0	U E G
gi|16741739|gb|BC016665.1| Homo sapiens thymus high mobility ...	1168	0.0	U G
gi|7021964|dbj|AK000971.1| Homo sapiens cDNA FLJ10109 fis, cl...	1160	0.0	U G
gi|34366619|emb|BX647462.1|HSM807607 Homo sapiens mRNA; cDNA ...	1148	0.0	U G
gi|76634394|ref|XM_604247.2| PREDICTED: Bos taurus similar to...	1096	0.0	G
gi|73999419|ref|XM_544093.2| PREDICTED: Canis familiaris simi...	636	2e-179	G
gi|74179787|dbj|AK161578.1| Mus musculus adult male pituitary...	462	7e-127	G
gi|26332746|dbj|AK038671.1| Mus musculus adult male hypothala...	462	7e-127	U E G
gi|24433537|gb|BC038873.1| Mus musculus thymocyte selection-a...	462	7e-127	U E G
gi|51593440|gb|BC080732.1| Mus musculus thymocyte selection-a...	462	7e-127	U G
gi|31543884|ref|NM_145711.2| Mus musculus thymocyte selection...	462	7e-127	U E G
gi|28300582|emb|AL831740.9| Mouse DNA sequence from clone RP2...	462	7e-127	
gi|26325627|dbj|AK029694.1| Mus musculus adult male testis cD...	456	5e-125	U E G
gi|74225561|dbj|AK133397.1| Mus musculus adult male testis cD...	454	2e-124	G
gi|12838418|dbj|AK005704.1| Mus musculus adult male testis cD...	157	6e-35	U E G
gi|74206040|dbj|AK137964.1| Mus musculus 16 days neonate thym...	121	3e-24	G
gi|74184115|dbj|AK162821.1| Mus musculus adult male hypothala...	121	3e-24	G
gi|27877142|gb|AC135895.2| Homo sapiens 12 BAC RP11-168J19 (R...	48.1	0.039	
gi|5262435|emb|AL050401.5|HSJ519P24 Human DNA sequence from c...	46.1	0.16	
gi|38323093|emb|BX088644.9| Zebrafish DNA sequence from clone...	44.1	0.61	
gi|21358750|gb|AC105074.5| Homo sapiens chromosome 18, clone RP1	44.1	0.61	
gi|20377040|gb|AC104376.6| Homo sapiens chromosome 8, clone CTD-	44.1	0.61	
gi|17921225|gb|AC093303.2| Homo sapiens chromosome 5 clone RP11-	44.1	0.61	
gi|13431065|gb|AC023842.5|AC023842 Homo sapiens chromosome 8, cl	44.1	0.61	
gi|60301747|gb|AC154914.3| Pan troglodytes BAC clone RP43-172...	44.1	0.61	
gi|7159230|gb|AF221878.1|AF221878 Gyrinomimus sp. NI118 speci...	44.1	0.61	
gi|38228945|emb|BX470219.6| Zebrafish DNA sequence from clone...	44.1	0.61	
gi|23496883|gb|AE014850.1| Plasmodium falciparum 3D7 chromoso...	42.1	2.4	
gi|77020681|gb|AC163623.5| Mus musculus BAC clone RP23-123D6 ...	42.1	2.4	
gi|3217882|emb|AL023839.1|CEY39A1C Caenorhabditis elegans YAC Y3	42.1	2.4	
gi|70908345|emb|CR956629.5| Pig DNA sequence from clone PigE-...	42.1	2.4	
gi|1843447|emb|Z82201.1|HS345P10 Human DNA sequence from clon...	42.1	2.4	E
gi|15717972|emb|AL590702.17| Human DNA sequence from clone RP...	42.1	2.4	
gi|15787728|emb|AL355338.33| Human DNA sequence from clone RP...	42.1	2.4	
gi|46485782|gb|AC137746.2| Oryza sativa (japonica cultivar-gr...	42.1	2.4	
gi|11544743|emb|AL122016.15|HSJ161C16 Human DNA sequence from...	42.1	2.4	
gi|34610309|gb|AC116096.3| Homo sapiens chromosome 3 clone RP11-	42.1	2.4	
gi|51174248|emb|BX677667.10| Zebrafish DNA sequence from clon...	42.1	2.4	
gi|72096057|gb|AC160535.3| Mus musculus chromosome 7, clone RP24	42.1	2.4	
gi|21322174|gb|AC002088.2| Homo sapiens BAC clone CTB-13P7 fr...	42.1	2.4	
gi|18449556|gb|AC068308.12| Homo sapiens 3 BAC RP11-275H4 (Ro...	42.1	2.4	
gi|58530791|dbj|AP008211.1| Oryza sativa (japonica cultivar-g...	42.1	2.4	
gi|19807856|gb|AC107622.2| Homo sapiens chromosome 3 clone RP11-	42.1	2.4	
gi|18497251|gb|AC096577.3| Homo sapiens BAC clone RP11-556I14 fr	42.1	2.4	
gi|42415100|emb|BX293558.19| Mouse DNA sequence from clone RP...	42.1	2.4	
gi|66841667|gb|AC156637.2| Mus musculus BAC clone RP24-241I18...	42.1	2.4	
gi|10140837|gb|AC021019.5|AC021019 Homo sapiens BAC clone RP11-4	42.1	2.4	
gi|66730824|gb|AC111051.26| Mus musculus chromosome 7, clone RP2	42.1	2.4	
gi|66510452|ref|XM_396494.2| PREDICTED: Apis mellifera simila...	42.1	2.4	G
gi|66506611|ref|XM_396589.2| PREDICTED: Apis mellifera simila...	42.1	2.4	G